Universidade do Minho
Escola de Engenharia

Hélder Daniel Peixoto da Silva

Development and characterization of lipid-based nanosystems for controlled release of bioactive compounds

November 2015

Universidade do Minho
Escola de Engenharia

Hélder Daniel Peixoto da Silva

Development and characterization of lipid-based nanosystems for controlled release of bioactive compounds

PhD in Chemical and Biological Engineering

Supervisor:
António Augusto Martins de Oliveira Soares Vicente, PhD
Co-supervisor:
Miguel Ângelo Parente Ribeiro Cerqueira, PhD

November 2015

STATEMENT OF INTEGRITY

I hereby declare having conducted my thesis with integrity. I confirm that I have not used plagiarism or any form of falsification of results in the process of the thesis elaboration.

I further declare that I have fully acknowledged the Code of Ethical Conduct of the University of Minho.

University of Minho, November 20, 2015

Full name: Hélder Daniel Peixoto da Silva

Signature: 

"Uma vez que aprendas a voar nunca mais
caminharás sobre a terra sem para os céus olhar,
pois já lá estiveste e para lá a tua alma deseja
voltar."

Leonardo da Vinci

À minha família.
Porque são insubstituíveis!

ACKNOWLEDGEMENTS/AGRADECIMENTOS

O desenvolvimento deste Doutoramento foi uma experiência enriquecedora que para além do conhecimento científico adquirido, nos embarca numa jornada onde o desenvolvimento pessoal é único e digno de registo. Várias foram as etapas ultrapassadas, que seriam difíceis de superar sem ajuda dos meus orientadores, da minha família, amigos e colegas de trabalho. Assim, e após esta longa e árdua, mas frutífera etapa, não posso deixar de reconhecer o contributo de algumas pessoas que me acompanharam e apoiaram na concretização deste trabalho. Ficará sempre a minha amizade por todos.

Gostaria de agradecer em primeiro lugar ao Doutor António Vicente, muito mais que a oportunidade de realizar um doutoramento, agradeço-lhe pela confiança em mim depositada. Agradeço-lhe pela sua disponibilidade, orientação e estímulo científico, mas sobretudo pela amizade sempre presente. Ao Doutor Miguel Cerqueira pela orientação, disponibilidade infindável, conhecimento científico e amizade proporcionada.

To Prof. Giovanna Ferrari I am deeply thankful for having welcomed me in the ProdAl Scarl at Salerno University. It was a privilege to work in such environment and team. I thank you also and for sharing your knowledge with me.

To Dr. Francesco Donsì and Dr. Mariarenata Sessa I thank you for your co-supervising during my stay at ProdAl, for all your scientific support, the incentives, your creativity and your kindness.

À Doutora Catarina Duarte por me ter recebido no seu laboratório e pelo conhecimento adquirido.

A todos os meus colegas e amigos do Departamento de Engenharia Biológica, especialmente aos do Laboratório de Indústria e Processo pelo apoio dados nos últimos anos e pelo carinho: ao Ricardo, à Joana, ao Bruno, à Cristiana, ao Mota, à Maria, ao Duda, ao Héctor, ao Bartô ao Luís, ao Filipe, ao Óscar, ao Rui, ao Artur, ao André e à Professora Graça. Em especial, ao Miguel, à Isabel, ao Philippe, à Cristina e ao Flávio por tantos bons momentos que partilhamos juntos, pelo apoio mútuo, compreensão e incentivo.

À Diana e ao João. Por todo o carinho, forte amizade e força transmitida. Não chega dizer obrigado, terão sempre a minha amizade e carinho.

To all the ProdAI team: Roberta, Gianluca, Serena, Mert, Maria Rosaria, Mauro, Abu, Antonio, and Gianpiero Pataro, I thank you for your friendship, for being always so kind to me and for showing me another perspective of life.

Às colegas do Instituto de Tecnologia Química e Biológica, em especial à Joana e à Teresa, agradeço a ajuda na análise da viabilidade celular.

Ao Sr. Santos e Engª Madalena Vieira pela disponibilidade em colaborar sempre que solicitava a vossa ajuda.

Um agradecimento especial à Diana, pelo amor incondicional, amizade, carinho e dedicação. Por me ter acompanhado e ajudado a superar todas as dificuldades deste capítulo da minha vida. Obrigado pelo suporte incansável pelos sorrisos e abraços que sempre me ajudaram a manter focado e determinado em alcançar sempre mais.

À minha família. Aos meus pais, Madalena e Fernando, e aos meus irmãos Pedro e Rúben dirijo um agradecimento especial por serem um exemplo de integridade, de bondade, de força na família, por saber que tenho alguém que me ajuda sempre a levantar e que me recebe de braços abertos.

A elaboração deste trabalho foi suportada por uma bolsa de doutoramento financiada pela Fundação para a Ciência e Tecnologia (FCT) com a referência SFRH/BD/81288/2011 financiada pelo Programa Operacional Potencial Humano Quadro de Referência Estratégico Nacional (POPH – QREN) - Tipologia 4.1 - Formação Avançada, comparticipado pelo Fundo Social Europeu (FSE) e por fundos nacionais do Ministério da Ciência, Tecnologia e Ensino Superior (MCTES).

ABSTRACT

DEVELOPMENT AND CHARACTERIZATION OF LIPID-BASED NANOSYSTEMS FOR CONTROLLED RELEASE OF BIOACTIVE COMPOUNDS

The application of nanotechnology to food industry has received great attention from the scientific community. Driven by the increasing consumers' demand for healthier and safer food products and the need for food grade systems able to encapsulate, protect, and release bioactive compounds, researchers are currently focusing their efforts in nanotechnology to address issues relevant to food and nutrition. Lipid-based nanosystems used as delivery systems are particularly suited for the encapsulation of lipophilic bioactive compounds as it prevents their degradation and improves their bioavailability during gastrointestinal passage. These nanosystems have the potential to revolutionize food industry, once they will allow designing and developing novel functional food products, improving water solubility, thermal stability and bioavailability of bioactive/functional compounds, and enhance sensory attributes and physiological performance of products such as: soft drinks, milk, ice cream, salad dressings, soups, mayonnaise, sauces, dips, butter and margarine. Despite their functionalities, key challenges such as their behaviour within the human gastrointestinal tract and possible toxicity, should first be addressed.

Having this background in mind, this thesis aims at developing lipid-based nanosystems for controlled release of lipophilic bioactive compounds, while evaluating their behaviour under gastrointestinal tract conditions and at the

same time evaluates the developed nanosystems toxicity towards humans, in model Caco-2 cells. In order to achieve these premises this work a) defines the influence of surfactants and processing conditions in nanoemulsions development; b) evaluates the influence of surface composition in the nanosystems behaviour under gastrointestinal conditions; and c) studies the nanosystems toxicity and their ability to deliver curcumin through Caco-2 cells monolayer.

The work performed has shown that nanoemulsions can be produced using high-pressure homogenization and surface composition can be modified using the layer-by-layer (LbL) electrostatic deposition technique. The influence of surfactant and processing conditions on the development and stability of nanoemulsions were evaluated and results showed that processing parameters such as homogenization pressure, surfactant concentration and oil:water ratio significantly affected the Hydrodynamic diameter (H_d) and Polydispersity Index (*PdI*) values of nanoemulsions. The developed nanoemulsions showed a good kinetic stability (evaluated after centrifugation, heating-cooling cycles and thermal stress) upon measuring the H_d during 28 and 35 days of storage, without visual evidence of creaming and phase separation. Surface composition modification carried through LbL technique resulted in kinetically stable multilayer nanoemulsions. Results showed an encapsulation efficiency of 99.8 ± 0.8 % and a loading capacity of 0.53 ± 0.03 % (w/w) for the nanoemulsion. The presence of the multilayer leads to an increase of the H_d of the nanosystems, from 80.0 ± 0.9 nm (nanoemulsion) to 130.1 ± 1.5 nm (multilayer nanoemulsion). Curcumin release profiles from the nanosystem were evaluated at different conditions and by fitting a linear superimposition model to experimental data the results suggested an anomalous behaviour, being the relaxation of the surfactant and polyelectrolytes the rate-determining phenomena in curcumin release.

The effect of the deposition of chitosan and alginate layers onto nanoemulsion systems on curcumin bioaccessibility during *in vitro* digestion was studied using a dynamic gastrointestinal system that mimicked stomach, duodenum, jejunum and ileum conditions. Results showed that the deposition of a polyelectrolyte layer significantly improved the antioxidant capacity of curcumin during *in vitro*

digestion. In addition, whenever a polyelectrolyte layer was deposited on the nanoemulsion droplets, was observed a better control of the rate and the extent of lipid digestibility by decreasing the hydrolytic activity of lipase when compared to uncoated nanoemulsions.

The construction of a chitosan layer increased the bioaccessibility of curcumin, whereas cellular antioxidant activity studies revealed that nanoemulsions and multilayer nanoemulsions had respectively 9 and 10 times higher antioxidant capacity at the cellular level, when compared to pure curcumin. Permeability assays showed that the use of a chitosan layer significantly increased ($p<0.05$) the apparent permeability coefficient of curcumin through Caco-2 cells by 1.55-fold.

In conclusion, this works shows that lipid-based nanosystems can be tailored to increase lipophilic bioactive compounds bioaccessibility or modulate the satiety response by retarding lipid digestion, which can be rather important for the development of functional foods designed for combating obesity, showing great potential for application in food industry.

RESUMO

DESENVOLVIMENTO E CARACTERIZAÇÃO DE NANOSISTEMAS LIPÍDICOS PARA LIBERTAÇÃO CONTROLADA DE COMPOSTOS BIOACTIVOS

A aplicação da nanotecnologia na indústria alimentar tem recebido grande atenção por parte da comunidade científica. Impulsionada pela crescente preocupação dos consumidores por produtos alimentares mais saudáveis e seguros e pela necessidade de sistemas edíveis capazes de encapsular, proteger e libertar compostos bioativos, os investigadores estão atualmente a concentrar os seus esforços no uso da nanotecnologia de forma a responder a questões relevantes à alimentação e nutrição. Os nanosistemas lipídicos como sistemas de libertação são particularmente interessantes para a encapsulação de compostos lipofílicos bioativos, uma vez que impedem a sua degradação e melhoram a sua biodisponibilidade durante a passagem gastrointestinal. Estes nanosistemas tem o potencial de revolucionar a indústria alimentar, uma vez que permitirão o desenvolvimento de novos produtos nutraceuticos, melhorar a solubilidade em água, a estabilidade térmica, a biodisponibilidade, atributos sensoriais e o desempenho fisiológico de produtos tais como refrigerantes, leite, gelados, molhos para saladas, sopas, maioneses, manteiga e margarina. No entanto, apesar das suas funcionalidades, existem ainda alguns desafios tais como o seu comportamento no trato gastrointestinal humano e possível toxicidade, que devem de ser abordados.

Com estes desafios em mente, esta tese visou o desenvolvimento de nanosistemas lipídicos para a libertação controlada de compostos bioativos lipofílicos, avaliar o seu comportamento sob condições do trato gastrintestinal e, ao mesmo tempo avaliar a toxicidade dos nanosistemas desenvolvidos em células Caco-2. De forma a cumprir estas premissas, este trabalho consistiu em: a) avaliar a influência dos surfactantes e das condições do processo no desenvolvimento de nanoemulsões; b) avaliar a influência da composição de

superfície no comportamento nanosistemas sob condições gastrointestinais; e c) determinar a toxicidade e a capacidade dos nanosistemas no transporte de curcumina através de uma monocamada de células Caco-2.

O trabalho realizado demonstrou que as nanoemulsões podem ser produzidos utilizando homogeneização de alta pressão e que a composição de superfície das mesmas pode ser alterada utilizando a técnica de deposição eletrostática camada-a-camada (LbL). A influência do surfactante e das condições de processamento foram avaliadas no desenvolvimento e estabilidade das nanoemulsões. Os resultados mostraram que as condições de processamento, tais como pressão de homogeneização, concentração de surfactante e proporção óleo:água afetou significativamente os valores do diâmetro hidrodinâmico e do índice de polidispersibilidade das nanoemulsões. As nanoemulsões desenvolvidas demonstraram boa estabilidade cinética (avaliada após ciclos de centrifugação, de aquecimento e de arrefecimento e stress térmico) através da medição da diâmetro hidrodinâmico durante 28 e 35 dias de armazenamento, sem evidência visual de *creaming* e separação de fases. A modificação da composição da superfície realizada através da técnica LbL resultou em nanoemulsões multicamadas cineticamente estáveis. Os resultados mostraram uma eficiência de encapsulação de 99,8 ± 0,8 % e uma capacidade de *loading* de 0,53 ± 0,03 % (w/w) para a nanoemulsão. A presença das multicamadas originou um aumento do diâmetro hidrodinâmico das nanoemulsões de 80,0 ± 0,9 nm (nanoemulsão) para 130,1 ± 1,5 nm (nanoemulsão multicamada). Os perfis de libertação da curcumina dos nanosistemas foram avaliados em diferentes condições. A modelação dos dados experimentais através do modelo linear de sobreposição sugeriu que o transporte da curcumina é devido a um comportamento anómalo, sendo o relaxamento do surfactante e dos polielectrólitos os fenómenos determinantes para a libertação controlada da curcumina.

O efeito da deposição de camadas de quitosano e alginato em nanoemulsões foi avaliado com base na bioacessibilidade da curcumina durante digestões *in vitro*, utilizando um sistema gastrointestinal dinâmico que mimetiza as condições do estômago, duodeno, jejuno e íleo. Os resultados mostraram que

a deposição de camadas de polielectrólitos melhorou significativamente a capacidade antioxidante de curcumina durante a digestão *in vitro*. Além disso, a deposição de camadas de polielectrólitos permitiu um melhor controlo da taxa e extensão da digestibilidade lipídica através da diminuição da atividade hidrolítica da lipase.

A construção de uma camada de quitosano aumentou a biodisponibilidade da curcumina, enquanto que estudos de atividade antioxidante celular revelaram que nanoemulsões e nanoemulsões multicamada obtiveram respectivamente 9 e 10 vezes maior capacidade antioxidante a nível celular, quando comparado com a curcumina pura. Ensaios de permeabilidade mostraram que o uso de uma camada de quitosano aumenta significativamente ($p<0.05$) o coeficiente de permeabilidade aparente da curcumina através de células Caco-2 em 1,55 vezes.

Em conclusão, esta trabalho demonstra que os nanosistemas lipídicos podem ser personalizados para aumentar a biodisponibilidade de compostos bioativos lipofílicos ou modular a saciedade ao retardar a digestão dos lípidos, o que pode ser importante para o desenvolvimento de alimentos funcionais concebidos para o combate à obesidade, mostrando um grande potencial para futuras aplicações na indústria alimentar.

TABLE OF CONTENTS

LIST OF FIGURES

Chapter 2

Chapter 3

Chapter 4

Chapter 5

Chapter 6

LIST OF TABLES

Chapter 2

Chapter 3

LIST OF GENERAL NOMENCLATURE

Symbols

(d*x*/d*t*) – terminal settling velocity

(d*x*/d*t*)' – settling velocity

∫*CA* – integrated area of the control curve

∫*SA* – integrated area under the sample fluorescence versus time curve

a – particle size

A – surface area of the membrane

A_0 – absorbance at 517 nm of DPPH

A_b – absorbance at 517 nm of sample without DPPH

A_s – absorbance at 517 nm of sample and DPPH

A_{sp} – specific surface area

C'_s – Concentration of surfactant at the continuous phase

Co – initial nanosystem concentration in the donor compartment

CP – Central point

$Curcumin_{free}$ – free/unabsorbed curcumin in filtrate

$Curcumin_{total}$ – total amount of curcumin added to the system

dQ/dt – cumulative transport rate

Ev – Specific energy

F – resonance frequency

f_a – fraction affected

FFA – Free fatty acids

f_u – fraction unaffected

g – gravity

HE – Total height of the emulsion

HS – height of the serum layer

k_F – Fickian diffusion rate constant

k_{Ri} – relaxation rate constant

$M_{\infty,F}$ – compound release at equilibrium

$M_{\infty,Ri}$ – contributions of the relaxation processes for compound release

$Mass_{nanoemulsion}$ – total weight of nanoemulsions after drying

M_F – total mass of compound released by Fickian transport

M_{lipid} – molecular weight of the MCTs oil

m_{NaOH} – molarity of the sodium hydroxide used (in mol L^{-1})

M_R – total mass of compound released by polymer relaxation

M_t – total amount of sorption per unit weight of nanosystems at time *t*

$M_{t,F}$ – Fickian contribution at time *t*

M_{tR} – Polymer relaxation contribution at time *t*

M_w – Molecular weight

n – Number of cycles

P_{app} – apparent permeability coefficient

pI – Isoelectric point

pK_a – acid dissociation constant

R – radii of curvature

R_1 – radii of curvature

R^2 – coefficient of determination

R_2 – radii of curvature

R_{blank} – resistance of the filter membrane

R_{min} – theoretical minimum size

$R_{monolayer}$ – resistance of the cell monolayer along with the filter membrane

T – Temperature

t – Time

v_{NaOH} – volume of sodium hydroxide required to neutralize the FFA

w_{lipids} – total weight of MCTs oil initially present

Greek symbols

$\gamma\Delta A$ – interfacial area

ΔS – entropy of the dispersion

$\Delta G_{formation}$ – Gibbs energy of formation

Δp – Laplace pressure

ΔF – resonant frequency

ΔP – Homogenization pressure

γ – Interfacial tension

Γ – Surface load

ϕ – Disperse phase volume

R – radii of curvature

ρ – density

η – viscosity

Abbreviations

A.L – absence of light

AFM – Atomic Force Microscopy

BHA – Butylated hydroxyanisole

BHT – Butylated hydroxytoluene

CAA – Cellular antioxidant activity

$CaCl_2$ – Calcium chloride

CLSM – Confocal laser scanning microscopy

DLS – Dynamic Light Scattering

DMSO – Dimethyl sulfoxide

DPPH – 1,1-diphenyl-2-picrylhydrazyl

DSC – Differential Scanning Calorimetry

DTAB – dodecyltrimethylammonium bromide

EC_{50} – median effective concentration

EE – Encapsulation efficiency

EFSA – European Food Safety Agency

EU – European Union

FBS – Fetal Bovine Serum

FDA – Food and Drug Admnistration

FFF – Flow Field Fractionation

FITC – fluorescent-labelled

FTIR – Fourier Transform Infrared

GRAS – Generally Recognized As Safe

HBSS – Hanks' salanced salt solution

HCl – Hydrochloric acid

H_d – Hydrodynamic diameter

HLB – hydrophilic/lipophilic balance

HPLC – High Pressure Liquid Chromatography

IC_{50} – concentrations resulting in a 50 % decrease of cell viability

IEC – ion exchange chromatography

KCl – Potassium chloride

LbL – layer-by-layer

LC – Loading capacity

LSM – linear superimposition model

MCT – Medium chain triglyceride

MTS – CellTiter 96® AQueous One Solution Cell Proliferation Assay reagent

NaCl – sodium chloride

$NaHCO_3$ – Sodium bicarbonate

NaOH – sodium hidroxide

NMR – Nuclear Magnetic Resonance

O/W – Oil-in-water

P.L – presence of light

PBS – phosphate buffered saline

PdI – Polydispersity index

PS – Penicillin-Streptomycin

Psi – Pounds per square inch

QCM – Quartz Crystal Microbalance

QE – Quercitin equivalents

RMSE – squared root mean square error

rpm – Revolutions per minute

RSA – radical scavenging activity

SAXS – Small-Angle X-ray Scattering

SDS – sodium dodecyl sulfate

SEC – size-exclusion chromatography

SEM – Scanning Electron Microscopy

SHW % – standardised halved width

SIES – Small intestinal electrolyte solution

Span 20 – Sorbitan laurate

Span 80 – Sorbitan monooleate

SSE – sum of the squared residues

TEER – Transepithelial electrical resistance

TEM – Transmission Electron Microscopy

Tween 20 – Polysorbate 20

Tween 80 – Polysorbate 80

U.S. – United States dollars

USA – United States of America

Uv-vis – ultraviolet-visible

WPI – Whey protein isolate

XRD – X-Ray Diffraction

Zp – Zeta potential

LIST OF PUBLICATIONS

This thesis is based on the work presented in the following publications:

Silva, H. D., Cerqueira, M, A,. & Vicente, A, A. (2012). Nanoemulsions for Food Applications: Development and Characterization. *Food and Bioprocess Technology, 5*(3), 854-867.

Cerqueira, M. A., Bourbon, A. I., Pinheiro, A. C., Silva, H. D., Quintas, M. A. C., & Antonio, A. V. (2013). Edible Nano-Laminate Coatings for Food Applications. In *Ecosustainable Polymer Nanomaterials for Food Packaging* (pp. 221-252): CRC Press.

Silva, H. D., Cerqueira, M. A., & Vicente, A. A. (2015). Chapter 56 - Nanoemulsion-Based Systems for Food Applications. In B. I. Kharisov (Ed.), *CRC Concise Encyclopedia of Nanotechnology*. USA: CRC Press by Taylor and Francis Group.

Silva, H. D., Cerqueira, M. A. & Vicente, A. A. (2015). Influence of surfactant and processing conditions in the stability of oil-in-water nanoemulsions. *Journal of Food Engineering,* 167(Part B), 89-98*.*

Pinheiro, A.C., Bourbon, A.I., Silva, H.D., Martins J.T. & A.A. Vicente. Chapter 8 - Multilayer nanocapsules as a vehicle for release of bioactive compounds. In J. Moreno (Ed.), *Innovative Processing Technologies for Foods with Bioactive Compounds*. USA: CRC Press by Taylor and Francis Group (submitted).

Cerqueira, M, A., Ramos, O. L., Pinheiro, A. C., Bourbon A. I., Silva H. D. & Vicente A. A. Chapter 2 – Advances in food nanotechnology. In R. Busquets (Ed.), *Emerging Nanotechnologies in Food Science*. USA: Elsevier (submitted).

Silva, H. D., Donsì, F., Pinheiro, A. C., Cerqueira, M. A., Ferrari, G. & Vicente, A. A. Development and characterization of lipid-based nanosystems: Effect of interfacial composition on nanoemulsions behaviour. *Food Hydrocolloids* (Submitted).

Silva, H. D., Poejo, J., Pinheiro, A. C., Donsì, F., Serra, A. T., Duarte C. M., Ferrari, G., Cerqueira, M. A. & Vicente, A. A. Development and characterization of lipid-based nanosystems: Effect of interfacial composition on nanoemulsions behaviour. *Food Hydrocolloids* (Submitted).

Silva, H. D., Beldíková, E., Poejo, J., Abrunhosa, L., Serra, A. T., Duarte C. M., Bránykib, T., Cerqueira, M. A., Pinheiro, A. C. & Vicente, A. A. Evaluating the effect of chitosan layer on bioaccessibility and cellular uptake of curcumin nanoemulsions. *Food Hydrocolloids* (Submitted).

CHAPTER 1

MOTIVATION AND OUTLINE

This chapter provides a general overview of the thesis, including the motivation, research aims and outline of the work performed.

1.1 Thesis motivation

Nowadays consumers are demanding for new and healthier food products, so food industry seeks for new methodologies that lead to sustainable products and processes. The creation of new methodologies of encapsulation using nanotechnology allows the protection and release of bioactive compounds with several advantages when compared with microencapsulation, whereas the development of functional products without affecting their quality is one of researchers' focuses (M. A. Cerqueira, et al., 2013; H. Silva, Cerqueira, & Vicente, 2012). In this context, lipid-based nanosystems appear as an emerging tool that holds potential to provide the food industry with a variety of applications once they can act as carriers or delivery systems for lipophilic bioactive compounds, such as nutraceuticals, drugs, flavours, antioxidants and antimicrobials, while offering the potential to improve bioavailability during gastro-intestinal passage and their solubility in aqueous media (Quintanilla-Carvajal, et al., 2010; H. D. Silva, et al., 2011). Lipid-based nanosystems can be used for the food and beverage industry for the encapsulation of lipophilic compounds, while allowing the preservation of their unique properties, releasing them at the desired target, and simultaneously preserving the organoleptic and nutritional properties of food products (Plaza-Oliver, et al., 2015).

Nevertheless, key challenges must be addressed for a total and safe implementation of these systems by the industry, such as: the production of nanosystems without toxicity, targeting human consumption; the development of functional nanosystems with affordable scale-up technologies; the understanding of nanosystems behaviour during gastrointestinal conditions and informative actions towards the application of nanotechnology in the food industry focused to consumers (Cerqueira, et al., 2014). In order to answer to these challenges the following purposes must be achieved: a) development of nanosystems using food grade materials, simple and economically affordable methods easy to scale-up, such as nanoemulsions and multilayer nanoemulsions; b) knowledge of the nanosystems behaviour when subjected to the physicochemical and physiological processes occurring in human

gastrointestinal tract using realistic *in vitro* gastrointestinal models, where ideally *in vivo* models should be used (Pinheiro, Coimbra, & Vicente, 2016). Consumers' awareness and knowledge towards nanotechnology should be enlarged through accurate information regarding the state of the art, potential benefits and safety of nanotechnology (Roco & Bainbridge, 2005).
The potential of nanotechnology to create new and healthier foods were thus the major motivations for the development of this thesis.

1.2 Research aims

The main purpose of this thesis was the development of lipid-based nanosystems for controlled release of lipophilic bioactive compounds. In particular:

- Physicochemical characterization of developed nanosystems: nanoemulsions and multilayer nanoemulsions;
- Incorporation of bioactive compounds into the developed nanosystems;
- Evaluation of the stability of nanosystems under different environmental conditions;
- Study of the transport properties of nanosystems in food simulants;
- Study of the behaviour of nanosystems in a dynamic artificial gastrointestinal system;
- Evaluation of the cytotoxicity of nanosystems in a Caco-2 cell line;
- Study of the apparent permeability coefficient of curcumin in nanosystems through Caco-2 cells.

1.3 Thesis outline

Based on the main purpose and following the research aims this thesis was organized in a total of seven chapters. Chapter 1 provides the motivation, research aims and outline of this thesis. Chapter 2 provides an overview regarding the development of nanoemulsions and multilayer nanoemulsions. Chapters 3 to 6 report the main experimental results and further discussion, while Chapter 7 presents the main conclusions and future remarks.

More specifically, Chapter 3 presents the influence of surfactants, lipid phase and process conditions in the development and stability of nanoemulsions. In Chapter 4, curcumin nanoemulsions were produced using high-pressure homogenization and multilayer nanoemulsions were developed through layer-by-layer (LbL) electrostatic technique being the release properties of the nanosystems evaluated. In Chapter 5 the behaviour of the nanosystems developed in Chapter 4 were studied under *in vitro* gastrointestinal conditions. Also, the effect of the surface composition of the nanoemulsion on curcumin bioaccessibility was evaluated. Chapter 6 presents the development of food grade nanoemulsions and multilayer nanoemulsions, while evaluating the effect of surface composition under gastrointestinal conditions. Equally, the evaluation of the cytotoxicity and apparent permeability coefficient of curcumin from nanosystems on Caco-2 cells was performed.

Chapter 7 presents the main achievements of this thesis and future recommendations.

1.4 References

Cerqueira, M., Pinheiro, A., Silva, H., Ramos, P., Azevedo, M., Flores-López, M., Rivera, M., Bourbon, A., Ramos, Ó., & Vicente, A. (2014). Design of Bio-nanosystems for Oral Delivery of Functional Compounds. *Food Engineering Reviews, 6*(1-2), 1-19.

Cerqueira, M. A., Bourbon, A. I., Pinheiro, A. C., Silva, H. D., Quintas, M. A. C., & Antonio, A. V. (2013). Edible Nano-Laminate Coatings for Food Applications. In *Ecosustainable Polymer Nanomaterials for Food Packaging* (pp. 221-252): CRC Press.

Pinheiro, A. C., Coimbra, M. A., & Vicente, A. A. (2016). In vitro behaviour of curcumin nanoemulsions stabilized by biopolymer emulsifiers – Effect of interfacial composition. *Food Hydrocolloids, 52*, 460-467.

Plaza-Oliver, M., Baranda, J. F. S. d., Rodríguez Robledo, V., Castro-Vázquez, L., Gonzalez-Fuentes, J., Marcos, P., Lozano, M. V., Santander-Ortega, M. J., & Arroyo-Jimenez, M. M. (2015). Design of the interface of edible nanoemulsions to modulate the bioaccessibility of neuroprotective antioxidants. *International Journal of Pharmaceutics, 490*(1–2), 209-218.

Quintanilla-Carvajal, M., Camacho-Díaz, B., Meraz-Torres, L., Chanona-Pérez, J., Alamilla-Beltrán, L., Jimenéz-Aparicio, A., & Gutiérrez-López, G. (2010). Nanoencapsulation: A New Trend in Food Engineering Processing. *Food Engineering Reviews, 2*(1), 39-50.

Roco, M. C., & Bainbridge, W. S. (2005). Societal implications of nanoscience and nanotechnology: Maximizing human benefit. *Journal of Nanoparticle Research, 7*(1), 1-13.

Silva, H., Cerqueira, M., & Vicente, A. (2012). Nanoemulsions for Food Applications: Development and Characterization. *Food and Bioprocess Technology, 5*(3), 854-867.

Silva, H. D., Cerqueira, M. A., Souza, B. W. S., Ribeiro, C., Avides, M. C., Quintas, M. A. C., Coimbra, J. S. R., Carneiro-da-Cunha, M. G., & Vicente, A. A. (2011). Nanoemulsions of β-carotene using a high-energy emulsification-evaporation technique. *Journal of Food Engineering, 102*(2), 130-135.

CHAPTER 2

GENERAL INTRODUCTION

This chapter provides an overview of the production methods of nanoemulsions and multilayer nanoemulsions, of the materials used (solvents, emulsifiers and bioactive compounds) and of the current analytical techniques that can be used for the identification and characterization of nanoemulsions and multilayer nanosystems. Finally, nanotechnological applications in foods currently marketed are reported and the societal challenges in food nanotechnology are addressed.

This Chapter was adapted from:

Silva, H. D., Cerqueira, M, A,. & Vicente, A, A. (2012). Nanoemulsions for Food Applications: Development and Characterization. *Food and Bioprocess Technology, 5*(3), 854-867.

Silva, H. D., Cerqueira, M. A., & Vicente, A. A. (2015). Chapter 56 - Nanoemulsion-Based Systems for Food Applications. In B. I. Kharisov (Ed.), *CRC Concise Encyclopedia of Nanotechnology*. USA: CRC Press by Taylor and Francis Group.

Cerqueira, M. A., Bourbon, A. I., Pinheiro, A. C., Silva, H. D., Quintas, M. A. C., & Antonio, A. V. (2013). Edible Nano-Laminate Coatings for Food Applications. In *Ecosustainable Polymer Nanomaterials for Food Packaging* (pp. 221-252): CRC Press.

Pinheiro, A.C., Bourbon, A.I., Silva, H.D., Martins J.T. & A.A. Vicente (submitted). Chapter 8 - Multilayer nanocapsules as a vehicle for release of bioactive compounds. In J. Moreno (Ed.), *Innovative Processing Technologies for Foods with Bioactive Compounds*. USA: CRC Press by Taylor and Francis Group.

Cerqueira, M, A., Ramos, O. L., Pinheiro, A. C., Bourbon A. I., Silva H. D. & Vicente A. A (submitted). Chapter 2 – Advances in food nanotechnology. In R. Busquets (Ed.), *Emerging Nanotechnologies in Food Science*. USA: Elsevier.

2.1 Introduction

Nanotechnology is an emerging technology that holds potential to change food industry (Huang et al., 2010; Luykx et al., 2008). Nanotechnology involves research, technology development, and control of structures within sizes ranged between 1 and 100 nm (Quintanilla-Carvajal et al., 2010). The development of technologies able to manipulate or assemble materials at the nanometer scale (10^{-9} m) can provide commercial, technological and scientific opportunities for the industry (Huang et al., 2010). The application of nanotechnology to the food field may allow the modification of macroscale characteristics of food, such as texture, taste, other sensory attributes, colouring strength, processability, and stability during shelf life, which can lead to a great number of new products.

Bioactive compounds, claimed to provide health benefits as prevention or treatment of diseases (Chu et al., 2007b), are already available in the marketplace in the form of capsules or tablets. Nevertheless, it has become evident that these solutions may not sustain the health benefits of these bioactive compounds, mainly because of their low bioavailability. This is particularly the case of lipophilic compounds (Chen et al., 2006; Chu et al., 2007b; Spernath & Aserin, 2006). Improving the bioavailability of bioactive compounds often means enhancing their absorption in the gastro-intestinal tract, referred as a critical requirement. In this field nanotechnology offers solutions for improving water solubility and bioavailability of lipophilic bioactive compounds (Chu et al., 2007b).

Nanoemulsions technology can allow the modification of food characteristics such as: texture, taste, other sensory attributes, colouring strength, processability and stability during the shelf life of the food products, leading to the production of new food products (McClements et al., 2007; Ziani et al., 2012). Nanoemulsions are one the examples of structures which uses nanotechnology to improve the water solubility, thermal stability and the bioavailability of lipophilic bioactive compounds. The development of these structures can lead to the commercialization of edible systems able to encapsulate, protect and release lipophilic functional compounds (Huang et al., 2010; McClements et

al., 2007). They can also be used in the incorporation of lipophilic bioactive compounds into aqueous-based foods or beverages that needs to remain stable and optically transparent during the shelf-life, e.g. fortified waters, soft drinks, sauces and dips (Velikov & Pelan, 2008). In this way, the food and beverage industries have a considerable interest in encapsulate, protect and deliver lipophilic functional compounds, such as: flavours, colours, essential oils, antioxidants, antimicrobials, micronutrients, vitamins and nutraceuticals (Sanguansri & Augustin, 2006; Yang et al., 2012). This interest is due to their insolubility in water and weakly solubility in oil at ambient temperature, low bioavailability, sensitivity to light, oxygen and heat and poor chemical stability that limits their use in the food industry (McClements et al., 2007; McClements & Li, 2010).

This chapter reviews nanoemulsion production methods (high energy and low energy) as well as the materials used for nanoemulsion preparation (solvents and emulsifiers, as well as bioactive compounds) that are already in use or can be used. An overview on the layer-by-layer (LbL) technique for the build up of multilayer nanoemulsions is also provided. A description of analytical techniques used for nanoemulsions characterization is covered, being these techniques divided in three categories: separation techniques (such as High Pressure Liquid Chromatography – HPLC and Flow Field Fractionation – FFF), physical techniques (such as Dynamic Light Scattering – DLS, zeta potential – *Zp*, Differential Scanning Calorimetry – DSC, Fourier Transform Infrared – FTIR, Nuclear Magnetic Resonance – NMR and X-Ray Diffraction – XRD) and imaging techniques (such as Transmission Electron Microscopy – TEM, Scanning Electron Microscopy – SEM and Atomic Force Microscopy – AFM). Despite some of these techniques being mostly applied to nanoparticles, they can be applied to characterize nanoemulsions as well.

Finally, a brief statement regarding the societal challenges of nanotechnology in foods is presented, and some examples of nanotechnology-based foods and food-ingredients which are being marketed or very close from it are showed.

2.2 Materials and lipophilic bioactive compounds used in nanoemulsions fabrication

A great variety of materials can be used to produce nanoemulsions, and these are divided in three different classes: oily phase materials, surfactants and bioactive compounds. In order to build nanoemulsions, the appropriate materials should be employed in order to achieve the desired properties. A special attention to the nature of these materials should be given, where only food-grade ingredients (Generally Recognized As Safe – GRAS) should be used; moreover these materials should be: a) matrix compatible, in order to not affect the appearance, texture, flavour and stability of the products; b) stable during food processing, being able to undergo the various processing operations experienced by the food products, during the manufacture, storage, distribution and shelf-life during the utilization; and c) economic, in order to avoid additional costs to the food product (McClements & Li, 2010; Rao & McClements, 2013; Ziani et al., 2012).

Table 2.1 and Table 2.2 present examples of oils and surfactants used in the production of nanoemulsions, which can be applied to the food industry. Whereas in Table 2.3 some examples of lipophilic bioactive compounds are presented.

2.3 Production of nanoemulsions

Emulsifiers have a major role in the formation of nanoemulsions due their ability to form a protective coating (interfacial layer) surrounding the oil droplets. This is due their ability to low the interfacial tension between two immiscible liquids (e.g. oil in the dispersed phase and water in the aqueous phase), reducing the required amount of energy needed to disrupt the droplets, leading to smaller sizes and preventing the coalescence (McClements, 2005; Silva et al., 2012; Silva et al., 2011b; Silva et al., 2011c). Oil-in-water (o/w) nanoemulsions is a mixture of two immiscible liquids, where thin interfacial layer of emulsifier molecules surrounds the oil droplets promotes the dispersion of the oil phase in the continuous phase (Acosta, 2009; Silva et al., 2012; Silva et al., 2011b; Tadros et al., 2004). In water-in-oil (w/o) nanoemulsions the oil is the continuous phase, where the emulsifier surrounds the water droplets (disperse phase);

the emulsifiers can also be dispersed in the continuous phase or in the dispersed phase, depending on their hydrophilic-lipophilic balance (Khalid et al., 2013).

Table 2.1 – Lipids used in the production of nanoemulsions for the food industry

Lipids	Droplet Size (nm)	Solubility (mg/ml)	Studied parameters	Release[1] %	Charge[1] (mV)	Function[1]	Reference
Medium chain triglyceride (MCT)	81 - 311	46.30 mg ml^{-1} of ezetimibe	In vitro release studies	100 % in 30 min	n.a	MCTs are directly transported from the blood to the systemic circulation	(Bandyopadhyay et al., 2012)
Sunflower oil	35	n.a	Oxidative stability	n.a	n.a	n.a	(Lante & Friso, 2013)
Corn oil	181	0.30 % wt of curcumin in corn oil	In vitro digestion and bioaccessability	n.a	n.a	n.a	(Ahmed et al., 2012)
Sesame oil	20 - 90	n.a	Antibacterial activity of the eugenol nanoemulsion	n.a	n.a	Antibactericidal nanoemulsions	(Ghosh et al., 2014)
D-limonene	40 - 229	n.a	Influence of the oil phase in the nanoemulsions production	n.a	n.a	n.a	(Li et al., 2013)
Orange oil	< 200	n.a	In vitro digestions proved that the orange oil is indigestible	n.a	n.a	Flavour oil	(Qian et al., 2012b)

[1] If applicable; n.a – not available

Table 2.2 – Surfactants used in the production of nanoemulsions for the food industry

Surfactants	Droplet Size (nm)	HLB	Encapsulation efficiency	Release[1] %	Charge[1] (mV)	Studied parameter	Reference
Span 20	86	8.6		± 100 µg cm^{-2} Q10 permeated through the skin after 24 h	-16	Permeation of Q10 through skin	(Schwarz et al., 2013)
Span 80	214 – 277	4.3	n.a	n.a	-16	Effect of variables (hlb, concentration and type of surfactant)	(Manchun et al., 2014)
Tween 20	87 – 92	16.7	0.5 % w/w of ß-carotene	n.a	n.a	Oxidation rate of ß-carotene nanoemulsions	(Qian et al., 2012a)
Tween 80	4 – 35	15	1 % v/v of lemongrass essential oil	n.a	-17 to -55	Antimicrobial activity assay	(Salvia-Trujillo et al., 2014)
Cremophor El	14 – 118	14	n.a	74% after 24h	-6 to +5 neutral	Cytotoxic studies and *in vitro* release	(Sood et al., 2014)
Sodium caseinate	160	14	n.a	n.a	-30	Thermal analysis	(Truong et al., 2014)
Lipoid (lecithin)	64 – 154	6	n.a	n.a	n.a	Optimization of nanoemulsions and artificial neural network models	(Rezaee et al., 2014)

HLB – Hydrophilic-Lipophilic Balance; n.a – not available

Table 2.3 – Bioactive compounds used in the production of nanoemulsions for the food industry

Bioactive compound	Droplet Size (nm)	Solubility (mg ml^{-1})	Studied parameter	Release[1] %	Charge[1] (mV)	Benefits[1]	Reference
β-carotene	124-328	n.a	Rate of lipolysis	n.a	n.a	Source of provitamin A, antioxidant	(Yi et al., 2014)
Curcumin	14 – 118	50 mg ml^{-1} in Capmul MCM	Release studies	74 % after 24h	-12 to -25	Antioxidant	(Sood et al., 2014)
Quercetin	282	0.05 % w/w of quercetin	Release and *in vitro* permeation studies	55 % released within the first 2h	-36	Antioxidant	(Bose & Michniak-Kohn, 2013)
Omega 3	167 – 390	88.5 % of entrapment efficiency	In vitro antioxidant activity and in vitro release	99 % released after 27h	-29 to -34.5	Antinflamatory, decreases the levels of triglycerides and LDL cholesterol	(Lacatusu et al., 2013)
Vitamin D	170 - 380	4 mg ml^{-1} in ethanol	Oxidation of the vitamin was stable during 21 days of storage	n.a	n.a	Diminish the colon, breast and prostate cancer	(Israeli-Lev & Livney, 2014)

Co-enzyme Q10	86	5 % w/w in cetiol oil	In vitro skin studies ± 100 µg cm^{-2} of Co Enzyme Q10 permeated through the skin after 24 h	n.a	-16	Antioxidant	(Schwarz et al., 2013)
Resveratrol	128 - 211	0.01 % w/w	Caco-2 cells uptake % (0.5 to 1.5); *in vitro* release studies; transport through CaCo-2 cell monolayers and cytotoxicity of nanoemulsions	60 % after 24h		Antioxidant	(Sessa et al., 2014)
Eugenol	20 - 90	1 to 6 % w/w	Nanoemulsion characterization; antibacterial activity and application in a orange juice with shelf-life evaluation (72 h)	n.a	n.a	Antibacterici dal	(Ghosh et al., 2014)

n.a – not available

Table 2.1 – Lipids used in the production of nanoemulsions for the food industry

Lipids	Droplet Size (nm)	Solubility (mg/ml)	Studied parameters	Release[1] %	Charge[1] (mV)	Function[1]	Reference
Medium chain triglyceride (MCT)	81 - 311	46.30 mg ml^{-1} of ezetimibe	In vitro release studies	100 % in 30 min	n.a	MCTs are directly transported from the blood to the systemic circulation	(Bandyopadhyay et al., 2012)
Sunflower oil	35	n.a	Oxidative stability	n.a	n.a	n.a	(Lante & Friso, 2013)
Corn oil	181	0.30 % wt of curcumin in corn oil	In vitro digestion and bioaccessability	n.a	n.a	n.a	(Ahmed et al., 2012)
Sesame oil	20 - 90	n.a	Antibacterial activity of the eugenol nanoemulsion	n.a	n.a	Antibactericidal nanoemulsions	(Ghosh et al., 2014)
D-limonene	40 - 229	n.a	Influence of the oil phase in the nanoemulsions production	n.a	n.a	n.a	(Li et al., 2013)
Orange oil	< 200	n.a	In vitro digestions proved that the orange oil is indigestible	n.a	n.a	Flavour oil	(Qian et al., 2012b)

[1] If applicable; n.a – not available

Table 2.2 – Surfactants used in the production of nanoemulsions for the food industry

Surfactants	Droplet Size (nm)	HLB	Encapsulation efficiency	Release[1] %	Charge[1] (mV)	Studied parameter	Reference
Span 20	86	8.6		± 100 µg cm^{-2} Q10 permeated through the skin after 24 h	-16	Permeation of Q10 through skin	(Schwarz et al., 2013)
Span 80	214 – 277	4.3	n.a	n.a	-16	Effect of variables (hlb, concentration and type of surfactant)	(Manchun et al., 2014)
Tween 20	87 – 92	16.7	0.5 % w/w of ß-carotene	n.a	n.a	Oxidation rate of ß-carotene nanoemulsions	(Qian et al., 2012a)
Tween 80	4 – 35	15	1 % v/v of lemongrass essential oil	n.a	-17 to -55	Antimicrobial activity assay	(Salvia-Trujillo et al., 2014)
Cremophor El	14 – 118	14	n.a	74% after 24h	-6 to +5 neutral	Cytotoxic studies and *in vitro* release	(Sood et al., 2014)
Sodium caseinate	160	14	n.a	n.a	-30	Thermal analysis	(Truong et al., 2014)
Lipoid (lecithin)	64 – 154	6	n.a	n.a	n.a	Optimization of nanoemulsions and artificial neural network models	(Rezaee et al., 2014)

HLB – Hydrophilic-Lipophilic Balance; n.a – not available

Table 2.3 – Bioactive compounds used in the production of nanoemulsions for the food industry

Bioactive compound	Droplet Size (nm)	Solubility (mg ml^{-1})	Studied parameter	Release[1] %	Charge[1] (mV)	Benefits[1]	Reference
β-carotene	124-328	n.a	Rate of lipolysis	n.a	n.a	Source of provitamin A, antioxidant	(Yi et al., 2014)
Curcumin	14 – 118	50 mg ml^{-1} in Capmul MCM	Release studies	74 % after 24h	-12 to -25	Antioxidant	(Sood et al., 2014)
Quercetin	282	0.05 % w/w of quercetin	Release and *in vitro* permeation studies	55 % released within the first 2h	-36	Antioxidant	(Bose & Michniak-Kohn, 2013)
Omega 3	167 – 390	88.5 % of entrapment efficiency	In vitro antioxidant activity and in vitro release	99 % released after 27h	-29 to -34.5	Antinflamatory, decreases the levels of triglycerides and LDL cholesterol	(Lacatusu et al., 2013)
Vitamin D	170 - 380	4 mg ml^{-1} in ethanol	Oxidation of the vitamin was stable during 21 days of storage	n.a	n.a	Diminish the colon, breast and prostate cancer	(Israeli-Lev & Livney, 2014)

Co-enzyme Q10	86	5 % w/w in cetiol oil	In vitro skin studies ± 100 µg cm^{-2} of Co Enzyme Q10 permeated through the skin after 24 h	n.a	-16	Antioxidant	(Schwarz et al., 2013)
Resveratrol	128 - 211	0.01 % w/w	Caco-2 cells uptake % (0.5 to 1.5); *in vitro* release studies; transport through CaCo-2 cell monolayers and cytotoxicity of nanoemulsions	60 % after 24h		Antioxidant	(Sessa et al., 2014)
Eugenol	20 - 90	1 to 6 % w/w	Nanoemulsion characterization; antibacterial activity and application in a orange juice with shelf-life evaluation (72 h)	n.a	n.a	Antibacterici dal	(Ghosh et al., 2014)

n.a – not available

Nanoemulsions can be produced using a broad range of approaches that are classified in high-energy and low-energy approaches. High-energy approaches use mechanical energy from devices to create intensive disruption forces that leads to the breakup of oil and water phases and along with the emulsifiers, that allows to reduce the interfacial tension, leads to the formation of o/w nanoemulsions (Anton et al., 2008; Leong et al., 2009; Silva et al., 2012; Velikov & Pelan, 2008). Low-energy approaches are based in the intrinsic physicochemical properties of the system formulation (e.g. interfacial tension, surfactant and co-surfactant structure and concentration, oil physical properties and excipients of the formulation), where the nanoemulsions can be produced almost spontaneously due to the phase transitions that take place during the emulsification process, which can be carried out at constant temperature, changing the composition or keeping constant the composition, in this case changing the temperature (Bouchemal et al., 2004; Freitas et al., 2005; Rang & Miller, 1999; Shinoda & Saito, 1968; Silva et al., 2012).

2.3.1 High-Energy Approach

The use of mechanical forces or processes to produce nanoemulsions is normally divided in three categories based on used devices: a) high-pressure homogenizers, b) ultrasounds and c) high shear stirring or high-speed devices (Sanguansri & Augustin, 2006; Silva et al., 2012). This approach is governed by the amount of energy applied and by the surfactant and bioactive compounds chosen. It has been stated that the devices that are able to supply the available energy in the shortest time and with the most homogeneous flow can produce smaller nanoemulsions (Solans et al., 2005; Walstra, 1996).

Briefly, when a high-pressure homogenizer is used the mixture is forced to go through a nozzle, by the very high pressures, promoting shear, impact and cavitation forces, that leads to the formation of the nanoemulsions (Anton et al., 2008; Lee et al., 2009; Quintanilla-Carvajal et al., 2010; Sanguansri & Augustin, 2006; Silva et al., 2012). Table 2.4 presents some examples of nanoemulsions produced by high-energy methods. In the ultrasound technique when a mixture of two immiscible liquids and surfactants are subject to high-intensity sound waves, nanoemulsions are produced due to the cavitation forces, once it

causes the formation of high-speed liquid jets responsible by the creation of the nanoemulsions. Ultrasounds deeply depend on the power of the devices and on the surfactants used (Anton et al., 2008; Bondy & Sollner, 1935; Maa & Hsu, 1999; Mason, 1992; Pongsawatmanit et al., 2006; Silva et al., 2012). High-speed devices such as Ultra-Turrax do not provide the same efficiency of the other two methods, being the resulting energy manly dissipated into heat (Anton et al., 2008; Walstra, 1993). Despite the ability of these techniques to produce nanoemulsions, there are some drawbacks. High-pressure homogenizers are very expensive devices and depending on the molecules used it can cause degradation the molecules (Solans et al., 2005); ultrasound devices are only efficient for small batches (Solans et al., 2005); and high-speed devices do not provide a good dispersion and most of the energy is dissipated in heat (Anton et al., 2008; Walstra, 1993). Figure 2.1 represents a TEM microphotograph of nanoemulsions produced using the high-pressure homogenization technique at 15 000 Psi, during 10 cycles, using Tween 20 at 1 % (w/w) as surfactant, dispersed in the aqueous phase, and using corn oil as the lipid phase.

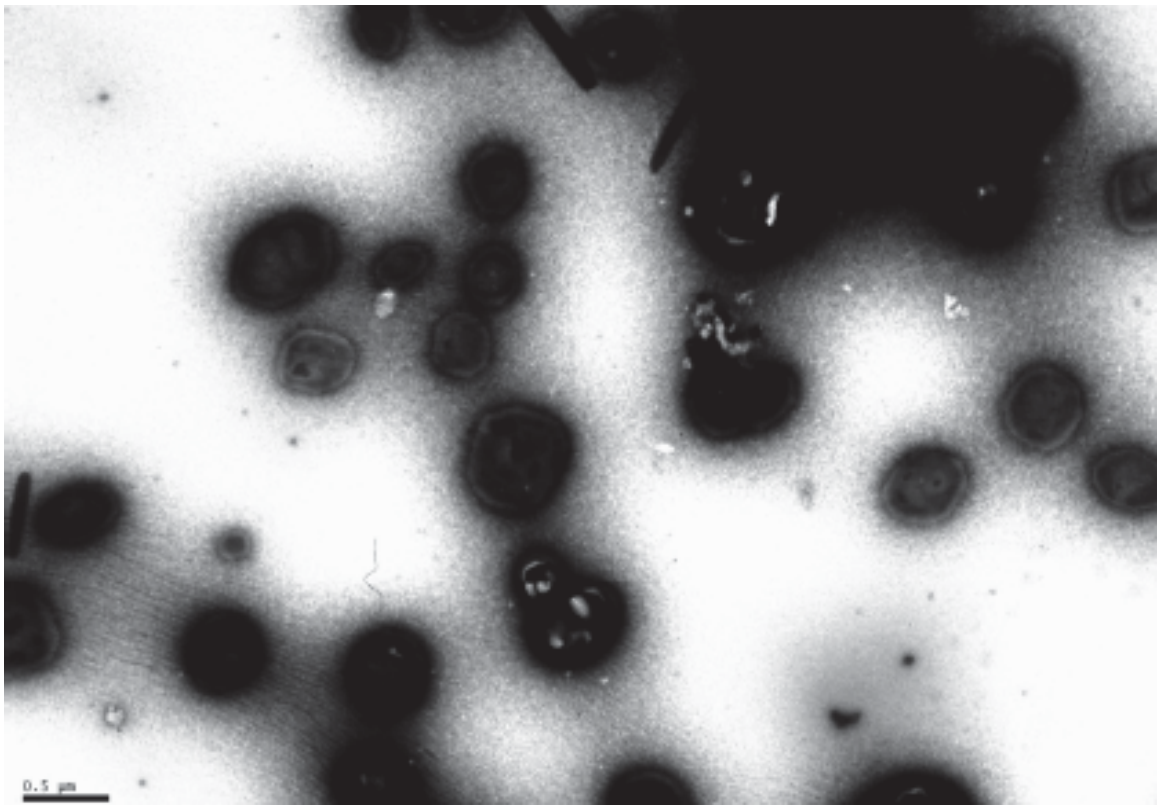

Figure 2.1 – TEM microphotograph of negatively stained nanoemulsion with uranyl 1 % w/w.

Table 2.4 – Examples of high and low-energy approaches, materials used, size and polydispersity (*PdI*), scale-up possibility and process costs

Technique	Materials	Size (nm)	*PdI*	Release properties	Scale-up[1]	Scale-up challenge	Cost[2]	Reference
High-pressure homogenization	Peanut oil, ethanol, Tween 20, glycerol monooleate and resveratrol	128	0.12	60 % released after 24 h	Complex -	Prices of the homogenizer	€€	(Sessa et al., 2014)
Ultrasound	Lemongrass oil, Tween 80, and sodium alginate	4 - 35	n.a	n.a	Very complex --	Only for small batches	€€	(Salvia-Trujillo et al., 2014)
Ultraturrax	Softisan 100, Precirol ATO5, Compritol 888ATO, glycerol, Lutrol F68, Tween 80 and lactoferrin	100 - 200	n.a	n.a	Simple +	Only for small batches	€	(Balcão et al., 2013)
Solvent displacement + ultraturrax (nanomemulsion)	Hexane, Tween 20 and ß-carotene	9 - 280	n.a.	n.a.	Simple +	Evaporation step	€€	(Silva et al., 2011b)
Spontaneous	Cremophor® RH 40, Tween 60 and	16	0.170	70 % released	Very simple	Knowledge on the intrinsically	€	(Badran et

emulsification	meloxicam			after 40 min	++	properties, evaporation step		al., 2014)
Phase inversion temperature	Solutol® HS 15, MCT, Lipoid S75-3® and sodium chloride	< 300	< 0.1	n.a	Simple +	Knowledge on the intrinsically properties, evaporation step	€	(Anton et al., 2007b)
Phase inversion composition	Hexadecane, tween 20 and span 80	40	n.a	n.a	Simple +	Knowledge on the intrinsically properties, evaporation step	€	(Nazarzadeh et al., 2013)

[1] For the upscale are considered: very complex – –, complex –, simple +, very simple ++

[2] For the cost are considered: low cost €, medium cost €€ and high cost €€€

2.3.2 Low-Energy Approaches

Low-energy approaches are based in the physicochemical properties of the system; nanoemulsions are obtained due to the phase transitions that takes place during the emulsification process (Rang & Miller, 1999; Silva et al., 2012; Solans et al., 2005; Solans & Solé, 2012). Two major groups of methods are proposed: a) the spontaneous phenomena that is divided in the spontaneous emulsification and in the solvent displacement, and b) the phase inversion methods, that include phase inversion temperature and phase inversion composition (Anton et al., 2008; Solans & Solé, 2012; Tadros et al., 2004; Usón et al., 2004). Briefly, spontaneous emulsification uses the rapid diffusion of surfactant and water-soluble solvent molecules from the oily phase to the aqueous phase, when the phases are mixed to produce stable nanoemulsions (Anton et al., 2008; Bouchemal et al., 2004; Solans et al., 2005; Solans & Solé, 2012). Nanoemulsions produced by spontaneous emulsification depends on the interfacial tension, phase transition, surfactant structure and concentration, surface tension and oil physical properties (Anton et al., 2008; Bouchemal et al., 2004; López-Montilla et al., 2002; Silva et al., 2012). Despite being a low energy method has some limitations, besides the low oil content also a water-soluble solvent is required as well as the solvent removal after the process (Bouchemal et al., 2004; Solans et al., 2005; Solans & Solé, 2012). Solvent displacement consists in the quick diffusion of organic solvents like acetone or ethanol from the disperse phase to the continuous phase containing surfactant promoting the formation of nanoemulsions with a high encapsulation efficiency (Anton et al., 2008; Chu et al., 2007a; Quintanar-Guerrero et al., 1999; Ribeiro et al., 2008; Silva et al., 2012; Yin et al., 2009). Nevertheless, this technique is limited to water-soluble solvents; the use of organic solvents requires their removal under reduced pressure by evaporation (Ribeiro et al., 2008; Silva et al., 2011b; Yin et al., 2009). Phase inversion technique is an organic and solvent free technique, which uses the specific capacity of surfactants, normally nonionic, to modify their affinity to water and oil in function of temperature (phase inversion temperature) or composition (phase inversion composition) at fixed composition and temperature, respectively. This process involves the surfactant film inversion, is a simple process and easy to scaled up (Anton et al., 2008; Anton

et al., 2007a; Izquierdo et al., 2001; Izquierdo et al., 2004; Shinoda & Saito, 1968, 1969; Silva et al., 2012; Solans et al., 2005; Solans & Solé, 2012).

Table 2.4 summarizes some examples of high and low-energy approaches for the production of nanoemulsions, the materials used, size, polydispersity index (*PdI*), scale-up possibility and process costs.

2.4 Advantages and limitations of nanoemulsions

Nanoemulsions are delivery systems able to encapsulate hydrophilic, amphiphilic and lipophilic bioactive compounds, despite being major explored to encapsulate lipophilic compounds, due to the oil in their composition (Berton-Carabin et al., 2013). For instance the lipophilic compound would be encapsulated in the oil phase, being the hydrophilic compound solubilized in the aqueous phase and linked to the polar head of the surfactant used for hydrophilic bonding (McClements, 2005; McClements et al., 2007). Is possible to create nanoemulsions with different rheological properties (e.g. viscous liquids, viscoelastic liquids, viscoelastic solids, plastics, or elastic solids) by controlling the composition and structure of the surfactant, co-surfactant and oil physical properties, normally increasing the droplet concentration leads to higher values of viscosity (Genovese et al., 2007; McClements et al., 2007). Nanoemulsions can be used directly (solution) or as powder by the food industry, according the final application (Desai & Jin Park, 2005; Jafari et al., 2008; McClements et al., 2007; Soottitantawat et al., 2003; Vega & Roos, 2006). Despite these advantages, nanoemulsions also have some limitations, namely: a) under environmental stresses like heating, chilling, freezing, drying and pH nanoemulsions are prone to physical instability (McClements et al., 2007); b) limited control over the oxidation and of the functional compounds due to the very thin interfacial layer (McClements et al., 2007); and c) only few surfactants can be used to form the interfacial layer surrounding the oil droplets in the food industry, restricting the ability to create nanoemulsions with different release characteristics (Dickinson, 2003; Drusch, 2007; McClements et al., 2007).

In order to overcome these limitations, a strategy has been created aiming in the improvement of nanoemulsions properties, and consists in creating an interfacial layer of polyelectrolyte around oil droplets and the layer of emulsifier using a LbL electrostatic deposition technique (Guzey & McClements, 2006; Li et al., 2010b; Li & McClements, 2014; McClements et al., 2007; McClements & Li, 2010).

2.5 The LbL technique applied to build-up multilayers nanoemulsions

The method selected for the development of multilayer nanoemulsions is a crucial step, since it allows achieving to different properties and performances. Properties such as: particle size, surface area, shape, solubility, encapsulation efficiency and the release mechanism will strongly influence the final application of the developed systems (Cerqueira et al., 2014; Ezhilarasi et al., 2013; Rao & Geckeler, 2011). Nanosystems designed for bioactive compounds delivery should possess the following characteristics (Shchukina & Shchukin, 2011):

a) Enhanced solubilization: The decrease in the nanoemulsions size should improve the bioactive compound solubility in water and stability during the gastrointestinal tract;

b) Prolongation of gastric residence time: Higher residence times allow better dissolution of bioactive compounds at absorption sites, improving the absorption;

c) Controlled release of the bioactive compounds;

d) High encapsulation efficiency, absence of cytotoxicity and protection of the bioactive compounds from degradation;

e) Bioavailability of the lipophilic bioactive compounds; enhancing the stimulation of the intestinal lymphatic transport pathway;

f) Selective transport of the bioactive compounds;

g) Versatility to allow the delivery of both hydrophilic and lipophilic bioactive compounds;

h) Economically affordable when cost to benefit ratio is considered.

Nevertheless, so far nanoemulsions do not meet all the above-mentioned requirements and are mostly monofunctional, lacking versatility and multifunctionality (Shchukina & Shchukin, 2011). One of the most promising techniques to accomplish additional functionalities to the nanoemulsions is change their surface properties through the LbL electrostatic deposition technique (Cerqueira et al., 2014; Cerqueira et al., 2013; Shchukina & Shchukin, 2011).

The LbL allows obtaining multilayer nanoemulsions with well-defined chemical and structural properties, offering a precise control over thickness and morphology (Cui et al., 2014; Mora-Huertas et al., 2010). Offering the possibility of tailoring different functionalities, through the encapsulation of both hydrophilic and lipophilic bioactive compounds inside the nanoemulsions and in the shell, offering controlled release of the encapsulated bioactive compounds (Shchukina & Shchukin, 2011).

2.5.1 LbL electrostatic deposition technique

LbL is frequently viewed as a surface engineering technique aiming to modify the properties of interfaces, maintaining the properties of the bulk system (Costa et al., in press). Decher and co-workers firstly described LbL in the 1990s, where a protocol for development of ultrathin multilayer films on a solid surface was implemented (Decher, 1997; Decher et al., 1992). Donath et al (1998) and Sukhorukov et al (1998) applied the LbL technique into colloidal templates, transferring this technique from planar films to multilayer capsules (del Mercato et al., 2014; Donath et al., 1998; Mora-Huertas et al., 2010; Sukhorukov et al., 1998).

Briefly, LbL technique consists in the deposition of polyelectrolytes on charged colloidal templates due to strong electrostatic attraction between the colloidal surface and the charged polyelectrolyte. An oppositely charged polyelectrolyte is added to the solution, adsorbing to the colloidal template surface producing a layer of polyelectrolyte in the colloidal template, leading to the formation of the “first layer” by electrostatic deposition. The adsorption of the following layer is

achieved by the simple addition of an oppositely charged polyelectrolyte, promoting the “second layer” adsorption on top of the first layer of polyelectrolytes. This procedure can be repeated to form multilayer nanoemulsions coated by interfaces containing three or more layers of polyelectrolytes. The number of layers will be defined by the final application of these systems (Cerqueira et al., 2014; Martins et al., 2015; Mora-Huertas et al., 2010).

However, between new layers formed around the nanoemulsions, it is frequently necessary to assure that little or no free polyelectrolyte is present in the solution. The presence of free polyelectrolyte will interact with the new appositely charged polyelectrolytes off the following solution, being necessary to remove any excess of polyelectrolyte, in order to avoid interferences with the multilayer formation around the nanoemulsions, which would be difficult to separate from the nanoemulsions (Guzey & McClements, 2006; Szczepanowicz et al., in press). Due this, a number of strategies were developed in order to overcome particles aggregation (Cui et al., 2014; Guzey & McClements, 2006; Mora-Huertas et al., 2010).

a) Centrifugation method: In the presence of excess of polyelectrolyte (non-adsorbed) it is necessary to centrifuge the solution in order to separate the free polyelectrolytes from the coated nanoemulsions. Nonetheless, this procedure requires multiple centrifugation and washing steps, being time-consuming, labor-intensive and expensive. Additionally, centrifugation can promote particle aggregation;

b) Filtration method: The excess of free polyelectrolyte is removed from the nanoemulsions by membrane filtration, which allows the passage of the excess polyelectrolytes, due a pressure differential that forces the non-adsorbed polyelectrolyte through the filter but not the nanoemulsions. In order to avoid close proximity between nanoemulsions, a buffer solution can be added, keeping the volume of the system constant. This method allows a large quantity of multilayer nanoemulsions to be produce in an automated way. Also, it is not necessary to have density differences between nanoemulsions and polyelectrolyte solution. Nonetheless, the

appropriate selection of the filter material is crucial, in order to prevent polyelectrolyte adsorption to the filter and to avoid filter fouling, that leads to filter obstruction. Dialysis membranes can be used as an alternative, however this requires long time and a large amount of buffer solutions.

c) Electrophoretic method: This approach allows a continuous LbL process, since nanoemulsions remain suspend, and lowers their tendency to agglomerate. In this method an agarose hydrogel is used to suspend the nanoemulsions and layer deposition is achieved by electrophoresesis of the polyelectrolytes through the agarose gel. Despite this approach allowing a diverse size range of nanoemulsions to be multilayered, the success of this approach relies in mobile materials in electroosmotic flow. Also in order to recover the multilayer nanoemulsions it is necessary to heat and centrifuge the agarose gel;

d) Saturation method: In this method is possible to completely coat nanoemulsions using precise concentrations of polyelectrolyte, without the need of centrifugation. For each different nanoemulsion the saturation concentration needs to be determined empirically by monitoring changes in the *Zp* measurements after mixing with the polyelectrolyte. The addition of the optimal concentration of polyelectrolyte should be carefully added (drop by drop) in order to prevent bridging flocculation and to avoid depletion flocculation. The optimum concentration will usually correspond to the *Zp* value of the polyelectrolyte in solution. Bridging flocculation happens if the polyelectrolyte adsorbs to the surface of more than one particle, linking the nanoemulsions together. Depletion flocculation will occur if the free polyelectrolyte concentration in the continuous phase is high enough to generates an attractive osmotic force, strong enough to overcome the repulsive forces. The osmotic forces will remove the polyelectrolytes from the nanoemulsions surfaces. Nevertheless, this method leads to systematic dilution of the nanoemulsions at each step of layer adsorption.

As stated above usually the development of multilayer nanoemulsions is confirmed through the measurements of the *Zp*, after each polyelectrolyte adsorption, resulting in a saw like profile (Szczepanowicz et al., in press; Szczepanowicz et al., 2010a). Alternatively, fluorescently labeled polyelectrolytes spectroscopic or spectrofluorimetric, confocal or Fourier transform infrared spectroscopy can be used to confirm the success of the layer deposition through LbL electrostatic technique (Berth et al., 2002; Caruso et al., 1998; Szczepanowicz et al., in press; Szczepanowicz et al., 2010b).

2.5.2 Factors effecting properties of layers

Factors such as pH and ionic strength significantly influence the amount of polyelectrolytes adsorbed in each layer, due conformation variations. Also salts are able to rearrange the conformation of the polyelectrolytes, shielding the electrostatic repulsion within the polyelectrolytes chains (del Mercato et al., 2014).

a) pH – One of the most essential factors responsible for the formation and properties of multilayer nanoemulsions is the solution pH, either during and after formation of the interface. For an appropriate LbL technique the pH of the solution should be properly selected in order to have sufficiently high opposite charges between the nanoemulsions surface and the adsorbing polyelectrolyte. Therefore the order of the charge signal at the surface of the nanoemulsions depends on the type and concentration of molecules attached to the surface, influenced by the solution conditions (Ai et al., 2003; Guzey & McClements, 2006; Israelachvili, 2011). It is often observed a critical pH where adsorption first occurs; this depends of the magnitude and sign of the charges on the nanoemulsions surface and polyelectrolyte. It is important to refer that, a polyelectrolyte is able to adsorb to nanoemulsions with the same charge, under special conditions, such as the presence of oppositely charged patches in the nanoemulsions surface (Gu et al., 2005; Guzey & McClements, 2006). After multilayer nanoemulsions formation, small variations in the pH may adjust the properties of the polyelectrolyte multilayer interface that surrounds the nanoemulsions. These variations

can change the electrostatic interactions between nanoemulsions surface and the adsorbed polyelectrolyte, between adsorbed polyelectrolytes in different layers or even between adsorbed and non-adsorbed polyelectrolytes. These changes in pH can modify the thickness, packing and integrity of the new interface (Guzey & McClements, 2006).

b) Salt – The presence of salt during the construction of polyelectrolyte multilayers may affect the composition, structure and thickness of the polyelectrolyte layers, since the ionic strength of the solution will determine the strength of intra- and inter-molecular electrostatic interactions (Decher et al., 1992; Guzey & McClements, 2006). An increase in the ionic strength of the solution decreases the magnitude of the electrostatic interactions between polyelectrolytes and nanoemulsions, due the accumulation of counter-ions surrounding the surface, being this referred as electrostatic screening (Guzey & McClements, 2006; McClements, 2005). In the presence of salt, due to weaker intra-molecular repulsion, the polyelectrolytes layers are often thicker, since they have a more compact chain conformation. Increasing the ionic strength weakens the attractive interactions between polyelectrolyte molecules in different layers thereby causing an increase of interfacial porosity. In the absence of salt, polyelectrolytes should form thin layers with flat chains against the colloidal template surface. This behavior is related with the strong intramolecular electrostatic repulsion of the polyelectrolyte molecules which are in a highly extended conformation (Guzey & McClements, 2006).

c) Polyelectrolyte characteristics – The nature of the polyelectrolytes used has a major importance in the formation, stability and properties of the multilayer nanoemulsions. Characteristics such as chain length, rigidity, degree of branching and electrical charge influences the ability of polyelectrolytes to adsorb to nanoemulsions surfaces, reflecting in different thicknesses, structures, porosities and environmental triggers sensitivity (Guzey & McClements, 2006). Characteristics like flexibility and packing will depend on the relative position of the polyelectrolytes

within the multilayer, since polyelectrolytes within inner layers are prone to be packed and their motion is restricted by those in the outside layer (Guzey & McClements, 2006). Environmental triggers such as pH, ionic strength and temperature lead to changes in the electrical charge, conformation and hydrophobicity, that influences the amount of polyelectrolyte adsorbed to the nanoemulsions surface. Therefore, due proper selection of polyelectrolytes is possible to create new interfaces with different environmental responses and may lead to different electrical characteristics of the trapped polyelectrolyte. Due their local electrostatic environment a shift in the pK_a of the ionizable groups of the polyelectrolytes from the value of the polyelectrolyte in an aqueous solution can occur (Guzey & McClements, 2006). Finally, the amount of polyelectrolyte should be high enough to saturate the surface of the nanoemulsions, reversing the charge of the nanoemulsions (or previous layers), in order to create a strong electrostatic repulsion between the multilayer nanoemulsions. This amount will be influenced by the molecular characteristics of the polyelectrolyte, such as chain length, conformation, flexibility and electrical charge (Guzey & McClements, 2006).

As explained above, multilayer nanoemulsions can be developed using the LbL electrostatic deposition technique through sequential adsorption of oppositely charged polyelectrolytes surrounding the surface of nanoemulsions (del Mercato et al., 2014). The proper development of nanoemulsions and the choice of polyelectrolytes are crucial factors for the development of multilayer nanoemulsions with distinct properties. The nanoemulsions will determine the size and shape, while the polyelectrolyte will determine the properties of the multilayer nanoemulsions (Cui et al., 2014).

Adamczak and co-workers (2014) developed multilayer nanoemulsions using the membrane emulsification method to prepare nanoemulsions. Briefly, sodium bis (2−ethyl hexyl) sulfosuccinate (AOT) was solubilized in squalene and then pumped through a hydrophilic ceramic membrane into 50 ml of poly(allyaminehydrochloride) polyelectrolytes. The multilayer nanoemulsions formation was achieved by the LbL technique, using the saturation method

described above. The nanoemulsions stabilized by AOT and poly(allyaminehydrochloride) were then added to the polysodium 4 – styrenesulfonate polyelectrolyte solution, while mixing at 300 rpm. This procedure was repeated until the desired number of layers was created (10 layers), without an intermediate rinsing step (Adamczak et al., 2014). Adamczak and co-workers (2014) successfully developed multilayer nanoemulsions with 120 nm of diameter using squalene nanoemulsions with 80 nm of diameter as templates. The advantage of using nanoemulsions by membrane emulsification consists in its higher encapsulation efficiency and due the fact that using a membrane unit it is possible to work in a continuous mode, producing higher volumes of multilayer nanoemulsions. Szczepanowicz and co-workers (2014) successfully developed multilayer nanoemulsions, using an emulsion system with silica. A fluorescent dye (coumarine-6 as lipophilic substance) was solubilized in the oil phase (chloroform) containing dimethyloctadecyl[3-(trimethoxysilyl) propyl]ammonium chloride a surface active silane that can be utilized as emulsifier and emulsion stabilizer (Szczepanowicz et al., 2014). The nanoemulsions were prepared by continuous mixing during one night and due hydrolysis and condensation of dimethyloctadecyl[3-(trimethoxysilyl) propyl]ammonium chloride a positively charged interface was developed, achieving a droplet diameter of 70 nm. The multilayer nanoemulsions were then created by sequential adsorption of polyelectrolytes using the saturation method. Different pairs of polycation/polyanion were chosen to form the multilayer nanocapsules. The adsorption of 5 bilayers of alginate/poly (diallyldimethylammoniumchloride resulted in an increase of the average diameter, from 70 to 122 nm; when 5 bilayers of poly (styre-nesulfonate)/poly (allylamine)hydrochloride was used, the same result was achieved (122 nm); when 5 bilayers of poly (styre-nesulfonate)/poly (diallyldimethylammoniumchloride were used, a slighter average diameter was achieved, 106 nm (Szczepanowicz et al., 2014). These authors developed multilayer nanoemulsions with tunable thickness and permeability based in different polyelectrolytes. Bazylinska and co-workers (2011), developed multilayer nanoemulsions using nanoemulsion templates prepared by the conjugation of spontaneous emulsification followed by ultrasonication, achieving a template with less then 100 nm of diameter (Bazylinska et al., 2011).

Nanoemulsion templates were then surrounded by LbL adsorption of poly (sodium 4-styrenesulfonate) and poly(diallyldimethylammonium chloride) using the saturation method, in order to develop multilayer nanoemulsions with less than 200 nm of diameter (Bazylinska et al., 2011). In this study, the authors verified that one bilayer delayed the compound release in four times, whereas five bilayers caused a delay in compounds released of 285 times. The developed multilayer nanoemulsions can provide an efficient system for the encapsulation of lipophilic bioactive compounds while being an effective barrier for the compound release (Bazylinska et al., 2011). This study showed that varying the number of polyelectrolyte layers can tune the release rate of the bioactive compounds (Bazylinska et al., 2011). Li and co-workers (2010) have shown that is possible to prepare nanoemulsions multilayer by the LbL technique. In their work, a globular protein (β-lactoglobulin) was used to form the inner layer of the multilayer (1st layer), used a cationic polysaccharide (chitosan) as an intermediate layer (2nd layer) and as an outer layer (3rd layer) they used an anionic polysaccharide (pectin or alginate). The nanoemulsion was unstable and droplet aggregation happens at intermediary pH values due the low net charge. The secondary layer nanoemulsions, were stable from pH 3 to 6, however were highly unstable at higher pH values. Nanoemulsions that had an outer layer (alginate or pectin) were unstable to droplet aggregation at pH 3, but stable at higher pH values. Li and co-workers (2010) study states that the addition of polysaccharides trough the LbL technique can improve the physical stability of the nanoemulsions, as well reducing the rate of lipid digestion by restricting the access of lipase to the emulsified triacylglycerol's (Li et al., 2010b). Also trough LbL technique, Madrigal-Carballo and co-workers (2010) developed a novel delivery system for ellagic acid by deposition of biopolymers (chitosan and dextran sulphate) onto soybean lecithin liposomes. The study performed in this work revealed that the biopolymers' addition there is a better thermal and pH stability of the system, as well as better release properties (Madrigal-Carballo et al., 2010). Preetz and co-workers (2010) developed through LbL a nanocapsule system with a nanoemulsion as a core. It was used as emulsifier an OSA starch and as polysaccharides chitosan and k-carrageenan. The addition of the polysaccharides promotes a higher stiffness of the wall with the increasing number of shell layers, this was observed using

atomic force microscopic. A stiffer capsule might be advantageous during storage due to the better mechanical resistance and the strong barrier. Therefore nanocapsules developed by LbL might present a prolonged release of the bioactive compounds in the system in contrast to nanoemulsions (Preetz et al., 2010). Aoki and co-workers (2005) have used a three-step process based on LbL technique to produce multilayer nanoemulsions. Nanoemulsion was prepared using high-pressure homogenization, stabilized by sodium dodecyl sulphate. Then, secondary layer was formed by chitosan and as a tertiary layer pectin was used. Aoki's work shows that nanoemulsion stability could be improved by coating the nanoemulsion droplets with two or more layers. Nanoemulsions with a third layer had a good stability against aggregation and creaming at high temperatures (90 ºC), freeze-thaw cycles (-20 ºC for 22 h/30 ºC for 2 h), high salt concentrations (NaCl 500 mM) and a wide range of pH values (pH 3 – 8). The improve stability showed by this multilayer nanoemulsion can be attributed to the increase of the repulsive interactions between the droplets (e.g. electrostatic and steric) and/or the increase of resistance of the membrane against rupture (Surh et al., 2005). Pongsawatmanit and co-workers (2006) improved the stability of a nanoemulsion trough the adsorption of sodium alginate to the emulsifier (β-lactoglobulin). The addition of sodium alginate to the nanoemulsions improved their stability at pH 4 and 5 against flocculation (lower creaming index) and against environmental stresses (pH, ionic strength and temperature), possibly because the alginate molecules adsorbed to the nanoemulsions surfaces and increase electrostatic and steric repulsion between them (Pongsawatmanit et al., 2006).

The formation of the multilayers on the nanoemulsions is schematically shown in Figure 2.2.

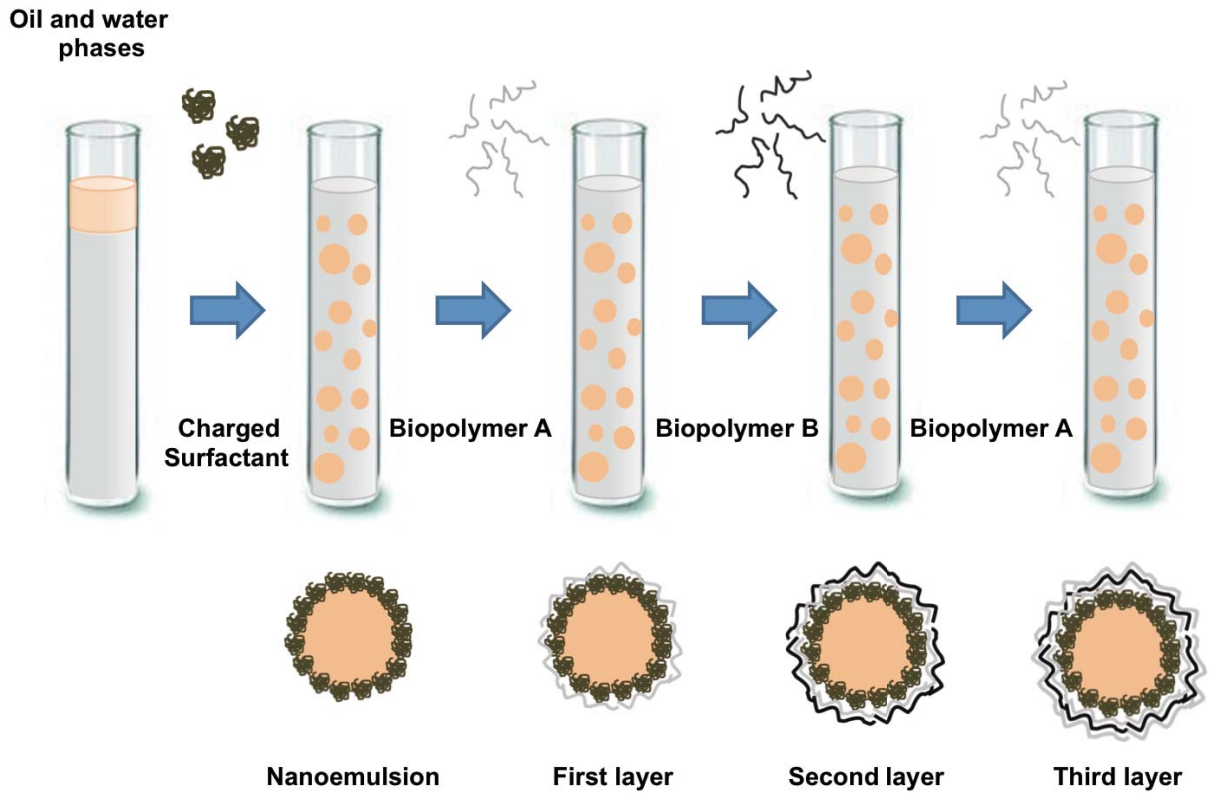

Figure 2.2 – Representative scheme of multilayer nanoemulsion after LbL deposition onto nanoemulsion templates.

2.6 Advantages and limitations of multilayers nanoemulsions

A benefit of using multilayers nanoemulsions as delivery systems is that they can be fabricated based on natural food grade components (i.e. lipids, proteins, polysaccharides) using simple processing operations (homogenization, mixing), with possibility of being tailored made. The physical stability to environmental stresses can be improved by controlling the composition and properties of the interfacial layers (Aoki et al., 2005; Costa et al., in press; Decher, 2003; Grigoriev & Miller, 2009; Guzey & McClements, 2006). The chemical stability of the bioactive compounds is improved controlling the thickness and charge of the interfacial layer, which minimizes the interaction between the bioactive compounds and transition metal ions (Klinkesorn et al., 2005; McClements & Decker, 2000; McClements et al., 2007). LbL allows a precise control over shell properties, such as thickness and morphology (Cui et al., 2014). Due to the ability to control the thickness and properties of the interfacial layer by varying the number of the adsorbed layers is possible to build delivery systems with a

better control of the release rate (Costa et al., in press; Decher, 2003). This delivery system can be applied to design novel functional food as well as applied to food products (Li et al., 2010b; McClements, 2010; McClements et al., 2007; McClements & Li, 2010). The multilayer structure of these nanoemulsions enables the combination of different properties in one system, mostly governed by the material used. These systems can be developed to be responsive to different external stimuli and they can be loaded with bioactive compounds of different polarities (Costa et al., in press; Cui et al., 2014).

They also can be designed to control the digestion and absorption of bioactive compounds within the gastrointestinal tract. Can be used to control the release of bioactive compounds at specific locations of the gastrointestinal tract (i.e. mouth, stomach, small intestine or colon), due to the ability to trigger the release in response of specific environmental conditions (i.e. pH and ionic strength) (Li et al., 2010b; McClements, 2010; McClements et al., 2007; McClements & Li, 2010).

The LbL technique offers a promising way to improve the stability of the actual delivery systems. Nevertheless, the optimization of this technique depends on the preparation conditions (bioactive compound concentration, pH, ionic strength, temperature), the choice of appropriate emulsifiers and polyelectrolyte and the combination of the two, as well the physicochemical knowledge of the principles involved and depending the development method could require the removal of the core template, leaving traces of solvent (Guzey & McClements, 2006; Li et al., 2010b; McClements, 2010; McClements et al., 2007; McClements & Li, 2010; Szczepanowicz et al., in press). It implicates long construction times, with the assembly of a single layer taking typically only few minutes which is dependent on the nature of the polyelectrolyte used (Costa et al., in press). The formation of stable multilayer nanoemulsions requires meticulous control of the system construction and composition in order to avoid droplet aggregation (Guzey & McClements, 2006). Another limitation is the fact that LbL method is based in electrostatic interactions, and they can be disrupted by changes in the pH and ionic strengths (McClements, 2010; McClements & Li, 2010). Despite the simple method for producing multilayer nanoemulsions, additional processing steps are needed over the nanoemulsions formation and

at the present it is only possible to produce diluted multilayer nanoemulsions (McClements et al., 2007). One strategy to overcome the dilution is adding an evaporation step in order to concentrate the multilayers nanoemulsions; nevertheless this additional step will increase the costs of the production. Another strategy to overcome the dilution effect is the use of a nano spray dryer for the construction of multilayer nanoemulsions; this possible strategy will be able to concentrate multilayer nanoemulsions while enhancing their stability, in a matter of seconds (Chan & Kwok, 2011; del Mercato et al., 2014; Li et al., 2010a; Maher et al., 2014). Nevertheless, there is a limited number of polyelectrolytes available for the use of spray dryer, since the polyelectrolytes should be soluble in solvents used in the food industry and able to seal and hold the bioactive compounds within the nanosystem during the process (Desai & Jin Park, 2005; Fang & Bhandari, 2010). From a scale-up perspective, despite LbL devices did not receive significant attention, some automated devices have been proposed but only for the production of multilayer films, namely dipping and sputtering machines (Costa et al., in press). Nonetheless, efforts in developing devices able to produce multilayer nanoemulsions in an automated way have been reported (Costa et al., in press; Kantak et al., 2011; Priest et al., 2008).

2.7 Techniques for the identification and characterization of nanoemulsions

Detection, identification and characterization of lipid-based nanosystems are essential for the understanding of the benefits as well as the potential toxicity of these systems (Luykx et al., 2008). In this section, the analytical techniques that can be used for the identification and characterization of nanoemulsions are described. The analytical approaches have been subdivided into three groups: separation techniques, characterization techniques and imaging techniques. The principles of the techniques together with their advantages and drawbacks are reported.

2.7.1 Separation techniques

Some analytical techniques can be used for *in situ* identification of nanoemulsions, however in most cases it is not possible to detect them in the food matrices. Therefore, separation techniques are necessary to isolate the nanoemulsions from food prior to their characterization. This section describes the most important separation techniques for isolation of nanoemulsions.

Chromatography

Because size and/or charge are typical characteristics of nanoemulsions, (SEC) and/or ion exchange chromatography (IEC) are the most suitable types of liquid chromatography for the separation of nanoemulsions from the food matrix. In the case of SEC, compounds are separated on the basis of size; larger molecules elute faster than smaller ones. However, the shape of the compound could affect elution. In the case of IEC, compounds are separated on the basis of charge; low-charged compounds elute faster than highly charged ones (Luykx et al., 2005; Luykx et al., 2008).

High-Performance Liquid Chromatography (HPLC) is a form of liquid chromatography to separate, analyse, and quantify compounds that are dissolved in solution. Compounds are separated by injecting the sample mixture (carried by mobile phase) onto a column. Depending on the type of stationary phase, compounds can be separated based on their charge (weak/strong cation or anion exchange chromatography), molecular mass (size exclusion chromatography), hydrophobicity/polarity (reversed-phase HPLC, hydrophobic interaction chromatography), and specific characteristics (affinity chromatography). The most common detectors for HPLC are ultraviolet-visible (UV-Vis) light absorbance, fluorescence, electrochemical, and diffraction detectors (Luykx et al., 2008). HPLC has been used in food analysis for measuring numerous compounds, for example, carbohydrates, vitamins, additives, mycotoxins, amino acids, proteins, triglycerides in fats and oils, lipids, chiral compounds, and pigments. It is a straightforward, robust, and reproducible technique. Sensitive selective detectors are available for HPLC, and their selection depends mostly on the compound to be analysed (Luykx et

al., 2008). HPLC was also used to quantify bioactive compounds encapsulated in the nanoemulsions, some examples are: β-carotene (Tan & Nakajima, 2005a; Tan & Nakajima, 2005b); (Yin et al., 2009), α-tocopherol (Cheong et al., 2008) and thalidomide (Araújo et al., 2011).

Field Flow Fractionation

Field Flow Fractionation (FFF) is a flow-assisted technique for the separation of analytes, from macromolecules, such as proteins (nanometer range), to micrometer-sized particles, such as whole cells. In a one single run, very broad ranges of molecular sizes can be separated (Luykx et al., 2008). FFF can also separate particles due to their Stokes radius (Dulog & Schauer, 1996; Jores et al., 2004). In this technique, smaller particles are transported faster and elute earlier if a parabolic flow is used; if a cross flow is used with particles of the same volume and different shape, the isometric particles will be eluted first than the asymmetric particles (Jores et al., 2004). FFF has advantages over other separation techniques such as higher biocompatibility, reduction of sample carry-over, and simple sterility issues. The separation times typically range from a few minutes up to 30 min. Despite these advantages, the FFF has the disadvantage of being easily overloaded by higher concentrations of the compounds. In order to overcome this, dilutions should be made. Nevertheless, the detection of trace amounts of compounds is limited by the sensitivity of an appropriate detector system (Luykx et al., 2008).

2.7.2 Physical characterization techniques

This section describes the techniques that are used to characterize nanoemulsions from a physical perspective (e.g. size, size distribution, zeta potential and crystallinity of the nanoemulsions).

Dynamic Light Scattering

Dynamic Light Scattering (DLS) also known as Photon Correlation Spectroscopy or Quasi-Elastic Light Scattering is a technique used for rapid determination of the size distribution profile of small particles in suspensions or

polymers in solution. DLS measures Brownian motion and relates this to the size of the particles through Stokes-Einstein equation. Through the illumination of the particles with a laser and analysing the intensity fluctuations in the scattered light, DLS allows calculating the size of the particles. DLS provides a fast and adequate evaluation of the size of nanoemulsions and is often used to evaluate the size distribution of nanosystems, as well their size stability through storage (Araújo et al., 2011; Preetz et al., 2010; Silva et al., 2011a).

Zeta potential

Zp is a scientific term for electrokinetic potential in colloidal systems (Mills et al., 1993). In colloidal chemistry literature, *Zp* is the potential difference between the dispersion medium and the stationary layer of fluid attached to the dispersed particle. A value of 30 mV (positive or negative) can be taken as the arbitrary value that separates low-charged surfaces from highly-charged surfaces (Preetz et al., 2010). *Zp* value can be related to the stability of colloidal dispersions, indicating the degree of repulsion between adjacent, similarly charged particles in dispersion. For molecules and particles that are small enough, a high *Zp* will confer stability, i.e., the solution or dispersion will resist to aggregation. When the potential is low, attraction exceeds repulsion and the dispersion will break and flocculate. So, colloids with high *Zp* (negative or positive) are electrically stabilized while colloids with low *Zp* tend to coagulate or flocculate. Briefly, *Zp* values from 0 to ± 30 mV indicate instability, while *Zp* values higher than ± 30 mV indicate stability (ASTM, 1985). The *Zp* of nano-scaled particles is influenced by many factors, such as the source of particles and the treatment with different surfactants, electrolyte concentration (ionic strength), particle morphology and size, pH of the solution and state of hydration (Simunkova et al., 2009). For instance, Araújo et al. (2011), Gao et al. (2011), and Preetz et al. (2010), evaluated the *Zp* of nanoemulsions and multilayer nanoemulsions: the information given by the *Zp* allows stating that the nanoemulsions with highly-charged surfaces are stable and will resist to droplet aggregation.

Differential Scanning Calorimetry

Differential Scanning Calorimetry (DSC) is a thermo-analytical technique in which the difference in the amount of heat required to increase the temperature of a sample and reference is measured as a function of temperature. Both the sample and reference are maintained at nearly the same temperature throughout the experiment. Generally, the temperature program for a DSC analysis is designed such that the sample holder temperature increases linearly as a function of time. The reference sample should have a well-defined heat capacity over the range of temperatures to be scanned (Salmah et al., 2008; Venturini et al., 2011). DSC can be used to detect phase transitions including the melting of crystalline regions, and to analyse the proportion of solid fat or the proportion of ice crystals in emulsions (Thanasukarn et al., 2004). Thanasukarn and co-workers (2004) showed that fat crystallization affects the emulsion stability depending on the emulsifier used, showing that the thermal decomposition follows the melting of the drug encapsulated (Thanasukarn et al., 2004). Usón et al. (2004) have shown that DSC can be used to determine the crystallisation temperature of a mixture of surfactants.

Fourier Transform Infrared

Fourier Transform Infrared (FTIR) spectroscopy is based in an infrared radiation that passes through a sample where it is mostly absorbed by the sample and some of it is transmitted. The resulting spectrum represents the molecular absorption and transmission, creating a molecular fingerprint of the sample. Each sample fingerprint presents its characteristic absorption peaks that correspond to the frequencies of vibrations between the bonds of the atoms of the material. Because each different material is a unique combination of atoms, no two compounds produce the exact same infrared spectrum (Nicolet, 2001). Therefore, infrared spectroscopy can result in a positive identification of different materials. In addition, the size of the peaks in the spectrum is a direct indication of the amount of material present in the sample. The major advantages of FTIR are the fact that it can determine the amount of components in a mixture, it can determine the quality or consistency of a sample, the small time required for analyses (because all frequencies are

measured simultaneously), the fact that it is a very sensitive method, relatively simple to work with and internally calibration. These advantages make FTIR measurements extremely accurate and reproducible (Nicolet, 2001). Araújo and co-workers (2011) reported the encapsulation of thalidomide in nanoemulsions by spontaneous emulsification, where the crystallization process was studied through FTIR analysis of the crystals; when present in a nanoemulsion, these crystals were found to be in a different polymorphic form than that found before in the nanoemulsions preparation (Araújo et al., 2011). Lawrie and co-workers (2007) studied the interactions between alginate and chitosan in the alginate-chitosan polyelectrolyte complexes in the form of a film trough FTIR (Lawrie et al., 2007). Also, Silva and co-workers 2015 showed the deposition of chitosan and alginate onto nanoemulsions, developing multilayer nanoemulsions (Silva et al., 2015b).

Nuclear Magnetic Resonance

Nuclear Magnetic Resonance (NMR) is a powerful and complex analytical tool that allows the study of compounds in either liquid or solid state and serves equally in quantitative as in structural analysis. It is very efficient in gathering structural information regarding molecular compounds. It can be used as a complementary technique to methods of optical spectroscopy and mass spectrometry leading to precise information concerning the structural formula, stereochemistry, information about the preferred conformation of molecules; it may also be used to identify the compound in study (Rouessac F. & Rouessac, 2007). The application of NMR to nanoemulsions characterization has been only slightly exploited. Jenning et al. (2000) successfully incorporated medium chain triglycerides oil in a matrix of a solid long chain glyceride (glyceryl behenate) and the structure of the liquid lipids inside the matrix of solid lipid nanoparticles was characterized through ^{1}H-NMR. Information about the mobility, the arrangement and the environment of the oil molecules (Jenning et al., 2000b) was obtained. Casadei et al (2006), determined the amount of unloaded ibuprofen and the entrapment efficiency of this compound within solid lipid particles through ^{1}H-NMR analysis (Casadei et al., 2006).

X-Ray Diffraction

X-Ray Diffraction (XRD) techniques are a family of non-destructive analytical techniques that reveals information about the crystallographic structure, chemical composition and physical properties of materials. XRD is based on observing the scattered intensity of an X-ray beam hitting a sample as a function of incident and scattered angles, polarization and wavelength or energy (Azároff et al., 1974). XRD is mostly used for the identification of crystalline compounds by their diffraction pattern. Nevertheless, it covers a lot of specific uses such as: identification of single phase materials, determination of the crystal structure, identification and structural analysis of samples, recognition of amorphous materials in partially crystalline mixtures, determination of crystallite size from analysis of peak broadening, determination of crystallite shape from the study of peak symmetry and the study of thermal expansion in crystal structures using *in-situ* heating stage equipment (Connolly, 2007). Mulik (2010) showed that the diffraction pattern of curcumin is significantly different from the diffraction pattern of solid lipid nanoparticles loaded with curcumin. The diffraction pattern of loaded solid lipid nanoparticles indicates that curcumin is entrapped in the lipid core of the nanoparticles, while the diffraction pattern of the unloaded solid lipid nanoparticle indicates that the addition of curcumin has not changed the nature of the solid lipid nanoparticles (Mulik et al., 2010).

Small-Angle X-ray Scattering

Small-Angle X-ray Scattering (SAXS) is a technique for the study of structural features of colloidal size particles where the elastic scattering of X-rays by a sample that has inhomogeneities in the nanometric range, is recorded at very low angles (typically 0.1 – 10º). This angular range can give information about: the shape and size of macromolecules, characteristic distances of partially ordered materials and pore sizes. SAXS is capable to give structural information on macromolecules between 5 and 25 nm and on repeating distances in partially ordered systems of up to 150 nm (Glatter & Kratky, 1982). Through the scattering patterns information on the structure, shape and size of macromolecules can be achieved. This method is non-destructive and requires a minimum sample preparation. One of the disadvantages of SAXS data

analysis is that only a one-dimension scattering pattern can be obtained (Luykx et al., 2008). Jennings et al. studied the influence of the oily constituent of their particles on the subcell parameters and long spacings of solid Compritol nanocyrstals through SAXS, which was used to confirm the polymorphism behavior found through DSC measurements (Jenning et al., 2000a). Also, through SAXS, Venturini and co-workers (2011) showed that sorbitan monostearate is interacting with the oily phase, in the core of the solid-lipid-nanoparticle (Venturini et al., 2011).

Quartz Crystal Microbalance

Quartz Crystal Microbalance (QCM) is based on the piezoelectric effect, where the mass is deposited onto the crystal surface, and the piezoelectric properties of the quartz crystal change its oscillation frequency (Marx, 2003). It can detect monolayer surface coverage by small molecules or polymer films, providing information about the energy dissipating properties. QCM can characterize surface film mass, thickness, viscoelasticity, hydrophobicity, roughness, energy dissipative or viscoelastic behaviour (Marx, 2003; Pinheiro et al., 2011a; Pinheiro et al., 2011b), allowing a direct observation of the adsorption process in situ (Channasanon et al., 2007; Indest et al., 2009). Channasanon and co-workers (2007) used QCM as a tool to follow the assembly process of chitosan-poly(sodium styrenesulfonate) nanolaminated films by monitoring the frequency change as a function of the number of depositions. Indest and co-workers (2009) observed *in situ* the adsorption behaviour of fucoidan to a chitosan layer, using the same process. Recently, Pinheiro and co-workers (2011) confirmed trough QCM measurements that the alternating deposition of k-carrageenan and chitosan resulted in the formation of a stable multilayer structure.

2.7.3 Imaging techniques

Microscopy can be used as a direct imaging technique for nanoemulsions; nevertheless the type of microscopy used depends on the kind of matrix to be analyzed. This technique enables information regarding the size, shape, and

aggregation state of the nanoemulsions. Some of the imaging methods that are used for the characterization of nanoemulsions are presented below.

Transmission Electron Microscopy

Transmission Electron Microscopy (TEM) is a technique capable of a resolution on the order of the 0.2 nm (Luykx et al., 2008; Wang, 2000). It is widely used in the study of materials for science/metallurgy and biological sciences; in both cases the samples must be very thin and able to withstand the high vacuum present inside the instrument. Nevertheless, this technique has some drawbacks (Luykx et al., 2008; Wang, 2000). Some materials require extensive sample preparation to produce a sample thin enough to be electron transparent, which makes TEM analysis a relatively time-consuming process with a low throughput of samples. The structure of the sample may be changed during the preparation process; the field of view is relatively small and the electron beam may damage the sample. Bouchemal and co-workers (2004) studied the morphology and structure of the nanoemulsions using TEM; the combination of bright field imaging at increasing magnification and of diffraction modes were used to reveal the form and size of the emulsions and to determine the amorphous or crystalline character of the components. They direct observation enabled the possibility to perform selected area electron diffraction in order to check the crystallinity of the emulsion core components (Bouchemal et al., 2004). Chu et al. (2007) observed the microstructure and the particle-size distribution in their nanoemulsions, concluding that β-carotene particles exhibited spherical morphology with a mean diameter of 20 nm, confirming the results obtained by DLS (Chu et al., 2007b).

Scanning Electron Microscopy

Scanning Electron Microscopy (SEM) is capable of producing high-resolution images of a sample surface (Luykx et al., 2008; Reimer, 2000). SEM images have a characteristic three-dimensional appearance and are useful for judging the surface structure. Generally TEM resolution is about an order of magnitude higher than SEM resolution; however, because the SEM image relies on surface processes rather than transmission, it is able to image bulky samples

and has a much greater depth of field and so can produce images that are a good representation of the 3D structure of the sample. In particular, the significantly large depth of field available in SEM allows a large amount of the sample to be in focus at one time. It is also capable to produce high-resolution images at higher magnification. The combination of higher magnification, larger depth of field, greater resolution, and ease of sample observation makes SEM one of the most heavily used methods in research areas today (Luykx et al., 2008). Nevertheless, SEM is also an expensive technique and requires high vacuum and a relatively high sample conductivity (Luykx et al., 2008). The presence of surfactants during nanoemulsions preparation can sometimes inhibit their characterization via SEM due to the formation of a smooth camouflaging coating on the particle surfaces (Luykx et al., 2008). Tan and Nakajima (2005b) observed great differences between coarse and nanodispersed β-carotene samples through SEM. The analysis of coarse crystalline β-carotene showed particles with irregular shapes and sizes ranging from a few μm to more than 10 μm, as opposed to the nanodispersions. SEM particle sizes were confirmed through DLS (Tan & Nakajima, 2005b).

Atomic Force Microscopy

Atomic Force Microscopy (AFM) is a recently developed microscopy technique (Edwards & Baeumner, 2006; Luykx et al., 2008; Ruozi et al., 2005). The high resolution (± 0.1 nm) achieved by AFM has been used to directly view single atoms or molecules that have dimensions of a few nanometers. AFM relies on the raster scanning of a nanometer-sized sharp probe over a sample that has been immobilized onto a carefully selected surface (mica or glass), resulting in a high-resolution three-dimensional profile of the surface under study. AFM has the advantage of imaging almost any type of surface, including polymers, ceramics, composites, glass, and biological samples. AFM allows biomolecules to be imaged not only under physiological conditions but also during biological processes. The advantage of directly observing biomolecular systems in their native environment opens the possibility of analysing their structural and functional properties at the submolecular level. Surface irregularities observed by SEM are absent in AFM inspection. AFM's disadvantages are related with

the analysis of surfaces that are soft, sticky, or have loose particles floating, as the tip is in direct contact with the actual surface and will run into difficulties in those cases. Nevertheless, AFM works on most materials and has been used in a range of applications from biology and chemistry, to electronics. AFM images are complementary to other established techniques. AFM can be used for the structural characterization of e.g. proteins, polysaccharides and liposomes (Luykx et al., 2008; Moraru et al., 2003). Preetz and co-workers (2010) showed the differences between nanoemulsions and multilayer nanoemulsions by studying the shape, morphology and mechanical properties of the emulsion and capsule shell through AFM, and were able to demonstrate that the shell around an oil droplet increases their thickness with increasing amounts of polyelectrolytes.

Confocal Laser Scanning Microscopy

Confocal laser scanning microscopy (CLSM) allows obtaining high-resolution optical images with depth selectivity. The key feature of confocal microscopy is the ability to acquire in-focus images from selected depths, a process known as optical sectioning, allowing three-dimensional reconstructions of topologically complex objects. Being this useful for surface profiling in opaque specimens. In non-opaque specimens, is possible to see interior structures with enhanced quality of image over simple microscopy. Confocal microscopy provides the capacity for direct, non-invasive, serial optical sectioning of intact, thick, living specimens with a minimum of sample preparation as well as a marginal improvement in lateral resolution. Biological samples are often treated with fluorescent dyes to make selected objects visible. However, the actual dye concentrations can be low to minimize their disturbance on biological systems (some instruments can track single fluorescent molecules) (Richert et al., 2003). Using CSLM and fluorescent-labelled (FITC) chitosan Richert et al. (2003) studied the diffusion ability of chitosan and showed that the chitosan-FITC added at the outermost layer of the film diffused through the whole film up to the substrate.

2.8 Nanoemulsions: industrial perspectives and applications in the food market

Nowadays, consumers in the industrialized world are demanding for novel food products that: a) address to specific health benefits, b) have specific bioactive compounds; c) with reduced fat content and d) ingredients that have health sustaining properties. Based on this, researchers seek for new food-grade nanoemulsions, able to be used as an effective delivery systems aiming the encapsulation, protection and release bioactive compounds (McClements & Rao, 2011). A recent report ("Food Encapsulation: A Global Strategic Business Report," Global Industry Analysts, Inc., San Jose, CA) on the food encapsulation market estimated that in 2015 this market would reach to 39 billions U.S. dollars (Global et al., 2010; McClements & Rao, 2011). The same behaviour is expected for the nanotechnology industry, once it is expected that the overall market reach the one trillion U.S. dollars (Neethirajan & Jayas, 2011). Commercial applications of nanoemulsions are one of the emerging fields of nanotechnology applied to food industry. Nanoemulsions can be applied to different types of food products; for instance the German company Aquanova portfolio is divided into two categories: healthy functional compounds with the NovaSol beverages solutions and natural colorants with the NovaSol BCS (AquaNova, 2013a, 2013b). The Portuguese company Improveat, incorporate bioactive compounds (nanoemulsions is one of the ways) in the BioNutriCoat, a nutritional edible coating for foods (Improveat, 2014). The American company Life Enhancement developed the NanoResveratrol, a food supplement that increases the bioavailability of resveratrol (Life Enhancement, 2013). Another example is a fortified oil created by the Israeli company Shemen Industries, the Canola Active Oil, an oil reinforced with phytosterol that can inhibit the transportation of cholesterol from the digestive system into the bloodstream (Shemen Industries, 2013). In Figure 2.3, there are some commercial applications of nanoemulsions already in the food and beverage market.

Despite of nanotechnology already being applied to the food industry, there is still a major gap in the regulatory framework, and most countries are still relying

on existing legislation to regulate nanomaterials (Gruère et al., 2011). Improving the actual legislation framework is a crucial step to prevent consumers' misinformation regarding nanotechnology applied to foods. Such misinformation was the main responsible for the actual suspicions that many consumers have towards genetically modified organisms and their use in foods; a great deal of care is needed to prevent that from happening with nanotechnology. While legislation is still being adapted, other actions may be taken to improve consumers' confidence in foods integrating nanotechnology-based ingredients, such as the guarantee of use of food grade materials for nanosystems production.

Another important aspect to the industry implementation is the cost, the scaling-up of high-energy approaches is still very expensive due the pressures needed to process high volumes. Such costs need to be reduced, either by further technical improvements in the methods or by adoption of simpler methods for nanoemulsion production. As a general recommendation when applied to the food industry, nanotechnology needs to be affordable, simple to use and with readily perceived advantages in order to be a real alternative to the standard methodologies.

- NutraLease beverages (NutraLease, 2011a);
- NovaSol beverages (AquaNova, 2013a);
- SunActive Iron beverage (High Vive, 2013).

- NovaSol BCS (AquaNova, 2013b);
- Colour emulsion (Wild Flavors Inc, 2013)

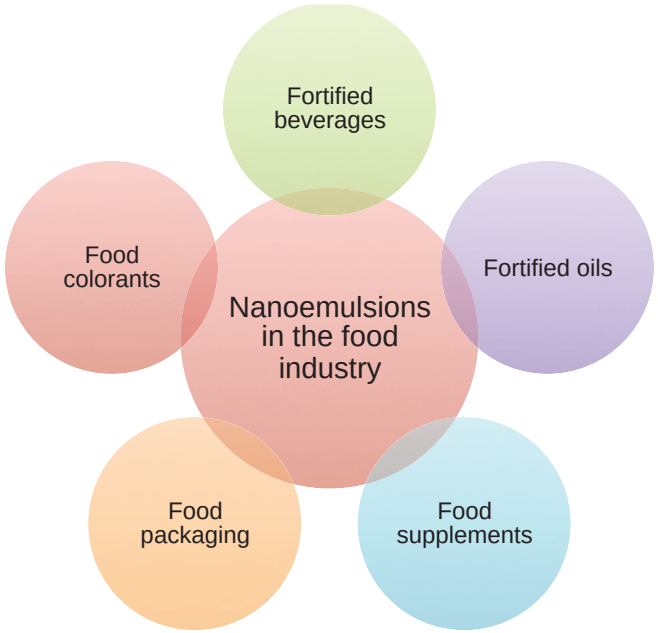

- Canola Active Oil (Shemen Industries,

- BioNutriCoat (Improveat, 2014)

- NanoResveratrol (Life Enhancement, 2013);
- Spray for Life (NanoSinergy, 2013);
- Nutri-Nano^{TM}CoQ-10 3.1x Softgels (Solgar, 2013);

Figure 2.3 – Commercial applications of nanoemulsions and food markets where they were applied.

2.9 Societal challenges in food nanotechnology

Nanotechnology offers a vast number of opportunities to agri-food industry in several aspects and within a broad number of areas. The primary production sector could benefit of new pesticides with improved action, improved efficacy and nutrition of animal feeds, through the use of enriched supplements, smart sensors for animal disease diagnostics or sensors for the detection of pathogenic in waters. Food production sector may improve the detection and control of chemical and microbiological hazards, promoting food safety, sanitisation of equipment; equipment's could be optimised to reduce heat loss, lowering energy costs. Food packaging, one of the utmost operational areas of nanotechnology in the food industry could incorporate antimicrobials to extend shelf life, new active/intelligent packaging could be designed to act as sensors,

alerting for the quality or freshness of the food products, create new food contact materials able to preserve the organoleptic properties of the food products and to protect against microorganism growth. Also the nutritional value of food products could be improved through the use of nanotechnology, that would allow the incorporation of bioactive compounds, such as antioxidants, vitamins, polyphenols, omega-3 fatty acids and more, while increasing the bioavailability of them. Also, individual dietary and health requirements could be prepared, allowing the consumers to safely choose the one of interest. The agri-food companies could trigger new market opportunities, with product differentiation leading to economical gains (Amenta et al., 2015; Handford et al., 2014; Neethirajan & Jayas, 2011). Despite all the potential benefits that nanotechnology could bring to the agri-food industry, some risks are associated such as: the environment harmful effects, the concern for workers safety and potential human health effects, like: oxidative damage, inflammation of the gastrointestinal system, cancers and lesions of liver and kidneys due to acute toxic responses (Dasgupta et al., 2015; Neethirajan & Jayas, 2011).

Nevertheless, due the potential benefits of nanotechnology application to the agri-food industry, nanotechnology is considered by the European Union (EU) as a major tool to help address key societal challenges, included in the EU Framework Programme for Research and Innovation, the Horizon 2020. This program targets to diminishes the gap between research and markets, while contributing to economical sustainable growth, competitiveness of smaller companies, promoting specialized jobs and at the same time increasing the quality of life (Commission, 2014). In order to address this challenges, the EU pretends to scale-up laboratory experiences to industrial scale, while establishing the viability of these new manufacturing technologies, aiming at developing and marketing food products nano-labelled as multifunctional, economic and environmentally friendly. The safety of nanotechnology applied to food products will also be analysed in terms of potential impact on health and environment and tools for risk assessment and management will be provided along life cycle of the agri-food products (Commission, 2014). The EU expects to support competitiveness by accelerating market acceptance of nano-labelled products; continuous improvements in the manufacturing processes and

industrial productivity; promote safe approaches crafting towards regulatory strategies, while increasing technical knowledge, with the final goal to provide societal benefits such as enhanced health care and better-quality of life (Commission, 2014).

Nanotechnology capability to solve societal challenges, such as food security, nutrition, food safety and environmental protection was also recognized by the U.S. Department of Agriculture, that funds nine research projects within the nanotechnology area in the value of $3.8 million to support solutions to the societal challenges (USDA, 2015).

As cited before, there is a lack of regulation on nanomaterials for food industry applications, at a worldwide level. Due this, in the recent years FDA and EFSA make efforts in developing guidelines in nanotechnology or nanomaterials for food industry guidance (Costa et al., in press; Silva et al., 2015a). These guidelines provide recommendations for both manufacturers and consumers awareness regarding safety, effectiveness and other product attributes in a case-by-case analysis (Costa et al., in press). EFSA states that a product involves nanotechnology if it refers to materials with a minimum of one dimension below or equal to 100 nm. Additionally to the nano-size, physic-chemical parameters such as shape, solubility, surface charge and reactivity should be considered of high importance when determining the properties and potential biological effect of the nanostructures (EFSA, 2011; Handford et al., 2014; Rossi et al., 2014). Size for instance, should be evaluated by a minimum of two independent methods, being electron microscopy one of them. Also the reactivity of the main functional groups should be taken into consideration, since this may bind the nanostructures with biopolymers. This may lead to catalytic activity, which could trigger unexpected reactions in the foods or body after ingestion (EFSA, 2011). For instance FDA, claims that nanomaterials should exhibited at least one dimension between 1 and 100 nm, exhibiting physical or chemical properties and biological effects, due to their dimensions, even when presents sizes higher than the nanoscale range (e.g. 1000 nm) (Amenta et al., 2015; Costa et al., in press; Silva et al., 2015a). FDA developed useful guidance for industry, regarding criteria for helping food industry to identify potential implications that could arise from the application of nanotechnology on

the food and feed sector. In this guidance, FDA recommends the food industry to consult FDA during the beginning of the development process, in order to simplify the understanding of the specific scientific and regulatory issues involved in their nanotechnology products (Administration, 2014a; Costa et al., in press). Also, FDA provided information regarding with identification of potential issues related to safety or regulatory status to food for animals, which could contain nanostructures or involving nanotechnology (Administration, 2014b; Costa et al., in press). Despite the lack of specific regulation regarding the use of nanotechnology in the food industry, there are clear instructions and guidance to safely develop nanotechnological products applied in the food industry. These documents were developed not only to provide information to manufacturers but also to improve the awareness of the consumers to the potential benefits, effectiveness and safety of food products developed with nanotechnology (Administration, 2014a, b; Costa et al., in press). Recently, some papers regarding the awareness, trust, acceptability and willingness of consumers to pay for food products developed with nanotechnology, are being published, that could give a bright insight on how the consumers reply to nanotechnology in the food industry. For instance, Rooses and co-workers analysed the trust and willingness of consumers to pay for food products developed with nanotechnology, recurring to online surveys in Canada and Germany. These authors also analysed the acceptance on functional food attribute (vitamin enrichment and protection) and if the trust of the consumers changes when consumers learn that this attribute was created using nanotechnology (Roosen et al., 2015). This paper showed that the use of nanotechnology in the food products is a real concern for consumers. However it was unclear to understand if the consumers concerns were related to the lack of information regarding nanotechnology in general or the lack of knowledge of the uses of nanotechnology in the food industry (Roosen et al., 2015). Additionally, these authors conclude that the use of nanotechnology is considered “bad news”, being this results consistent in Canada and Germany (Roosen et al., 2015). Consumers concern about the use of nanotechnology was also expressed in studies realised in U.S. and Switzerland (Roosen et al., 2015). Siegrist and co-workers determined the factors that can have influence on the acceptability of nanotechnology on food products, through

questionnaires. In general, the participants were hesitant to buy nanotechnological food products, either foods or food with nanotechnology packaging. Although, nanotechnology packaging is seen as more beneficial than nanotechnology applied directly on foods. The results of the questionnaires suggested that social trust was a major factor that directly influenced the benefits claimed by the products. Indeed, the heuristic affect suggested that the affect has impact on the noticed benefits and observed risks. Where, the perceived benefits appears to be of furthermost importance predictor for the acceptability and willingness to buy food products manufactured with the help of nanotechnology (Siegrist et al., 2007). In conclusion, the benefits associated to the nanotechnology food products did not provide sufficient additional value, able to induce consumers to buy food products developed with the standard of nanotechnology. Zhou (2013) achieved similar conclusions, that consumers are more willing to accept nanotechnology when they are aware of the benefits. Given this, it would be beneficial if the food industry explored the potential benefits that nanotechnology could enhance for the well being of consumers (Zhou, 2013). Otherwise, Handford and co-workers, surveyed the awareness and attitudes to agri-food organizations on Ireland regarding the application of nanotechnology, through interviews (14 organizations) and on-line questionnaire (88 organizations). They found out that the knowledge of nanotechnology applications in the food industry are low and responses were not positive or negative. Also, the key benefits for the food industry can be safer food product, reduced waste and increased product shelf life. As key barriers to the full implementation of nanotechnology by the food industry were the unknown hazards to human health and environmental impacts, consumer approval and media framing (Handford et al., 2015). Given this, scientists, government bodies and agri-food industry need to cooperate in order to increase the understanding, awareness and acceptability of nanotechnology by media and more important consumers. All the involved parts should clarify the safety of nanotechnology food products and applications, addressing the potential benefits associated to the consumption of food products developed under nanotechnology, while implementing legislative framework for the application of nanotechnology in the agri-food industry.

Although, the lack of specific regulation, agri-food companies are already exploring the vast opportunities that nanotechnology can offer to the different agri-food industry sectors, from the improvement of the nutritional value of foods, to the food packaging sector, food processing and primary production, nanotechnology is expected to reach a overall market of almost one trillion U.S. dollars, while food encapsulation market is believed to reach 39 billion U.S. dollars (Global et al., 2010; Neethirajan & Jayas, 2011). The identification of the principal commercial applications of nanotechnology already present in the agri-food market is summarised in Table 2.5.

From the commercial applications already present in the agri-food market it is possible to see that fortification of food products using bioactive compounds for the improvement of the nutritional value of foods (nutrition sector) and nanopackaging applications are rapidly growing and are considered the most active sectors of the agri-food industry with a major impact in the commercialized products developed through the use of nanotechnology.

Table 2.5 – Commercial applications of nanotechnology products established in the agri-food industry

Product	Agri-food sector	Nanostructure type	Company	Country	References
Canoila active oil	Nutrition	Nanoemulsion	Shemen Industries	Israel	(Nanotechnologies, 2013)
NovaSol® beverages	Nutrition	Nanoemulsion	Aquanova	Germany	(AquaNova, 2013b)
Nutralease beverages	Nutrition	Nano-sized self-assembled structured liquids	Nutralease Ltd.	Israel	(Nanotechproject, 2011)
SunActive®	Nutrition	Nanoemulsions	Tayo International	Japan	(International, 2006)
Colors from Nature®	Nutrition	Nanoemulsions	Wild Flavours Inc	USA	(Wild Flavors Inc, 2013)
NanoResveratrol®	Nutrition	Nanoemulsions	Life Enhancement	USA	(Life Enhancement, 2013)
SprayforLife®	Nutrition	Nanoemulsions	NanoSynergy Worldwide	USA	(NanoSinergy, 2013)
Nutri-Nano™	Nutrition	Nanoemulsions	Solgar	USA	(Solgar, 2013)
Altrient®	Nutrition	Liposomes	Livon Laboratories	USA	(Laboratories)
Bioral™	Nutrition		Bioral Nutrient Delivery, LLC	USA	(Delivery)
BioNutriCoat	Nutrition/Food packaging	Nanoemulsions	Improveat	Portugal	(Improveat, 2014)
Fresh Box	Food packaging	Silver nanoparticles	BlueMoonGoods, LLC	USA	(Nanotechnologies, 2007a)
N-Coat	Food	Clay	Multifilm	USA	(Corporation)

	packaging	nanoparticles	Packaging Corporation		
FresherLonger™ Miracle Food Storage	Food packaging	Silver nanoparticles	Sharper Image	USA	(Nanotechnologies, 2007b)
Nano Silver Baby Mug Cup	Food packaging	Silver nanoparticles	Baby Dream® Co., Ltd.	Korea	(Nanotechnologies)
Imperm®	Food packaging	Clay nanoparticles	Nanocor®	USA	(Nanocor®)
Nansulate®	Food processing	Nanocomposite	Industrial Nanotech Inc.	USA	(Inc.)
Bioni nano paint	Food processing	Silver nanoparticles	Bioni	Germany	(Bioni, 2008)
Nano air-filter	Food processing	Silver nanoparticles	SongSing Nano Technology Co., Ltd.	Taiwan	(Nanotechnologies, 2007c)
Wifi nanosensors	Primary production	Nanosensors	Accenture	USA	(Handford et al., 2014)
Primo Maxx®	Primary production	Nanoemulsions	Syngenta	Switzerland	(Handford et al., 2014)

2.10 Conclusions

Nanoemulsions constitute one of the most promising systems to improve solubility, bioavailability and functionality of hydrophobic compounds. Food industry seeks to use these systems for the incorporation of e.g. lipophilic bioactive compounds in food matrices. While there are various techniques available to produce and characterize nanoemulsions, some of them have shown to be more suitable than others. LbL electrostatic technique is able to

change nanoemulsions surface, conferring new properties. In short, HPLC can be used for quantification of bioactive compounds, DLS may quickly determine the hydrodynamic diameter of a nanoemulsion, zeta potential can indicate the stability of the nanoemulsions and TEM may be used to confirm the hydrodynamic diameter given by DLS technique and to have a indication of the nanoemulsion morphology.

The application of these nanosystems to the food industry still needs to address some challenges in terms of the preparation of these nanosystems: including surfactants characteristics, mixing conditions, resistance to environmental stresses, composition of these systems to overcome the different phases of the gastrointestinal passage and the scale up for the production process. A special attention should given to the cost-benefits analysis of manufacturing these nanosystems. It is also crucial to improve the actual legislation framework in order to prevent consumers' misinformation concerning nanotechnology in the food industry. Such misinformation can raise consumers' suspicions about the security of applying nanotechnology to the food products.

2.11 References

Acosta E (2009) Bioavailability of nanoparticles in nutrient and nutraceutical delivery. Current Opinion in Colloid & Interface Science 14, 3-15.

Adamczak M, Kupiec A, Jarek E, Szczepanowicz K & Warszyński P (2014) Preparation of the squalene-based capsules by membrane emulsification method and polyelectrolyte multilayer adsorption. Colloids and Surfaces A: Physicochemical and Engineering Aspects 462, 147-152.

Administration UFaD (2014a). Considering Whether an FDA-Regulated Product Involves the Application of Nanotechnology, Available at: http://www.fda.gov/RegulatoryInformation/Guidances/ucm257698.htm. Accessed 17/09/15.

Administration UFaD (2014b). Guidance for Industry: Assessing the Effects of Significant Manufacturing Process Changes, Including Emerging Technologies, on the Safety and Regulatory Status of Food Ingredients and Food Contact Substances, Including Food Ingredients that Are Color Additives, Available at: http://www.fda.gov/Food/GuidanceRegulation/GuidanceDocumentsRegulatoryInformation/ucm300661.htm. Accessed 17/09/2015.

Ahmed K, Li Y, McClements DJ & Xiao H (2012) Nanoemulsion- and emulsion-based delivery systems for curcumin: Encapsulation and release properties. Food Chemistry 132(2), 799-807.

Ai H, Jones S & Lvov Y (2003) Biomedical applications of electrostatic layer-by-layer nano-assembly of polymers, enzymes, and nanoparticles. Cell Biochemistry and Biophysics 39(1), 23-43.

Amenta V, Aschberger K, Arena M, Bouwmeester H, Botelho Moniz F, Brandhoff P, Gottardo S, Marvin HJP, Mech A, Quiros Pesudo L, Rauscher H, Schoonjans R, Vettori MV, Weigel S & Peters RJ (2015) Regulatory aspects of nanotechnology in the agri/feed/food sector in EU and non-EU countries. Regulatory Toxicology and Pharmacology 73(1), 463-476.

Anton N, Benoit J-P & Saulnier P (2008) Design and production of nanoparticles formulated from nano-emulsion templates--A review. Journal of Controlled Release 128(3), 185-199.

Anton N, Gayet P, Benoit J-P & Saulnier P (2007a) Nano-emulsions and nanocapsules by the PIT method: An investigation on the role of the

temperature cycling on the emulsion phase inversion. International Journal of Pharmaceutics 344(1-2), 44-52.

Anton N, Gayet P, Benoit J-P & Saulnier P (2007b) Nano-emulsions and nanocapsules by the PIT method: An investigation on the role of the temperature cycling on the emulsion phase inversion. International Journal of Pharmaceutics 344(1,Äì2), 44-52.

Aoki T, Decker EA & McClements DJ (2005) Influence of environmental stresses on stability of O/W emulsions containing droplets stabilized by multilayered membranes produced by a layer-by-layer electrostatic deposition technique. Food Hydrocolloids 19(2), 209-220.

AquaNova (2013a). Available at: http://www.aquanova.de/media/public/pdf_produkte unkosher/NovaSOL_beverage.pdf. Accessed 13 November 2013.

AquaNova (2013b). Available at: http://www.aquanova.de/media/public/pdf_produkte unkosher/NovaSOL_BCS.pdf. Accessed 11 November 2013.

Araújo FA, Kelmann RG, Araújo BV, Finatto RB, Teixeira HF & Koester LS (2011) Development and characterization of parenteral nanoemulsions containing thalidomide. European Journal of Pharmaceutical Sciences 42(3), 238-245.

ASTM (1985) Zeta potential of colloids in water and waste water. American Society for Testing and Materials, D 4187-4182.

Azároff LV, Kaplow R, Kato N., Weiss RJ, Wilson AJC & Young RA, (1974). Crystal physics, diffraction, theoretical and general crystallography. McGraw-Hill, New York.

Badran MM, Taha EI, Tayel MM & Al-Suwayeh SA (2014) Ultra-fine self nanoemulsifying drug delivery system for transdermal delivery of meloxicam: Dependency on the type of surfactants. Journal of Molecular Liquids 190(0), 16-22.

Balcão VM, Costa CI, Matos CM, Moutinho CG, Amorim M, Pintado ME, Gomes AP, Vila MM & Teixeira JA (2013) Nanoencapsulation of bovine lactoferrin for food and biopharmaceutical applications. Food Hydrocolloids 32(2), 425-431.

Bandyopadhyay S, Katare OP & Singh B (2012) Optimized self nano-emulsifying systems of ezetimibe with enhanced bioavailability potential using long chain and medium chain triglycerides. Colloids and Surfaces B: Biointerfaces 100(0), 50-61.

Bazylinska U, Skrzela R, Szczepanowicz K, Warszynski P & Wilk KA (2011) Novel approach to long sustained multilayer nanocapsules: influence of surfactant head groups and polyelectrolyte layer number on the release of hydrophobic compounds. Soft Matter 7(13), 6113-6124.

Berth G, Voigt A, Dautzenberg H, Donath E & Möhwald H (2002) Polyelectrolyte Complexes and Layer-by-Layer Capsules from Chitosan/Chitosan Sulfate. Biomacromolecules 3(3), 579-590.

Berton-Carabin CC, Coupland JN & Elias RJ (2013) Effect of the lipophilicity of model ingredients on their location and reactivity in emulsions and solid lipid nanoparticles. Colloids and Surfaces A: Physicochemical and Engineering Aspects 431(0), 9-17.

Bioni (2008). Bioni's nano paint, Available at: http://www.bioni.de/en/index.php?page=news&lang=en - news040. Accessed 22 September 2015.

Bondy C & Sollner K (1935) On the mechanism of emulsification by ultrasonic waves. Transactions of the Faraday Society 31(0), 835-843.

Bose S & Michniak-Kohn B (2013) Preparation and characterization of lipid based nanosystems for topical delivery of quercetin. European Journal of Pharmaceutical Sciences 48(3), 442-452.

Bouchemal K, Briançon S, Perrier E & Fessi H (2004) Nano-emulsion formulation using spontaneous emulsification: solvent, oil and surfactant optimisation. International Journal of Pharmaceutics 280(1-2), 241-251.

Caruso F, Furlong DN, Ariga K, Ichinose I & Kunitake T (1998) Characterization of Polyelectrolyte−Protein Multilayer Films by Atomic Force Microscopy, Scanning Electron Microscopy, and Fourier Transform Infrared Reflection−Absorption Spectroscopy. Langmuir 14(16), 4559-4565.

Casadei MA, Cerreto F, Cesa S, Giannuzzo M, Feeney M, Marianecci C & Paolicelli P (2006) Solid lipid nanoparticles incorporated in dextran hydrogels: A new drug delivery system for oral formulations. International Journal of Pharmaceutics 325(1-2), 140-146.

Cerqueira M, Pinheiro A, Silva H, Ramos P, Azevedo M, Flores-López M, Rivera M, Bourbon A, Ramos Ó & Vicente A (2014) Design of Bio-nanosystems for Oral Delivery of Functional Compounds. Food Engineering Reviews 6(1-2), 1-19.

Cerqueira MA, Bourbon AI, Pinheiro AC, Silva HD, Quintas MAC & Antonio AV, (2013). Edible Nano-Laminate Coatings for Food Applications, *Ecosustainable Polymer Nanomaterials for Food Packaging*. CRC Press, pp. 221-252.

Chan H-K & Kwok PCL (2011) Production methods for nanodrug particles using the bottom-up approach. Advanced Drug Delivery Reviews 63(6), 406-416.

Channasanon S, Graisuwan W, Kiatkamjornwong S & Hoven VP (2007) Alternating bioactivity of multilayer thin films assembled from charged derivatives of chitosan. Journal of Colloid and Interface Science 316(2), 331-343.

Chen L, Remondetto GE & Subirade M (2006) Food protein-based materials as nutraceutical delivery systems. Trends in Food Science & Technology 17(5), 272-283.

Cheong JN, Tan CP, Man YBC & Misran M (2008) [alpha]-Tocopherol nanodispersions: Preparation, characterization and stability evaluation. Journal of Food Engineering 89(2), 204-209.

Chu B-S, Ichikawa S, Kanafusa S & Nakajima M (2007a) Preparation and Characterization of β-Carotene Nanodispersions Prepared by Solvent Displacement Technique. Journal of Agricultural and Food Chemistry 55(16), 6754-6760.

Chu B-S, Ichikawa S, Kanafusa S & Nakajima M (2007b) Preparation of Protein-Stabilized β-Carotene Nanodispersions by Emulsification–Evaporation Method. Journal of the American Oil Chemists' Society 84(11), 1053-1062.

Commission E (2014). The EU Framework Programme for Research and Innovation, Available at: http://ec.europa.eu/programmes/horizon2020/en/h2020-section/nanotechnologies. Accessed 18/09/2015.

Connolly JR (2007). Introduction to X-Ray Powder Diffraction., Available at: http://epswww.unm.edu/xrd/xrdclass/01-XRD-Intro.pdf. Accessed 14 January 2011.

Corporation MP N-Coat, Available at: http://multifilm.com/pouch-film/n-coat/. Accessed

Costa RR, Alatorre-Meda M & Mano JF (in press) Drug nano-reservoirs synthesized using layer-by-layer technologies. Biotechnology Advances.

Cui J, van Koeverden MP, Müllner M, Kempe K & Caruso F (2014) Emerging methods for the fabrication of polymer capsules. Advances in Colloid and Interface Science 207, 14-31.

Dasgupta N, Ranjan S, Mundekkad D, Ramalingam C, Shanker R & Kumar A (2015) Nanotechnology in agro-food: From field to plate. Food Research International 69, 381-400.

Decher G (1997) Fuzzy Nanoassemblies: Toward Layered Polymeric Multicomposites. Science 277(5330), 1232-1237.

Decher G, (2003). Polyelectrolyte Multilayers, an Overview, *Multilayer Thin Films*. Wiley-VCH Verlag GmbH & Co. KGaA, pp. 1-46.

Decher G, Hong JD & Schmitt J (1992) Buildup of ultrathin multilayer films by a self-assembly process: III. Consecutively alternating adsorption of anionic and cationic polyelectrolytes on charged surfaces. Thin Solid Films 210–211, Part 2, 831-835.

del Mercato LL, Ferraro MM, Baldassarre F, Mancarella S, Greco V, Rinaldi R & Leporatti S (2014) Biological applications of LbL multilayer capsules: From drug delivery to sensing. Advances in Colloid and Interface Science 207, 139-154.

Delivery BN Bioral, Available at: http://www.bloomberg.com/research/stocks/private/snapshot.asp?privcapId=4690005. Accessed 21 September 2015.

Desai KGH & Jin Park H (2005) Recent Developments in Microencapsulation of Food Ingredients. Drying Technology 23(7), 1361-1394.

Dickinson E (2003) Hydrocolloids at interfaces and the influence on the properties of dispersed systems. Food Hydrocolloids 17(1), 25-39.

Donath E, Sukhorukov GB, Caruso F, Davis SA & Möhwald H (1998) Novel Hollow Polymer Shells by Colloid-Templated Assembly of Polyelectrolytes. Angewandte Chemie International Edition 37(16), 2201-2205.

Drusch S (2007) Sugar beet pectin: A novel emulsifying wall component for microencapsulation of lipophilic food ingredients by spray-drying. Food Hydrocolloids 21(7), 1223-1228.

Dulog L & Schauer T (1996) Field flow fractionation for particle size determination. Progress in Organic Coatings 28(1), 25-31.

Edwards KA & Baeumner AJ (2006) Analysis of liposomes. Talanta 68(5), 1432-1441.

EFSA (2011). Guidance on the risk assessment of the application of nanoscience and nanotechnologies in the food and feed chain, Available at: http://www.efsa.europa.eu/sites/default/files/scientific_output/files/main_documents/2140.pdf. Accessed 10 September 2015.

Ezhilarasi PN, Karthik P, Chhanwal N & Anandharamakrishnan C (2013) Nanoencapsulation Techniques for Food Bioactive Components: A Review. Food and Bioprocess Technology 6(3), 628-647.

Fang Z & Bhandari B (2010) Encapsulation of polyphenols – a review. Trends in Food Science & Technology 21(10), 510-523.

Freitas S, Merkle HP & Gander B (2005) Microencapsulation by solvent extraction/evaporation: reviewing the state of the art of microsphere preparation process technology. Journal of Controlled Release 102(2), 313-332.

Genovese DB, Lozano JE & Rao MA (2007) The Rheology of Colloidal and Noncolloidal Food Dispersions. Journal of Food Science 72(2), R11-R20.

Ghosh V, Mukherjee A & Chandrasekaran N (2014) Eugenol-loaded antimicrobial nanoemulsion preserves fruit juice against, microbial spoilage. Colloids Surf B Biointerfaces 114(0), 392-397.

Glatter O & Kratky O, (1982). Small Angle X-ray Scattering. Academic Press.

Global, Industry & Analysts (2010). Food Encapsulation: A Global Strategic Business Report, Available at: http://www.ift.org/food-technology/daily-news/2010/july/07/global-food-encapsulation-market-to-reach-$39b-by-2015.aspx. Accessed 23/11/2013.

Grigoriev DO & Miller R (2009) Mono- and multilayer covered drops as carriers. Current Opinion in Colloid & Interface Science 14(1), 48-59.

Gu YS, Decker EA & McClements DJ (2005) Influence of pH and carrageenan type on properties of β-lactoglobulin stabilized oil-in-water emulsions. Food Hydrocolloids 19(1), 83-91.

Guzey D & McClements DJ (2006) Formation, stability and properties of multilayer emulsions for application in the food industry. Advances in Colloid and Interface Science 128-130, 227-248.

Handford CE, Dean M, Henchion M, Spence M, Elliott CT & Campbell K (2014) Implications of nanotechnology for the agri-food industry: Opportunities, benefits and risks. Trends in Food Science & Technology 40(2), 226-241.

Handford CE, Dean M, Spence M, Henchion M, Elliott CT & Campbell K (2015) Awareness and attitudes towards the emerging use of nanotechnology in the agri-food sector. Food Control 57, 24-34.

High Vive (2013). Available at: http://www.highvive.com/sunactiveiron.htm. Accessed 16 November 2013.

Huang Q, Yu H & Ru Q (2010) Bioavailability and Delivery of Nutraceuticals Using Nanotechnology. Journal of Food Science 75(1), R50-R57.

Improveat (2014). Available at: http://www.improveat.pt/en/products/. Accessed 9 January 2014.

Inc. IN Nansulate®, Available at: http://www.industrial-nanotech.com/main-page.html. Accessed 22 September 2015.

Indest T, Laine J, Johansson L-S, Stana-Kleinschek K, Strnad S, Dworczak R & Ribitsch V (2009) Adsorption of Fucoidan and Chitosan Sulfate on Chitosan Modified PET Films Monitored by QCM-D. Biomacromolecules 10(3), 630-637.

International T (2006). Available at: http://www.taiyointernational.com/products/sunactive/. Accessed 19 September 2015.

Israelachvili JN, (2011). Chapter 14 - Electrostatic Forces between Surfaces in Liquids, in: Israelachvili JN (Ed.), *Intermolecular and Surface Forces (Third Edition)*. Academic Press, San Diego, pp. 291-340.

Israeli-Lev G & Livney YD (2014) Self-assembly of hydrophobin and its co-assembly with hydrophobic nutraceuticals in aqueous solutions: Towards application as delivery systems. Food Hydrocolloids 35(0), 28-35.

Izquierdo P, Esquena J, Tadros TF, Dederen C, Garcia MJ, Azemar N & Solans C (2001) Formation and Stability of Nano-Emulsions Prepared Using the Phase Inversion Temperature Method. Langmuir 18(1), 26-30.

Izquierdo P, Esquena J, Tadros TF, Dederen JC, Feng J, Garcia-Celma MJ, Azemar N & Solans C (2004) Phase Behavior and Nano-emulsion Formation by the Phase Inversion Temperature Method. Langmuir 20(16), 6594-6598.

Jafari SM, Assadpoor E, He Y & Bhandari B (2008) Encapsulation Efficiency of Food Flavours and Oils during Spray Drying. Drying Technology 26(7), 816-835.

Jenning V, Mäder K & Gohla SH (2000b) Solid lipid nanoparticles (SLN(TM)) based on binary mixtures of liquid and solid lipids: a 1H-NMR study. International Journal of Pharmaceutics 205(1-2), 15-21.

Jenning V, Thünemann AF & Gohla SH (2000a) Characterisation of a novel solid lipid nanoparticle carrier system based on binary mixtures of liquid and solid lipids. International Journal of Pharmaceutics 199(2), 167-177.

Jores K, Mehnert W, Drechsler M, Bunjes H, Johann C & Mäder K (2004) Investigations on the structure of solid lipid nanoparticles (SLN) and oil-loaded solid lipid nanoparticles by photon correlation spectroscopy, field-flow fractionation and transmission electron microscopy. Journal of Controlled Release 95(2), 217-227.

Kantak C, Beyer S, Yobas L, Bansal T & Trau D (2011) A 'microfluidic pinball' for on-chip generation of Layer-by-Layer polyelectrolyte microcapsules. Lab on a Chip 11(6), 1030-1035.

Khalid N, Kobayashi I, Neves MA, Uemura K & Nakajima M (2013) Preparation and characterization of water-in-oil emulsions loaded with high concentration of l-ascorbic acid. LWT - Food Science and Technology 51(2), 448-454.

Klinkesorn U, Sophanodora P, Chinachoti P, McClements DJ & Decker EA (2005) Increasing the Oxidative Stability of Liquid and Dried Tuna Oil-in-Water Emulsions with Electrostatic Layer-by-Layer Deposition Technology. Journal of Agricultural and Food Chemistry 53(11), 4561-4566.

Laboratories L Altrient, Available at: http://www.livonlabs.com/europe.html. Accessed 21 of September 2015.

Lacatusu I, Mitrea E, Badea N, Stan R, Oprea O & Meghea A (2013) Lipid nanoparticles based on omega-3 fatty acids as effective carriers for lutein delivery. Preparation and in vitro characterization studies. Journal of Functional Foods 5(3), 1260-1269.

Lante A & Friso D (2013) Oxidative stability and rheological properties of nanoemulsions with ultrasonic extracted green tea infusion. Food Research International 54(1), 269-276.

Lawrie G, Keen I, Drew B, Chandler-Temple A, Rintoul L, Fredericks P & Grøndahl L (2007) Interactions between Alginate and Chitosan Biopolymers Characterized Using FTIR and XPS. Biomacromolecules 8(8), 2533-2541.

Lee S-H, Lef√®vre T, Subirade M & Paquin P (2009) Effects of ultra-high pressure homogenization on the properties and structure of interfacial protein layer in whey protein-stabilized emulsion. Food Chemistry 113(1), 191-195.

Leong TSH, Wooster TJ, Kentish SE & Ashokkumar M (2009) Minimising oil droplet size using ultrasonic emulsification. Ultrasonics Sonochemistry 16(6), 721-727.

Li X, Anton N, Arpagaus C, Belleteix F & Vandamme TF (2010a) Nanoparticles by spray drying using innovative new technology: The Büchi Nano Spray Dryer B-90. Journal of Controlled Release 147(2), 304-310.

Li Y, Hu M, Xiao H, Du Y, Decker EA & McClements DJ (2010b) Controlling the functional performance of emulsion-based delivery systems using multi-component biopolymer coatings. European Journal of Pharmaceutics and Biopharmaceutics 76(1), 38-47.

Li Y & McClements DJ (2014) Modulating lipid droplet intestinal lipolysis by electrostatic complexation with anionic polysaccharides: Influence of cosurfactants. Food Hydrocolloids 35(0), 367-374.

Li Y, Zhang Z, Yuan Q, Liang H & Vriesekoop F (2013) Process optimization and stability of d-limonene nanoemulsions prepared by catastrophic phase inversion method. Journal of Food Engineering 119(3), 419-424.

Life Enhancement (2013). Available at: http://www.life-enhancement.com/shop/product/nsr-nanoresveratrol. Accessed 21 November 2013.

López-Montilla JC, Herrera-Morales PE, Pandey S & Shah DO (2002) Spontaneous Emulsification: Mechanisms, Physicochemical Aspects, Modeling, and Applications. Journal of Dispersion Science and Technology 23(1-3), 219-268.

Luykx DMAM, Goerdayal SS, Dingemanse PJ, Jiskoot W & Jongen PMJM (2005) HPLC and tandem detection to monitor conformational properties of biopharmaceuticals. Journal of Chromatography B 821(1), 45-52.

Luykx DMAM, Peters RJB, van Ruth SM & Bouwmeester H (2008) A Review of Analytical Methods for the Identification and Characterization of Nano Delivery

Systems in Food. Journal of Agricultural and Food Chemistry 56(18), 8231-8247.

Maa Y-F & Hsu CC (1999) Performance of Sonication and Microfluidization for Liquid–Liquid Emulsification. Pharmaceutical Development and Technology 4(2), 233-240.

Madrigal-Carballo S, Lim S, Rodriguez G, Vila AO, Krueger CG, Gunasekaran S & Reed JD (2010) Biopolymer coating of soybean lecithin liposomes via layer-by-layer self-assembly as novel delivery system for ellagic acid. Journal of Functional Foods 2(2), 99-106.

Maher PG, Roos YH & Fenelon MA (2014) Physicochemical properties of spray dried nanoemulsions with varying final water and sugar contents. Journal of Food Engineering 126, 113-119.

Manchun S, Dass CR & Sriamornsak P (2014) Designing nanoemulsion templates for fabrication of dextrin nanoparticles via emulsion cross-linking technique. Carbohydrate Polymers 101(0), 650-655.

Martins J, Ramos Ó, Pinheiro A, Bourbon A, Silva H, Rivera M, Cerqueira M, Pastrana L, Malcata FX, González-Fernández Á & Vicente A (2015) Edible Bio-Based Nanostructures: Delivery, Absorption and Potential Toxicity. Food Engineering Reviews, 1-23.

Marx KA (2003) Quartz Crystal Microbalance: A Useful Tool for Studying Thin Polymer Films and Complex Biomolecular Systems at the Solution-Surface Interface. Biomacromolecules 4(5), 1099-1120.

Mason TJ (1992) Industrial sonochemistry: potential and practicality. Ultrasonics 30(3), 192-196.

McClements D, (2005). Food Emulsions: Principles, Practice, and Techniques., 2nd ed. CRC Press, Boca Raton, Florida.

McClements DJ (2010) Design of Nano-Laminated Coatings to Control Bioavailability of Lipophilic Food Components. Journal of Food Science 75(1), R30-R42.

McClements DJ & Decker EA (2000) Lipid Oxidation in Oil-in-Water Emulsions: Impact of Molecular Environment on Chemical Reactions in Heterogeneous Food Systems. Journal of Food Science 65(8), 1270-1282.

McClements DJ, Decker EA, Park Y & Weiss J (2009) Structural Design Principles for Delivery of Bioactive Components in Nutraceuticals and

Functional Foods. Critical Reviews in Food Science and Nutrition 49(6), 577-606.

McClements DJ, Decker EA & Weiss J (2007) Emulsion-Based Delivery Systems for Lipophilic Bioactive Components. Journal of Food Science 72(8), R109-R124.

McClements DJ & Li Y (2010) Structured emulsion-based delivery systems: Controlling the digestion and release of lipophilic food components. Advances in Colloid and Interface Science 159(2), 213-228.

McClements DJ & Rao J (2011) Food-Grade Nanoemulsions: Formulation, Fabrication, Properties, Performance, Biological Fate, and Potential Toxicity. Critical Reviews in Food Science and Nutrition 51(4), 285-330.

Mills I, Cvitas T, Homann K, Kallay N & Kuchitsu K, (1993). IUPAC Quantities, Units and Symbols in Physical Chemistry, 2nd ed. Blackwell Scientific Publications, Oxford.

Mora-Huertas CE, Fessi H & Elaissari A (2010) Polymer-based nanocapsules for drug delivery. International Journal of Pharmaceutics 385(1–2), 113-142.

Moraru CI, Panchapakesan CP, Huang Q, Takhistov P, Liu S & Kokini JL (2003) Nanotechnology, a new frontier in food science. Food Technology 57(12), 24–29.

Mulik RS, Mönkkönen J, Juvonen RO, Mahadik KR & Paradkar AR (2010) Transferrin mediated solid lipid nanoparticles containing curcumin: Enhanced in vitro anticancer activity by induction of apoptosis. International Journal of Pharmaceutics 398(1-2), 190-203.

Nanocor® Polymer Polymer-Clay Nanocomposites Clay Nanocomposites

- Better Plastics Better Plastics, Available at: http://www.epa.gov/oppt/nano/p2docs/casestudy2_lan.pdf. Accessed 21 September 2015.

NanoSinergy (2013). Available at: http://sprayforlife.com/. Accessed 18 November 2013.

Nanotechnologies TPoE Nanotechnology consumer products inventory, Available at: http://www.nanotechproject.org/cpi/products/nano-silver-baby-mug-cup/. Accessed 21 September 2015.

Nanotechnologies TPoE (2007a). Nanotechnology consumer products inventory, Available at: http://www.nanotechproject.org/cpi/products/bluemoongoodstm-fresh-box-silver-nanoparticle-food-storage-containers/. Accessed

Nanotechnologies TPoE (2007b). Nanotechnology consumer products inventory, Available at: http://www.nanotechproject.org/cpi/products/fresherlongertm-miracle-food-storage/. Accessed 21 September 2015.

Nanotechnologies TPoE (2007c). Nanotechnology consumer products inventory, Available at: http://www.nanotechproject.org/cpi/products/nano-air-filter/. Accessed 22 September 2015.

Nanotechnologies TPoE (2013). Nanotechnology consumer products inventory, Available at: http://www.nutritionaloutlook.com/article/big-potential. Accessed 16 September 2015.

Nanotechproject (2011). Available at: http://www.nutralease.com/Nutra/Templates/showpage.asp?DBID=1&LNGID=1&TMID=84&FID=767. Accessed 13 September 2015.

Nazarzadeh E, Anthonypillai T & Sajjadi S (2013) On the growth mechanisms of nanoemulsions. Journal of Colloid and Interface Science 397(0), 154-162.

Neethirajan S & Jayas D (2011) Nanotechnology for the Food and Bioprocessing Industries. Food and Bioprocess Technology 4(1), 39-47.

Nicolet T (2001). Introduction to fourier transform infrared spectrometry., Available at: http://mmrc.caltech.edu/FTIR/FTIRintro.pdf. Accessed 11 January 2011.

NutraLease (2011a). Available at: http://www.nutralease.com/Nutra/Templates/showpage.asp?DBID=1&LNGID=1&TMID=84&FID=767. Accessed 13 April 2011.

Pinheiro AC, Bourbon AI, Medeiros BGS, da Silva LHM, Silva MCH, Carneiro-da-Cunha MG, Coimbra MA & Vicente AA (2011a) Interactions between k-carrageenan and chitosan in nanolayered coatings – structural and transport properties evaluation. Carbohydrate Polymers in Press.

Pinheiro AC, Bourbon AI, Rocha C, Ribeiro C, Maia JM, GonÁalves MP, Teixeira JA & Vicente AA (2011b) Rheological characterization of [kappa]-carrageenan/galactomannan and xanthan/galactomannan gels: Comparison of

galactomannans from non-traditional sources with conventional galactomannans. Carbohydrate Polymers 83(2), 392-399.

Pongsawatmanit R, Harnsilawat T & McClements DJ (2006) Influence of alginate, pH and ultrasound treatment on palm oil-in-water emulsions stabilized by [beta]-lactoglobulin. Colloids and Surfaces A: Physicochemical and Engineering Aspects 287(1-3), 59-67.

Preetz C, Hauser A, Hause G, Kramer A & Mäder K (2010) Application of atomic force microscopy and ultrasonic resonator technology on nanoscale: Distinction of nanoemulsions from nanocapsules. European Journal of Pharmaceutical Sciences 39(1-3), 141-151.

Priest C, Quinn A, Postma A, Zelikin AN, Ralston J & Caruso F (2008) Microfluidic polymer multilayer adsorption on liquid crystal droplets for microcapsule synthesis. Lab on a Chip 8(12), 2182-2187.

Qian C, Decker EA, Xiao H & McClements DJ (2012a) Inhibition of β-carotene degradation in oil-in-water nanoemulsions: Influence of oil-soluble and water-soluble antioxidants. Food Chemistry 135(3), 1036-1043.

Qian C, Decker EA, Xiao H & McClements DJ (2012b) Nanoemulsion delivery systems: Influence of carrier oil on ß-carotene bioaccessibility. Food Chemistry 135(3), 1440-1447.

Quintanar-Guerrero D, Allémann E, Fessi H & Doelker E (1999) Pseudolatex preparation using a novel emulsion-diffusion process involving direct displacement of partially water-miscible solvents by distillation. International Journal of Pharmaceutics 188(2), 155-164.

Quintanilla-Carvajal M, Camacho-Díaz B, Meraz-Torres L, Chanona-Pérez J, Alamilla-Beltrán L, Jimenéz-Aparicio A & Gutiérrez-López G (2010) Nanoencapsulation: A New Trend in Food Engineering Processing. Food Engineering Reviews 2(1), 39-50.

Rang M-J & Miller CA (1999) Spontaneous Emulsification of Oils Containing Hydrocarbon, Nonionic Surfactant, and Oleyl Alcohol. Journal of Colloid and Interface Science 209(1), 179-192.

Rao J & McClements DJ (2013) Optimization of lipid nanoparticle formation for beverage applications: Influence of oil type, cosolvents, and cosurfactants on nanoemulsion properties. Journal of Food Engineering 118(2), 198-204.

Rao JP & Geckeler KE (2011) Polymer nanoparticles: Preparation techniques and size-control parameters. Progress in Polymer Science 36(7), 887-913.

Reimer L (2000) Scanning Electron Microscopy: Physics of Image Formation and Microanalysis, Second Edition. Measurement Science and Technology 11(12), 1826.

Rezaee M, Basri M, Raja Abdul Rahman RNZ, Salleh AB, Chaibakhsh N & Fard Masoumi HR (2014) A multivariate modeling for analysis of factors controlling the particle size and viscosity in palm kernel oil esters-based nanoemulsions. Industrial Crops and Products 52(0), 506-511.

Ribeiro HS, Chu B-S, Ichikawa S & Nakajima M (2008) Preparation of nanodispersions containing β-carotene by solvent displacement method. Food Hydrocolloids 22(1), 12-17.

Richert L, Lavalle P, Payan E, Shu XZ, Prestwich GD, Stoltz J-Fß, Schaaf P, Voegel J-C & Picart C (2003) Layer by Layer Buildup of Polysaccharide Films: Physical Chemistry and Cellular Adhesion Aspects. Langmuir 20(2), 448-458.

Roosen J, Bieberstein A, Blanchemanche S, Goddard E, Marette S & Vandermoere F (2015) Trust and willingness to pay for nanotechnology food. Food Policy 52, 75-83.

Rossi M, Cubadda F, Dini L, Terranova ML, Aureli F, Sorbo A & Passeri D (2014) Scientific basis of nanotechnology, implications for the food sector and future trends. Trends in Food Science & Technology 40(2), 127-148.

Rouessac F. & Rouessac A, (2007). Chemical Analysis: Modern Instrumentation Methods and Techniques., 2nd ed. Wiley, France.

Ruozi B, Tosi G, Forni F, Fresta M & Vandelli MA (2005) Atomic force microscopy and photon correlation spectroscopy: Two techniques for rapid characterization of liposomes. European Journal of Pharmaceutical Sciences 25(1), 81-89.

Salmah H, Ismail H & Bakar AA (2008) The effects of dynamic vulcanization and compatibilizer on properties of paper sludge-filled polypropylene/ethylene propylene diene terpolymer composites. Journal of Applied Polymer Science 107(4), 2266-2273.

Salvia-Trujillo L, Rojas-Grau MA, Soliva-Fortuny R & Martín-Belloso O (2014) Impact of microfluidization or ultrasound processing on the antimicrobial activity

against Escherichia coli of lemongrass oil-loaded nanoemulsions. Food Control 37(0), 292-297.

Sanguansri P & Augustin MA (2006) Nanoscale materials development - a food industry perspective. Trends in Food Science & Technology 17(10), 547-556.

Schwarz JC, Baisaeng N, Hoppel M, Low M, Keck CM & Valenta C (2013) Ultra-small NLC for improved dermal delivery of coenyzme Q10. International Journal of Pharmaceutics 447(1-2), 213-217.

Sessa M, Balestrieri ML, Ferrari G, Servillo L, Castaldo D, D'Onofrio N, Donsì F & Tsao R (2014) Bioavailability of encapsulated resveratrol into nanoemulsion-based delivery systems. Food Chemistry 147(0), 42-50.

Shchukina EM & Shchukin DG (2011) LbL coated microcapsules for delivering lipid-based drugs. Advanced Drug Delivery Reviews 63(9), 837-846.

Shemen Industries (2013). Available at: http://www.nutritionaloutlook.com/article/big-potential. Accessed 16 November 2013.

Shinoda K & Saito H (1968) The effect of temperature on the phase equilibria and the types of dispersions of the ternary system composed of water, cyclohexane, and nonionic surfactant. Journal of Colloid and Interface Science 26(1), 70-74.

Shinoda K & Saito H (1969) The stability of o/w type emulsions as a function of temperature and the hlb of emulsifiers: the emulsification by pit-method. Journal of Colloid and Interface Science 30(1), 258-263.

Siegrist M, Cousin M-E, Kastenholz H & Wiek A (2007) Public acceptance of nanotechnology foods and food packaging: The influence of affect and trust. Appetite 49(2), 459-466.

Silva H, Cerqueira M & Vicente A (2012) Nanoemulsions for Food Applications: Development and Characterization. Food and Bioprocess Technology 5(3), 854-867.

Silva HD, Cerqueira MA, Souza BWS, Ribeiro C, Avides MC, Quintas MAC, Coimbra JSR, Carneiro-da-Cunha MG & Vicente AA (2011a) Nanoemulsions of [beta]-carotene using a high-energy emulsification-evaporation technique. Journal of Food Engineering 102(2), 130-135.

Silva HD, Cerqueira MA, Souza BWS, Ribeiro C, Avides MC, Quintas MAC, Coimbra JSR, Carneiro-da-Cunha MG & Vicente AA (2011b) Nanoemulsions of

β-carotene using a high-energy emulsification-evaporation technique. Journal of Food Engineering 102(2), 130-135.

Silva HD, Cerqueira MA & Vicente AA (2011c) Nanoemulsions for food applications: development and characterization. Food and Bioprocess Technology in Press.

Silva HD, Cerqueira MA & Vicente AA, (2015a). Chapter 56 - Nanoemulsion-Based Systems for Food Applications, in: Kharisov BI (Ed.), *CRC Concise Encyclopedia of Nanotechnology*. CRC Press by Taylor and Francis Group, USA.

Silva HD, Pinheiro AC, Donsì F, Cerqueira MA, Ferrari G & Vicente AA, (2015b). Development and characterization of lipid-based nanosystems: Effect of interfacial composition on nanoemulsions behaviour.

Simunkova H, Pessenda-Garcia P, Wosik J, Angerer P, Kronberger H & Nauer GE (2009) The fundamentals of nano- and submicro-scaled ceramic particles incorporation into electrodeposited nickel layers: Zeta potential measurements. Surface and Coatings Technology 203(13), 1806-1814.

Solans C, Izquierdo P, Nolla J, Azemar N & Garcia-Celma MJ (2005) Nano-emulsions. Current Opinion in Colloid & Interface Science 10(3,Äì4), 102-110.

Solans C & Solé I (2012) Nano-emulsions: Formation by low-energy methods. Current Opinion in Colloid & Interface Science 17(5), 246-254.

Solgar (2013). Available at: http://www.solgar.com/SolgarProducts/Nutri-Nano-CoQ-10-Alpha-Lipoic-Acid-Softgels.htm. Accessed 17 November 2013.

Sood S, Jain K & Gowthamarajan K (2014) Optimization of curcumin nanoemulsion for intranasal delivery using design of experiment and its toxicity assessment. Colloids and Surfaces B: Biointerfaces 113(0), 330-337.

Soottitantawat A, Yoshii H, Furuta T, Ohkawara M & Linko P (2003) Microencapsulation by Spray Drying: Influence of Emulsion Size on the Retention of Volatile Compounds. Journal of Food Science 68(7), 2256-2262.

Spernath A & Aserin A (2006) Microemulsions as carriers for drugs and nutraceuticals. Advances in Colloid and Interface Science 128-130, 47-64.

Sukhorukov GB, Donath E, Lichtenfeld H, Knippel E, Knippel M, Budde A & Möhwald H (1998) Layer-by-layer self assembly of polyelectrolytes on colloidal particles. Colloids and Surfaces A: Physicochemical and Engineering Aspects 137(1–3), 253-266.

Surh J, Gu YS, Decker EA & McClements DJ (2005) Influence of Environmental Stresses on Stability of O/W Emulsions Containing Cationic Droplets Stabilized by SDS,àíFish Gelatin Membranes. Journal of Agricultural and Food Chemistry 53(10), 4236-4244.

Szczepanowicz K, Bazylińska U, Pietkiewicz J, Szyk-Warszyńska L, Wilk KA & Warszyński P (in press) Biocompatible long-sustained release oil-core polyelectrolyte nanocarriers: From controlling physical state and stability to biological impact. Advances in Colloid and Interface Science.

Szczepanowicz K, Dronka-Góra D, Para G & Warszyński P (2010a) Encapsulation of liquid cores by layer-by-layer adsorption of polyelectrolytes. Journal of Microencapsulation 27(3), 198-204.

Szczepanowicz K, Hoel HJ, Szyk-Warszynska L, Bielańska E, Bouzga AM, Gaudernack G, Simon C & Warszynski P (2010b) Formation of Biocompatible Nanocapsules with Emulsion Core and Pegylated Shell by Polyelectrolyte Multilayer Adsorption. Langmuir 26(15), 12592-12597.

Szczepanowicz K, Podgórna K, Szyk-Warszyńska L & Warszyński P (2014) Formation of oil filled nanocapsules with silica shells modified by sequential adsorption of polyelectrolytes. Colloids and Surfaces A: Physicochemical and Engineering Aspects 441, 885-889.

Tadros T, Izquierdo P, Esquena J & Solans C (2004) Formation and stability of nano-emulsions. Advances in Colloid and Interface Science 108-109, 303-318.

Tan CP & Nakajima M (2005a) [beta]-Carotene nanodispersions: preparation, characterization and stability evaluation. Food Chemistry 92(4), 661-671.

Tan CP & Nakajima M (2005b) Effect of polyglycerol esters of fatty acids on physicochemical properties and stability of β-carotene nanodispersions prepared by emulsification/evaporation method. Journal of the Science of Food and Agriculture 85(1), 121-126.

Thanasukarn P, Pongsawatmanit R & McClements DJ (2004) Influence of emulsifier type on freeze-thaw stability of hydrogenated palm oil-in-water emulsions. Food Hydrocolloids 18(6), 1033-1043.

Truong T, Bansal N, Sharma R, Palmer M & Bhandari B (2014) Effects of emulsion droplet sizes on the crystallisation of milk fat. Food Chemistry 145(0), 725-735.

USDA (2015). USDA Awards $3.8 Million in Grants for Nanotechnology Research, Available at: http://nifa.usda.gov/sites/default/files/resource/AFRI Nanotech Release 2015 Fact Sheet P1.pdf. Accessed 18/09/2015.

Usón N, Garcia MJ & Solans C (2004) Formation of water-in-oil (W/O) nano-emulsions in a water/mixed non-ionic surfactant/oil systems prepared by a low-energy emulsification method. Colloids and Surfaces A: Physicochemical and Engineering Aspects 250(1-3), 415-421.

Vega C & Roos YH (2006) Invited review: spray-dried dairy and dairy-like – emulsions compositional considerations. Journal of Dairy Science 89(2), 383-401.

Velikov KP & Pelan E (2008) Colloidal delivery systems for micronutrients and nutraceuticals. Soft Matter 4(10), 1964-1980.

Venturini CG, Jäger E, Oliveira CP, Bernardi A, Battastini AMO, Guterres SS & Pohlmann AR Formulation of lipid core nanocapsules. Colloids and Surfaces A: Physicochemical and Engineering Aspects In Press, Corrected Proof.

Venturini CG, Jäger E, Oliveira CP, Bernardi A, Battastini AMO, Guterres SS & Pohlmann AR (2011) Formulation of lipid core nanocapsules. Colloids and Surfaces A: Physicochemical and Engineering Aspects 375(1-3), 200-208.

Walstra P (1993) Principles of emulsion formation. Chemical Engineering Science 48(2), 333-349.

Walstra P, (1996). Emulsion stability, in: Becher P (Ed.), *Encyclopedia of emulsion technology*. Marcel Dekker, New York, pp. 1 – 62.

Wang ZL (2000) Transmission Electron Microscopy of Shape-Controlled Nanocrystals and Their Assemblies. The Journal of Physical Chemistry B 104(6), 1153-1175.

Wild Flavors Inc (2013). Available at: http://www.wildflavors.com/EMEA-EN/products/natural-flavor-ingredients/colors-from-nature/. Accessed 20 September 2015.

Yang Y, Marshall-Breton C, Leser ME, Sher AA & McClements DJ (2012) Fabrication of ultrafine edible emulsions: Comparison of high-energy and low-energy homogenization methods. Food Hydrocolloids 29(2), 398-406.

Yi J, Li Y, Zhong F & Yokoyama W (2014) The physicochemical stability and in vitro bioaccessibility of beta-carotene in oil-in-water sodium caseinate emulsions. Food Hydrocolloids 35(0), 19-27.

Yin L-J, Chu B-S, Kobayashi I & Nakajima M (2009) Performance of selected emulsifiers and their combinations in the preparation of β-carotene nanodispersions. Food Hydrocolloids 23(6), 1617-1622.

Zhou G, (2013). Nanotechnology in the Food System: Consumer Acceptance and Willingness to Pay, *Agricultural Economics*. University of Kentucky.

Ziani K, Fang Y & McClements DJ (2012) Encapsulation of functional lipophilic components in surfactant-based colloidal delivery systems: Vitamin E, vitamin D, and lemon oil. Food Chemistry 134(2), 1106-1112.

CHAPTER 3

INFLUENCE OF SURFACTANT AND PROCESSING CONDITIONS IN THE STABILITY OF OIL-IN-WATER NANOEMULSIONS

This chapter evaluates the influence of the type of surfactant (Tween 20, SDS and DTAB) and processing conditions (pressure, number of cycles and oil-to-water volume ratio) on the stability of oil-in-water nanoemulsions, through the determination of hydrodynamic diameter (H_d), polydispersity index (PdI) and zeta potential (Zp).

This Chapter was adapted from:

Silva, H. D., Cerqueira, M. A. & Vicente, A. A. (2015). Influence of surfactant and processing conditions in the stability of oil-in-water nanoemulsions. *Journal of Food Engineering,* 167(Part B), 89-98.

3.1 Introduction

Driven by consumers' demands for new and healthier food products the food industry seeks for new methodologies able to encapsulate, protect and release functional compounds. Based on this, researchers are focusing their efforts in relevant issues to food and nutrition regarding the improvement of food quality, through nanotechnology (Cerqueira et al., 2013; Silva et al., 2012).

Nanoemulsions are interesting for the food industry due to their potential applications as delivery systems of bioactive compounds while preventing their degradation and improving their bioavailability (Donsì et al., 2011; Guttoff et al., 2015; Silva et al., 2012). Nanoemulsions generally consist of lipid droplets between 10 and 200 nm dispersed in an aqueous phase, where surfactant molecules surround each oil droplet (Acosta, 2009; Cerqueira et al., 2014). Nanoemulsions can be produced using either low-energy or high-energy methods. Low-energy methods mainly depend on the intrinsic physicochemical properties of surfactants and oily phase, forming nanoemulsions by simple mixing procedures or by changing the system conditions such as temperature or composition (Komaiko and McClements, 2015; Silva et al., 2012; Solans and Solé, 2012). High-energy methods make use of devices that apply high mechanical energy inputs to disrupt and combine the oil and water phases, forming small droplets (Abbas et al., 2013; Cerqueira et al., 2014; Komaiko and McClements, 2015; Silva et al., 2012). High-pressure homogenization is pointed as the most appropriate method for industrial applications, due to the facility of operation, scalability, reproducibility, and high throughput (Cerqueira et al., 2014; Donsì et al., 2011).

Preparing a nanoemulsion by a high-energy method implies using an oily and an aqueous phase, a surfactant and energy (Tadros et al., 2004; Walstra, 1993). The nano emulsification process by high-pressure homogenization comprises both the deformation and disruption of the droplets with the subsequent increase of the surface area and at the same time the droplet stabilization occurs by means of adsorption of the emulsifiers at the interface of the droplets (Donsì et al., 2011; Stang et al., 2001). The difference in the interfacial free energy between the initial and final state is by definition equal to the increase on the surface area between the oily and aqueous phases

multiplied by the interfacial tension (McClements, 2005). The energy necessary to increase the interfacial area ($\gamma\Delta A$) is very high and positive (i.e. it increases after homogenization), while the small entropy of the dispersion, and the corresponding energy ($T\Delta S$) is also positive but cannot compensate the interfacial free energy (McClements, 2005; Schramm, 2006b; Tadros et al., 2004) and therefore Eq. 3.1 is always positive.

$$\Delta G_{formation} = \gamma \Delta A - T\Delta S \quad \text{Eq. 3.1}$$

Thus nanoemulsion formation is always thermodynamically unfavourable, due to the increase of the interfacial area after emulsification and to the energy required to produce the droplets (McClements, 2005; Tadros et al., 2004; Walstra, 1993). In order to break up a droplet into smaller ones, it must be strongly deformed and this is opposed by the Laplace pressure, Δp, which is the difference in pressure between the inside and outside of the droplet, being the pressure greater on the inside of the droplet, given by:

$$\Delta p = \gamma(1/R_1 + 1/R_2) \quad \text{Eq. 3.2}$$

Where R_1 and R_2 are the principal radii of curvature of the droplet. For a nanoemulsion, a spherical droplet yields $R_1 = R_2 = R$ (Schramm, 2006b; Tadros et al., 2004; Walstra, 1993).

$$\Delta p = 2\gamma/R \quad \text{Eq. 3.3}$$

Eq. 3.3 shows that the amount of energy needed to break the droplets increases when smaller droplets are produced; however, when lowering the interfacial tension Δp is reduced and therefore the amount of energy needed to break up a droplet is reduced. Lowering the interfacial tension is one of the roles of the surfactants; nevertheless, their most essential role is preventing the coalescence of the newly formed droplets (Schramm, 2006b; Tadros et al., 2004; Walstra, 1993).

Surfactants preferentially adsorbs to the interfaces, once their molecular structures have non-polar hydrocarbon tails that favour non-polar liquids.

Lowering the interfacial tension they will minimize the interfacial area between the continuous and dispersed phases and keep the interfaces smooth (Mason et al., 2006). Low molecular weight surfactants are able to decrease the interfacial tension in a greater extension than high molecular weight surfactants. This is mainly due differences in the orientation and configuration of the surfactants at the interface (Sari et al., 2015). Low molecular weight surfactants entirely adsorb and instantaneously orient themselves and the partitioning of the entire molecule between the two phases facilitates a maximum reduction in the interfacial tension (Sari et al., 2015). Also, a significant excess of surfactant in the continuous phase is needed this enables the new surface area of droplets to be quickly coated during emulsification, inhibiting disruption induced coalescence. This generally forms surfactant micelles that dissociate into monomers that rapidly adsorbs to the surface of the droplets (Mason et al., 2006; Rao and McClements, 2012). After adsorption of the surfactant to the surface of a droplet, surfactants most provide repulsive forces strong enough to prevent droplets aggregation. Ionic surfactants provide a great stability due electrostatic repulsions between droplets. Non-ionic surfactants provide stability due short-range repulsive forces, such as steric overlap, hydration, thermal fluctuation interactions, that prevents droplets from getting to close. Briefly, a surfactant must have three characteristics to be effective, first, rapidly adsorption to the surface of the new droplets; second, drastically reduce the interfacial tension and third form a membrane that prevents droplets from aggregating (McClements, 2002).

One of the aims of this work was to study the effects of different charge surfactants, an anionic surfactant, Sodium Dodecyl Sulphate (SDS); a cationic surfactant, dodecyltrimethylammonium bromide (DTAB) and a non-ionic surfactant, Tween 20. The effect of the process conditions i.e., pressure, number of cycles, surfactant concentrations and oil content in the mean hydrodynamic diameter (H_d), polydispersity index (*PdI*), zeta potential (*Zp*) and the stability of the nanoemulsion were also evaluated. Furthermore, the theoretical minimum mean droplet diameter, creaming, the specific surface area and the energy dispended to produce the nanoemulsions were evaluated.

The surfactants used in this study were applied as model surfactants based on their different charge. Despite, they are commonly used in biotechnology and

cosmetics industry, for EFSA, SDS and DTAB cannot be applied in foods, while Tween 20 is consider a food additive (EFSA, 2010). Nevertheless, considering FDA regulation SDS can be applied in food products as surfactant in fruit juice drinks under 25 ppm and in coatings on fresh citrus fruit (FDA, 2014a, b). Regarding DTAB, it can be used as an indirect food additives: adjuvants, production aids and sanitizers in contact with food products (FDA, 2014c).

3.2 Materials and Methods

3.2.1 Materials

Neobee 1053 medium chain triglycerides (MCTs) is caprylic/capric triglyceride oil with a fatty acid distribution of 55 % of C8:0 and 44 % of C10:0 was kindly provided by Stepan (The Netherlands) and was used without further purification. Tween 20 and SDS were purchased from Sigma-Aldrich (St Louis, MO, USA) and DTAB was acquired from Acros Organics (Geel, Belgium). Milli-Q water (Milli-Q apparatus, Millipore Corp., Bedford, MA, USA) was used to prepare all solutions.

3.2.2 Experimental Procedures

3.2.2.1. Preparation of non-ionic, cationic and anionic nanoemulsions by high-pressure homogenization

Oil-in-water (O/W) emulsions were prepared according to (Pinheiro et al., 2013) with some modifications. Briefly, the nanoemulsions were pre-mixed during 2 min at 5000 rpm using an Ultra-Turrax homogenizer (T 25, Ika-Werke, Germany) followed by passage through a high-pressure homogenizer (Nano DeBEE, BEE International, USA) according to the fractional factorial design (Table 3.1). To assess the effect of operational conditions on emulsion stability at the nanoscale, samples were evaluated during a 28, 35 and 365 days of storage. The stability at day 365 was only performed for the nanoemulsions with the best stability results at day 35. The produced emulsions were stored at 4 ºC in the absence of light, during the evaluation period.

3.2.2.2 Kinetic stability studies

Kinetic stability studies were performed through centrifugation, heating-cooling cycle and thermal stress as followed:

Centrifugation: formulations were centrifuged at 5000 *g* for 30 min. Those formulations that did not show any phase separation were taken for the heating-cooling cycle test.

Heating-cooling cycle: formulations were subjected to six cycles between 4 ºC and 45 ºC with a storage time higher than 48 h at each temperature. Those formulations, which were stable at these temperatures cycles, were further taken for size measurements (Shafiq et al., 2007).

Thermal stress: The influence of temperature on nanoemulsions stability was examined through DLS technique, by measuring the H_d of the nanoemulsions. Briefly, 1 mL of the formulations were submitted to a range of temperatures from 20 to 80 ºC, with increasing intervals of 10 ºC, during 10 min at each condition (Morais Diane and Burgess, 2014). The temperature was adjusted using a Nano ZS-90 equipment (Zetasizer Nano ZS-90, Malvern Instruments, Worcestershire, UK). The data was reported as the H_d, average ± standard deviation of three values obtained.

3.2.2.3 Nanoemulsion size measurements

The particle size distribution and *PdI* of nanoemulsions were determined using DLS (Zetasizer Nano ZS-90, Malvern Instruments, Worcestershire, UK). The nanoemulsion samples were diluted 10× in distilled water at ambient temperature. The data was reported as the mean droplet diameter (hydrodynamic diameter, H_d). *PdI* is a dimensionless and indicates the heterogeneity (monodisperse or polydisperse) of sizes of particles in a mixture (Malvern, 2011). Each sample was analysed in a disposable polystyrene cell (DTS0012, Malvern Instruments). The measurements were performed in duplicate, with three readings for each of them. The results are given as the average ± standard deviation of the six values obtained (Rao and McClements, 2013; Silva et al., 2011).

3.2.2.4. Nanoemulsion charge measurements

The droplet charge (*Zp*) of the nanoemulsions was determined using a particle micro-electrophoresis instrument (Zetasizer Nano ZS-90, Malvern Instruments, Worcestershire, UK). Samples were diluted 100× in distilled water prior to measurements in order to avoid multiple scattering effects at ambient temperature and placing the diluted emulsions into disposable capillary cells (DTS 1060, Malvern Instruments) (Ozturk et al., 2014; Rao and McClements, 2013).

3.2.2.5 Nanoemulsion creaming rate

Ten grams of nanoemulsion were transferred into a 15 mL conical centrifuge tube (Falcon™, Fisher Scientific), tightly sealed with a plastic cap, and then stored at 4 ºC) for approximately 24 h, 1 month, 3 months and 1 year. After storage, several emulsions separated into an opaque layer at the top, a turbid layer in the middle, and a transparent layer at the bottom. The “serum layer” was defined to be the sum of the turbid and transparent layers. The total height of the emulsion (*HE*) and the height of the serum layer (*HS*) were measured using a ruler (Li et al., 2010).

3.2.2.6 Microscopy

The morphology of nanoemulsions was evaluated by transmission electron microscopy (TEM) (EM 902A, ZEISS, Germany) operating at 80 kV. TEM samples were prepared by depositing the nanoemulsion suspensions on a carbon-coated copper grid, and negatively stained with 1 % (w/v) uranyl acetate for observation. Samples were air-dried before analyses.

3.2.2.7 Nanoemulsions viscosity measurements

Viscosity measurements of the nanoemulsion samples were conducted using a dynamic shear rheometer (TA Instruments, New Castle, DE) with a shear rate profile from 0.1 to 1000 s^{-1}. All the measurements were performed at 25 ºC. The values of these measurements were applied to equations 3.7 and 3.8.

3.2.2.8 Nanoemulsions density measurements

Density measurements of the nanoemulsion samples were conducted using a density-meter Densito 30PX (Mettler-Toledo, Inc., Columbus, OH) at 25 ºC. The values of these measurements were applied to equations 3.6, 3.7 and 3.8.

3.2.2.9 Nanoemulsions interfacial tension measurements

The interfacial tension of the nanoemulsions solution was measured by the pendant drop method using the Laplace–Young approximation, (Song and Springer, 1996), with a face contact angle meter (OCA 20, Dataphysics, Germany). The samples of the coatings were taken with a 500 µL syringe (Hamilton, Switzerland), with a needle of 0.75 mm of diameter. Three replicates were performed at 20 ºC. The values of these measurements were used in equations 3.1, 3.2 and 3.3.

3.2.3 Statistical procedures

3.2.3.1 Experimental Design

A multifactor model (2^4 fractional factorial design) was used to evaluate the independent variables (see Table 3.1): homogenization pressure (10000 to 20000 Psi), surfactant concentration (0.5 % to 1.5 % w/w), ratio between oily and water phase (O/W ratio) (5 % to 15 % v/v) and cycles between each homogenization (10 to 30) and evaluate the main effects and interaction effects of these formulations on the H_d, *PdI* and *Zp*. A total of 11 experiments for each surfactant were conducted with 3 centre points (in order to allow the estimation of pure error).

3.2.3.2 Data Analyses

Data analyses were performed using Microsoft Windows Excel 2011, using the Tukey's Multiple Comparison Test with a confidence interval of 95 % in GraphPad Prism 5 (GraphPad Software, Inc.) and using ANOVA in STATISTICA 7.0 (Statsoft, Tulsa, OK, USA).

Table 3.1 – Independent variables used in the 2^4 fractional factorial design: Pressure of homogenization (*expressed in terms of* Psi), number of cycles between each homogenization, surfactant concentration (expressed in % wt) and oil to water (O/W) volume ratio (expressed in % vol)

Sample	Pressure (Psi*1000)	Cycles	Surfactant	O/W ratio (% vol)
1	10	10	0.5	5
2	20	10	0.5	15
3	10	30	0.5	15
4	20	30	0.5	5
5	10	10	1.5	15
6	20	10	1.5	5
7	10	30	1.5	5
8	20	30	1.5	15
9	15	20	1	10
10	15	20	1	10
11	15	20	1	10

3.3 Results and Discussion

3.3.1 Effect of process conditions on nanoemulsions

The combination of surfactant and a high-energy homogenization process (using an Ultra-Turrax as a premix step followed by a high-pressure homogenization process) allowed the formation of nanoemulsions with different characteristics. For an initial screening, the H_d, *PdI* and *Zp* of nanoemulsions are the most studied parameters, once they give accurate information about the formed nanoemulsions and their stability (Cheong et al., 2008; Sood et al., 2014; Tan and Nakajima, 2005).

Table 3.2 shows the values of H_d for the nanoemulsions produced with Tween 20, SDS and DTAB. Values ranged between 171 to 341 nm for nanoemulsions produced with Tween 20; between 126 to 177 nm when produced with SDS and between 135 to 198 nm for DTAB. TEM confirmed the development of these nanoemulsions and validated the mean droplet diameters

achieved. As example Figure 3.1 presents a TEM microphotograph of the anionic (figure 3.1a), cationic (figure 3.1b) and non-ionic (figure 3.1c) nanoemulsions produced using the high-pressure homogenization technique at 1 % wt of surfactant, dispersed in the aqueous phase, and MCTs oil as the organic phase at 15 000 Psi, during 20 cycles. Also, TEM was performed to observe the morphology of the different charge nanoemulsions. In Figure 3.1a it is possible to see oil-droplet aggregations due dehydration conditions after the use of uranyl and sample preparation.

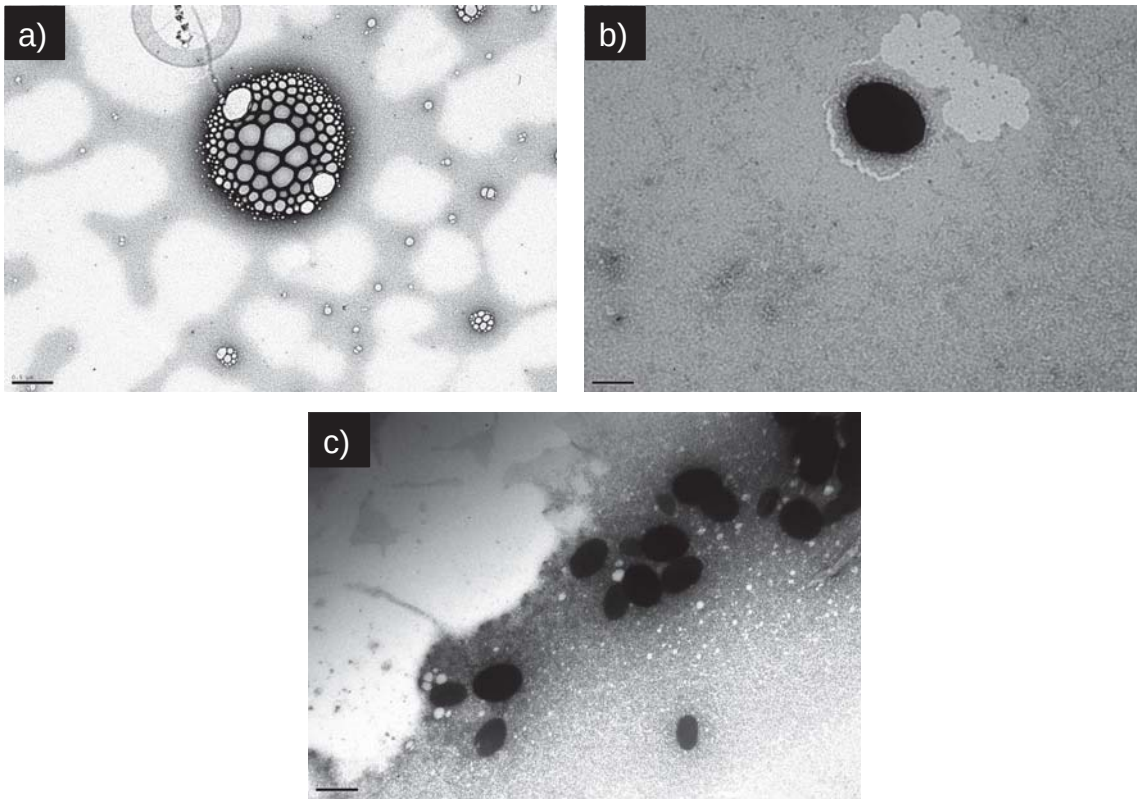

Figure 3.1 – TEM microphotograph of negatively stained nanoemulsions with uranyl 1 % w/w. a) anionic nanoemulsion; b) cationic nanoemulsion and c) non-ionic nanoemulsion.

In order to study the most influent factors on the dependent parameters (H_d, *PdI* and *Zp*) a multifactor model 2^4 was used, being the results analysed using ANOVA, which identifies the significant factors that affect the responses (Table 3.3). Results show that H_d is significantly influenced (p<0.05) by the homogenization pressure when SDS is used as surfactant; nevertheless, when DTAB was used as surfactants for the nanoemulsion production, H_d is significantly influenced (p<0.05) by homogenization pressure, surfactant

concentration and O/W ratio. In the case of nanoemulsions produced with Tween 20, H_d is significantly influenced (p<0.05) by homogenization pressure, the interaction between the homogenization pressure and the O/W ratio, by the surfactant concentration and the number of cycles. The nanoemulsions produced with SDS achieved the smallest value of H_d, followed by the nanoemulsions produced with DTAB and Tween 20, respectively. The differences in H_d values for the three surfactants used can be attributed to the molecular weight (M_w) of the surfactants (SDS < DTAB < Tween 20). In general small molecule surfactants can lead, under similar processing conditions, to smaller H_d values, which has been attributed to differences in adsorption rates (faster adsorption rates result in smaller sizes) and in interfacial properties (such as thickness, charge, permeability, and environmental responsiveness) (Donsì et al., 2011; McClements, 2010; Qian and McClements, 2011). Also, lowering the interfacial tension through the use of surfactants may facilitate droplet deformation and disruption (Brösel and Schubert, 1999).

As shown in Table 3.2 the mean H_d of nanoemulsions decreases with the increase of homogenization pressure and number of cycles. This behaviour is explained by the high intensity of shear forces produced during the homogenization process (Tan and Nakajima 2005). Also, increasing the homogenization pressure and the number of cycles will lead to a higher specific energy, *Ev* (Eq. 3.4), delivered to the emulsion by the high-pressure homogenizer, which is the mechanical energy input per unit of volume of the chamber where the droplets are disrupted. *Ev* can be calculated by the homogenization pressure (ΔP) times the number of cycles (n) (Donsì et al., 2011; Stang et al., 2001). This indicates that further increases of the dispersion energy levels lead to even smaller nanoemulsions (Donsì et al., 2011; Silva et al., 2011).

$$E_v = \Delta P * \mathrm{n} \qquad \text{Eq. 3.4}$$

Tables 3.2 and 3.3 present the H_d, *PdI* and *Zp* values of the produced nanoemulsions and showed that the increase of surfactant concentrations leads to lower values of H_d. This is due to the fact that more surfactant is present to cover any new droplet surfaces formed during homogenization and because the

droplet surfaces will be covered more quickly by the surfactants (Qian and McClements, 2011). Also, higher surfactant concentrations increase the interfacial area, while reducing the interfacial tension, leading to lower droplet sizes (Anton et al., 2007; Esquena et al., 2003; Liu et al., 2006).

Table 3.2 – Experimental H_d, *PdI* and *Zp* values for nanoemulsions produced with SDS, Tween 20 and DTAB as surfactants immediately after production, for the fractional factorial design

	SDS day 0			DTAB day 0			Tween 20 day 0		
Sample	H_d (nm)	*Zp* (mV)	*PdI*	H_d (nm)	*Zp* (mV)	*PdI*	H_d (nm)	*Zp* (mV)	*PdI*
1	168.6 ± 1.1	-69.4 ± 1.2	0.135 ± 0.01	174.9 ± 5.0	64.8 ± 0.3	0.158 ± 0.01	257.8 ± 2.7	-15.3 ± 1.0	0.242 ± 0.01
2	141 ± 4.6	-66.2 ± 1.8	0.150 ± 0.02	197.6 ± 5.5	43.0 ± 0.5	0.195 ± 0.02	171.2 ± 4.6	-30.1 ± 4.8	0.164 ± 0.01
3	147.7 ± 3.5	-69.3 ± 1.2	0.131 ± 0.01	187 ± 5.6	43.1 ± 2.4	0.202 ± 0.01	341.2 ± 8.1	-23.1 ± 0.7	0.224 ± 0.02
4	128.9 ± 3.7	-78.7 ± 1.7	0.153 ± 0.01	172.4 ± 4.8	71.0 ± 1.2	0.147 ± 0.01	323.3 ± 4.7	-16.6 ± 3.5	0.210 ± 0.01
5	177.1 ± 3.9	-73.1 ± 2.3	0.179 ± 0.02	163.0 ± 4.7	71.2 ± 2.5	0.148 ± 0.01	277.9 ± 8.8	-25.0 ± 0.5	0.236 ± 0.01
6	136.5 ± 5.3	-68.2 ± 1.9	0.130 ± 0.01	141.2 ± 3.4	70.3 ± 2.9	0.146 ± 0.01	256.2 ± 10.5	-20.1 ± 2.4	0.181 ± 0.02
7	157.5 ± 3.6	-84.2 ± 0.4	0.119 ± 0.01	134.9 ± 2.9	73.1 ± 3.1	0.171 ± 0.01	215.5 ± 6.1	-27.5 ± 1.0	0.177 ± 0.03
8	126.6 ± 3.8	-73.7 ± 2.2	0.148 ± 0.02	153.9 ± 4.8	74.6 ± 2.2	0.179 ± 0.01	195.8 ± 5.8	-20.4 ± 2.2	0.197 ± 0.01
CP	140.6 ± 12.3	-73.5 ± 3.8	0.145 ± 0.02	156.3 ± 2.7	75.7 ± 0.5	0.197 ± 0.02	237.4 ± 6.4	-24.7 ± 2.0	0.192 ± 0.01

Each value represents mean ± SD (n = 3); CP – Central point; H_d – Hydrodynamic diameter; *Zp* – Zeta potential; *PdI* – Polydispersity index.

Table 3.2 shows *PdI* values obtained for nanoemulsions, which ranges from 0.164 to 0.242, 0.119 to 0.179 and 0.146 to 0.202 for Tween 20, SDS and DTAB, respectively. The efficiency of droplet disruption increased for higher specific energy (i.e. homogenization pressure times the number of cycles), at the most severe conditions the smallest mean droplet diameter was achieved, nevertheless for the *PdI* this did not happen. This is due the fact that *PdI* may also be depend on emulsifier surface and dynamic properties (Donsì et al., 2011). Donsì et al. (2011) also verified that *PdI* was mainly affected by the kinetics of surface adsorption of the emulsifier.

ANOVA results (Table 3) show that the homogenization pressure significantly influenced (p<0.05) the *PdI* values of nanoemulsions produced with the different surfactants (SDS, DTAB and Tween 20). For the nanoemulsions produced with Tween 20 the interaction between pressure and O/W ratio and the interaction between pressure and the number of cycles also significantly influenced (p<0.05) *PdI* values. Regarding the nanoemulsions produced with DTAB, the interaction between pressure and O/W ratio and the interaction between pressure and the number of cycles also significantly influenced (p<0.05) *PdI*, as also did the number of cycles (p<0.05).

The influence of processing conditions on *Zp* was also evaluated, being of extremely importance due to the different charges of the surfactants used. *Zp* values ranged from -15 to -30 mV for nanoemulsions produced with Tween 20, a non-ionic surfactant. The high values of *Zp* obtained for the nanoemulsions produced with Tween 20 may be explained by the composition of the MCTs oil (free fatty acids and salts) and by the presence of MCTs oil at the interface of the surfactant, even at equilibrium, there is a continuous exchange of molecules between the interior of the droplets, the continuous phase and the interface, that will occur at a rate dependent of the mass transport of the molecules through the system (McClements, 2005). For nanoemulsions produced with SDS, an anionic surfactant, *Zp* values ranged between -66 mV to -84 mV. The *Zp* of the nanoemulsion has a negative value due to the presence of head sulphate groups of SDS molecules (Jadhav et al., 2015). Nanoemulsions produced with DTAB (cationic surfactant) displayed *Zp* values ranging from 43 mV to 76 mV. ANOVA results showed that the process parameters did not significantly influenced *Zp* for all the developed nanoemulsions (Table 3.3). These electrical

charges were expected as Tween 20, SDS and DTAB are non-ionic, anionic and cationic emulsifiers, respectively (Pinheiro et al., 2013).

Table 3.3 – ANOVA results for dependent parameters estimation

	Independent variable	*p*-value SDS	*p*-value Tween	*p*-value DTAB
H_d	Pressure	0.047301	0.014975	0.028920
	Pressure by O/W ratio	-	0.002528	-
	Surfactant concentration	-	0.014530	0.004790
	Cycles	-	0.024731	-
	Ratio	-	-	0.013720
PdI	Pressure	0.048942	0.013272	0.030854
	Pressure by O/W ratio	-	0.040542	0.010941
	Pressure by cycles	-	0.011017	0.022267
	Cycles	-	-	0.009264
Zp	Pressure	0.041880	-	-
	Pressure by cycles	-	0.049921	-

3.3.2 Kinetic stability of nanoemulsions during storage

It is important to distinguish thermodynamic stability from kinetic stability; while thermodynamics will tell if a process will or not occur (no matter the time to complete it), kinetics will give information about the rate (what time scale) and the degree of change, if it occurs. Kinetic stability tests were carried out to eliminate any unstable formulation, due to creaming or sedimentation. Tests were performed in terms of centrifugation and through heating and cooling cycles. Only those formulations that were found to be stable were selected for evaluation of H_d, *PdI* and *Zp* during storage (Table 3.4).

Table 3.4 – Experimental H_d values obtained for nanoemulsions produced with SDS, Tween 20 and DTAB as surfactants after 28 days of storage for the fractional factorial design

	SDS day 28			DTAB day 28			Tween 20 day 28		
Sample	H_d (nm)	Zp (mV)	*PdI*	H_d (nm)	Zp (mV)	*PdI*	H_d (nm)	Zp (mV)	*PdI*
1	159.8 ± 4.4	-61.2 ± 1.1	0.136 ± 0.03	172.0 ± 5.1	63.1 ± 0.8	0.168 ± 0.01	174.2 ± 2.4	-14.7 ± 0.1	0.194 ± 0.01
2	137.8 ± 3.0	-62.2 ± 1.3	0.141 ± 0.01	175.7 ± 1.4	58.3 ± 0.6	0.174 ± 0.01	166.1 ± 4.5	-32.3 ± 0.3	0.134 ± 0.01
3	147.4 ± 3.8	-62.3 ± 1.9	0.121 ± 0.01	194.8 ± 4.2	60.7 ± 0.9	0.185 ± 0.02	195.5 ± 6.8	-22.8 ± 1.1	0.197 ± 0.01
4	130.9 ± 4.6	-94.4 ± 1.9	0.165 ± 0.01	168.2 ± 2.0	67.0 ± 0.7	0.162 ± 0.01	253.9 ± 7.4	-15.1 ± 0.7	0.213 ± 0.01
5	164.6 ± 6.9	-63.5 ± 1.7	0.168 ± 0.03	159.9 ± 4.8	66.3 ± 1.9	0.156 ± 0.01	203.6 ± 3.7	-27.8 ± 0.4	0.131 ± 0.02
6	132.58± 2.6	-76.7 ± 2.3	0.141 ± 0.02	118.9 ± 1.5	76.8 ± 1.5	0.155 ± 0.02	245.9 ± 5.2	-19.5 ± 0.2	0.173 ± 0.01
7	159.4 ± 6.5	-62.5 ± 1.0	0.138 ± 0.01	142.9 ± 4.4	70.8 ± 1.9	0.227 ± 0.03	177.8 ± 4.2	-24.3 ± 0.3	0.140 ± 0.01
8	126.1 ± 5.2	-92.6 ± 1.8	0.139 ± 0.01	152.0 ± 3.1	74.9 ± 1.0	0.187 ± 0.01	196.7 ± 0.2	-25.7 ± 2.3	0.186 ± 0.01
CP	140.5 ± 4.0	-78.2 ± 1.4	0.155 ± 0.01	155.4 ± 3.0	73.6 ± 1.9	0.196 ± 0.01	204.6 ± 3.7	-26.3 ± 1.3	0.125 ± 0.01

Each value represents mean ± SD (n = 3); CP – Central point; Hd – Hydrodynamic diameter; Zp – Zeta potential; PdI – Polydispersity index.

3.3.2.1 Size distribution

Regarding centrifugation tests, all produced formulations (using all type of surfactants) showed no macroscopic instability phenomena (i.e. creaming or phase separation), and the sizes remained unchanged after centrifugation (data not shown), due to this all the formulations were subjected to the heating-cooling cycles. Once more the produced nanoemulsions showed no macroscopic instability phenomena (i.e. creaming or phase separation) and the sizes remained unchanged (data not shown) after the heating-cooling cycles' tests. Therefore, all formulations were evaluated by means of size stability during 28 days of storage, in order to evaluate the influence of the process conditions in the H_d during storage.

Table 3.4 shows the values of H_d, *PdI* and *Zp* of nanoemulsions after 28 days of storage. In general, it can be observed that these parameters remain unchanged after 28 days of storage. For the nanoemulsions produced with the anionic surfactant, SDS, only sample 5 shows an increase of 13 nm in size. Donsì et al. (2011) showed that SDS as a significantly short characteristic time for adsorbing to the oil-in-water interface, when compared to surfactants like polysorbates (e.g. Tween 20) (Donsì et al., 2011). Fast adsorption kinetics of the surfactant to the interface can significantly reduce the re-coalescence phenomena. This conjugated with the lower oil-in-water interfacial tension lead to stable nanoemulsions with size values ranged between 130 and 165 nm, depending on the processing conditions (Donsì et al., 2011).

The same behaviour was observed for nanoemulsions produced with DTAB (cationic surfactant), where the size values remained unchangeable during storage time. Li and McClements (2011) prepared stable nanoemulsions using DTAB, achieving size values of approximately 187 nm, indicating that these nanoemulsions were not susceptible to droplet aggregation; those authors also claim that the presence of DTAB in low concentrations increased the rate and extent the lipid digestion. One possible explanation is the fact that this surfactant may facilitate the adsorption of lipase to the nanoemulsion surface due to electrostatic attraction (Li and McClements, 2011). For nanoemulsions produced with the non-ionic surfactant, Tween 20, an increase in the size values of samples 1, 3, 4, 5 and 7 after storage was observed. This increase could be explained by the breakdown process of the emulsions, namely the

creaming effect, where the larger droplets move faster to the top of the container, due the fact that when the gravitational forces exceed the thermal motion of the droplets (Brownian motion) a concentration gradient is built up (Tadros, 2013). Silva et al. (2011) also found a similar behaviour for nanoemulsions produced with Tween 20. They showed that the samples with lower size values had a greater tendency to aggregate, since they were more susceptible to Brownian motion, which leads to a superior chance of collision, allowing aggregation to become a dominant mechanism for emulsion instability (Silva et al., 2011). The larger droplets produced when Tween 20 is used as surfactant can lead to lower nanoemulsion stability as measured in terms of particle size. These larger droplets result in lower specific surface areas, being more susceptible to surface area fluctuations, increasing creaming and coalescence phenomena (Tadros, 2013).

3.3.3 Selection of the most suitable process conditions

The results showed that for anionic nanoemulsions the smallest sizes were achieved using the highest pressure and highest number of cycles tested, 20000 Psi and 30 cycles of homogenization (Table 3.2). In fact, a higher homogenization pressure and number of cycles increase the specific energy delivered by the high-pressure homogenizer, which is responsible for increasing the disruption rates that, in the presence of enough surfactant, will lead to smaller sizes (Donsì et al., 2011). Nevertheless, performing a one-way ANOVA to the obtained size values it was possible to verify that there were no statistically significant differences between the results achieved with 15000 and 20000 Psi and between 20 and 30 cycles (p=0.2269). Being so, it can be concluded that 15000 Psi and 20 cycles are the most suitable process conditions to carry on the study of creaming during long-term storage. The surfactant concentration and the oil content did not show statistically significant differences in terms of H_d.

For the cationic nanoemulsions the most influent parameters were surfactant concentration (p=0.0048), followed by ratio between oily and aqueous phases (p=0.014) and pressure (p=0.0289). The increase of surfactant concentration leads to the formation of smaller nanoemulsions, once surfactant adsorption to the interface may lower the interfacial tension, resulting in a higher mechanical

resistance to rupture (McClements, 2005). Low oil content leads to the decrease of droplet size; this can be explained by the influence of oil in nanoemulsions viscosity (i.e. low oil content leads to lower viscosity values). Higher viscosities induce a flow resistance in the chamber of the high-pressure homogenizer diminishing the rate and efficiency of droplet disruption, leading to higher mean droplet sizes (McClements, 2005; Troncoso et al., 2012). For the nanoemulsions produced with non-ionic surfactant the significant parameters were the combination of pressure with oil content (p=0.0025), the surfactant concentration (p=0.0145), pressure (p=0.0150) and the number of cycles (p=0.0247). Here the increase in oil content lead to smaller H_d values, contrary to the usual assumption that the increase of the oil content increases H_d values due to the influence of oil in the viscosity (McClements, 2005; Troncoso et al., 2012). An increase in oil content results in the increase of the concentration of droplets (i.e. increase of the dispersed phase volume fraction) in an emulsion, which leads to higher frequency of droplet collisions and hence coalescence during emulsification. Also, the viscosity of the emulsion increases, which may change the flow from turbulent to laminar. The presence of more particles results in an increase of the velocity gradient. In turbulent flow, the increase of oil content can induce turbulence depression leading to larger droplet sizes. If the ratio between the surfactant and the continuous phase is constant, an increase in oil content results in a decrease of the surfactant concentration, resulting in larger droplets. Nevertheless, if the ratio between the surfactant concentration and the disperse phase is kept constant, then this is reversed, so at this point it is impossible to draw any conclusions regarding the mechanisms that may come into play (McClements, 2005; Schramm, 2006a; Tadros, 2013).

The selection of the most suitable process conditions for the three surfactants was rather difficult since for each surfactant different process parameters had different responses. However, due to the need to select one formulation for further study the central point formulation was selected (15000 Psi, 20 cycles, 1 % wt of surfactant and an oil content of 10% wt). The pressure of 20000 Psi and the 30 cycles of homogenization were not considered, due to the overheating that these conditions induced to the nanoemulsion solution, that could be harmful for bioactive compounds that could be encapsulated and that are heat sensitive. Also, increasing the pressure and the number of cycles

increases the energy consumption, which can increase the price of producing nanoemulsions. An oily/aqueous phase volume ratio of 10 % wt was used according to Silva et al. (2011) and Tan and Nakajima (2005). Tan and Nakajima (2005) studied the influence of phase ratios (1:9 and 2:8); as the oil content increases, the available surfactant decreases, reducing the number of molecules able to stabilize the formed droplets, thus favouring coalescence and resulting in higher mean droplet diameters. In addition, higher viscosity of the oily phase leads to a less favourable mixing efficiency (Tan and Nakajima, 2005).

3.3.4. Kinetic stability for the selected conditions

Kinetic stability tests are useful not only to provide information about the short-term stability of nanoemulsions, but also for predicting the long-term stability. The input of high temperature and centrifugal forces increases Brownian motion and allows the dispersed droplets to approach one another (McClements, 2005; Morais Diane and Burgess, 2014; Schramm, 2006b). Information such as the rate at which the properties of a nanoemulsion change with time (i.e. time dependence) is highly important for food industry (McClements, 2005; Schramm, 2006b; Walstra, 1993). The selected nanoemulsion formulations were studied in terms of centrifugation, heating-cooling cycles, creaming and size stability during storage (35 days) at 4 ºC. Creaming and size stability during storage were also evaluated after one year of storage at 4 ºC, in the absence of light.

Nanoemulsions produced with anionic, cationic and non-ionic surfactants showed no macroscopic sign of instability phenomena (i.e. creaming or phase separation) after centrifugation. The results showed that the nanoemulsions produced with the anionic, cationic and non-ionic surfactants maintained their mean droplet size and hence were stable even under a centrifugal stress of 5000 *g* (Table 3.5). Results showed that these nanoemulsions under centrifugal tests did not present statistically significant (p>0.05) differences in the values of H_d when compared to those maintained at 4 °C (see Table 3.5). Similar results were obtained following the heating-cooling tests (Table 3.5).

Table 3.5 – Experimental H_d and *PdI* values for nanoemulsions produced with SDS, Tween 20 and DTAB as surfactants after kinetic stability tests

	SDS		DTAB		Tween 20	
Treatment	H_d (nm)	*PdI*	H_d (nm)	*PdI*	H_d (nm)	*PdI*
After production	137.4 ± 0.6 [a]	0.128 ± 0.04 [a]	152.1 ± 2.1 [a]	0.178 ± 0.02 [a]	223.2 ± 1.4 [a]	0.218 ± 0.01 [a]
After centrifugation	134.8 ± 2.4 [a]	0.126 ± 0.03 [a]	155.4 ± 2.1 [a]	0.177 ± 0.01 [a]	225.6 ± 1.1 [a]	0.221 ± 0.02 [a]
After heating-cooling cycles	136.3 ± 3.0 [a]	0.121 ± 0.03 [a]	155.7 ± 2.6 [a]	0.176 ± 0.01 [a]	221.2 ± 4.6 [a]	0.217 ± 0.01 [a]
After 1 year of storage	138.5 ± 1.3 [a]	0.129 ± 0.05 [a]	n.a.	n.a.	n.a.	n.a.

Each value represents mean ± SD (n = 3). Tukey's Multiple Comparison Test with a confidence interval of 95 % was applied; [a] different letters between rows means values statistically different. n.a. – not available; H_d – Hydrodynamic diameter; *PdI* – Polydispersity index.

For the same process and formulation conditions nanoemulsions produced with SDS achieved lower sizes (i.e. H_d) compared to the cationic or non-ionic surfactant nanoemulsions (Figure 3.2). The differences in H_d values for the different surfactants can be attributed to the M_w of the surfactants (SDS < DTAB < Tween 20). In general small molecule surfactants can lead, under similar processing conditions, to smaller H_d values (Donsì et al., 2011; Qian and McClements, 2011). Within the homogenizer chambers small molecule surfactants are able to quickly adsorb to the newly formed droplets surface (Qian and McClements, 2011; Troncoso et al., 2012).

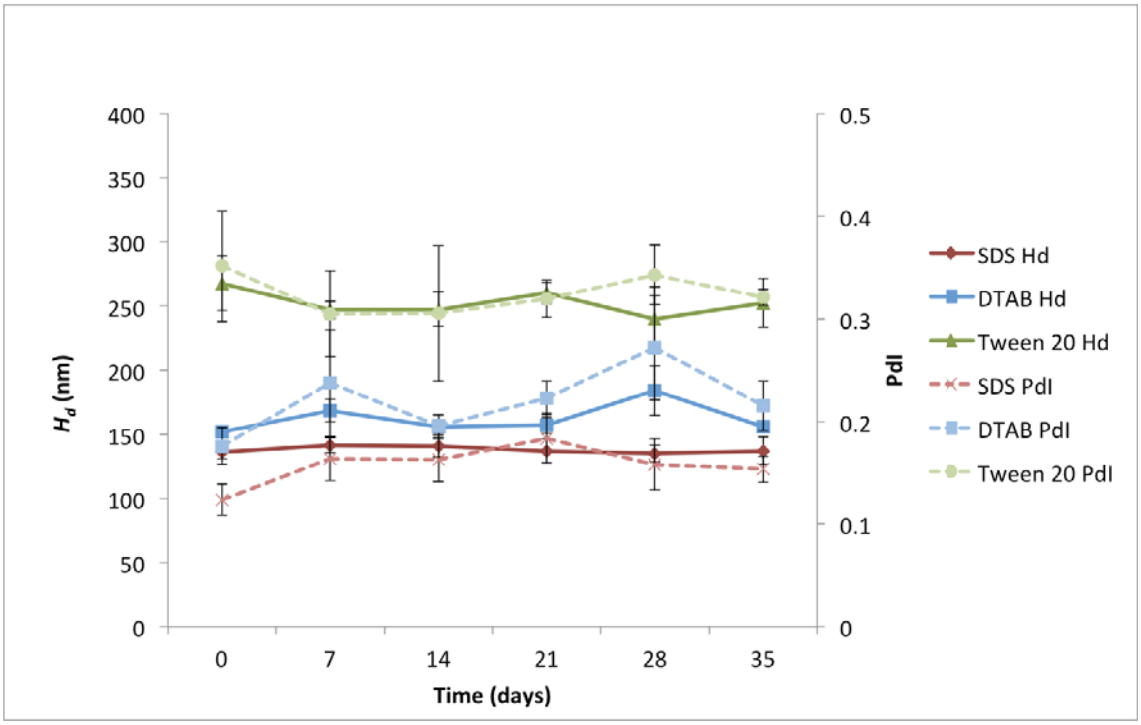

Figure 3.2 – Hydrodynamic diameter (H_d) and polydispersity index (*PdI*) during 35 days of storage. Bars indicate standard deviation (n = 3). Lines are for readers' guidance and do not represent a model prediction.

The theoretical minimum radius (R_{min}) of the produced nanoemulsions through high-pressure homogenization was calculated using Eq. 3.5.

$$R_{min} = (3 * \Gamma * \phi)/(c_s' * (1 - \phi)) \qquad \text{Eq. 3.5}$$

Here, Γ is the surface load of the surfactant at saturation (kg m^{-2}), ϕ is the disperse phase volume (dimensionless), and C'_s is the concentration of

surfactant at the continuous phase (kg m^{-3}) (Troncoso et al., 2012). The surface load of SDS, DTAB and Tween 20 were assumed as 1, 1 and 1.5 mg m^{-2}, respectively (Berton-Carabin et al., 2014). The minimum theoretical droplet diameter achieved was 67 nm for the anionic and cationic nanoemulsions and 100 nm for the non-ionic nanoemulsion. The experimental mean droplet diameter obtained in our study was 137 nm for the anionic nanoemulsion, 152 nm for the cationic nanoemulsion and 223 nm for the non-ionic nanoemulsion. These results are far from the theoretical ones, which suggests that there was not enough surfactant initially present to cover all droplets, or the homogenizer was incapable of generating enough disruptive forces for the process conditions used (Qian and McClements, 2011; Troncoso et al., 2012). The oil viscosity has an important role in the mean droplet sizes. Troncoso and co-workers (2012) showed that for more viscous oily phases the high-pressure homogenizer used to prepare the nanoemulsions was incapable of generating sufficiently intensive disruptive forces, while reducing the viscosity of the oil lead to similar results between the experimental work and the theoretical data (Troncoso et al., 2012).

Also the ability to lower oil:water interfacial tension and the faster kinetics of adsorption at the oil:water interface can explain the differences in the mean droplet size (Donsì et al., 2011). A decrease in interfacial tension, while leading to lower droplet sizes, also increases the surface area of nanoemulsions. The properties of colloidal systems' surface are very important and lead to unique physical properties (Schramm, 2006a, b, c). The specific surface area of nanoemulsions, considering n spheres of density ρ and radius R was determined (Eq. 3.6) for the selected conditions (Schramm, 2006a).

$$A_{sp} = 3/\rho R \qquad \text{Eq. 3.6}$$

The combination of high-pressure homogenization with the intrinsic properties of the anionic surfactant lead to a specific surface area of 44.3 m^2 g^{-1} of oil promoting, promoting an increase of ca. 37 000 times of the surface area which was of 0.0012 m^2 g^{-1} of oil before the high-pressure homogenization process. Higher specific surface areas (smaller droplets) are less susceptible to surface fluctuations and hence creaming and coalescence are reduced, explaining the

high stability of nanoemulsions (Tadros, 2013). As expected, due to the higher droplet sizes, cationic and non-ionic surfactants nanoemulsions had lower specific surface areas. The cationic nanoemulsion had 1.1 times less surface area when compared to the anionic nanoemulsion, achieving a specific surface area of 39.7 m^2 g^{-1} of oil. Non-ionic nanoemulsion had 1.9 times less surface area when compared to the anionic nanoemulsion, achieving a specific surface area of 22.6 m^2 g^{-1} of oil.

Consumers expect homogenous products, without the undesirable separation of emulsion into oily (opaque and rich in droplets) and aqueous phases (less opaque and without droplets). In order to evaluate emulsion homogeneity, creaming was determined after 1 year of storage at 4 ºC. Using Stokes equation (Eq. 3.7), where the terminal settling velocity (d*x*/d*t*) is proportional to gravity (*g*) and the square of particle size (*a*), and inversely proportional to the fluid viscosity (η), it is possible to predict the rate of creaming once it is proportional to the settling velocity.

$$(dx/dt) = (2a^2(\rho_2 - \rho_1)g)/(9\eta) \quad \text{Eq. 3.7}$$

Stokes law assumes that emulsions are uncharged and spherical; nevertheless, since the droplets will interact in the case of charged nanoemulsions stabilized with surfactants or polymers (opposite to what is assumed in Stokes' theory), underestimations or overestimations of the terminal velocity are expected (Schramm, 2006a). When the emulsions are charged an electrical potential is created; this speeds up the counter-ions and slows down the droplets, although this effect can be quickly dissipated at high enough electrolyte concentrations. Applying a correction factor to the Stokes' law it is possible to determine the settling velocity. Richardson-Zaki equation (Eq. 3.8) was applied for this, where Φ is the dispersed-phase volume fraction (Φ<1), for particles smaller than 1 µm in diameter the exponent found was 5.25 (Barnes, 1993; Schramm, 2006a).

$$(dx/dt)' = (dx/dt) * (1 - \phi)^{5.25} \quad \text{Eq. 3.8}$$

Anionic nanoemulsions showed no macroscopic sign of creaming or phase separation (Table 3.5); nevertheless, cationic and non-ionic nanoemulsions

presented a phase separation due to creaming with a height of 0.25 and 0.5 cm after 1 year of storage, respectively. The obtained creaming values for the nanoemulsions produced with Tween 20 are in agreement with the predicted values (0.42 cm $year^{-1}$); nevertheless, for anionic and cationic nanoemulsions the same behaviour was not verified. The predicted value for the cationic nanoemulsion was 0.09 cm $year^{-1}$, opposing to the obtained value of 0.25 cm $year^{-1}$. One possible explanation for this discrepancy is that even reducing droplet sizes to 155 nm this was not enough to overcome the density difference between dispersed and continuous phases. Here the gravitational forces exceed the Brownian motion, creating a concentration gradient that makes the larger droplets quickly move to the top of the container (Schramm, 2006a; Tadros, 2013). For the anionic nanoemulsion the predicted creaming value was 0.07 cm $year^{-1}$; nevertheless, no macroscopic sign of instability phenomena (i.e. creaming or phase separation) was visible. As the gravity force is proportional to R^3, if R is reduced 10 times the gravity force is reduced by 1000 times. Below 100 to 200 nm of droplet size (which also depends on the density difference between the oily and water phases), Brownian motion can exceed the gravity force and therefore creaming is prevented (Tadros, 2013). The smaller size obtained by the anionic nanoemulsions is one of the reasons that allow explaining why these nanoemulsions had higher stability than the cationic and non-ionic nanoemulsions. Also, increasing the surface charge of the droplets can slow down the creaming rate because of the increasing repulsive forces between the droplets (McClements, 2005).

After 1 year of storage at 4º C, the nanoemulsions produced with cationic and non-ionic surfactants showed visible creaming, presenting a creaming height of 0.25 and 0.5 cm, respectively (data not shown). The nanoemulsion produced with the anionic surfactant remained kinetically stable, without evidence of creaming and/or phase separation, showing an H_d of 138.5 nm.

Table 3.6 – Experimental H_d and *PdI* values for nanoemulsions produced with SDS, Tween 20 and DTAB as surfactants after thermal stress tests

	SDS		DTAB		Tween 20	
Treatment	H_d (nm)	*PdI*	H_d (nm)	*PdI*	H_d (nm)	*PdI*
After production	137.5 ± 0.2[a]	0.128 ± 0.04 [a]	152.1 ± 2.1 [a]	0.178 ± 0.02 [a]	223.2 ± 1.4 [a]	0.218 ± 0.01 [a]
20 ºC	138.1 ± 0.7 [a]	0.128 ± 0.01 [a]	153.4 ± 1.1 [a]	0.174 ± 0.02 [a]	223.3 ± 1.1 [a]	0.218 ± 0.01 [a]
30 ºC	139.0 ± 1.6 [a]	0.128 ± 0.02 [a]	156.2 ± 1.8 [a]	0.176 ± 0.01 [a]	226.8 ± 3.2 [a]	0.224 ± 0.06 [a]
40 ºC	139.5 ± 2.2 [a]	0.129 ± 0.02 [a]	157.6 ± 2.7 [a]	0.175 ± 0.02 [a]	225.5 ± 2.8 [a]	0.214 ± 0.03 [a]
50 ºC	139.0 ± 1.4 [a]	0.127 ± 0.01 [a]	155.6 ± 1.7 [a]	0.178 ± 0.03 [a]	224.3 ± 1.4 [a]	0.218 ± 0.01 [a]
60 ºC	138.2 ± 0.7 [a]	0.127 ± 0.03 [a]	157.5 ± 2.2 [a]	0.178 ± 0.01 [a]	227.7 ± 3.6 [a]	0.217 ± 0.02 [a]
70 ºC	139.6 ± 1.9 [a]	0.127 ± 0.01 [a]	155.7 ± 1.4 [a]	0.179 ± 0.02 [a]	226.6 ± 2.6 [a]	0.219 ± 0.01 [a]
80 º C	139.4 ± 2.1 [a]	0.126 ± 0.02 [a]	154.8 ± 1.9 [a]	0.178 ± 0.02 [a]	224.3 ± 1.6 [a]	0.219 ± 0.01 [a]

Each value represents mean ± SD (n = 3). Tukey's Multiple Comparison Test with a confidence interval of 95 % was applied; [a] different letters between rows means values statistically different; H_d – Hydrodynamic diameter; *PdI* – Polydispersity index.

3.3.5 Effect of temperature in size stability

The thermal stability tests performed to select nanoemulsions (please see topic 3.3.3) showed no macroscopic sign of instability phenomena (i.e. creaming or phase separation) after heating the samples from 20 to 80 ºC. For this test, H_d measurements were performed immediately after nanoemulsions' preparation and following the 30 min of heating at each temperature (20 to 80 ºC, refer to Table 3.6). Temperature increase did not have an immediate effect in the characteristics of nanoemulsions, e.g. statistical analysis showed that thermal stress did not provoke significant differences in the mean hydrodynamic diameter (Table 3.6). This is due the fact that unlike microemulsions, that change their morphology, size and shape as a function of temperature and/or composition, nanoemulsions stability is less sensitive to temperature increase, and this change does not promote a modification in the continuous phase, being the droplet sizes unchangeable (Anton and Vandamme, 2011; Gordon et al., 2014).

3.3.6 Energy consumption

One of the drawbacks of high-energy methods like high-pressure homogenization is the significant amount of energy required during the process (Tadros et al., 2004; Walstra, 1993). It is therefore important to evaluate the interfacial energy (Eq. 3.1), the mechanical energy (Eq. 3.4) and the % of energy dissipated into heat. Results showed that mechanical energy exceeded interfacial energy by several orders of magnitude. The interfacial energy values required for the formation of anionic, cationic and non-ionic nanoemulsions were 1.97, 1.92 and 0.91 J, respectively, while the mechanical energy was 2070 MJ for all the nanoemulsions. This means an efficiency of 0.1 %, while 99.9 % of the energy was dissipated as heat. These results are in agreement with the results present by Tadros et al. (2004) and Walstra (1993).

3.4 Conclusions

Homogenization pressure, surfactant type and oil concentration were found to be critical to achieve the desired hydrodynamic diameters, polydispersity index and zeta potential of nanoemulsions. Although nanoemulsions were produced at all levels of process and formulation parameters, the parameters' values for

the preparation of stable nanoemulsions with the smallest hydrodynamic diameter are: homogenization pressure of 20000 Psi, 20 cycles of homogenization, 1 % wt of surfactant and 10 % wt of oil. Results showed that differently charged nanoemulsions were kinetically stable during storage, 28 days (for fractional factorial design) and 35 days (for the selected formulations) at 4 ºC in terms of H_d, *PdI* and *Zp*. However, the anionic nanoemulsion displayed the highest stability against creaming after 1 year of storage. The use of small molecules' surfactants as SDS leads to smaller droplet sizes due to the faster adsorption kinetics to the interface that can reduce size and recoalescence phenomena. The increase of surface charge may slow down the creaming rate, due to the increase of the repulsive forces between droplets. This work showed that it is possible to tailor charged nanoemulsions' size through high-pressure homogenization and the appropriate choice of surfactant.

3.5 References

Abbas, S., Hayat, K., Karangwa, E., Bashari, M., Zhang, X., (2013). An Overview of Ultrasound-Assisted Food-Grade Nanoemulsions. Food Engineering Reviews 5(3), 139-157.

Acosta, E., (2009). Bioavailability of nanoparticles in nutrient and nutraceutical delivery. Current Opinion in Colloid & Interface Science 14, 3-15.

Anton, N., Gayet, P., Benoit, J.-P., Saulnier, P., (2007). Nano-emulsions and nanocapsules by the PIT method: An investigation on the role of the temperature cycling on the emulsion phase inversion. International Journal of Pharmaceutics 344(1-2), 44-52.

Anton, N., Vandamme, T., (2011). Nano-emulsions and Micro-emulsions: Clarifications of the Critical Differences. Pharmaceutical Research 28(5), 978-985.

AquaNova, (2013a). http://www.aquanova.de/media/public/pdf_produkte unkosher/NovaSOL_beverage.pdf.

AquaNova, (2013b). http://www.aquanova.de/media/public/pdf_produkte unkosher/NovaSOL_BCS.pdf.

Barnes, H.A.H., S.A., (1993). High Concentration Suspensions, in: Shamlou, P.A. (Ed.), *Preparation and Properties In Processing of Solid–Liquid Suspensions.* Butterworth-Heinemann, Boston, pp. 222–245.

Berton-Carabin, C.C., Ropers, M.-H., Genot, C., (2014). Lipid Oxidation in Oil-in-Water Emulsions: Involvement of the Interfacial Layer. Comprehensive Reviews in Food Science and Food Safety 13(5), 945-977.

Brösel, S., Schubert, H., (1999). Investigations on the role of surfactants in mechanical emulsification using a high-pressure homogenizer with an orifice valve. Chemical Engineering and Processing: Process Intensification 38(4–6), 533-540.

Cerqueira, M., Pinheiro, A., Silva, H., Ramos, P., Azevedo, M., Flores-López, M., Rivera, M., Bourbon, A., Ramos, Ó., Vicente, A., (2014). Design of Bio-nanosystems for Oral Delivery of Functional Compounds. Food Engineering Reviews 6(1-2), 1-19.

Cerqueira, M.A., Bourbon, A.I., Pinheiro, A.C., Silva, H.D., Quintas, M.A.C., Antonio, A.V., (2013). Edible Nano-Laminate Coatings for Food Applications,

Ecosustainable Polymer Nanomaterials for Food Packaging. CRC Press, pp. 221-252.

Cheong, J.N., Tan, C.P., Man, Y.B.C., Misran, M., (2008). [alpha]-Tocopherol nanodispersions: Preparation, characterization and stability evaluation. Journal of Food Engineering 89(2), 204-209.

Donsì, F., Sessa, M., Ferrari, G., (2011). Effect of Emulsifier Type and Disruption Chamber Geometry on the Fabrication of Food Nanoemulsions by High Pressure Homogenization. Industrial & Engineering Chemistry Research 51(22), 7606-7618.

EFSA, (2010). Call for scientific data on food additives permitted in the EU and belonging to the functional classes of emulsifiers, stabilisers and gelling agents.

Esquena, J., Sankar, Solans, C., (2003). Highly Concentrated W/O Emulsions Prepared by the PIT Method as Templates for Solid Foams. Langmuir 19(7), 2983-2988.

FDA, (2014a). CFR - Code of Federal Regulations Title 21.

FDA, (2014b). CFR - Code of Federal Regulations Title 21 - Food and Drugs.

FDA, (2014c). CFR - Code of Federal Regulations Title 21 - indirect food additives: adjuvants, production aids and sanitizers.

Gordon, V., Marom, G., Magdassi, S., (2014). Formation of hydrophilic nanofibers from nanoemulsions through electrospinning. Int J Pharm 478(1), 172-179.

Guttoff, M., Saberi, A.H., McClements, D.J., (2015). Formation of vitamin D nanoemulsion-based delivery systems by spontaneous emulsification: factors affecting particle size and stability. Food Chem 171(0), 117-122.

High Vive, (2013). http://www.highvive.com/sunactiveiron.htm.

Improveat, (2014). http://www.improveat.pt/en/products/.

Jadhav, A.J., Holkar, C.R., Karekar, S.E., Pinjari, D.V., Pandit, A.B., (2015). Ultrasound assisted manufacturing of paraffin wax nanoemulsions: process optimization. Ultrason Sonochem 23(0), 201-207.

Komaiko, J., McClements, D.J., (2015). Low-energy formation of edible nanoemulsions by spontaneous emulsification: Factors influencing particle size. Journal of Food Engineering 146(0), 122-128.

Li, Y., Hu, M., Xiao, H., Du, Y., Decker, E.A., McClements, D.J., (2010). Controlling the functional performance of emulsion-based delivery systems

using multi-component biopolymer coatings. European Journal of Pharmaceutics and Biopharmaceutics 76(1), 38-47.

Li, Y., McClements, D.J., (2011). Inhibition of lipase-catalyzed hydrolysis of emulsified triglyceride oils by low-molecular weight surfactants under simulated gastrointestinal conditions. European Journal of Pharmaceutics and Biopharmaceutics 79(2), 423-431.

Life Enhancement, (2013). http://www.life-enhancement.com/shop/product/nsr-nanoresveratrol.

Liu, W., Sun, D., Li, C., Liu, Q., Xu, J., (2006). Formation and stability of paraffin oil-in-water nano-emulsions prepared by the emulsion inversion point method. Journal of Colloid and Interface Science 303(2), 557-563.

Malvern, I., (2011). Dynamic light scattering common terms defined, in: Instruments, M. (Ed.), Worcestershire, UK.

Mason, T.G., Wilking, J.N., Meleson, K., Chang, C.B., Graves, S.M., (2006). Nanoemulsions: formation, structure, and physical properties. Journal of Physics: Condensed Matter 18(41), R635.

McClements, D., (2005). Food Emulsions: Principles, Practice, and Techniques., 2nd ed. CRC Press, Boca Raton, Florida.

McClements, D.J., (2002). Lipid-Based Emulsions and Emulsifiers, *Food Lipids*. CRC Press.

McClements, D.J., (2010). Emulsion Design to Improve the Delivery of Functional Lipophilic Components. Annual Review of Food Science and Technology 1(1), 241-269.

Morais Diane, J.M., Burgess, J., (2014). Vitamin E nanoemulsions characterization and analysis. International Journal of Pharmaceutics 465(1–2), 455-463.

NanoSinergy, (2013). http://sprayforlife.com/.

NutraLease, (2011). http://www.nutralease.com/Nutra/Templates/showpage.asp?DBID=1&LNGID=1&TMID=84&FID=767.

Ozturk, B., Argin, S., Ozilgen, M., McClements, D.J., (2014). Formation and stabilization of nanoemulsion-based vitamin E delivery systems using natural surfactants: Quillaja saponin and lecithin. Journal of Food Engineering 142(0), 57-63.

Pinheiro, A.C., Lad, M., Silva, H.D., Coimbra, M.A., Boland, M., Vicente, A.A., (2013). Unravelling the behaviour of curcumin nanoemulsions during in vitro digestion: effect of the surface charge. Soft Matter 9(11), 3147-3154.

Qian, C., Decker, E.A., Xiao, H., McClements, D.J., (2012). Physical and chemical stability of β-carotene-enriched nanoemulsions: Influence of pH, ionic strength, temperature, and emulsifier type. Food Chemistry 132(3), 1221-1229.

Qian, C., McClements, D.J., (2011). Formation of nanoemulsions stabilized by model food-grade emulsifiers using high-pressure homogenization: Factors affecting particle size. Food Hydrocolloids 25(5), 1000-1008.

Rao, J., McClements, D.J., (2012). Lemon oil solubilization in mixed surfactant solutions: Rationalizing microemulsion & nanoemulsion formation. Food Hydrocolloids 26(1), 268-276.

Rao, J., McClements, D.J., (2013). Optimization of lipid nanoparticle formation for beverage applications: Influence of oil type, cosolvents, and cosurfactants on nanoemulsion properties. Journal of Food Engineering 118(2), 198-204.

Sari, T.P., Mann, B., Kumar, R., Singh, R.R.B., Sharma, R., Bhardwaj, M., Athira, S., (2015). Preparation and characterization of nanoemulsion encapsulating curcumin. Food Hydrocolloids 43(0), 540-546.

Schramm, L.L., (2006a). Dispersion and Dispersed Species Characterization, *Emulsions, Foams, and Suspensions*. Wiley-VCH Verlag GmbH & Co. KGaA, pp. 13-51.

Schramm, L.L., (2006b). Interfacial Energetics, *Emulsions, Foams, and Suspensions*. Wiley-VCH Verlag GmbH & Co. KGaA, pp. 53-100.

Schramm, L.L., (2006c). Introduction, *Emulsions, Foams, and Suspensions*. Wiley-VCH Verlag GmbH & Co. KGaA, pp. 1-12.

Shafiq, S., Shakeel, F., Talegaonkar, S., Ahmad, F.J., Khar, R.K., Ali, M., (2007). Development and bioavailability assessment of ramipril nanoemulsion formulation. European Journal of Pharmaceutics and Biopharmaceutics 66(2), 227-243.

Shemen Industries, (2013). http://www.nutritionaloutlook.com/article/big-potential.

Silva, H., Cerqueira, M., Vicente, A., (2012). Nanoemulsions for Food Applications: Development and Characterization. Food and Bioprocess Technology 5(3), 854-867.

Silva, H.D., Cerqueira, M.A., Souza, B.W.S., Ribeiro, C., Avides, M.C., Quintas, M.A.C., Coimbra, J.S.R., Carneiro-da-Cunha, M.G., Vicente, A.A., (2011). Nanoemulsions of β-carotene using a high-energy emulsification-evaporation technique. Journal of Food Engineering 102(2), 130-135.

Solans, C., Solé, I., (2012). Nano-emulsions: Formation by low-energy methods. Current Opinion in Colloid & Interface Science 17(5), 246-254.

Solgar, (2013). http://www.solgar.com/SolgarProducts/Nutri-Nano-CoQ-10-Alpha-Lipoic-Acid-Softgels.htm.

Song, B., Springer, J., (1996). Determination of Interfacial Tension from the Profile of a Pendant Drop Using Computer-Aided Image Processing: 2. Experimental. Journal of Colloid and Interface Science 184(1), 77-91.

Sood, S., Jain, K., Gowthamarajan, K., (2014). Optimization of curcumin nanoemulsion for intranasal delivery using design of experiment and its toxicity assessment. Colloids and Surfaces B: Biointerfaces 113(0), 330-337.

Stang, M., Schuchmann, H., Schubert, H., (2001). Emulsification in High-Pressure Homogenizers. Engineering in Life Sciences 1(4), 151-157.

Tadros, T., Izquierdo, P., Esquena, J., Solans, C., (2004). Formation and stability of nano-emulsions. Advances in Colloid and Interface Science 108-109, 303-318.

Tadros, T.F., (2013). Emulsion Formation, Stability, and Rheology, *Emulsion Formation and Stability*. Wiley-VCH Verlag GmbH & Co. KGaA, pp. 1-75.

Tan, C.P., Nakajima, M., (2005). [beta]-Carotene nanodispersions: preparation, characterization and stability evaluation. Food Chemistry 92(4), 661-671.

Troncoso, E., Aguilera, J.M., McClements, D.J., (2012). Influence of particle size on the in vitro digestibility of protein-coated lipid nanoparticles. Journal of Colloid and Interface Science 382(1), 110-116.

Walstra, P., (1993). Principles of emulsion formation. Chemical Engineering Science 48(2), 333-349.

Wild Flavors Inc, (2013). http://www.wildflavors.com/NA-EN/assets/File/1Ins_Colors_Emulsions_1_.pdf.

CHAPTER 4

DEVELOPMENT AND CHARACTERIZATION OF LIPID-BASED NANOSYSTEMS: EFFECT OF INTERFACIAL COMPOSITION ON NANOEMULSIONS BEHAVIOUR

In this chapter multilayer nanoemulsions were developed through high-pressure homogenization, followed by the LbL technique for the deposition of chitosan and alginate polyelectrolytes multilayers. The effect of polyelectrolytes concentration in the development of multilayer nanoemulsions was evaluated in terms of H_d, *PdI*, *Zp*. The release profiles of curcumin were evaluated at different conditions and fitted to a linear superimposition model.

This Chapter was adapted from:

Silva, H. D., Donsì, F., Pinheiro, A. C., Cerqueira, M. A., Ferrari, G. & Vicente, A. A. Development and characterization of lipid-based nanosystems: Effect of interfacial composition on nanoemulsions behaviour. *Food Hydrocolloids* (Submitted).

4.1 Introduction

Food industry in recent years has focused its attention on lipophilic bioactive compounds due to their health-promoting properties and encapsulation related issues, such as low solubility in aqueous mediums and low bioaccessibility (McClements & Xiao, 2012; Pinheiro et al., 2016). Curcumin [1,7-bis(4-hydroxy-3-methoxyphenyl)-1,6-hepadiene-3,5-dione], a natural polyphenol, extracted from the rhizome of *Curcuma longa*, has been reported to have a wide range of biological activities, such as antioxidant, anti-inflammatory, antimicrobial and anticancer properties (Kaur et al., 2015; Liu et al., 2016). Nonetheless, the application of curcumin to food products has been limited due their low solubility in water (11 ng mL^{-1}), rapid degradation in aqueous systems due to oxidative processes, pH and temperature changes during manufacturing or storage of the food products, and their effect on the organoleptic properties of foods (Plaza-Oliver et al., 2015; Zhao et al., 2012). The need to overcome these limitations has led the food and beverage industries to consider the use of nanotechnology, with a special attention to lipid-based nanosystems due to their ability to encapsulate lipophilic bioactive compounds efficiently, protect them and act as delivery systems, while helping their incorporation into food products (Cerqueira et al., 2014; Pinheiro et al., 2016; Plaza-Oliver et al., 2015; Spigno et al., 2013).

The use of lipid-based nanosystems, such as nanoemulsions, is an interesting option for the food and beverage industry to encapsulate lipophilic bioactive compounds, protecting their unique properties, while releasing them at the desired target. The distinctive characteristics of nanoemulsions, such as high optical clarity, good physical stability, and protection of the incorporated bioactive compounds from degradation, while also improving their bioavailability (Guttoff et al., 2015; Saberi et al., 2015; Silva et al., 2015b) can help preserving the organoleptic and nutritional properties of food products (Plaza-Oliver et al., 2015). Nevertheless, nanoemulsions present some drawbacks such as limited stability to heat, chilling, freezing-thawing and dehydration (Cerqueira et al., 2014; Silva et al., 2015a). Previous studies have shown that the surface properties of nanoemulsions can be modified through the addition of a

polyelectrolyte layer (Li et al., 2010; Pinheiro et al., 2016; Saberi et al., 2015). This deposition can be performed through the LbL electrostatic deposition technique, a powerful tool for the alternate deposition of polyelectrolytes and thus the development of multilayer nanoemulsions with improved stability against environmental stresses (Cerqueira et al., 2014; Li et al., 2010; Pinheiro et al., 2016). LbL deposition of polyelectrolytes changes the surface properties of nanoemulsions, creating the possibility of tailoring the properties of lipid-based systems, offering a precise control over thickness and morphology, while allowing the controlled release of the lipophilic bioactive compounds (Cui et al., 2014). LbL deposition relies on the electrostatic interactions between a charged polyelectrolyte deposited on the surface of an oppositely charged system (Figure 4.1). However, the development of the composition of these systems must be carefully controlled in order to avoid particle aggregation due to bridging or depletion flocculation (Cui et al., 2014; Saberi et al., 2015).

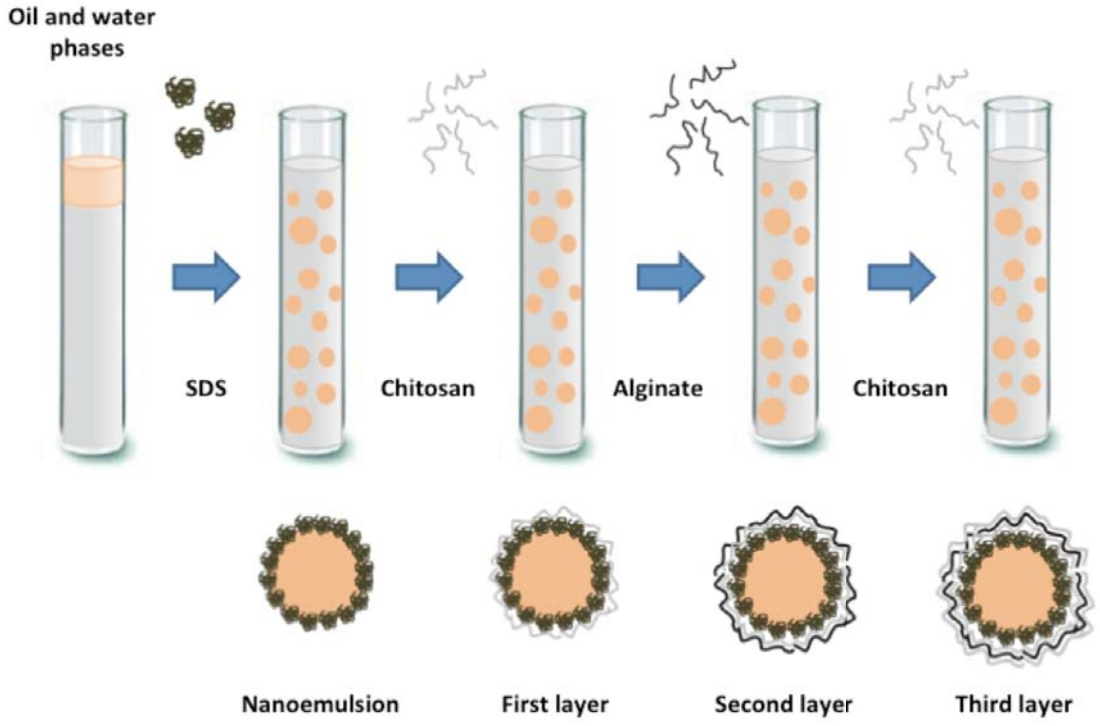

Figure 4.1 – Representative scheme of multilayer nanoemulsions after LbL deposition of polyelectrolytes onto the nanoemulsion.

In this work, multilayer nanoemulsions were produced using high-pressure homogenization, followed by the alternate deposition of chitosan and alginate

layers. The nanosystems stability, responsiveness to environmental triggers and release mechanisms were evaluated. The effects of environmental conditions such as temperature and acceptor medium (solvent) on curcumin release and transport behaviours were also studied.

4.2 Materials and Methods

4.2.1 Materials

Neobee 1053 medium chain triglycerides (MCTs) is caprylic/capric triglyceride oil with a fatty acid distribution of 55 % of C8:0 and 44 % of C10:0 which was kindly provided by Stepan (The Netherlands) and used without further purification. SDS, curcumin (Mw = 368.38 Da) and 1,1-diphenyl-2-picrylhydrazyl (DPPH) were purchased from Sigma-Aldrich (St Louis, MO, USA). Chitosan (deacetylation degree ≥ 95 %) was purchased from Golden-Shell Biochemical CO., LTD (Zhejiang, China) and sodium alginate from Manutex RSX, Kelco 104 International, Ltd. (Portugal) with Mw ≈ 15,900 Da and viscosity ≈ 200 cp (1 % aqueous solution with Brookfield Model LV – 60 rpm at 25 ºC). Lactic acid (90 %) was obtained from Acros Organics (Geel, Belgium) and ethanol was obtained from Panreac (Spain). Distilled water (Milli-Q apparatus, Millipore Corp., Bedford, MA, USA) was used to prepare all solutions.

4.2.2 Experimental Procedures

4.2.2.1 Preparation of curcumin nanosystems

4.2.2.1.1 Curcumin nanoemulsion preparation

Oil-in-water (O/W) nanoemulsions were prepared according to Silva et al., (2015b), with minor modifications. Briefly, 0.1 % (w/w) of curcumin was solubilized at 90 ºC in MCTs (Yu et al., 2012; Yucel et al., 2015). This oily phase was then added to an aqueous phase containing 1 % (w/w) of SDS in distilled water. According to previous works (Silva et al., 2011; Silva et al., 2015b) an oily phase and aqueous phase volume ratio of 1:9 was used. The nanoemulsions were pre-mixed during 2 min at 5000 rpm using an Ultra-Turrax

homogenizer (T 25, Ika-Werke, Germany) followed by 20 passages through a high-pressure homogenizer equipped with a zirconia nozzle (Z4 nozzle) with 100 μm of orifice (Nano DeBEE, BEE International, USA) at 15000 Psi. The surfactant used in this study was applied as model surfactant based on its negative charge, since one of the aims of this study was to produce multilayer nanoemulsions using the LbL electrostatic deposition technique.

4.2.2.1.2 Curcumin multilayer nanoemulsion preparation

The multilayer nanoemulsions were formed through adsorption of consecutive deposition of layers of polyelectrolytes onto the curcumin nanoemulsions using the LbL electrostatic deposition technique. The saturation method was applied, i.e. the layers were constructed by subsequent adsorption of polyelectrolytes from their solutions without the intermediate rinsing step (Adamczak et al., 2014). Briefly, anionic curcumin nanoemulsions were coated with alternating layers of positively charged chitosan solution and negatively charged sodium alginate (volume ratio of 1:1, respectively) until the desired number of polyelectrolyte layers was achieved. The polyelectrolyte solutions were added dropwise with a syringe pump (NE-1000, New Era Pump Systems, Inc., USA) to fresh curcumin nanoemulsions, under stirring for 15 min. The concentrations of polyelectrolyte solutions used to form each layer were selected on the basis of the results of zeta potential measurements (Adamczak et al., 2014; Madrigal-Carballo et al., 2010).

4.2.2.2 Size measurements

The H_d and the *PdI* of nanoemulsions and multilayer nanoemulsions were determined using Dynamic Light Scattering (DLS) (Zetasizer Nano ZS-90, Malvern Instruments, Worcestershire, UK). The nanoemulsion samples were diluted 10× in distilled water at room temperature, without affecting H_d and *PdI*. Data were reported as the mean droplet diameter (hydrodynamic diameter, H_d). The *PdI* is a dimensionless number and indicates the heterogeneity (monodisperse or polydisperse) of sizes of particles in a mixture (Malvern, 2011). Each sample was analysed in a disposable polystyrene cell (DTS0012, Malvern Instruments). The measurements were performed in duplicate, with

three readings for each of them. The results are given as the average ± standard deviation of the six values obtained (Rao & McClements, 2013; Silva et al., 2011).

4.2.2.3 Charge measurements

The droplet charge (zeta potential) of the nanoemulsions and multilayer nanoemulsions was determined using a particle micro-electrophoresis instrument (Zetasizer Nano ZS-90, Malvern Instruments, Worcestershire, UK). Samples were diluted 100× in distilled water prior to measurements in order to avoid multiple scattering effects at ambient temperature and placing the diluted emulsions into disposable capillary cells (DTS 1060, Malvern Instruments) (Ozturk et al., 2014; Rao & McClements, 2013).

4.2.2.4 Evaluation of temperature and pH responsiveness

Thermal stress: The influence of temperature on nanoemulsions stability was evaluated through DLS, by measuring the H_d of the nanoemulsions. Briefly, 1 mL of the formulations were submitted to a range of temperatures from 10 to 80 ºC, with increasing intervals of 10 ºC, during 10 min at each condition (Morais Diane & Burgess, 2014). The temperature was adjusted using a Nano ZS-90 equipment (Zetasizer Nano ZS-90, Malvern Instruments, Worcestershire, UK). The occurrence of creaming was visually checked during experiment, and excluded if it was the case. Data were reported as H_d, average ± standard deviation of the three values obtained.

pH stress: The pH-responsive behaviour of the nanosystems was analyzed by measuring the droplets mean diameter to responses to dynamic pH values change using DLS, Zetasizer Nano ZS operating with a 633 nm laser source equipped with a MPT-2 Autotitrator. The pH value of the nanosystems was adjusted to 2 and gradually increased to 12 using 0.1 mol L^{-1} and 0.5 mol L^{-1} NaOH solution and 0.1 mol L^{-1} HCl solution. Measurements of the H_d were collected at 25 ºC and pH intervals of 1 (Liechty et al., 2013).

4.2.2.5 Encapsulation efficiency and loading capacity of curcumin nanoemulsions

The encapsulation efficiency (*EE*) and loading capacity (*LC*) were determined by measuring the amount of curcumin that was not encapsulated in the nanoemulsions. Briefly, 0.5 mL of the curcumin nanoemulsion solution was placed into an Amicon® Ultra 0.5 centrifugal filter with 10 kDa cut-off (Amicon® Ultra – 0.5 mL device, Millipore Corp., Ireland) and centrifuged at 14,000 *g* for 15 min. Efficient recovery of the concentrated sample (retained species) is achieved by a reverse spin step at 14,000 *g* after collecting the filtrate. This allowed the separation of the unabsorbed curcumin (filtered) from the nanoemulsions with encapsulated curcumin (supernatant). In order to measure the EE (Eq. 4.1), the free curcumin in the filtrate was assayed spectrophotometrically at 425 nm, the maximum absorbance peak of curcumin, in Elisa Biotech Synergy HT (Biotek, USA). This procedure was performed twice, being the unabsorbed curcumin removed by two repeated cycles of centrifugation. For LC determination (Eq. 4.2) the filtered nanoemulsions were dried and weighted.

$$EE\% = \frac{Curcumin_{total} - Curcumin_{free}}{Curcumin_{total}} \times 100 \qquad \text{Eq. 4.1}$$

$$LC\% = \frac{Curcumin_{total} - Curcumin_{free}}{Mass_{nanoemulsion}} \times 100 \qquad \text{Eq. 4.2}$$

$Curcumin_{total}$ represents the total amount of curcumin added to the system, $curcumin_{free}$ is the free/unabsorbed curcumin in filtrate and $Mass_{nanoemulsion}$ is the total weight of nanoemulsions after drying (Azevedo et al., 2014).

4.2.2.6 Antioxidant activity of curcumin nanosystems

The free-radical scavenging capacity of curcumin and curcumin nanosystems were analysed using the DPPH test according to the methodology described by Pinheiro et al (2015), with some modifications. Briefly, 0.2 mL of ethanol and 0.3 mL of the curcumin dissolved in ethanol (concentrations ranging from 0.05 to 5.0 mg mL^{-1}) was mixed in a 10 mL test tube with 2.5 mL of DPPH

(60 μmol L^{-1} in ethanol), achieving a final volume of 3.0 mL. The solution was kept at room temperature for 30 min and the absorbance was measured at 517 nm (Pinheiro et al., 2015; Rufino et al., 2007; Souza et al., 2012). Butylated hydroxytoluene (BHT) and butylated hydroxyanisole (BHA) were used as positive controls. The DPPH scavenging effect was calculated as follows:

$$Scavenging\ effect\ (\%) = \frac{A_0 - (A_s - A_b)}{A_0} \times 100 \qquad \text{Eq. 4.3}$$

where A_0 is the absorbance at 517 nm of DPPH without sample, A_s is the absorbance at 517 nm of sample and DPPH and A_b is the absorbance at 517 nm of sample without DPPH. The absorbance measurements were performed in Elisa Biotech Synergy HT (Biotek, USA) (Pinheiro et al., 2015).

4.2.2.7 Fourier transform infrared (FTIR) spectroscopy

In order to confirm the successful development of the multilayer nanoemulsions, FTIR analyses were carried out with a Thermo Nicolet 6700 spectrometer (Thermo Scientific, Waltham, MA, USA) in the wavenumber region of 600–4000 cm^{-1} using 16 scans for each sample. The nanosystems were air dried prior to FTIR measurements. Each spectrum was baseline corrected and the transmittance was normalised between 0 and 1.

4.2.2.8 Quartz crystal microbalance

The adsorption behaviour of the polyelectrolytes onto the curcumin nanoemulsions was evaluated using a quartz crystal microbalance (QCM 200, purchased from Stanford Research Systems, SRS, USA), equipped with AT-cut quartz crystals (5 MHz) with optically flat polished chrome/gold electrodes on contact and liquid sides. Before carrying out the experiments, the crystal was cleaned by successive sonication (40 kHz, 30 min) in ultra-pure water, ethanol and ultra-pure water, followed by drying with a flow of nitrogen. Adsorption measurements were performed by alternate immersion of the crystal in nanoemulsions (pH 5.0), chitosan (pH 3.0), alginate (pH 7.0) and chitosan (pH 3.0) solutions, for 15 min. The variations of the resonance frequency (*F*)

were simultaneously measured as a function of time and the analyses were performed at 25 ºC, in triplicate (Pinheiro et al., 2015).

4.2.2.9 Microscopy

The morphology of nanosystems was evaluated by transmission electron microscopy (TEM) (EM 902A, ZEISS, Germany) operating at 80 kV. TEM samples were prepared by depositing the nanoemulsion suspensions on a carbon-coated copper grid, and negatively stained with 1 % (w/v) uranyl acetate for observation. Samples were air-dried before analyses.

4.2.2.10 Curcumin release from nanosystems

The *in vitro* release kinetics of curcumin was performed by the dialysis method (Azevedo et al., 2014; Pinheiro et al., 2015). 2 mL of aqueous curcumin nanosystems were added into a dialysis membrane (molecular weight cut-off 15 kDa; Cellu-Sep H1, Membrane filtration products, USA). The sealed dialysis membrane was then placed into 50 mL of acceptor medium (10 %, 20 % and 50 % v/v of ethanol and 5 % w/w of SDS) under magnetic stirring at 4 ºC, 25 ºC and 37 ºC. At appropriate time intervals, 0.5 mL of supernatant were taken and 0.5 mL of fresh acceptor medium was added to keep the volume of the release medium constant. The released amount of curcumin from the nanosystems was evaluated by measuring the absorbance at 425 nm, maximum absorbance peak (Elisa Biotech Synergy HT, Biotek, USA). All release tests were run in duplicate or triplicate. In order to evaluate the release mechanism of curcumin from nanosystems the linear superimposition model (LSM) was applied (Eq. 4.4). This kinetic model accounts for both Fickian and Case II transport effects (Berens & Hopfenberg, 1978).

$$M_t = M_{t,F} + M_{t,R} \qquad \text{Eq. 4.4}$$

Where M_t is the total amount of sorption per unit weight of nanosystems at time t, being $M_{t,F}$ and M_{tR} are the Fickian and polymer relaxation contributions, respectively, at time t. Pure Fickian diffusion can be described by equation (4.5).

$$M_{t,F} = M_{\infty,F}\left[1 - \frac{6}{\pi^2}\sum_{n=1}^{\infty}\frac{1}{n^2}\exp(-n^2 k_F t)\right]M_{t,R} \quad \text{Eq. 4.5}$$

where, $M_{\infty,F}$ is the compound release at equilibrium and k_F is the Fickian diffusion rate constant. Equation (4.5) can be simplified using the first term of the Taylor series (Pinheiro et al., 2015; Pinheiro et al., 2012).

Polymer relaxation (Eq. 4.6) is driven by the swelling ability of the polymer being then related to the dissipation of stress induced by the entry of the penetrant and can be described as a distribution of relaxation times, each assuming a first order-type kinetic equation (Berens & Hopfenberg, 1978).

$$M_{t,R} = \sum_i M_{\infty,R_i}\left[1 - exp\left(-k_{R_i} t\right)\right] \quad \text{Eq. 4.6}$$

where, $M_{\infty,Ri}$ are the contributions of the relaxation processes for compound release and k_{Ri} are the relaxation rate constants. For most cases, there is only one main polymer relaxation that influences transport and thus the above equation can be simplified using i= 1. Therefore, equation (4.7) can describe the linear superimposition model for curcumin release from nanosystems.

$$\frac{M_t}{M_\infty} = M_F\left[1 - \frac{6}{\pi^2}\exp(k_F t)\right] + M_R[1 - exp(k_R t)] \quad \text{Eq. 4.7}$$

where M_F is the total mass of compound released by Fickian transport and M_R is the total mass of compound released by polymer relaxation. The experimental data were analysed by fitting equation (4.7) (linear superimposition model) in order to assess the transport mechanism involved in the curcumin release from nanosystems at different temperatures and acceptor media (Pinheiro et al., 2015).

4.2.2.11 Stability of the nanosystems under storage

In order to evaluate the stability of nanoemulsion and multilayer nanoemulsion during storage, the H_d, *PdI* and *Zp* were evaluated during three months of storage at 4 ºC in the absence of light.

4.2.3 Statistical procedures

4.2.3.1 Data Analyses

Data analyses were performed using Microsoft Windows Excel 2011, using Tukey's Multiple Comparison Test with a confidence interval of 95 % in GraphPad Prism 5 (GraphPad Software, Inc.) and using ANOVA in STATISTICA 7.0 (Statsoft, Tulsa, OK, USA).

4.2.3.2 Non-linear regression analysis

The equations 5 and 7 were fitted to data by non-linear regression, using STATISTICAT 7.0 (Statsoft. Inc, USA). The Levenberg–Marquardt algorithm for the least squares function minimization was applied. The quality of the regressions was evaluated on the basis of the determination coefficient, R^2, the squared root mean square error, RMSE (i.e., the square root of the sum of the squared residues (SSE) divided by the regression degrees of freedom) and residuals visual inspection for randomness and normality. R^2 and SSE were obtained directly from the software. The precision of the estimated parameters was evaluated by the standardised halved width (SHW %), which was defined as the ratio between the 95 % standard error (obtained from the software) and the value of the estimate (Pinheiro et al., 2015).

4.3 Results and Discussion

4.3.1 Curcumin nanosystems

4.3.1.1 Characterization of the curcumin nanoemulsion

The use of high-energy emulsification methods, such as high-pressure homogenization, resulted very efficient in creating stable nanoemulsions encapsulating curcumin, with a final mean droplet diameter of 80.0 ± 0.9 nm. Regarding the *PdI* and *Zp*, the obtained values were, 0.177 ± 0.009 and -65.8 ± 5.8 mV, respectively. The highly negative *Zp* can be explained by the fact that SDS, an anionic surfactant, was used to stabilize the nanoemulsions, as seen in chapter 3.

The theoretical minimum size of the curcumin nanoemulsions produced by high-pressure homogenization at 1 % (w/w) of surfactant was calculated using equation (4.8)

$$R_{min} = \frac{3*\Gamma*\phi}{c_s'*(1-\phi)} \qquad \text{Eq. 4.8}$$

Here, Γ is the surface load of the surfactant at saturation (kg m^{-2}), ϕ is the disperse phase volume (dimensionless), and C'_s is the concentration of surfactant at the continuous phase (kg m^{-3}) (Troncoso et al., 2012). Assuming a surface load of SDS of 1 mg m^{-2} (Berton-Carabin et al., 2014), the minimum theoretical droplet diameter is 67 nm, while the experimental mean droplet diameter obtained for the curcumin nanoemulsion was 80 nm. This result suggests not only that the concentration of 1 % (w/w) of SDS used was sufficient to cover all droplets, but also that SDS quickly adsorbed on the droplet interface during the homogenization process, which was capable of generating enough disruptive forces (Qian & McClements, 2011; Silva et al., 2015b; Troncoso et al., 2012). In chapter 3, where the authors prepared nanoemulsions using the same equipment and process conditions but a nozzle with an orifice of 200 µm diameter instead of 100 µm, a mean droplet size of 137 nm was obtained, being of 57 nm larger than the value of 80 nm obtained in this work. The geometry of the nozzle is in fact of major importance when developing nanoemulsions (Donsì et al., 2011), with the reduction in nozzle diameter allowing the generation of enough disruptive forces, which led to a reduction in H_d.

The encapsulation efficiency (*EE*) and loading capacity (*LC*) of curcumin using nanoemulsions was determined using equations 1 and 2. The values of EE and LC obtained were 99.8 ± 0.8 % and 0.53 ± 0.03 %, respectively. The low *LC* may be related with the large number of droplets present with very small sizes, which leads to a higher surface area, where 1 mg of nanoemulsion contains 5.3 µg of curcumin. Sari et al (2015) prepared curcumin-loaded nanoemulsions using whey protein isolate and Tween 80, achieving an EE of 90.65 %, having droplet sizes of 142 nm (Sari et al., 2015). Friedrich et al. (2015) also reported

an *EE* of 100 % for curcumin nanocapsules developed with sorbitan monostearate and poly(ε-caprolactone) (Friedrich et al., 2015).

4.3.1.2 Polyelectrolytes adsorption onto nanoemulsions

The saturation method was used to determine the optimum chitosan and sodium alginate concentrations required to prepare the multilayer nanoemulsions. For polyelectrolytes concentrations below a critical value, the polyelectrolyte molecules adsorb on more than one droplet, leading to bridging flocculation. In contrast, the presence of free polyelectrolyte (excess) in the aqueous phase will cause interaction with the polyelectrolytes of the following layer, leading to interferences in the development of the multilayer nanoemulsion. If the free polyelectrolyte is in excess at high enough concentration, this could generate attractive osmotic forces able to remove the polyelectrolytes from nanoemulsion surface, overcoming the repulsion forces and leading to depletion flocculation (Cui et al., 2014; Guzey & McClements, 2006; Szczepanowicz et al., in press). The addition of polyelectrolytes at the optimum concentration was determined by *Zp* measurements, being the polyelectrolyte carefully added drop by drop in order to prevent bridging and depletion flocculation.

The influence of chitosan concentration was initially evaluated on the properties of the nanoemulsion with the first layer, i.e. H_d, *PdI* and *Zp*. The H_d, *PdI* and *Zp* of the multilayer nanoemulsion (first layer) were measured immediately after production. For concentrations ranging between 0.02 % and 0.05 % (w/w), these properties were also evaluated after 24 h of storage. Figure 4.2a shows that the addition of chitosan leads to a change of *Zp* values, where the increase of chitosan concentrations (from 0.0005 % to 0.08 %) leads to higher *Zp* values (from negative to positive). This change reached a positive constant value around +16 mV, when the concentration ranged between 0.04 % and 0.08 % (w/w). This change in the *Zp* values suggests that the polyelectrolytes effectively adsorbed on the surface of the nanoemulsion, with the deposition of the first layer (Szczepanowicz et al., in press). At chitosan concentrations ranging from 0.0025 % and 0.015 % (w/w) a few “clumps” and oily droplets were observed at the upper surface of the samples. This can be explained by

the insufficient mass of chitosan present to coat all the nanoemulsions, which is reflected in the *Zp* of the samples, causing a decrease from -68.5 mV to -39.9 mV and consequent aggregation. The presence of clumps at these concentrations suggests that bridging flocculation occurred. Charged polyelectrolytes are known to promote bridging flocculation; if there is insufficient chitosan to completely coat the nanoemulsion droplets, a chitosan molecule could adsorb to the surface of more than one droplet, bridging the nanoemulsions droplets together (Cui et al., 2014; Guzey & McClements, 2006; Mora-Huertas et al., 2010). A similar phenomenon was observed by Aoki and co-workers (2005), who reported that mixing low concentrations of a chitosan solution with a nanoemulsion led to droplets with negative surfaces, which allowed chitosan molecules to adsorb on the surface of two or more droplets simultaneously (Aoki et al., 2005). In the range of chitosan concentration from 0.03 % to 0.08 % (w/w) a change from negative to positive electrical charge was observed, which indicates that chitosan fully adsorbed on the surface of the nanoemulsion droplets.

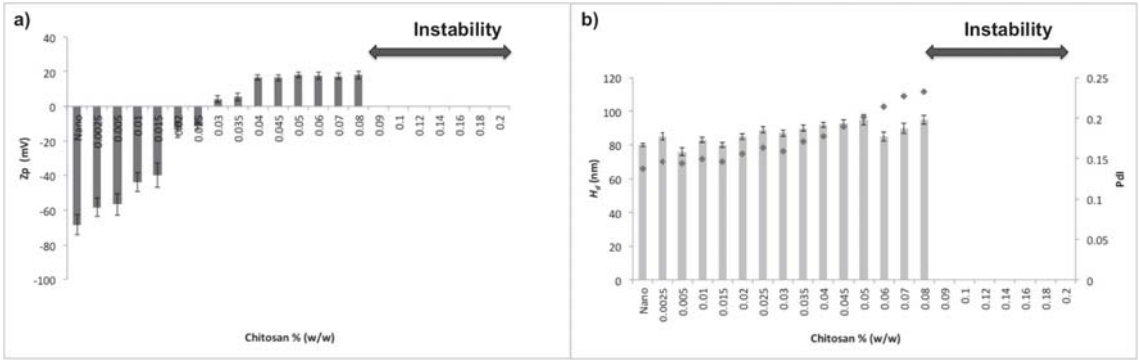

Figure 4.2 – Values of a) zeta potential (*Zp*), and b) hydrodynamic diameter (H_d) and polydispersity index (*PdI*) as a function of chitosan concentrations for nanoemulsions coated with the 1st layer.

Despite the shift from negative to positive electrical charge, from 0.05 % to 0.08 % (w/w) chitosan some clumps were observed, this time without oil droplets, at the surface of the solutions. At high concentrations (from 0.09 % to 0.2 % w/w) the presence of large clumps was even more evident, making impossible to measure H_d, *PdI* and *Zp* for nanoemulsions coated with this range of chitosan concentrations. From 0.05 % to 0.2 % (w/w), chitosan induced a depletion attraction between the nanoemulsion droplets that lead to the

flocculation of particles. The presence of a high concentration of free chitosan in the continuous phase was able to generate an attractive osmotic force, capable of overcoming the repulsive forces, removing the polyelectrolytes from the surface of the nanoemulsions droplets (Cui et al., 2014; Guzey & McClements, 2006; Szczepanowicz et al., in press). A similar behaviour was described by Mun and co-workers (2005), where chitosan concentrations below the amount of chitosan required to saturate the droplet surfaces formed extremely large droplet aggregates. While stable nanoemulsions were formed above the concentration of saturation, at higher chitosan concentrations the electrostatic repulsive forces were not high enough to avoid depletion flocculation (Mun et al., 2005). Another study of Mun and co-workers (2006) revealed that the molecular weight of chitosan did not have any influence on the charge of the multilayer nanoemulsion, or on the tendency to the formation of clumps due to bridging flocculation. However, high levels of chitosan were reported to cause depletion flocculation, inducing droplet aggregation. The tendency to form aggregates increased with the increase of the molecular weight. This study also showed that the electrical charge of the SDS-chitosan droplets depended on the degree of deacetylation, where higher degrees of deacetylation lead to higher electrical charges (Mun et al., 2006). Despite the low electrical charge observed in this study, the samples were stable during 24 h (data not shown), due to both electrostatic and steric repulsions. Mun and co-workers (2006) showed that if the charge density of the polyelectrolytes is not too low, the final electrical charge is largely independent of the charge density of the adsorbed polyelectrolytes. Otherwise, if the charge density of the polyelectrolyte is sufficiently high, when the surface charge reaches a critical value, there will be a strong electrostatic repulsion between the surface (nanoemulsion) and the similarly charged polyelectrolytes in the aqueous phase that further limits the adsorption of the polyelectrolytes. Due to this, the final electrical charge of the multilayer nanoemulsion is determined by this critical value, rather than the charge density of the polyelectrolyte (Mun et al., 2006). This seems to be the case, since the high charge density of chitosan leads to a critical electrical charge, opposing to further adsorption due to electrostatic repulsion between template and the non-adsorbed polyelectrolyte. Therefore, the concentration of

0.04 % (w/w) of chitosan was selected to carry on the development of the multilayer nanoemulsions.

For the development of the 2nd layer sodium alginate, an anionic polyelectrolyte was used. The effect of the concentration of alginate in the H_d, *PdI* and *Zp* was evaluated, for concentration ranging from 0.01 % to 0.06% (w/w). The increase of alginate concentration caused a switch in the electrical charge, from positive to negative, reaching a constant negative value around -50 mV, for an alginate concentration ≥ 0.04 % (w/w), approximately corresponding to the electrical charge of alginate solution. Usually the optimum concentration of polyelectrolytes corresponds to the polyelectrolyte *Zp* value in solution (Cui et al., 2014). This suggests that the anionic alginate molecules adsorbed to the surfaces of SDS-stabilized nanoemulsions until they became saturated with alginate (Figure 4.3a).

From Figure 4.3b it is possible to see that the increase of alginate concentration leads to an increase of the mean droplet diameter, from 110 nm (1st layer) to 128 nm (0.1 % w/w of alginate). The increase of alginate concentration (from 0 to 0.1 % w/w) also leads to higher values of *PdI*, from 0.177 to 0.231 without and with 0.1 % (w/w) of alginate, respectively. This behaviour suggests that the nanoemulsions were saturated with alginate, not being susceptible to droplet aggregation by bridging and not prone to depletion flocculation, due to strong electrostatic repulsions between the multilayer nanoemulsions (Li et al., 2010; Pinheiro et al., 2016). Hence, 0.04 % (w/w) of alginate was selected for the preparation of the 2nd layer of the multilayer nanoemulsion, since the chitosan-SDS-stabilized multilayer nanoemulsions were completely surrounded by alginate molecules, without significant excess of polyelectrolytes in solution.

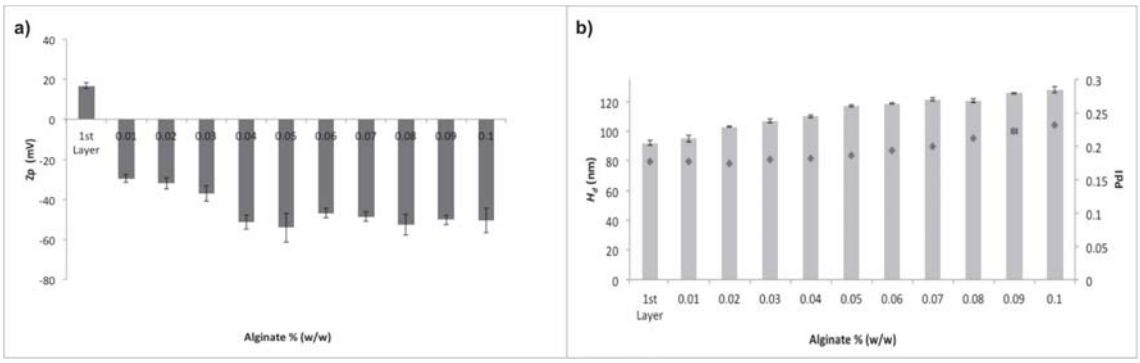

Figure 4.3 – Values of a) zeta potential (*Zp*), and b) hydrodynamic diameter (H_d) and polydispersity index (*PdI*) as a function of alginate concentrations for nanoemulsions coated with the 2nd layer.

The results of adding chitosan to build the 3rd and last layer are shown in Figure 4.4. Chitosan concentrations ranging from 0.01 % to 0.1 % (w/w) were tested. However, for concentrations ≥ 0.03 % (w/w) large yellowish clumps were formed, surrounded by a transparent aqueous phase, making it impossible to evaluate the H_d, *PdI* and *Zp*. Due to the presence of a high concentration of chitosan in the continuous phase, chitosan induced depletion flocculation, leading to the aggregation of the particles (Cui et al., 2014; Guzey & McClements, 2006; Szczepanowicz et al., in press). Figure 4.4a shows that at a chitosan concentration of 0.015 % (w/w) the neutralization of the electrical charge occurred. At this concentration, there was enough chitosan adsorbed on the anionic groups of alginate capable of neutralizing the anionic groups on the adsorbed alginate layer (Li et al., 2010). A similar behaviour was observed by Li and co-workers (2010), while depositing an anionic layer of alginate and pectin onto the cationic layer of chitosan. They were able to neutralize the cationic groups of the adsorbed chitosan. The positively charged molecules of chitosan continued to adsorb to the surface of the SDS-Chitosan-Alginate multilayer nanoemulsions until the charges became positive, up to a certain level of saturation at 0.025 % (w/w) despite attaining higher values of H_d and *PdI* when compared to the ones obtained at 0.02 % (w/w) (see Figure 4.4b). At this concentration, a critical electrical charge was reached (+11 mV), opposing to further adsorption due to electrostatic repulsion between the template and the non-adsorbed polyelectrolyte. Therefore, a chitosan concentration of 0.02 % (w/w) was selected to build the 3rd layer.

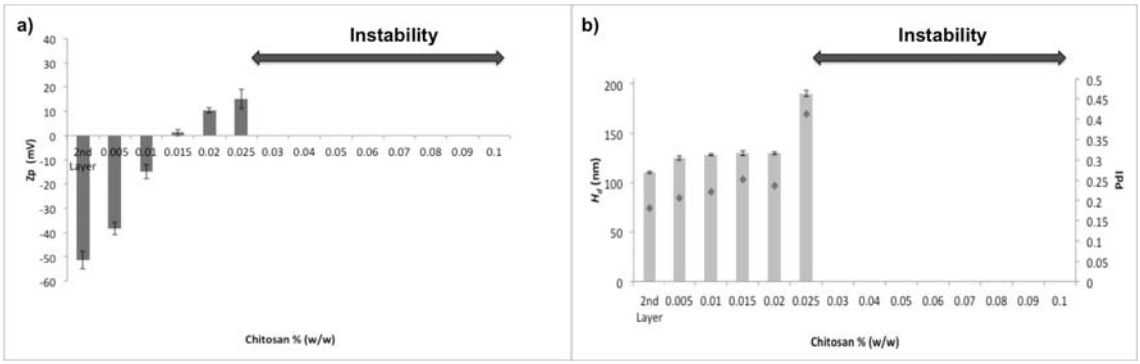

Figure 4.4 – Values of a) zeta potential (*Zp*), and b) hydrodynamic diameter (H_d) and polydispersity index (*PdI*) as a function of chitosan concentrations for nanoemulsions coated with the 3rd layer.

Transmission Electron Microscopy (TEM) confirmed the values of the H_d measured by DLS, supporting the hypothesis of successful multilayer deposition and formation of a multilayer nanoemulsion. Figure 4.5a and 4.5b show the TEM microphotographs of the nanoemulsion and multilayer nanoemulsion, respectively. Figure 4.5b shows the affinity that uranyl ions have towards chitosan, evidencing the successful development of the multilayer nanoemulsion (Tegge, 1989).

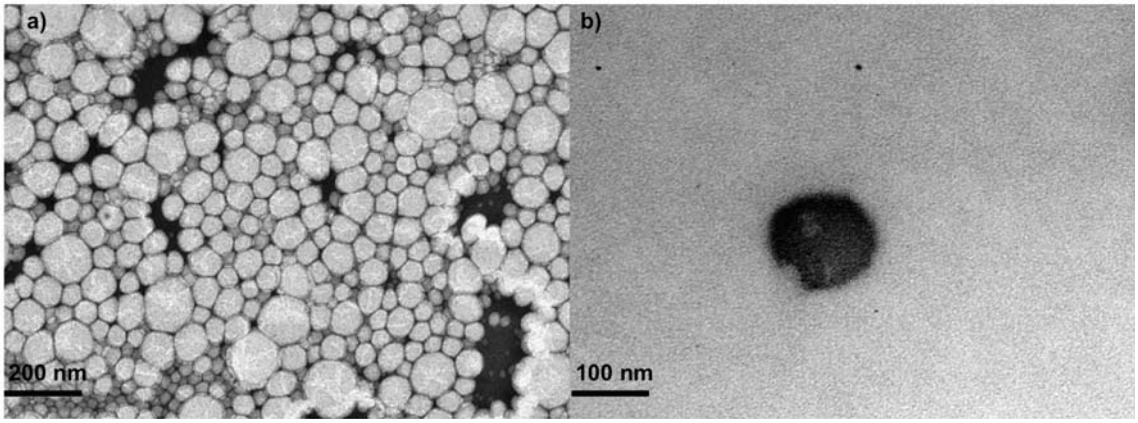

Figure 4.5 – TEM microphotograph of negatively stained nanosystems with uranyl 1 % w/w. a) nanoemulsion and b) multilayer nanoemulsion.

4.3.2 Evaluation of the interactions between polyelectrolytes and nanoemulsion

The adsorption of the polyelectrolyte solutions by electrostatic interactions between the polyelectrolytes and the nanoemulsion droplets during the

construction of the multilayer nanoemulsion were evaluated *in situ* through QCM.

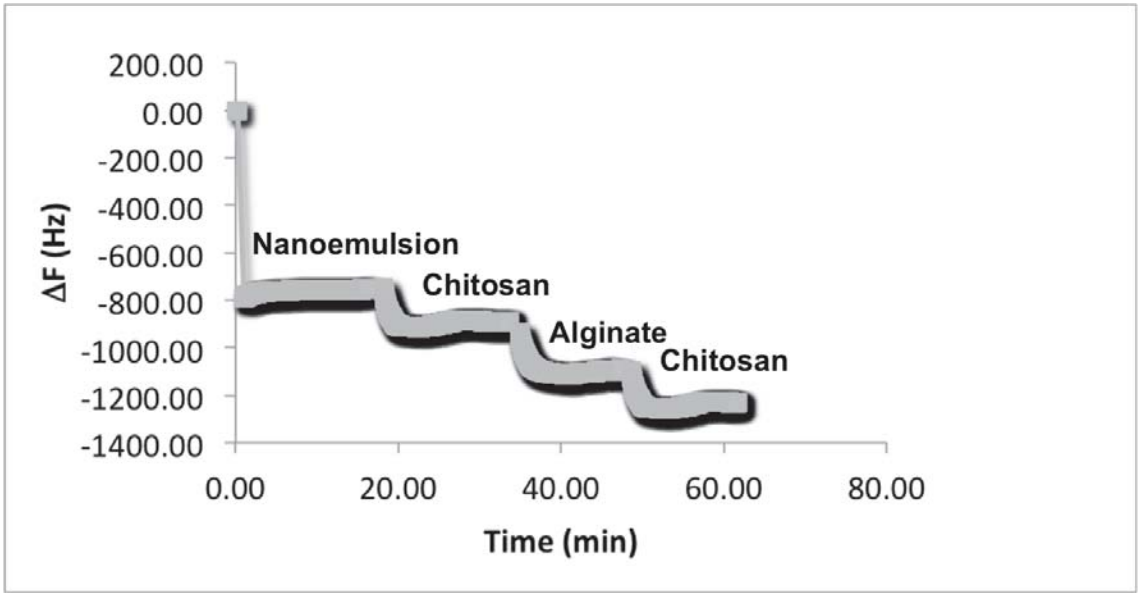

Figure 4.6 – Real time monitoring of polyelectrolytes onto nanoemulsions, QCM response signal (resonant frequency, Δ*F*) for the sequential adsorption of nanoemulsion, chitosan, alginate and chitosan onto a gold electrode surface.

Figure 4.6 shows the consecutive decrease of frequency after the alternate immersion of the QCM crystal in nanoemulsion, chitosan, alginate and chitosan solutions, which means that the mass of polyelectrolytes is being successfully deposited. In addition, Figure 4.6 shows that the adsorption of alginate results in higher changes of frequency leading to a higher mass deposition, when compared to chitosan. This may possibly be related with the more hydrophilic character of alginate: its deposition can be accompanied by solvent entrapment, resulting in a more viscoelastic system. On the other hand chitosan, a more hydrophobic polymer, may entrap air, resulting in a smaller measured mass. Similar behaviour was observed for alginate/chitosan multilayers (Martins et al., 2010) for chitosan/fucoidan multilayer nanocapsules (Pinheiro et al., 2015) and lactoferrin-GMP nanohydrogels (Bourbon et al., 2015).

When mixing oils, surfactants, bioactive compounds and polyelectrolytes, physical bonds and chemical interactions are reflected by changes in characteristic bonds, which can be evaluated by FTIR. The characteristic bands

for curcumin, SDS, MCTs, chitosan and alginate are presented in the supplementary material, Table S4.1.

Figure 4.7 show that the FTIR spectrum of the nanoemulsion majorly presents the characteristic spectra of the MCTs. Nevertheless, from comparing the FTIR profile for the curcumin nanoemulsion with that of pure curcumin and of curcumin in MCTs (data not shown), it is possible to observe that a shift in the out-of-plane bending CH of aromatic and skeletal CCH occurred, from 855 cm^{-1} in the pure curcumin, to 872 cm^{-1} in the curcumin + MCTs and to 836 cm^{-1} when encapsulated into the nanoemulsion (Hee-Je Kim et al., 2013). In addition, a shift also occurred in the bending vibrations of CH bond of alkene group ($RCH=CH_2$) from 962 cm^{-1} in the pure curcumin to 969 cm^{-1} in the nanoemulsion. The nanoemulsion presents a peak at 1017 cm^{-1} when compared to the curcumin in MCTs profile. The in-plane bending of the CH_2 group at 1465 cm^{-1} indicates a reduction of side-by-side chain interactions and an increase in chain motion, which is normally associated with the SDS in the liquid state (Viana et al., 2012). This indicates that the SDS membrane is surrounding the droplets of oil with encapsulated curcumin. The stretching vibration of the CO ester groups present in the MCTs also exhibited a slight shift from 1153 to 1154 cm^{-1} and from 1222 to 1224 cm^{-1}. The FTIR profile for the nanoemulsion further confirmed that the nanoemulsion does not contain SDS micelles. Normally the stretching of CH_2 band of SDS micelles is observed between 2936–2928 cm^{-1}, a peak that it is not present in the nanoemulsion spectrum. This confirms the hypothesis that under the processing conditions used in the homogenization process, SDS micelles were not formed (Viana et al., 2012).

With the adsorption of chitosan for the construction of the 1st layer, the FTIR spectrum shows three new peaks at 1045, 1649 and a broad band at 3408 cm^{-1}, that correspond to characteristic peaks of chitosan, skeletal vibration of the C-O stretching, carbonyl (C=O) stretching of the secondary amide (amide I band) and to the amine and hydroxyl groups, respectively (Lawrie et al., 2007; Li et al., 2008; Pawlak & Mucha, 2003). Also, the shift of some characteristic peaks of the oil phase, such as the stretching vibration of the C-O ester groups from 1154 and 1222 to 1159 and 1218 cm^{-1} and the SDS in-plane bending of the CH_2 group shifted from 1465 to 1460 cm^{-1} reveals that chitosan is now the outer

layer (Lawrie et al., 2007; Viana et al., 2012; Vlachos et al., 2006; Yang et al., 2005).

The deposition of alginate as the 2nd layer was characterized by two new peaks at 1080 and 1631 cm^{-1}, responsible for the asymmetrical stretch of the C-O-C and a asymmetrical stretch vibration of the carboxyl groups (COO), respectively (Lawrie et al., 2007; Shi et al., 2006). The deposition of alginate also leads to a shift in the skeletal vibration of the C-O stretching vibration from 1045 to 1055 cm^{-1} and to a small shoulder at 3455 cm^{-1} due OH stretching vibration (Lawrie et al., 2007).

After the development of the 3rd layer, it is possible to observe that residual lactic acid is evident at 1710 cm^{-1}, which corresponds to carbonyl vibration of the carboxylic acid (Bourbon et al., 2011; Lawrie et al., 2007). There is also a shift in the in the skeletal vibration of the C-O stretching from 1055 to 1043 cm^{-1} and a shift in the carbonyl (C=O) stretching of the secondary amide (amide I band) from 1649 to 1643 cm^{-1}. Additionally, the OH stretching vibration band of the multilayer nanoemulsion (3rd layer) was broader and shifted to a lower wave number, 3386 cm^{-1}, suggesting that intermolecular hydrogen bonds also existed in the multilayer nanoemulsions (Shi et al., 2006). It is then plausible to assume that hydrogen bonding can also play an important role in the LbL assembly (Martins et al., 2010).

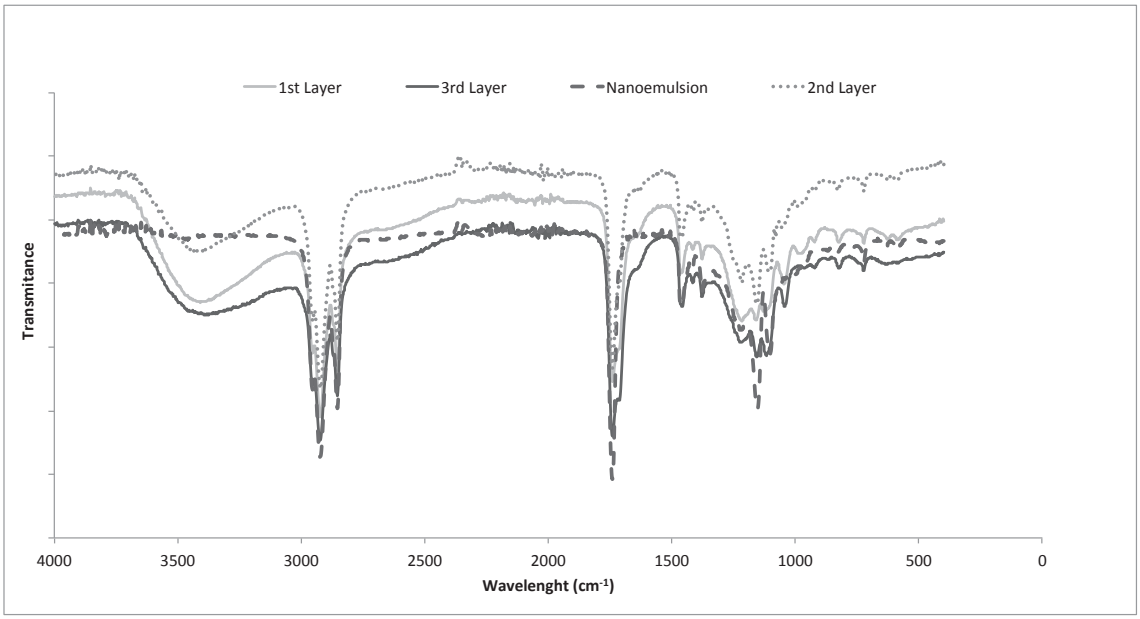

Figure 4.7 – FTIR spectra of nanoemulsions, 1st layer nanoemulsion; 2nd layer nanoemulsion and 3rd layer nanoemulsion (multilayer nanoemulsion).

4.3.3 Evaluation of temperature and pH responsiveness

The thermal stress tests performed on the nanosystems (see section 4.2.2.4) showed no macroscopic sign of instability phenomena (i.e. creaming or phase separation) after heating the samples from 10 to 80 ºC. For this test, H_d measurements were performed immediately after nanoemulsions preparation and following the 30 min of heating at each temperature (10 to 80 ºC, please refer to Table 4.1). The temperature increase did not have an immediate effect in the characteristics of the nanosystems. Table 4.1 shows that thermal stress did not influence significantly (p>0.05) the values of H_d. This can be explained by the fact that nanoemulsions and multilayer nanoemulsions do not change their morphology, size and shape as a function of temperature, having low sensibility to the increase of the temperature. Temperature changes do not promote a modification in the continuous phase, being the droplet sizes stable to temperature changes (Anton & Vandamme, 2011; Gordon et al., 2014; Silva et al., 2015b).

Table 4.1 – Experimental H_d and *PdI* values obtained for the nanosystems after thermal stress tests

	Nanoemulsion		*Multilayer nanoemulsion*	
Treatment	H_d (nm)	*PdI*	H_d (nm)	*PdI*
After production	80.0 ± 1.6 [a]	0.137 ± 0.04 [a]	129.8 ± 3.2 [a]	0.237 ± 0.03 [a]
10 ºC	80.8 ± 1.7 [a]	0.134 ± 0.02 [a]	125.2 ± 2.1 [a]	0.235 ± 0.02 [a]
20 ºC	81.2 ± 1.6 [a]	0.131 ± 0.03 [a]	125.1 ± 2.8 [a]	0.241 ± 0.02 [a]
30 ºC	82.8 ± 2.1 [a]	0.133 ± 0.03 [a]	125.8 ± 2.7 [a]	0.236 ± 0.01 [a]
40 ºC	83.3 ± 1.5 [a]	0.137 ± 0.03 [a]	124.7 ± 2.9 [a]	0.242 ± 0.02 [a]
50 ºC	82.7 ± 1.7 [a]	0.133 ± 0.02 [a]	125.7 ± 3.2 [a]	0.239 ± 0.02 [a]
60 ºC	82.6 ± 1.9 [a]	0.134 ± 0.02 [a]	124.3 ± 3.3 [a]	0.238 ± 0.01 [a]
70 ºC	82.9 ± 1.9 [a]	0.129 ± 0.04 [a]	125.8 ± 2.4 [a]	0.237 ± 0.03 [a]
80 ºC	84.7 ± 3.1 [a]	0.134 ± 0.02 [a]	128.5 ± 2.9 [a]	0.241 ± 0.03 [a]

Each value represents mean ± SD (n = 3). Different letters between rows means statistically different results (p<0.05).

Figure 4.8 show that changes in pH values did not affect the nanoemulsion H_d. A similar behaviour was observed by Tang and co-workers (2012), which developed a nanoemulsion loaded with aspirin using Cremophore EL through ultrasound cavitation, obtaining droplet sizes between 200 to 300 nm and a *PdI* of about 0.30. These nanoemulsions were subjected to changes in the pH, revealing to be stable under the range of pH tested (2 – 9), even at pH values close to their isoelectric point, i.e. 2.54 (Tang et al., 2012).

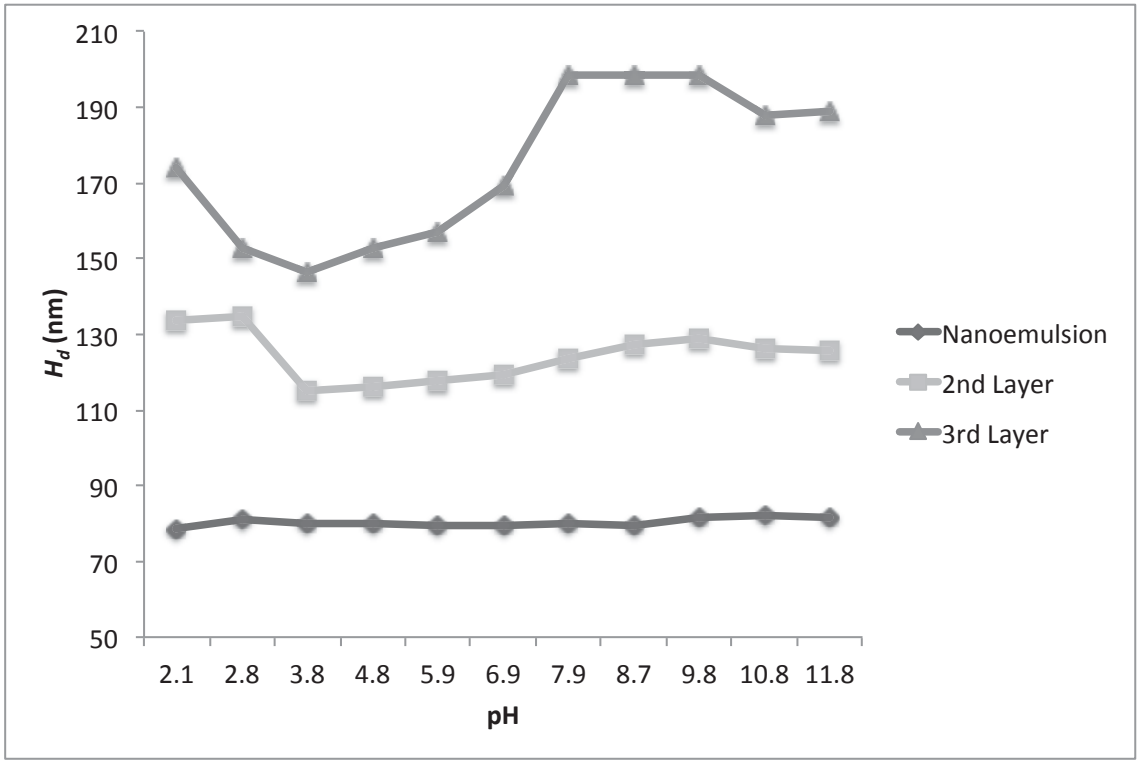

Figure 4.8 – pH-responsiveness of the nanosystems in terms of hydrodynamic diameter (H_d).

The H_d of the nanoemulsions with the 2nd layer and 3rd layer increased when the pH was below 3 and above 7 (Figure 4.8), with a larger increase in H_d for the multilayer nanoemulsion with 3rd layers, from 150 to 200 nm. The increase of H_d at acidic pH (below 3) can be attributed to the anionic groups of alginate, which are carboxylic acids with pK_a values around 3.5 (Harnsilawat et al., 2006; Li et al., 2010). Nevertheless, alginate layer desorbs from the droplet surfaces in the multilayer system at acidic conditions, even though the electrical charges were supposed to be nearly 0 mV. This effect might be due the fact that alginate layer

retained some negative charges at pH below the pK_a. Interestingly, the same behaviour was found for pH above 7, i.e. above the pK_a of chitosan, reported to be around 6.5. At basic pH the amino groups are completely deprotonated and then contribute to the loss of solubility of the chain segments (Vachoud et al., 2000). However, it can be presumed that the chitosan layers retained some positive charge at neutral and basic pH values. This is corroborated by previous research that pK_a values of charged groups on polyelectrolytes can change appreciably when they are entangled between two oppositely charged polyelectrolytes, increasing the stability of the multilayer system to pH (Burke & Barrett, 2003a, b; Li et al., 2010). Despite the increase in the H_d for the multilayer nanoemulsion when varying pH, no visual instability phenomena (i.e. creaming or phase separation) was observed.

4.3.4. Antioxidant activity

The antioxidant activity values of curcumin encapsulated in the nanosystems was not significantly different from the values obtained for free curcumin, when determined by DPPH tests. The radical scavenging activity of the free curcumin was 9.4 ± 0.5 μmol L^{-1} Trolox mg^{-1} curcumin, while for the nanoemulsion was it 9.4 ± 0.3 μmol L^{-1} Trolox mg^{-1} curcumin and for the multilayer nanoemulsion it was 9.3 ± 0.6 μmol L^{-1} Trolox mg^{-1} curcumin. Sari and co-workers (2015) produced curcumin nanoemulsions using whey protein isolate, where 10 to 40 mg of curcumin were added to 100 mL of total emulsion and achieved a lower radical scavenging activity of approximately 3.33 ± 0.02 μmol L^{-1} Trolox mg^{-1} curcumin, for the nanoemulsion system, whereas for native curcumin the value was 3.53 ± 0.11 μmol L^{-1} Trolox mg^{-1} curcumin. In the present study, the radical scavenging activity for the nanosystems was measured during 35 days of storage, at 4 ºC and 25 ºC and in absence of light (A.L) and in the presence of light (P.L). Figure 4.9 clearly shows that curcumin is degraded during storage, since the radical scavenging activity (RSA) decreases during storage. From Figure 4.9 it is possible to see that samples that were kept in the dark had a significantly lower (p<0.05) decrease in the RSA when compared to the ones that were kept under light. This was expected due the fast degradation of curcumin when exposed to light (Khurana & Ho, 1988). For the nanoemulsions, losses around 18.7 ± 1.2 % to 25.5 ± 1.5 % were observed when samples were

kept in the dark at 4 ºC and exposed to light at 25 ºC. For pure curcumin solubilized in MCTs in the same conditions, a decrease in the RSA of 21.9 ± 1.4 % and 26.6 ± 1.1 % was observed. Despite lipids and surfactants are known for significantly decreasing the curcumin degradation, it was expected that nanoencapsulation decreased even further the degradation of curcumin (Priyadarsini, 2009). Opposite to the expected, the development of layers around the nanoemulsion did not decrease the RSA during storage, on the contrary, a significantly decrease in RSA during storage was observed (Figure 4.9). The addition of consecutive layers led to a decrease in the antioxidant activity of the curcumin, especially in the presence of light at 25 ºC. It is a known fact that curcumin is very sensitive to light, pH, solvent system and oxygen (Siviero et al., 2015). For the 1st layer, the decrease of RSA when exposed to light and at 25 ºC was of 43.7 ± 1.7 % against the decrease of 26.9 ± 1.3 % when stored in the dark at the same temperature. For the 3rd layer, the same behaviour was observed, achieving a loss of 73.8 ± 1.2 % at 25 ºC in the presence of light against 66.0 ± 1.8 % when stored in the dark. It was possible to follow this degradation visually, since the solution turned colourless for the 3rd layer at 25 ºC in the presence of light. The processes behind curcumin degradation are very complex, since polarity, π-bonding nature, hydrogen bond donating and accepting properties of the solvent influence the excited state photophysics of curcumin (Priyadarsini, 2009). The mechanism of photodegradation is still not clear, nevertheless the presence or absence of the phenolic OH group does not play a significant role in the degradation of curcumin, being the degradation mainly governed by the breaking of β-diketone link forming smaller phenolic compounds (Priyadarsini, 2009). Tomren and co-workers (2007) showed that curcumin in cyclodextrin solutions was more resistant to hydrolysis than free curcumin; nevertheless, curcumin in cyclodextrin showed to be equally or more susceptible to photochemical degradation, depending on the medium. They observed that stability depends either on the presence of organic solvents or the absence of water (Tomren et al., 2007). Nevertheless, the RSA values for the nanoemulsion and the multilayer nanoemulsion (3rd layer) was around 50 % lower for the multilayer nanoemulsion. This could be explained by the difference in the aqueous

medium. The multilayer nanoemulsion was developed using the saturation method that generates massive dilutions; each layer deposition increases the dilution, performing a 8-fold dilution, achieving a final pH of 5, which excludes degradation of curcumin to basic pH. This difference in the aqueous phase volume could lead to higher hydrogen binding ability, promoting the degradation of curcumin (Priyadarsini, 2009). The hydrogen donation reaction from curcumin leads to the oxidation of curcumin (Priyadarsini, 2014). In addition, during the deposition of the chitosan layers free radicals could be entrapped within the polymers net with air (Lander et al., 2000; Martins et al., 2010). If this was the case, the presence of labile hydrogens is crucial for the H-atom donating ability of the curcumin, leading to a decrease of the RSA during storage (Jovanovic et al., 1999). Moreover, the presence of air within the polymer net can be responsible for the oxidation of curcumin, in which two oxygen molecules are included into the heptadienone chain connecting the curcumin phenolic rings resulting in the formation of dioxygenated bicyclopentadione product, being the oxidative degradation of curcumin a consequence of its activity as a ROS scavenger (Thangavel et al., 2015).

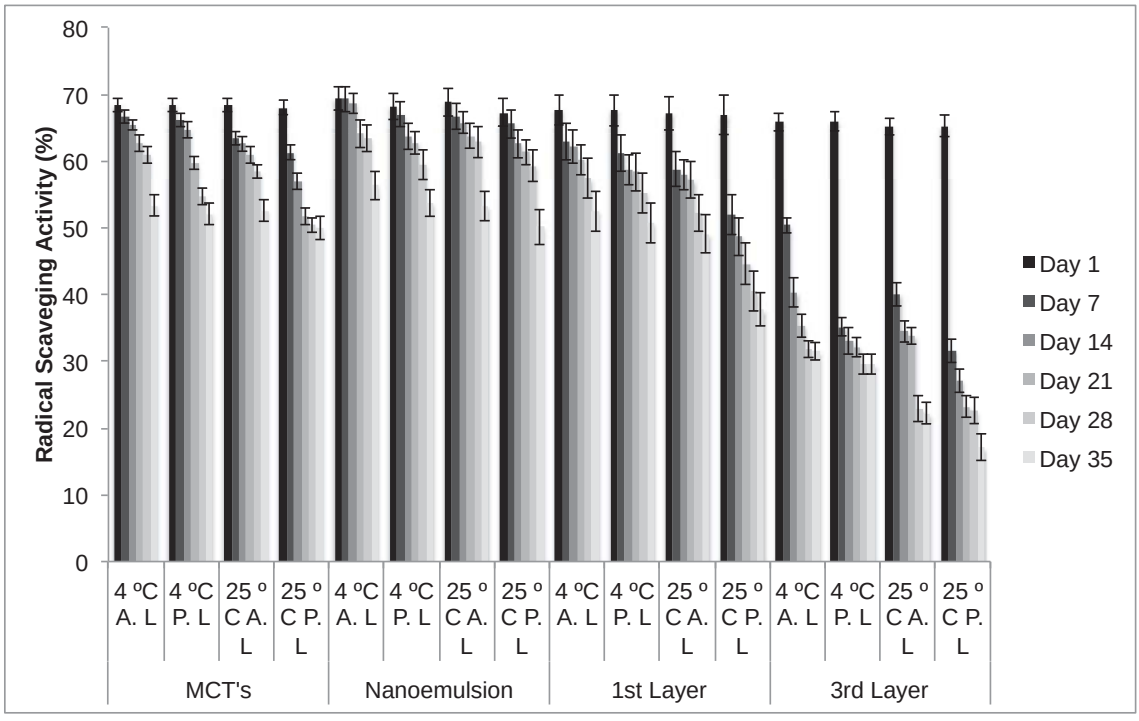

Figure 4.9 – Encapsulated curcumin radical scavenging activity during 35 days of storage. MCTs – Medium Chain Triglycerides; A. L – Absence of light; P. L – Presence of light.

4.3.5 Curcumin release from the nanosystems

The release behaviour of curcumin from the developed nanosystems was evaluated at 4 ºC, 25 ºC and 37 ºC in four different acceptor mediums, ethanol at 10 %, 20 % and 50 % (v/v) and 5 % (v/v) of SDS, always maintaining the sink conditions for curcumin.

Ethanol at 10 % and 20 % (v/v) solutions are food simulants assigned for foods that have a hydrophilic character and are able to extract hydrophilic substances. Ethanol at 20 % (v/v) shall be used for alcoholic foods with an alcohol content of up to 20 % and for those foods that contain a relevant amount of organic ingredients that render the food more lipophilic. In contrast, food simulants like ethanol at 50 % (v/v) are assigned for foods that have a lipophilic character and are able to extract lipophilic substances. Ethanol at 50 % (v/v) shall be used for alcoholic foods with an alcohol content of above 20 % and for oil.in-water emulsions (EC, 2011).

Concerning the release tests using 10 % and 20 % (v/v) of ethanol as the acceptor medium at 4 ºC and 25 ºC, it was observed that both nanosystems were unable to release curcumin (data not shown), maintaining the curcumin entrapped within the nanosystems. These nanosystems also showed H_d stability during the period of the release assays (55 h), whereas the mean droplet diameter was 80.0 ± 0.9 nm and 130.1 ± 1.5 nm for the nanoemulsion and multilayer nanoemulsion, respectively, before the assay, being after the release assay 79.2 ± 1.5 and 127.3 ± 2.8 nm, respectively, when using 10 % (v/v) of ethanol. For 20 % (v/v) of ethanol, the H_d after the assays were 77.2 ± 2.4 and 125.4 ± 3.9 nm, respectively for the nanoemulsion and multilayer nanoemulsion. The stability evidenced by the nanosystems gives an idea of which food products are best suited for the incorporation of the developed nanosystems (e.g. mayonnaise, mustard, salad creams, ice creams, non-alcoholic beverages and alcoholic beverages up to 20 % v/v).

For 50 % (v/v) ethanol at 25 ºC and for 5 % (v/v) SDS at 25 ºC and 37 ºC the LSM fitting curves adequately describe the experimental data (Figure 4.10) with good regression quality (R^2 > 0.87), and most parameters were estimated with good precision. This suggests that this model can be used to describe the transport mechanisms involved in curcumin release for both nanosystems.

From the parameters presented in Table 4.2 it can be seen that Brownian motion of curcumin in the nanosystems cannot describe the transport mechanism for itself, i.e. it does not strictly follow Fick's behaviour, but is governed by both Fickian and Case II transport, with only one main relaxation phenomenon (i.e. surfactant and polyelectrolytes relaxation. Figure 4.10a shows that the release of curcumin from nanoemulsions, when using SDS as the acceptor medium at 37 ºC, happens in the first 10 h, while at 25 ºC the release of curcumin from the nanoemulsion is much slower, happening during 48 h until achieving a stagnant phase. It is also possible to observe that at 37 ºC the mass of curcumin released (≈ 100 µg) is 2.5 times higher than the one released at 25 ºC (≈ 40 µg). Data in Table 4.2 show that relaxation is the main mechanism of transport, since it is responsible for 90 % of the curcumin released, M_R, while Brownian motion is responsible for only 10 %, M_F.

The relaxation effect is understood as a time-dependent phenomenon whose characteristic time constant reflects the reformation process of the surface layer (Atsumi et al., 1994). Briefly, there are two relaxation processes involved in surfactant micellar solutions. The first is a fast relaxation time, associated with the collision of surfactant monomers with micelles, generally in the order of the microseconds. The second relaxation time is related to the micelle formation and dissolution process, being an indicator of the micelle stability (Atsumi et al., 1994). Surfactant molecules maintain an equilibrium surface concentration (nanoemulsion stability) through a continuous dynamic exchange with surfactant monomers (and possibly larger assemblies such as surfactant micelles) in the continuous phase (Mason et al., 2006). Due to this, in the presence of high concentrations of SDS, nanoemulsion droplets can quickly exchange monomers with the surfactant monomers or even micelles, promoting the release of curcumin (Atsumi et al., 1994; Mason et al., 2006; Paruchuri et al., 2006).

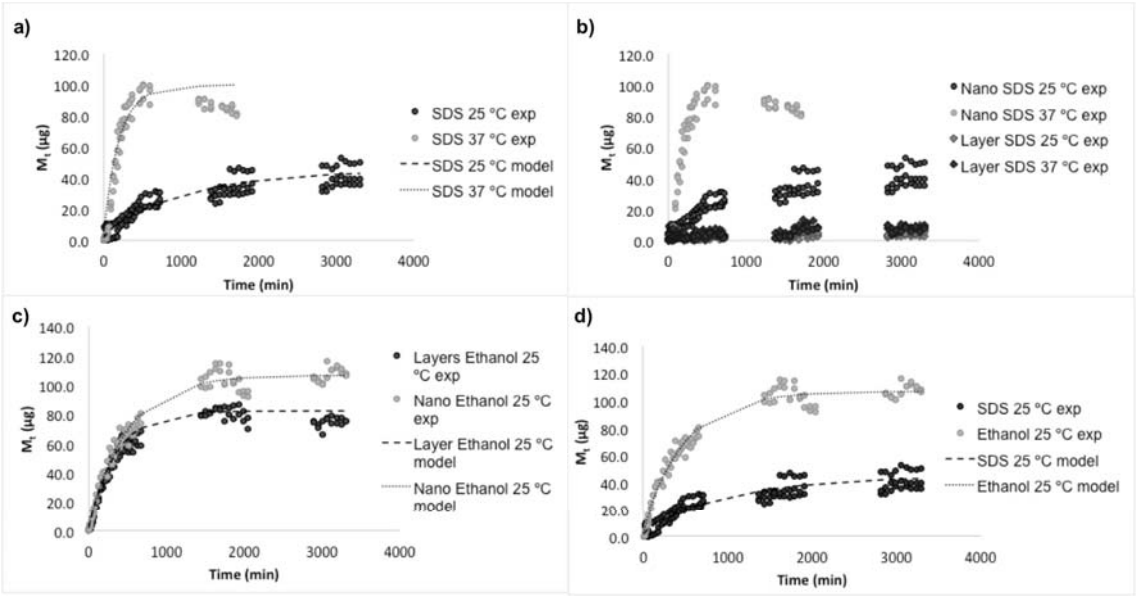

Figure 4.10 – Profile of curcumin release from nanosystems. a) effect of temperature, using 5 % (w/w) SDS as acceptor medium; b) effect of polyelectrolytes at 25 ºC and 37 ºC, using 5 % (w/w) SDS as acceptor medium; c) effect of polyelectrolytes at 25 ºC, using 50 % (v/v) ethanol as acceptor medium; d) effect of acceptor medium (ethanol vs SDS) at 25 ºC.

The effect of temperature on the total of mass released by relaxation can be explained by the influence of a higher temperature in the decrease of the second relaxation rate, that is able to promote instability, while leading to a decrease in the first relaxation time (Atsumi et al., 1994; Milcovich & Asaro, 2012; Paruchuri et al., 2006). In addition, it is known that high temperatures increase the solubility of bioactive compounds, which can be associated with the decrease in the first relaxation time and trigger a higher amount of M_R with the temperature increase, contributing to a slower rate of release. The multilayer nanoemulsion system was unable to perform a release, maintaining curcumin entrapped (Figure 4.10b). Here the addition of polyelectrolyte layers reinforced the stability of these structures, avoiding curcumin release, probably by inhibiting the exchange of monomers with the surfactant monomers or micelles from the acceptor medium. For the assays at 37 ºC, another possible explanation for the release behaviour can be pointed, is the fact that alginate and chitosan exhibit a gel form, which can further prevent the release of curcumin (Azevedo et al., 2014; Carreira et al., 2010). The effect of polyelectrolyte layers in the release properties was also evaluated, at 50 % (v/v) of ethanol at 25 ºC. From the parameters presented in Table 4.2 it can be

observed that relaxation was the phenomenon responsible for curcumin release ($M_R > M_F$). Ethanol is a water-soluble solvent that has the ability to modify the bulk physicochemical properties of aqueous solutions, such as density, refractive index, and interfacial tension, while changing their structural properties, such as the optimum curvature, solubility, and phase behaviour (Saberi et al., 2013). Due to this, ethanol may induce surfactant and polymer relaxation. Ethanol it is also known for its ability to create pores; although not fully understood, it may be related to a partial removal of the hydration water between surfactants and polyelectrolytes, resulting in segregation of the surfactant or polyelectrolyte network in the presence of ethanol (Delcea et al., 2011). Figure 4.10c shows that the creation of the multilayer on the nanoemulsion did not slow down the initial burst phase, nevertheless, after 4 h (240 min) a reduction in the released curcumin was observed, while reducing the final amount of released curcumin, from M_T= 82.37 to M_T= 106.76 μg, for multilayer nanoemulsion and nanoemulsion respectively. A similar behaviour was described by Sharipova and co-workers (in press), which observed that the build-up of polymer-surfactant complexes leads to a decrease in the release of α-tocopherol, promoting the release of α-tocopherol during 80 h. Nevertheless, in that work the emulsion used as control showed an initial burst up to 100 % of the encapsulated α-tocopherol within 1 h, due to the instability of the emulsion in the ethanol mixture (Sharipova et al., in press). Table 4.2 shows that M_R of curcumin released from nanoemulsions is higher (100.98 μg) than that obtained from multilayer nanoemulsions (77.37 μg). The addition of the polyelectrolyte layers may slow down the partial removal of the hydration water between surfactants and polyelectrolytes, which resulted in the segregation of the polyelectrolyte network, in the presence of ethanol. Moreover, a solvent like ethanol plays an important role in the establishment of hydrogen bonds (Delcea et al., 2011). As showed in FTIR section, the construction of the multilayer nanoemulsions showed hydrogen bonds between alginate and chitosan, that in the presence of ethanol may be disrupted, explaining the lower amount of curcumin released into the acceptor medium.

The influence of the acceptor medium was also evaluated. The experimental data and parameters present in Figure 4.10d and Table 4.2 show that considerably higher amounts of curcumin were released from the

nanoemulsions, when 50 % (v/v) ethanol was used as the acceptor medium, achieving a M_T of 106.76 µg, while for the 5 % (v/v) SDS, the M_T was 41.13 µg. These differences may be explained by the ability of ethanol to create pores in the nanosystems, increasing the amount of released curcumin, due to the partial removal of hydration water between the surfactants (Delcea et al., 2011). This effect is even more pronounced when observing the multilayer nanoemulsions release profile, while the polyelectrolytes in the SDS medium were able to maintain the curcumin entrapped, avoiding the relaxation phenomena, ethanol through hydrogen-bound disruption and pore creation ability, leading to an M_T of 82.37 µg.

Table 4.2 – Results of fitting the LSM to experimental data of the curcumin release profile. Evaluation of the quality of the regression on the basis of R^2

Nanosystem	Acceptor medium	T (ºC)	R^2	M_F (µg)	K_F (cm^{-1})	M_R (µg)	K_R (cm^{-1})	M_T (µg)
Nanoemulsion	SDS	25	0.8758	4.44	0.0047	36.69	0.0012	41.13
		37	0.9280	10.00	0.0010	90.97	0.0054	100.97
Nanoemulsion	50% vol. Ethanol	25	0.9889	5.78	0.014	100.98	0.0020	106.76
Multilayer nanoemulsion	50% vol. Ethanol	25	0.9845	5.00	0.0029	77.37	0.0029	82.37

T, Temperature; M_F, equilibrium amount of sorption in unrelaxed polymer; M_R, Equilibrium sorption of the relation process; K_F, Fick rate constant; K_R, relaxation rate constant.

4.3.6 Nanosystems stability under storage conditions

Curcumin nanoemulsions and multilayer nanoemulsions showed no macroscopic sign (visual observation) of instability phenomena (i.e. creaming or phase separation) after three months of storage. The results show that curcumin nanoemulsions and multilayer nanoemulsions maintained the values of H_d and *PdI* (Figure 4.11) during storage. Results showed that after storage H_d values did not present statistically significant (p>0.05) differences when compared to the values obtained immediately after production (see Figure 4.11).

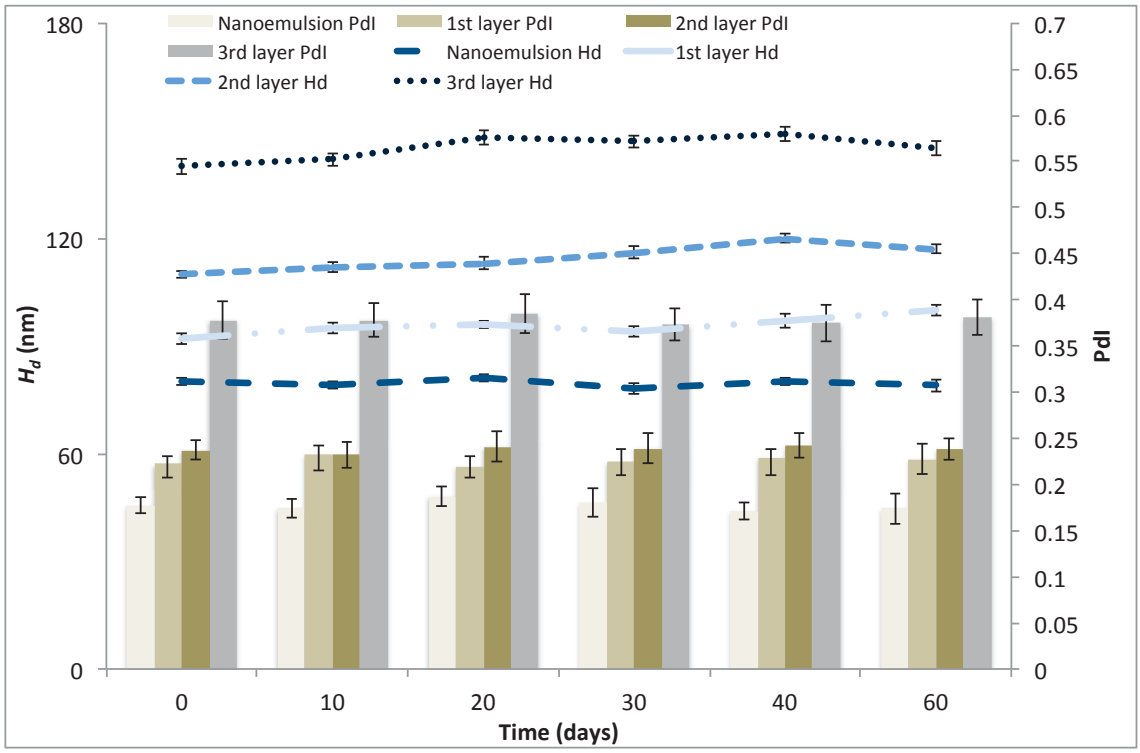

Figure 4.11 – Hydrodynamic diameter (H_d) and polydispersity index (*PdI*) during 60 days of storage. Bars indicate standard deviation (n = 3). Lines are for readers' guidance and do not represent a model prediction.

4.4 Conclusions

Layer-by-layer assembly could successfully change the surface characteristics of nanoemulsions. These nanosystems showed stability under storage conditions in terms of H_d and *PdI*, being stable to changes in temperature and being pH-responsiveness. From QCM measurements it is possible to conclude that deposition of chitosan and alginate results in the formation of a stable multilayer structure, mainly due electrostatic interactions between the polyelectrolytes, while FTIR showed that interactions such as hydrogen bonds might also be involved. Fitting the linear superimposition model to experimental data of curcumin release suggested an anomalous behaviour, being relaxation of the polymers/surfactant the main transport phenomenon observed. This work clarifies the release mechanism involved when two different acceptor media are used, enlightening the impact of temperature, solvent and surface properties in the controlled release.

4.5 References

Adamczak M, Kupiec A, Jarek E, Szczepanowicz K & Warszyński P (2014) Preparation of the squalene-based capsules by membrane emulsification method and polyelectrolyte multilayer adsorption. Colloids and Surfaces A: Physicochemical and Engineering Aspects 462, 147-152.

Anton N & Vandamme T (2011) Nano-emulsions and Micro-emulsions: Clarifications of the Critical Differences. Pharmaceutical Research 28(5), 978-985.

Aoki T, Decker EA & McClements DJ (2005) Influence of environmental stresses on stability of O/W emulsions containing droplets stabilized by multilayered membranes produced by a layer-by-layer electrostatic deposition technique. Food Hydrocolloids 19(2), 209-220.

Atsumi O, Akiko M, Keiji S & Kenshiro T (1994) Dynamic Properties of Soluble Monolayer of Sodium Dodecyl Sulfate (SDS) on Aqueous Solution. Japanese Journal of Applied Physics 33(10B), L1468.

Azevedo MA, Bourbon AI, Vicente AA & Cerqueira MA (2014) Alginate/chitosan nanoparticles for encapsulation and controlled release of vitamin B2. International Journal of Biological Macromolecules 71, 141-146.

Berens AR & Hopfenberg HB (1978) Diffusion and relaxation in glassy polymer powders: 2. Separation of diffusion and relaxation parameters. Polymer 19(5), 489-496.

Berton-Carabin CC, Ropers M-H & Genot C (2014) Lipid Oxidation in Oil-in-Water Emulsions: Involvement of the Interfacial Layer. Comprehensive Reviews in Food Science and Food Safety 13(5), 945-977.

Bourbon AI, Pinheiro AC, Carneiro-da-Cunha MG, Pereira RN, Cerqueira MA & Vicente AA (2015) Development and characterization of lactoferrin-GMP nanohydrogels: Evaluation of pH, ionic strength and temperature effect. Food Hydrocolloids 48, 292-300.

Bourbon AI, Pinheiro AC, Cerqueira MA, Rocha CMR, Avides MC, Quintas MAC & Vicente AA (2011) Physico-chemical characterization of chitosan-based edible films incorporating bioactive compounds of different molecular weight. Journal of Food Engineering 106(2), 111-118.

Burke SE & Barrett CJ (2003a) Acid−Base Equilibria of Weak Polyelectrolytes in Multilayer Thin Films. Langmuir 19(8), 3297-3303.

Burke SE & Barrett CJ (2003b) pH-Responsive Properties of Multilayered Poly(l-lysine)/Hyaluronic Acid Surfaces. Biomacromolecules 4(6), 1773-1783.

Carreira AS, Gonçalves FAMM, Mendonça PV, Gil MH & Coelho JFJ (2010) Temperature and pH responsive polymers based on chitosan: Applications and new graft copolymerization strategies based on living radical polymerization. Carbohydrate Polymers 80(3), 618-630.

Cerqueira M, Pinheiro A, Silva H, Ramos P, Azevedo M, Flores-López M, Rivera M, Bourbon A, Ramos Ó & Vicente A (2014) Design of Bio-nanosystems for Oral Delivery of Functional Compounds. Food Engineering Reviews 6(1-2), 1-19.

Cui J, van Koeverden MP, Müllner M, Kempe K & Caruso F (2014) Emerging methods for the fabrication of polymer capsules. Advances in Colloid and Interface Science 207, 14-31.

Delcea M, Möhwald H & Skirtach AG (2011) Stimuli-responsive LbL capsules and nanoshells for drug delivery. Advanced Drug Delivery Reviews 63(9), 730-747.

Donsì F, Sessa M & Ferrari G (2011) Effect of Emulsifier Type and Disruption Chamber Geometry on the Fabrication of Food Nanoemulsions by High Pressure Homogenization. Industrial & Engineering Chemistry Research 51(22), 7606-7618.

EC, (2011). Plastic materials and articles intended to come into contact with food., in: Commission E (Ed.), *COMMISSION REGULATION (EU) No 10/2011*, Official Journal of the European Union.

EFSA (2010). Call for scientific data on food additives permitted in the EU and belonging to the functional classes of emulsifiers, stabilisers and gelling agents, Available at: http://www.efsa.europa.eu/en/dataclosed/call/ans091123.pdf. Accessed 17/03/2015.

FDA, (2014a). CFR - Code of Federal Regulations Title 21.

FDA, (2014b). CFR - Code of Federal Regulations Title 21 - Food and Drugs.

Friedrich RB, Kann B, Coradini K, Offerhaus HL, Beck RCR & Windbergs M (2015) Skin penetration behavior of lipid-core nanocapsules for simultaneous

delivery of resveratrol and curcumin. European Journal of Pharmaceutical Sciences 78, 204-213.

Gordon V, Marom G & Magdassi S (2014) Formation of hydrophilic nanofibers from nanoemulsions through electrospinning. Int J Pharm 478(1), 172-179.

Guttoff M, Saberi AH & McClements DJ (2015) Formation of vitamin D nanoemulsion-based delivery systems by spontaneous emulsification: factors affecting particle size and stability. Food Chem 171(0), 117-122.

Guzey D & McClements DJ (2006) Formation, stability and properties of multilayer emulsions for application in the food industry. Advances in Colloid and Interface Science 128-130, 227-248.

Harnsilawat T, Pongsawatmanit R & McClements DJ (2006) Characterization of β-lactoglobulin–sodium alginate interactions in aqueous solutions: A calorimetry, light scattering, electrophoretic mobility and solubility study. Food Hydrocolloids 20(5), 577-585.

Hee-Je Kim, Dong- Jo Kim, Karthick SN, Hemalatha KV, C. Justin Raj, Sunseong Ok & Choe Y (2013) Curcumin Dye Extracted from Curcuma longa L. Used as Sensitizers for Efficient Dye-Sensitized Solar Cells. International Journal of Electrochemical Science(8), 8320 - 8328.

Jovanovic SV, Steenken S, Boone CW & Simic MG (1999) H-Atom Transfer Is A Preferred Antioxidant Mechanism of Curcumin. Journal of the American Chemical Society 121(41), 9677-9681.

Kaur K, Kumar R & Mehta SK (2015) Nanoemulsion: A new medium to study the interactions and stability of curcumin with bovine serum albumin. Journal of Molecular Liquids 209, 62-70.

Khurana A & Ho C-T (1988) High Performance Liquid Chromatographic Analysis of Curcuminoids and Their Photo-oxidative Decomposition Compounds in Curcuma Longa L. Journal of Liquid Chromatography 11(11), 2295-2304.

Lander R, Manger W, Scouloudis M, Ku A, Davis C & Lee A (2000) Gaulin Homogenization: A Mechanistic Study. Biotechnology Progress 16(1), 80-85.

Lawrie G, Keen I, Drew B, Chandler-Temple A, Rintoul L, Fredericks P & Grøndahl L (2007) Interactions between Alginate and Chitosan Biopolymers Characterized Using FTIR and XPS. Biomacromolecules 8(8), 2533-2541.

Li P, Dai Y-N, Zhang J-P, Wang A-Q & Wei Q (2008) Chitosan-Alginate Nanoparticles as a Novel Drug Delivery System for Nifedipine. International Journal of Biomedical Science : IJBS 4(3), 221-228.

Li Y, Hu M, Xiao H, Du Y, Decker EA & McClements DJ (2010) Controlling the functional performance of emulsion-based delivery systems using multi-component biopolymer coatings. European Journal of Pharmaceutics and Biopharmaceutics 76(1), 38-47.

Liechty WB, Scheuerle RL & Peppas NA (2013) Tunable, responsive nanogels containing t-butyl methacrylate and 2-(t-butylamino)ethyl methacrylate. Polymer 54(15), 3784-3795.

Liu Y, Cai Y, Jiang X, Wu J & Le X (2016) Molecular interactions, characterization and antimicrobial activity of curcumin–chitosan blend films. Food Hydrocolloids 52, 564-572.

Madrigal-Carballo S, Lim S, Rodriguez G, Vila AO, Krueger CG, Gunasekaran S & Reed JD (2010) Biopolymer coating of soybean lecithin liposomes via layer-by-layer self-assembly as novel delivery system for ellagic acid. Journal of Functional Foods 2(2), 99-106.

Malvern I, (2011). Dynamic light scattering common terms defined, in: Instruments M (Ed.), Worcestershire, UK.

Martins GV, Mano JF & Alves NM (2010) Nanostructured self-assembled films containing chitosan fabricated at neutral pH. Carbohydrate Polymers 80(2), 570-573.

Mason TG, Wilking JN, Meleson K, Chang CB & Graves SM (2006) Nanoemulsions: formation, structure, and physical properties. Journal of Physics: Condensed Matter 18(41), R635.

McClements DJ & Xiao H (2012) Potential biological fate of ingested nanoemulsions: influence of particle characteristics. Food & Function 3(3), 202-220.

Milcovich G & Asaro F, (2012). Insights into Catanionic Vesicles Thermal Transition by NMR Spectroscopy, in: Starov V & Griffiths, P (Eds.), *UK Colloids 2011*. Springer Berlin Heidelberg, pp. 35-38.

Mora-Huertas CE, Fessi H & Elaissari A (2010) Polymer-based nanocapsules for drug delivery. International Journal of Pharmaceutics 385(1–2), 113-142.

Morais Diane JM & Burgess J (2014) Vitamin E nanoemulsions characterization and analysis. International Journal of Pharmaceutics 465(1–2), 455-463.

Mun S, Decker EA & McClements DJ (2005) Influence of Droplet Characteristics on the Formation of Oil-in-Water Emulsions Stabilized by Surfactant−Chitosan Layers. Langmuir 21(14), 6228-6234.

Mun S, Decker EA & McClements DJ (2006) Effect of molecular weight and degree of deacetylation of chitosan on the formation of oil-in-water emulsions stabilized by surfactant–chitosan membranes. Journal of Colloid and Interface Science 296(2), 581-590.

Ozturk B, Argin S, Ozilgen M & McClements DJ (2014) Formation and stabilization of nanoemulsion-based vitamin E delivery systems using natural surfactants: Quillaja saponin and lecithin. Journal of Food Engineering 142(0), 57-63.

Paruchuri VK, Nalaskowski J, Shah DO & Miller JD (2006) The effect of cosurfactants on sodium dodecyl sulfate micellar structures at a graphite surface. Colloids and Surfaces A: Physicochemical and Engineering Aspects 272(3), 157-163.

Pawlak A & Mucha M (2003) Thermogravimetric and FTIR studies of chitosan blends. Thermochimica Acta 396(1–2), 153-166.

Pinheiro AC, Bourbon AI, Cerqueira MA, Maricato É, Nunes C, Coimbra MA & Vicente AA (2015) Chitosan/fucoidan multilayer nanocapsules as a vehicle for controlled release of bioactive compounds. Carbohydrate Polymers 115, 1-9.

Pinheiro AC, Bourbon AI, Quintas MAC, Coimbra MA & Vicente AA (2012) K-carrageenan/chitosan nanolayered coating for controlled release of a model bioactive compound. Innovative Food Science & Emerging Technologies 16(0), 227-232.

Pinheiro AC, Coimbra MA & Vicente AA (2016) In vitro behaviour of curcumin nanoemulsions stabilized by biopolymer emulsifiers – Effect of interfacial composition. Food Hydrocolloids 52, 460-467.

Plaza-Oliver M, Baranda JFSd, Rodríguez Robledo V, Castro-Vázquez L, Gonzalez-Fuentes J, Marcos P, Lozano MV, Santander-Ortega MJ & Arroyo-Jimenez MM (2015) Design of the interface of edible nanoemulsions to

modulate the bioaccessibility of neuroprotective antioxidants. International Journal of Pharmaceutics 490(1–2), 209-218.

Priyadarsini K (2014) The Chemistry of Curcumin: From Extraction to Therapeutic Agent. Molecules 19(12), 20091.

Priyadarsini KI (2009) Photophysics, photochemistry and photobiology of curcumin: Studies from organic solutions, bio-mimetics and living cells. Journal of Photochemistry and Photobiology C: Photochemistry Reviews 10(2), 81-95.

Qian C & McClements DJ (2011) Formation of nanoemulsions stabilized by model food-grade emulsifiers using high-pressure homogenization: Factors affecting particle size. Food Hydrocolloids 25(5), 1000-1008.

Rao J & McClements DJ (2013) Optimization of lipid nanoparticle formation for beverage applications: Influence of oil type, cosolvents, and cosurfactants on nanoemulsion properties. Journal of Food Engineering 118(2), 198-204.

Rufino MdSM, Alves RE, Brito ESd, Morais SMd, Sampaio CdG, Pérez - Jiménez J & Saura-Calixto FD (2007). Metodologia científica: determinação da atividade antioxidante total em frutas pela captura do radical livre DPPH., Available at: http://www.infoteca.cnptia.embrapa.br/handle/doc/426953. Accessed 22/08/2015.

Saberi AH, Fang Y & McClements DJ (2013) Fabrication of vitamin E-enriched nanoemulsions by spontaneous emulsification: Effect of propylene glycol and ethanol on formation, stability, and properties. Food Research International 54(1), 812-820.

Saberi AH, Zeeb B, Weiss J & McClements DJ (2015) Tuneable stability of nanoemulsions fabricated using spontaneous emulsification by biopolymer electrostatic deposition. Journal of Colloid and Interface Science 455, 172-178.

Sari TP, Mann B, Kumar R, Singh RRB, Sharma R, Bhardwaj M & Athira S (2015) Preparation and characterization of nanoemulsion encapsulating curcumin. Food Hydrocolloids 43, 540-546.

Sharipova AA, Aidarova SB, Grigoriev D, Mutalieva B, Madibekova G, Tleuova A & Miller R (in press) Polymer–surfactant complexes for microencapsulation of vitamin E and its release. Colloids and Surfaces B: Biointerfaces.

Shi X, Du Y, Sun L, Zhang B & Dou A (2006) Polyelectrolyte complex beads composed of water-soluble chitosan/alginate: Characterization and their protein release behavior. Journal of Applied Polymer Science 100(6), 4614-4622.

Silva HD, Cerqueira MA, Souza BWS, Ribeiro C, Avides MC, Quintas MAC, Coimbra JSR, Carneiro-da-Cunha MG & Vicente AA (2011) Nanoemulsions of β-carotene using a high-energy emulsification-evaporation technique. Journal of Food Engineering 102(2), 130-135.

Silva HD, Cerqueira MA & Vicente AA, (2015a). Chapter 56 - Nanoemulsion-Based Systems for Food Applications, in: Kharisov BI (Ed.), *CRC Concise Encyclopedia of Nanotechnology*. CRC Press by Taylor and Francis Group, USA.

Silva HD, Cerqueira MA & Vicente AA (2015b) Influence of surfactant and processing conditions in the stability of oil-in-water nanoemulsions. Journal of Food Engineering.

Siviero A, Gallo E, Maggini V, Gori L, Mugelli A, Firenzuoli F & Vannacci A (2015) Curcumin, a golden spice with a low bioavailability. Journal of Herbal Medicine 5(2), 57-70.

Souza BWS, Cerqueira MA, Bourbon AI, Pinheiro AC, Martins JT, Teixeira JA, Coimbra MA & Vicente AA (2012) Chemical characterization and antioxidant activity of sulfated polysaccharide from the red seaweed Gracilaria birdiae. Food Hydrocolloids 27(2), 287-292.

Spigno G, Donsì F, Amendola D, Sessa M, Ferrari G & De Faveri DM (2013) Nanoencapsulation systems to improve solubility and antioxidant efficiency of a grape marc extract into hazelnut paste. Journal of Food Engineering 114(2), 207-214.

Szczepanowicz K, Bazylińska U, Pietkiewicz J, Szyk-Warszyńska L, Wilk KA & Warszyński P (in press) Biocompatible long-sustained release oil-core polyelectrolyte nanocarriers: From controlling physical state and stability to biological impact. Advances in Colloid and Interface Science.

Tang SY, Manickam S, Wei TK & Nashiru B (2012) Formulation development and optimization of a novel Cremophore EL-based nanoemulsion using ultrasound cavitation. Ultrasonics Sonochemistry 19(2), 330-345.

Tegge G (1989) Yalpani, M.: Polysaccharides - Synthesis, Modifications and Structure/Property Relations (Vol. 36 of the series “Studies in Organic Chemistry”). Elsevier Science Publishers, Amsterdam – Oxford – New York – Tokyo 1988. ISBN 0–444–43022–9. 522 pages, with over 40 tables and 130

schemes and illustrations. Price US $ 171,-; Dfl 325,-. Available from : P.O. Box 211, 1000 AE Amsterdam (The Netherlands) or P.O. Box 1663, Grand Central Station. New York, NY 10163 (U.S.A.). Starch - Stärke 41(6), 244-244.

Thangavel S, Yoshitomi T, Sakharkar MK & Nagasaki Y (2015) Redox nanoparticles inhibit curcumin oxidative degradation and enhance its therapeutic effect on prostate cancer. Journal of Controlled Release 209, 110-119.

Tomren MA, Másson M, Loftsson T & Tønnesen HH (2007) Studies on curcumin and curcuminoids: XXXI. Symmetric and asymmetric curcuminoids: Stability, activity and complexation with cyclodextrin. International Journal of Pharmaceutics 338(1–2), 27-34.

Troncoso E, Aguilera JM & McClements DJ (2012) Influence of particle size on the in vitro digestibility of protein-coated lipid nanoparticles. Journal of Colloid and Interface Science 382(1), 110-116.

Vachoud L, Zydowicz N & Domard A (2000) Physicochemical behaviour of chitin gels. Carbohydrate Research 326(4), 295-304.

Viana RB, da Silva ABF & Pimentel AS (2012) Infrared Spectroscopy of Anionic, Cationic, and Zwitterionic Surfactants. Advances in Physical Chemistry 2012, 14.

Vlachos N, Skopelitis Y, Psaroudaki M, Konstantinidou V, Chatzilazarou A & Tegou E (2006) Applications of Fourier transform-infrared spectroscopy to edible oils. Analytica Chimica Acta 573–574, 459-465.

Yang H, Irudayaraj J & Paradkar MM (2005) Discriminant analysis of edible oils and fats by FTIR, FT-NIR and FT-Raman spectroscopy. Food Chemistry 93(1), 25-32.

Yu H, Shi K, Liu D & Huang Q (2012) Development of a food-grade organogel with high bioaccessibility and loading of curcuminoids. Food Chemistry 131(1), 48-54.

Yucel C, Quagliariello V, Iaffaioli RV, Ferrari G & Donsì F (2015) Submicron complex lipid carriers for curcumin delivery to intestinal epithelial cells: Effect of different emulsifiers on bioaccessibility and cell uptake. International Journal of Pharmaceutics 494(1), 357-369.

Zhao L, Du J, Duan Y, Zang Yn, Zhang H, Yang C, Cao F & Zhai G (2012) Curcumin loaded mixed micelles composed of Pluronic P123 and F68:

Preparation, optimization and in vitro characterization. Colloids and Surfaces B: Biointerfaces 97, 101-108.

CHAPTER 5

EVALUATING THE EFFECT OF SURFACE COMPOSITION ON CURCUMIN NANOEMULSIONS DURING *IN VITRO* DIGESTIONS

In this chapter the effect of the deposition of chitosan and alginate layers onto nanoemulsion systems on curcumin bioaccessibility during *in vitro* digestions was studied using a dynamic gastrointestinal system.

This Chapter was adapted from:

Silva, H. D., Poejo, J., Pinheiro, A. C., Donsì, F., Serra, A. T., Duarte C. M., Ferrari, G., Cerqueira, M. A. & Vicente, A. A. Development and characterization of lipid-based nanosystems: Effect of interfacial composition on nanoemulsions behaviour. *Food Hydrocolloids* (Submitted).

5.1 Introduction

Consumers' demands for new and healthier functional food products encouraged the food industry to seek for new strategies to fortify food products with bioactive compounds, with increased nutritional value, turning foods into products that promote health and wellness (Cerqueira et al., 2013; Silva et al., 2012; Silva et al., 2015b). Many of these bioactive compounds are lipophilic often resulting in low bioavailability, whereas some are pH- and temperature-sensitive, being prone to oxidative and chemical degradation (Guttoff et al., 2015; Mayer et al., 2013; McClements, 2015; Zou et al., 2015). Lipid-based delivery systems can be designed to encapsulate, protect, control the release and digestion of lipophilic bioactive compounds in the gastrointestinal tract, while improving their bioavailability (Li et al., 2010; McClements & Li, 2010; Sun et al., 2015). In this field nanoemulsions can inhibit the chemical and oxidative degradation of bioactive compounds, moreover their large surface area can enhance lipid digestibility rates, improve the release of bioactive compounds, promote the faster formation of mixed micelles, while enhancing the permeability of bioactive compounds across the mucus layer and epithelium cells (Cerqueira et al., 2014; Sun et al., 2015; Ting et al., 2014). Nonetheless, nanoemulsions present some drawbacks, and their stability can be influenced by their behaviour towards dehydration, temperature changes (e.g. heating, chilling and freezing-thawing) and the passage through the gastrointestinal tract (Cerqueira et al., 2014; Silva et al., 2015a). Multilayer nanoemulsions can improve the stability of nanoemulsions under environmental stresses, while controling lipids digestibility and release of bioactive compounds in response to specific environmental triggers (Cerqueira et al., 2014; Li et al., 2010; Pinheiro et al., 2016). Multilayer nanoemulsions can be produced using the LbL technique, based on the deposition of charged polyelectrolytes onto oppositelly charged lipid droplets (Li et al., 2010; Pinheiro et al., 2016). The characteristics of a multilayer nanoemulsion are known for being largely influenced by the properties of the outer polyelectrolyte layer, such as molecular weight, charge density, ionic composition and pK_a. However, the functional properties can be designed according to the type of polyelectrolyte, sequence of the polyelectrolyte layers, number of layers and the conditions to which the solution

is subjected during the construction of the system (Li et al., 2010). The proper selection of the lipid nanosystem should be based on the final application. For instance, lipid-based nanosystems can be used to increase the bioavailability of bioactive compounds, trigger the controlled release at specific locations within the gastrointestinal tract or be designed to slow down the digestability rate of lipids, being able to stimulate ileal brake mechanism responsible for regulating hunger, satiety and satiation, thereby reducing the caloric intake of food products (Li et al., 2010; Maljaars et al., in press; Pinheiro et al., 2016). In fact, the higher specific area of nanoemulsions allows the increase of the rate and extent of lipids digestion, which make them interesting for addressing humam disorders that inhibit lipid digestion or absorption (Troncoso et al., 2012). On the contrary, changing the interfacial properties through the deposition of polyelectrolyte layers may help controlling lipid's digestibility by enhancing the coating integrity, preventing lipase and other enzymes from reaching the encapsulated lipids (McClements & Li, 2010; Troncoso et al., 2012). Therefore, the understanding of the behavior of lipid-based nanosystems within the gastrointestinal tract is of great importance, being important for the development of tailored lipid nanosystems (Pinheiro et al., 2016). With this view the main purpose of this study was to evaluate the influence of the interfacial composition of nanoemulsions on their behavior under *in vitro* gastrointestinal conditions. The cytotoxicity of the developed nanosystems was also evaluated prior to *in vitro* digestion.

5.2 Materials and Methods

5.2.1 Materials

Neobee 1053 medium chain triglycerides (MCTs), composed by caprylic/capric triglyceride oil with a fatty acid distribution of 55 % of C8:0 and 44 % of C10:0, was kindly provided by Stepan (The Netherlands) and was used without further purification. SDS, curcumin (Mw = 368.38 Da), DPPH, pepsin from porcine gastric mucosa (600 U mL^{-1}), lipase from porcine pancreas (40 U mL^{-1}), pancreatin from porcine pancreas (8 × USP), bile extract porcine and the salts used for preparing the gastric and small intestinal electrolyte solutions,

hydrochloric acid, sodium bicarbonate, Nile Red 9-diethylamino-5H-benzo[α]phenoxazine-5-one and dimethyl sulfoxide were purchased from Sigma-Aldrich (St Louis, MO, USA). Chitosan (deacetylation degree ≥ 95 %) was purchased from Golden-Shell Biochemical CO., LTD (Zhejiang, China) and sodium alginate with Mw ≈ 15,900 Da and viscosity ≈ 200 cp (1 % aqueous solution with Brookfield Model LV – 60 rpm at 25 ºC) from Manutex RSX, Kelco 104 International, Ltd. (Portugal). Lactic acid (90 %) was purchased from Acros Organics (Geel, Belgium). Sodium hydroxide and phenolphthalein were obtained from Panreac (Barcelona, Spain). Chloroform was obtained from Fisher Scientific (NJ, USA) and acetone from Fisher Chemical (Loughborough, UK). All cell culture media and supplements, namely RPMI 1640, Fetal Bovine Serum (FBS), Penicillin-Streptomycin (PS) and trypsin/EDTA, were obtained from Invitrogen (Paisley, UK). For cytotoxicity experiments phosphate buffered saline (PBS) powder was purchased from Sigma-Aldrich (St. Louis, USA) and CellTiter 96® AQueous One Solution Cell Proliferation Assay was obtained from Promega (Wisconsin, USA). Distilled water (Milli-Q apparatus, Millipore Corp., Bedford, MA, USA) was used to prepare all solutions.

5.2.2 Experimental Procedures

5.2.2.1 Preparation of curcumin nanosystems

5.2.2.1.1 Curcumin nanoemulsion preparation

Oil-in-water (O/W) nanoemulsions were prepared according to (Silva et al., 2015b), with slight modifications. Briefly, 0.1 % (w/w) of curcumin was solubilized at 90 ºC in MCTs during 30 min. The oil-to-aqueous phase containing 1 % (w/w) of SDS in distilled water. An oily phase to aqueous phase volume ratio of 1:9 was used. The nanoemulsions were pre-mixed during 2 min at 5000 rpm using an Ultra-Turrax homogenizer (T 25, Ika-Werke, Germany) followed by 20 cycles of homogenization through a high-pressure homogenizer equipped with a zirconia nozzle (Z4 nozzle) with 100 μm of orifice (Nano DeBEE, BEE International, USA) at 15000 Psi (103 MPa).

5.2.2.1.2 Curcumin multilayer nanoemulsion preparation

The multilayer nanoemulsions were produced according to chapter 4 through adsorption of consecutive deposition of layers of polyelectrolytes onto the curcumin nanoemulsions using the LbL electrostatic deposition technique. The saturation method was applied, i.e. the layers were constructed by subsequent adsorption of polyelectrolytes from their solutions without the intermediate rinsing step. Briefly, anionic curcumin nanoemulsions were coated with alternating layers of positively charged chitosan solution at pH 3 and negatively charged sodium alginate at pH 7 (volume ratio of 1:1, respectively) until the desired number of biopolymer layers was achieved. The polyelectrolyte solutions were used at pH values where the polyelectrolytes were strongly charged and added dropwise with a syringe pump (NE-1000, New Era Pump Systems, Inc., USA) to fresh curcumin nanoemulsions, under stirring for 15 min.

5.2.2.2 Nanosystems size measurements

The particle size distribution and polydispersity index (*PdI*) of nanoemulsions and multilayer nanoemulsions were determined using Dynamic Light Scattering (DLS) (Zetasizer Nano ZS-90, Malvern Instruments, Worcestershire, UK). The nanoemulsion samples were diluted 10× in distilled water at room temperature. Data were reported as the mean droplet diameter (hydrodynamic diameter, H_d). *PdI* is a dimensionless and indicates the heterogeneity (monodisperse or polydisperse) of particles' size in a mixture (Malvern, 2011). Each sample was analysed in a disposable polystyrene cell (DTS0012, Malvern Instruments). The measurements were performed in duplicate, with three readings for each of them. The results are given as the average ± standard deviation of the six values obtained (Rao & McClements, 2013; Silva et al., 2011).

5.2.2.3 Nanosystems charge measurements

The droplet charge (*Zp*) of the nanoemulsions and multilayer nanoemulsions was determined using a particle micro-electrophoresis instrument (Zetasizer Nano ZS-90, Malvern Instruments, Worcestershire, UK). Samples were diluted 100× in distilled water prior to measurements in order to avoid multiple scattering effects at ambient temperature and the diluted emulsions were

placed into disposable capillary cells (DTS 1060, Malvern Instruments) (Ozturk et al., 2014; Rao & McClements, 2013).

5.2.2.4 Nanosystems stability and curcumin release at gastrointestinal conditions

The stability of curcumin nanosystems under gastrointestinal environmental conditions was evaluated by the dialysis method. 2 mL of aqueous curcumin nanosystems were added into a dialysis membrane (molecular weight cut-off 15 kDa; Cellu-Sep H1, Membrane filtration products, USA). The sealed dialysis membrane was then placed into 50 mL of buffer solution (phosphate buffer, PBS, for pH 7.4 and KCl–HCl buffer for pH 2) under magnetic stirring at 37 ºC. At appropriate time intervals, 0.5 mL of supernatant were taken and 0.5 mL of fresh acceptor medium was added to keep the volume of the release medium constant. The stability of the nanosystems and the released amount of curcumin from the nanosystems was evaluated by measuring the H_d after 54 h and the absorbance at 425 nm, maximum absorbance peak (Elisa Biotech Synergy HT, Biotek, USA), respectively. All tests were run at least in duplicate.

5.2.2.5 In vitro *digestion*

5.2.2.5.1 Dynamic gastrointestinal model

A dynamic gastrointestinal system was used for the *in vitro* digestion experiments, using the model developed by Pinheiro et al. (2016). This model simulates the main events that occur during digestion and consists of four compartments simulating the stomach, duodenum, jejunum and ileum. Each compartment consists of two connected glass reactors with a flexible wall inside and water is pumped around the flexible walls to maintain the temperature at 37 ºC and to enable the simulation of the peristaltic movements (by the alternate compression and relaxation of the flexible walls). The changes in water pressure are achieved by peristaltic pumps, which alter the flow direction according to the time controlling devices connected to them. The compartments are connected by silicone tubes and, at a predefined time, a constant volume of chyme is transferred. All compartments are equipped with pH electrodes and pH values are controlled by the secretion of HCl (1 mol L^{-1}) into the stomach and $NaHCO_3$ (1 mol L^{-1}) into the intestinal compartments. The gastric and

intestinal secretions are added via syringe pumps at pre-set flow rates. The jejunum and ileum compartments are connected with hollow-fibre devices (SpectrumLabs Minikros®, M20S-100-01P, USA) to absorb digestion products and water from the chyme and to modify electrolyte and bile salts concentration of the chyme (Pinheiro et al., 2016; Reis et al., 2008). It should be noted that, although at the mouth stage there may be changes in emulsions' size and interfacial characteristics, influencing the emulsions' fate in the GI tract (McClements & Xiao, 2012; Pinheiro et al., 2016), this phase was not included because the sample is liquid (and therefore the mastication is not relevant and the residence time in the mouth is very low) and does not contain starch (i.e. the primary enzyme present in saliva, amylase, would not act) (Pinheiro et al., 2016).

5.2.2.5.2 Experimental conditions

In vitro digestion was performed as described by other authors (Pinheiro et al., 2016; Reis et al., 2008) with minor modifications. A volume of 40 mL of curcumin and curcumin-loaded nanosystems (i.e. nanoemulsions and multilayer nanoemulsions) was added to the dynamic gastrointestinal system (gastric compartment) and run for a total of 5 h, simulating average physiological conditions of GI tract by the continuous addition of gastric, duodenal, jejunal and ileal secretions. The gastric secretion consisted of pepsin and lipase in a gastric electrolyte solution (NaCl 4.8 g L^{-1}, KCl 2.2 g L^{-1}, $CaCl_2$ 0.22 g L^{-1} and $NaHCO_3$ 1.5 g L^{-1}), secreted at a flow rate of 0.33 mL min^{-1}. The pH was controlled to follow a predetermined curve (from 4.8 at t = 0 to 1.7 at t = 120 min) by secreting HCl (1 mol L^{-1}). The duodenal secretion consisted of a mixture of 4 % (w/v) porcine bile extract, 7 % (w/v) pancreatin solution and small intestinal electrolyte solution (SIES) (NaCl 5 g L^{-1}, KCl 0.6 g L^{-1}, $CaCl_2$ 0.25 g L^{-1}) secreted at a flow rate of 0.66 mL min^{-1}. The jejunal secretion fluid consisted of SIES containing 10 % (v/v) porcine bile extract solution at a flow rate of 2.13 mL min^{-1}. The ileal secretion fluid consisted of SIES at a flow rate of 2.0 mL min^{-1}. The pH in the different compartments of small intestine was controlled by the addition of 1 mol L^{-1} $NaHCO_3$ solution to set points of 6.5, 6.8 and 7.2 for simulated duodenum, jejunum and ileum, respectively. During *in vitro* digestion, samples were collected directly from the lumen of the different

compartments (or jacket reactor), from the stomach, duodenal, jejunal and ileal filtrates and from the ileal delivery. The jejunal and ileal filtrates and ileal delivery were used to determine the bioaccessibility of curcumin. The samples were analysed in terms of H_d, *Zp* and amount of released free fatty acids. Both curcumin nanosystems were tested in the dynamic gastrointestinal model at least in triplicate.

5.2.2.6 Microscopy

The morphology of nanosystems was evaluated by transmission electron microscopy (TEM) (EM 902A, ZEISS, Germany) operating at 80 kV. TEM samples were prepared by depositing the nanoemulsion suspensions on a carbon-coated copper grid, and negatively stained with 1 % (w/v) uranyl acetate for observation. Samples were air-dried prior to be analysed. Also, the oil droplets in the emulsions were studied using an epifluorescence microscope (BX51 OLYMPUS, Tokyo, Japan) with a ×100 oil immersion objective lens. Samples were stained with Nile Red (9-diethylamino-5H-benzo[α]phenoxazine-5-one, 0.25 mg mL^{-1} in dimethyl sulfoxide, 1:10 (dye:sample, v/v), which enabled the oil droplets to become visible. Slides were prepared by taking 10 µL of the stained emulsion solution and placing in a glass microscope slide and covering with a glass cover slip.

5.2.2.7 Free fatty acids release

The extent of lipolysis was evaluated by determining the amount of free fatty acids (FFA) released from curcumin nanoemulsions using a titration method (Pinsirodom, 2005). Briefly, 5 mL of jejunal filtrate, ileal filtrate and ileal delivery samples were collected and 10 mL of acetone were added to quench the enzymes' activity, then three drops of 1 % (w/v) of phenolphthalein were added as an indicator. A direct titration using 0.1 mol L^{-1} NaOH was performed and the volume of NaOH added until the titration end point was determined and used to calculate the concentration of FFA produced by lipolysis. Therefore, the percentage of FFA released was calculated from the number of moles of NaOH required to neutralize the FFA divided by the number of moles of FFA that could be produced from triglycerides if they were all digested (assuming 2 FFA produced per 1 triacylglycerol molecule) (Li et al., 2011):

$$\% \, FFA = 100 \times \left(\frac{v_{NaOH} \times m_{NaOH} \times M_{lipid}}{w_{lipid} \times 2} \right) \quad \text{Eq. 5.1}$$

where v_{NaOH} is the volume of sodium hydroxide required to neutralize the FFA generated (in mL), m_{NaOH} is the molarity of the sodium hydroxide used (in mol L^{-1}), w_{lipids} is the total weight of MCTs oil initially present and M_{lipid} is the molecular weight of the MCTs oil (based on their average fatty acid composition, the molecular weight of MCTs oil was considered to be 503 g mol^{-1}).

5.2.2.8 Curcumin bioaccessibility

It is assumed that the fraction of the original curcumin that ended up in the micelle phase was a measure of curcumin bioaccessibility (Ahmed et al., 2012; Pinheiro et al., 2016) and that the mixed micelles that contained the bioaccessible curcumin fraction were able to pass the hollow-fibre membranes (i.e. corresponds to jejunal filtrate and ileal filtrate samples), while undigested emulsions were retained (Minekus et al., 2005; Pinheiro et al., 2016). Curcumin bioaccessibility was determined based on the methodology described by other authors (Ahmed et al., 2012; Pinheiro et al., 2016). Briefly, 5 mL of the sample (jejunal or ileal filtrate) were vortexed with 5 mL of chloroform, and then centrifuged (Sigma 4K15, Germany) at 651 *g*, at room temperature, for 10 min. The bottom chloroform layer was collected and the extraction procedure was repeated with the top layer. The second bottom chloroform layer was added to the previously set aside chloroform layer, mixed, and analysed in a UV-VIS spectrophotometer (Elisa Biotech Synergy HT, Biotek, USA) at 425 nm (maximum absorbance peak of curcumin). The concentration of curcumin was determined from a previously prepared calibration curve of absorbance versus curcumin concentration in chloroform.

5.2.2.9 Antioxidant activity of curcumin

The free-radical scavenging capacity of curcumin and curcumin nanosystems was analysed using the DPPH test according to the method described by Pinheiro et al (2015), with some modifications. Briefly, 0.2 mL of ethanol and 0.3 mL of the curcumin dissolved in ethanol (concentrations ranging from 0.05

to 5.0 mg mL^{-1}) or curcumin from the digested nanosystems were mixed in a 10 mL test tube with 2.5 mL of DPPH (60 µmol L^{-1} in ethanol), achieving a final volume of 3.0 mL. For the antioxidant activity of curcumin during the digestion steps, nanosystems without curcumin were used as controls. The solution was kept at room temperature for 30 min and the absorbance was measured at 517 nm (Pinheiro et al., 2015; Rufino et al., 2007; Souza et al., 2012).
The DPPH scavenging effect was calculated as follow:

$$Scavenging\ effect\ (\%) = \frac{A_0 - (A_s - A_b)}{A_0} \times 100 \qquad \text{Eq. 5.2}$$

where A_0 is the absorbance at 517 nm of DPPH without sample, A_s is the absorbance at 517 nm of sample and DPPH and A_b is the absorbance at 517 nm of sample without DPPH. The absorbance measurements were performed in Elisa Biotech Synergy HT (Biotek, USA) (Pinheiro et al., 2015).

5.2.2.10 Cell culture

The human colon carcinoma Caco-2 cells were purchased from Deutsche Sammlung von Mikroorganismen und Zellkulturen (DSMZ, Braunschweig, Germany). This cell line, originally obtained from human colon adenocarcinoma, undergoes in a process of spontaneous differentiation that leads to the formation of a monolayer of cells, expressing several morphological and functional characteristics of the mature enterocyte (Sambuy et al., 2005). Caco-2 cells were routinely grown in a standard medium: RPMI 1640 supplemented with 10 % (v/v) of inactivated FBS and 1 % (v/v) of PS. Stock cells were maintained as monolayers in 80 cm^2 culture flasks. Cells were subcultured every week at a split ratio of 1 to 4 by treatment with trypsin/EDTA (0.25 %) and incubated at 37 ºC in a 5 % CO_2 humidified atmosphere. For cytotoxicity experiments cells were used between passages 40 and 50.

5.2.2.11 Cytotoxicity assay

Caco-2 were harvested and seeded in 96-well plates at a density of 2×10^4 cells/well and the medium was changed every 48 h. After cells reach confluence (~96 hours), 100 µL of nanoemulsion or multilayer nanoemulsions were added

to cells in a concentration ranging between 0.15 and 4.75 µg of curcumin mL^{-1}. Also, the components of the nanosystems (curcumin, SDS and chitosan) were tested for toxicity in Caco-2 cell line. The curcumin stock solution was prepared in pure ethanol while the SDS and chitosan stock solutions were prepared in distilled water, all at a final concentration of 4 mg mL^{-1}. After 4 h of incubation at 37 ºC in a 5 % CO_2 humidified atmosphere cells were rinsed twice with PBS to remove traces of samples and 100 µL of a CellTiter 96® AQueous One Solution Cell Proliferation Assay reagent (MTS) previously diluted in RPMI 1640 medium was added to each well and left to react for 2 hours. MTS is bio-reduced by cells into a colored formazan product that is soluble in tissue culture medium. The quantity of formazan produced was measured spectrophotometrically at 490 nm in a microplate reader (EPOCH, Bio-Tek, USA) and is directly proportional to the number of living cells in culture. Results were expressed in terms of percentage of cellular viability relative to a group control (cells only with RPMI medium). Experiments were performed in triplicate in three independent assays.

5.2.3 Statistical procedures

5.2.3.1 Data analyses

Data analyses were performed using Microsoft Windows Excel 2011, using the Tukey's Multiple Comparison Test with a confidence interval of 95 % in GraphPad Prism 5 (GraphPad Software, Inc.) and using ANOVA in STATISTICA 7.0 (Statsoft, Tulsa, OK, USA).

5.3 Results and Discussion

5.3.1 Curcumin nanosystems

5.3.1.1 Curcumin nanosystems characteristics

The process conditions used for the development of the nanoemulsions were established in chapter 3, and lead to a final mean droplet diameter of 80.0 ± 0.9 nm, being particularly efficient for the development of small droplet sizes (<100 nm). *PdI* and *Zp* values were 0.177 ± 0.009 and -65.8 ± 5.8 mV, respectively.

The LbL technique was applied for the development of the multilayer nanoemulsion, being chitosan, alginate and chitosan subsequently deposited (in this order) onto the nanoemulsions under magnetic agitation. The final polyelectrolyte concentrations onto the nanoemulsions were determined using the saturation method. The multilayer nanoemulsion produced in chapter 4 was used in this chapter, with a H_d of 130 ± 1.5 nm, a *PdI* of 0.237 ± 0.004 and a *Zp* of 10.4 ± 0.9 mV. The concentration of the encapsulated curcumin within the nanosystems was 78 ± 0.8 μg mL^{-1}. Figure 5.1 (Initial) presents the TEM microphotographs of the nanoemulsion and multilayer nanoemulsion, confirming the development of the nanosystems and validating the mean droplet diameters obtained by DLS.

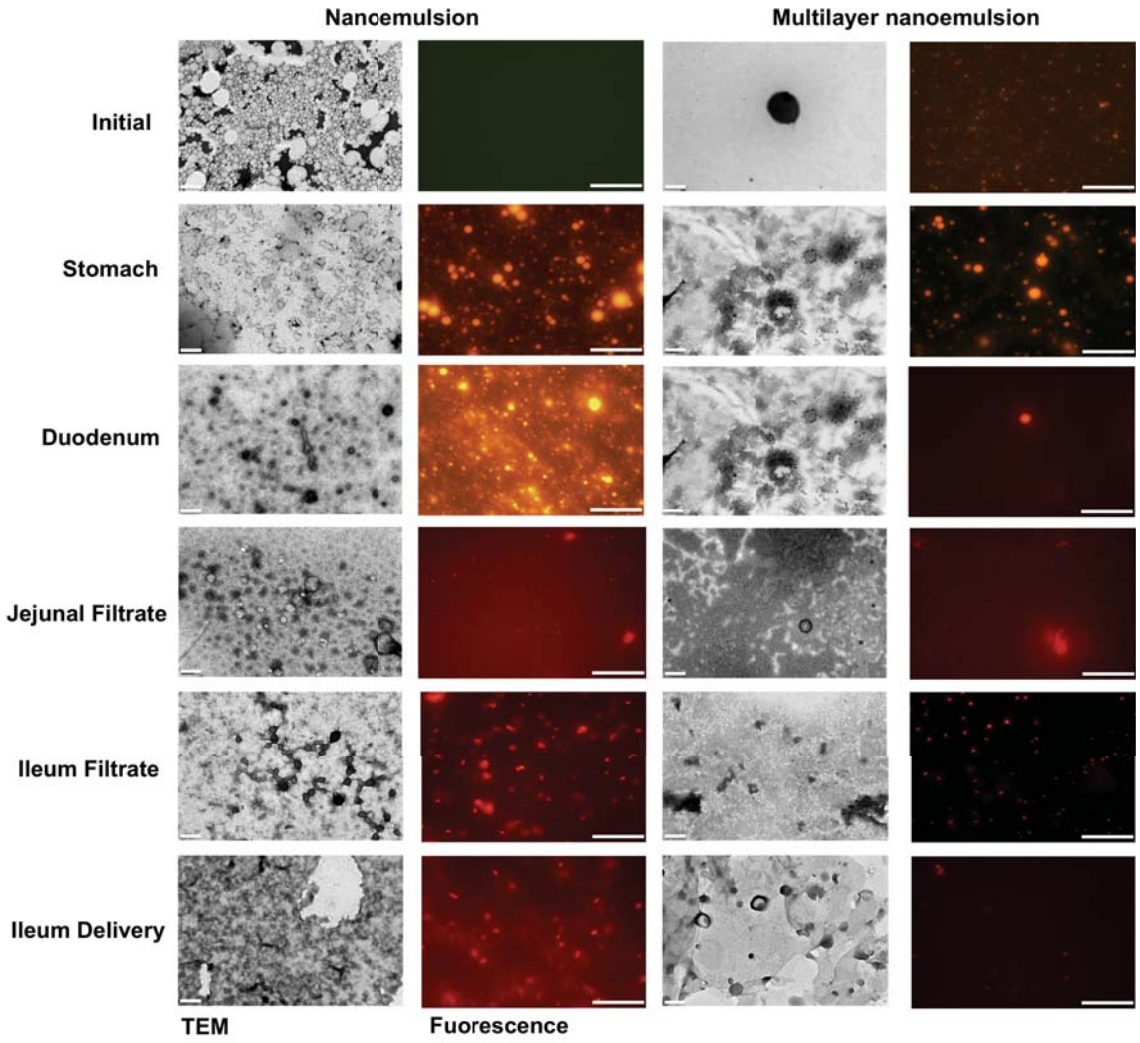

Figure 5.1 – TEM microphotographs of nanosystems (nanoemulsion and multilayer nanoemulsion) negatively stained with uranyl 1 % w/w and epifluorescence microphotographs of nanosystems stained with Nile Red, as they undergo the different stages of dynamic *in vitro* digestion. The scale bars of TEM and epifluorescent images are 400 nm and 20 μm, respectively.

5.3.2 Evaluation of nanosystems responsiveness under gastrointestinal conditions

The stability/responsiveness of the nanosystems under gastrointestinal pH conditions, i.e. pH 2 and 7.4 at 37 ºC, was assessed through release assays by measuring the absorbance of curcumin in the acceptor media. After 54 h of release assays, the H_d and *PdI* of the nanosystems were also determined and changes in their structural characteristics were evaluated. At the tested conditions, both nanosystems were unable to release curcumin. This was confirmed by measuring the content of curcumin in the acceptor media, which

was 0 μg mL^{-1} (below the detection limit of 0.01 ± 0.001 μg mL^{-1}) and by measuring the curcumin that remained encapsulated (77.5 ± 1.5 μg mL^{-1}), which did not show any significant difference when compared with the curcumin initially present within the nanostructures (77.9 ± 0.8 μg mL^{-1}). Regarding size stability, at pH 7.4 the nanosystems showed the ability to maintain their initial size (p>0.05), after 54 h of assay, with 82.3 ± 1.7 nm for the nanoemulsion and 139.8 ± 9.4 nm for the multilayer nanoemulsion. At this pH, above the pK_a of chitosan, the amino groups are entirely deprotonated and could contribute to loss of solubility of the chain segments (Vachoud et al., 2000). It is also possible that chitosan layers held some positive charge at pH 7.4; previous works showed that when polyelectrolyte chains are entangled between oppositely charged polyelectrolytes, the pK_a of the charged groups can considerably change, increasing the stability of the multilayer nanoemulsion to pH changes (Burke & Barrett, 2003a, b; Li et al., 2010). At pH 2, the nanosystems presented signs of creaming and phase separation, being unstable at this pH after 54 h of assay. At pH values below the pK_a of the carboxylic acid groups present in alginate these groups are deprotonated, thereby the alginate layer could desorb from the droplets' surface, inducing phase separation (Harnsilawat et al., 2006; Li et al., 2010). Also the low solubility of curcumin in aqueous systems, reported to be 11 ng mL^{-1} (Zhao et al., 2012) could explain the lack of curcumin release to both acceptor media, since sink conditions were not established (Jelezova et al., 2015). Nevertheless, this assay allows understanding the stability of developed nanosystems under the pH values used in the *in vitro* gastrointestinal system.

5.3.3 Dynamic in vitro digestion

The development of multilayer nanoemulsions by LbL allows to modify the surface composition of the nanoemulsion systems, offering the possibility to increase their stability under gastrointestinal tract conditions, while delaying lipid digestion (Hu et al., 2011; Klinkesorn & Julian McClements, 2010; Yang et al., 2014). The aim of these experiments was to evaluate the influence of polyelectrolytes layers in the behaviour of the nanosystems within the gastrointestinal tract.

5.3.3.1 Influence of polyelectrolytes on nanosystems behaviour during in vitro *digestion*

The effect of the polyelectrolytes layers in the nanosystem values of H_d, *PdI*, *Zp* and morphology were evaluated at each stage of the *in vitro* digestion. As stated before, the initial droplet diameters were 80 nm and 130 nm for the nanoemulsion and multilayer nanoemulsion, respectively. At the stomach stage, a increase of H_d of the nanoemulsion system was observed, from 80 nm to 104.1 ± 5.9 nm (please see Figure 5.2). On the contrary, a significant increase in the *PdI* was observed from 0.180 to 0.380 ± 0.05, which evidences the occurrence of coalescence phenomena, further confirmed by the epifluorescence microscopy (Figure 5.1 – stomach). For the multilayer nanoemulsion was observed an increase of the H_d values to 214.9 ± 27.6 nm under gastric conditions. This increase and the higher *PdI* values observed (0.572 ± 0.190) reveals that phenomena of coalescence occurred. This was confirmed by the epifluorescence microscopy (Figure 5.1 – stomach) although the TEM micrographs show that droplets in the nano-size range are still present. The behaviour of the multilayer nanoemulsion is related with the interfacial effect of the layers. One explanation could be the deprotonation of alginate under gastric conditions, which starts to desorb from the droplets surface inducing phase separation in this stage (Harnsilawat et al., 2006; Li et al., 2010). Also under gastric conditions nanoemulsion droplets have a highly negative charge of -64 ± 8 mV (Figure 5.3), exhibiting a strong electrostatic repulsion between them, able to avoid droplets flocculation, coalescence and aggregation. In contrast, the multilayer nanoemulsions present low *Zp* values (17.5 ± 1.3 mV, Figure 5.3), and despite of the electrical repulsion, the forces involved are not enough to completely inhibit the coalescence phenomena. The electrostatic attraction between alginate (inner layer) and chitosan (outer layer) is weakened due the partial loss of charges that alginate undergoes at acidic pH, below the alginate pK_a, leading to some aggregation of the particles that was visible through epifluorescence microscopy shown in Figure 5.1 (Pinheiro et al., 2016; Tokle et al., 2012; Tokle et al., 2010). The electrical charge of the multilayer nanoemulsion becomes more positive in the stomach, which is justified by various phenomena, such as: the increase of the electrical charge of chitosan due to pH and ionic strength of the solutions, maintaining the

electrostatic repulsion between polyelectrolytes and surfactant; adsorption of enzymes from the gastric solution to the chitosan outer layer; or polyelectrolytes displacement by the active materials present in the gastric solution (Hur et al., 2009; Pinheiro et al., 2016). TEM micrographs show that multilayer nanoemulsions have particles within the nano-size range; this might be explained by the alginate layer retaining some negative charges, despite at these conditions their electrical charge should be nearly 0 mV. When charged groups of polyelectrolytes are entangled between two or more oppositely charged polyelectrolytes, a change in the pK_a values can occur, increasing the stability of multilayers to changes in pH (Burke & Barrett, 2003a, b; Li et al., 2010).

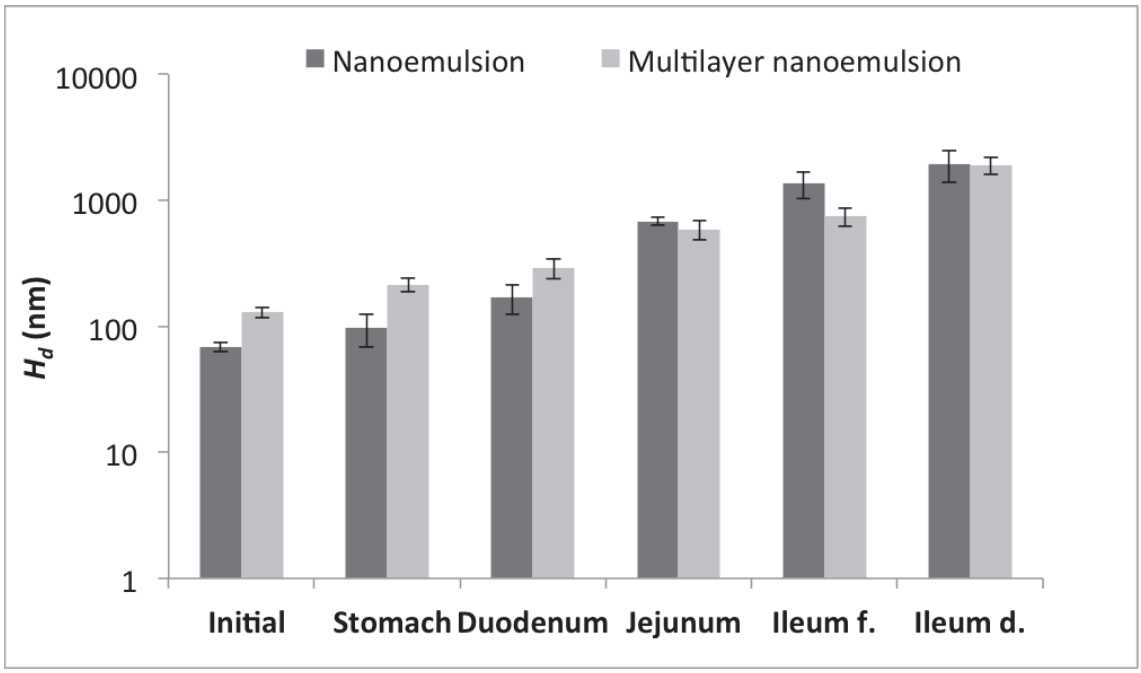

Figure 5.2 – Hydrodynamic diameter (H_d) of the nanosystems (nanoemulsion and multilayer nanoemulsion) as they undergo the different stages of dynamic *in vitro* digestion. The results are presented as the mean values of triplicate experiments. For better reading the vertical axis is on log scale. Ileum f. – Ileum filtrate; Ileum d. – Ileum delivery

Under intestinal conditions, both nanosystems exhibited an increase of H_d and *PdI* values, possibly due to particle aggregation either by flocculation or coalescence of droplets (Figure 5.2). At the duodenal stage, the H_d, increased to 168.5 ± 44.1 nm and the *PdI* was 0.42 ± 0.12 for the nanoemulsion system with a *Zp* value of -44.1 ± 8.8 mV. For multilayer nanoemulsion the H_d

increased to 292.3 ± 53.5 nm with a *PdI* of 0.65 ± 0.28 and a *Zp* of -23.3 ± 2.9 mV. The microscopic evaluation (Figure 5.1 - duodenum) showed that at the duodenum stage, both nanosystems still exhibited droplets at the nano-scale, but at the same time exhibits droplets at the micro-scale, which confirms the wide droplet size distribution indicated by the *PdI* value. The jejunal secretion promots the increase of the H_d values of both nanosystems, to 681.2 ± 47.6 nm and 586.9 ± 101.8 nm for nanoemulsion and multilayer nanoemulsion, respectively. Ileal filtrate and ileal delivery exhibited higher H_d than the jejunal filtrate. At these stages of digestion, H_d *values* ranged between 1 and 2 μm where observed (Figure 5.2). However, TEM analyses showed that non-digested nanosystems were still present in the jejunum and ileum stages; these can contribute to the high values of *PdI* (higher than 0.5). The largest increase in the H_d observed at small intestine conditions may be due to the fact that bile salts are able to displace surfactants and polyelectrolytes from the droplets surface and lipase may induce the hydrolysis of the triacylglycerol molecules present into free fatty acids (FFA), monoacyglycerides and/or diacylglycerides (Pinheiro et al., 2016). Also, this hydrolysis can generate structures such as micelles, vesicles or other colloidal structures (Mu & Høy, 2004).

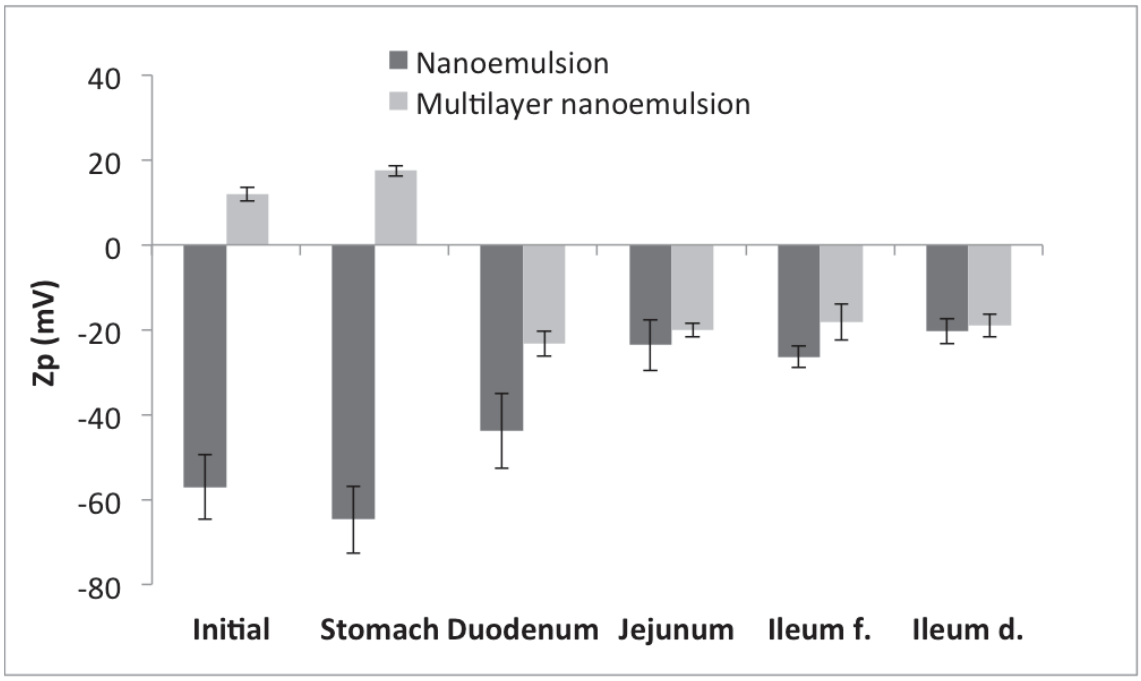

Figure 5.3 – Zeta potential values (*Zp*) of the nanosystems (nanoemulsion and multilayer nanoemulsion) as they undergo the different stages of dynamic *in vitro* digestion. The results are presented as the mean values of triplicate experiments. Ileum f. – Ileum filtrate; Ileum d. – Ileum delivery

Results showed that the electrical charges (expressed by the *Zp* values) at these stages of the digestion decreased in the case of nanoemulsion and completely changed in the case of the multilayer nanoemulsion (from positive to negative values), reaching a relatively constant value between -25 mV and -20 mV (Figure 5.3). These changes suggest that the bile salts or free fatty acids adsorbed to the surface of the nanoemulsions or to the surface of the chitosan layer present in the multilayer nanoemulsion or that the presence of the bile salts or free fatty acids promoted the displacement of the surfactant and polyelectrolytes from the droplets surface (Klinkesorn & Julian McClements, 2010; Salvia-Trujillo et al., 2015; Zou et al., 2015). From jejunum to ileum delivery stages of the digestion there were no significant differences ($p>0.05$) between the *Zp* values for both nanosystems.

5.3.3.2 Influence of polyelectrolytes on lipids digestion

The effect of the polyelectrolytes layers on the lipids digestion was evaluated by the hydrolysis of the triacylglycerol molecules into free fatty acids (FFA) at each stage of the small intestine digestion. The addition of the polyelectrolyte layers

to nanoemulsions had a significant effect on the extent of lipid digestion, reducing (p<0.05) the overall of FFA released (Figure 5.4), achieving 71.3 ± 3.5 % and 52.3 ± 10.6 % for nanoemulsion and multilayer nanoemulsion, respectively. This suggests that the presence of the layers in the multilayer nanoemulsion delayed lipid digestion, slowing down the release rate of the FFA. For both jejunal and ileal filtrate fractions lower amount of FFA was observed for the multilayer nanoemulsions when compared to the curcumin nanoemulsions, being these results in agreement with previous studies (Pinheiro et al., 2016). The decrease of the FFA release when using polyelectrolytes layers can be explained by the ability that bile salts have to form electrostatic complexes with the chitosan outer layer, reducing the digestibility of the lipids by sterically hindering the lipase, and thus their influence in the lipids phase (Klinkesorn & Julian McClements, 2010; Klinkesorn & McClements, 2009). Another possible justification is that at this stage of the digestion, since the cationic functional groups of chitosan have a pK_a value around pH 6.5, chitosan could lose most of its charges and form large chitosan aggregates that would impede the access of lipase to the lipids (Zhang et al., in press). Also, the presence of calcium ions that have a strong ability for binding with alginate may slow down the digestion of the FFA (Hu et al., 2010; Pinheiro et al., 2016). These results suggest that the addition of chitosan and alginate layers surrounding nanoemulsions may be useful to control the rate of lipid digestion and FFA adsorption within the gastrointestinal tract, delaying the lipids digestion. These findings could be important for the design of structures that are able to decrease the rate of lipids digestion, increasing the amount of undigested food at ileum, which can encourage the *ileal brake* mechanism responsible for the regulation of hunger, satiety and satiation, while also reducing the caloric content of food products (Li et al., 2010; McClements, 2010; McClements & Li, 2010).

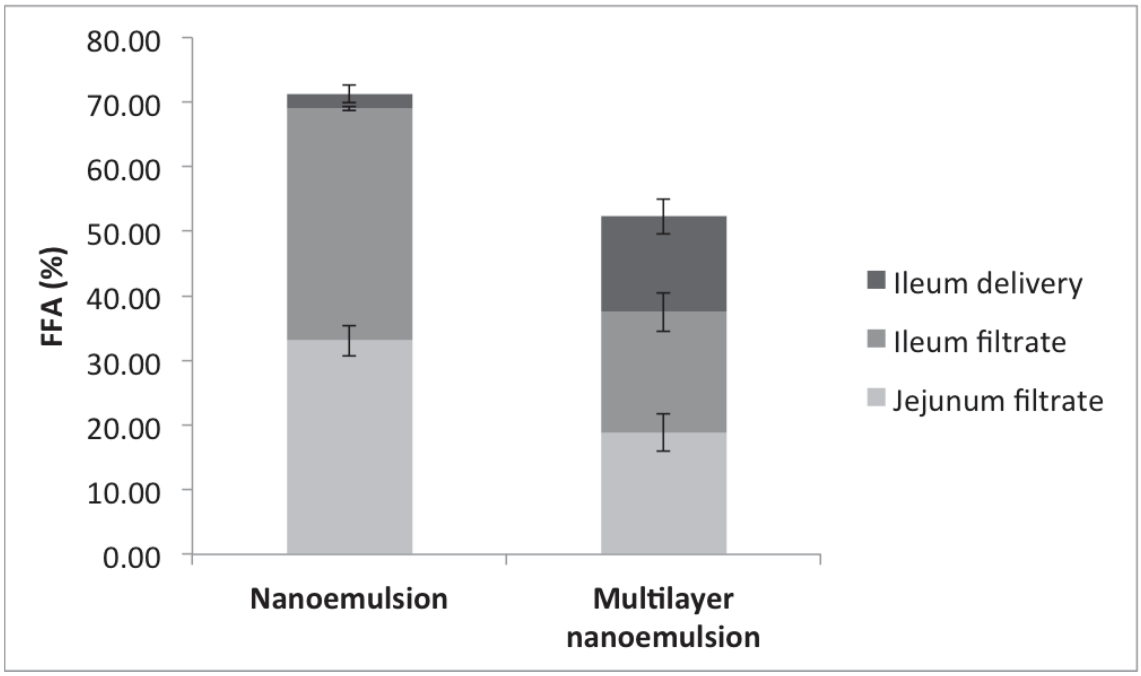

Figure 5.4 – Percentage of free fatty acids (FFA) released from the nanosystems (nanoemulsion and multilayer nanoemulsion) as they undergo the different stages of dynamic *in vitro* digestion. The results are presented as the mean values of triplicate experiments.

5.3.3.3 Influence of polyelectrolytes on curcumin bioaccessibility

The bioaccessibility of curcumin after digestion at jejunum, ileal filtrate and ileal delivery was studied for both nanosystems, being measured as the curcumin concentration presented in mixed micelles. Curcumin bioaccessibility increased during the digestion time (Figure 5.5), resulting in higher (p<0.05) bioaccessibility values for the nanoemulsion (43.64 ± 6.36 %) when compared to the values obtained for the multilayer nanoemulsion (26.98 ± 3.99 %). One possible explanation for this result can be the fact that polyelectrolyte layers were efficient in protecting the release of curcumin from the multilayer nanosystems, leading to undigested nanosystems able to retain curcumin; another explanation is the presence of less mixed micelles, which are necessary to solubilise the curcumin (Salvia-Trujillo et al., 2013; Zhang et al., in press). Another hypothesis is the fact that multilayer nanoemulsions, due to their larger sizes when compared to the nanoemulsion (130 nm to 80 nm), have a lower surface area, decreasing the bioaccessibility. This effect could be attributed to a lower amount of lipase present per mass of lipids (Salvia-Trujillo et al., 2013).

For both nanosystems the determined amount of curcumin was similar between the jejunal and ileum filtrates. However, nanoemulsions presented significantly higher concentrations of curcumin at both jejunal and ileum filtrate. These results are in agreement with FFA release results (Figure 5.4), i.e. both nanosystems had similar amounts of FFA found in those fractions. A crucial step for the bioavailability of bioactive compounds is the access of lipases to lipids, if there are no statistical differences between the FFA in the jejunal and ileal filtrate, there should not be statistical differences in the bioaccessibility of curcumin between jejunal and ileal compartments. Also, the digestion products can be part of the mixed micelles, increasing the solubility of curcumin and thus increasing the bioaccessibility in the small intestine (Pinheiro et al., 2016; Porter et al., 2007).

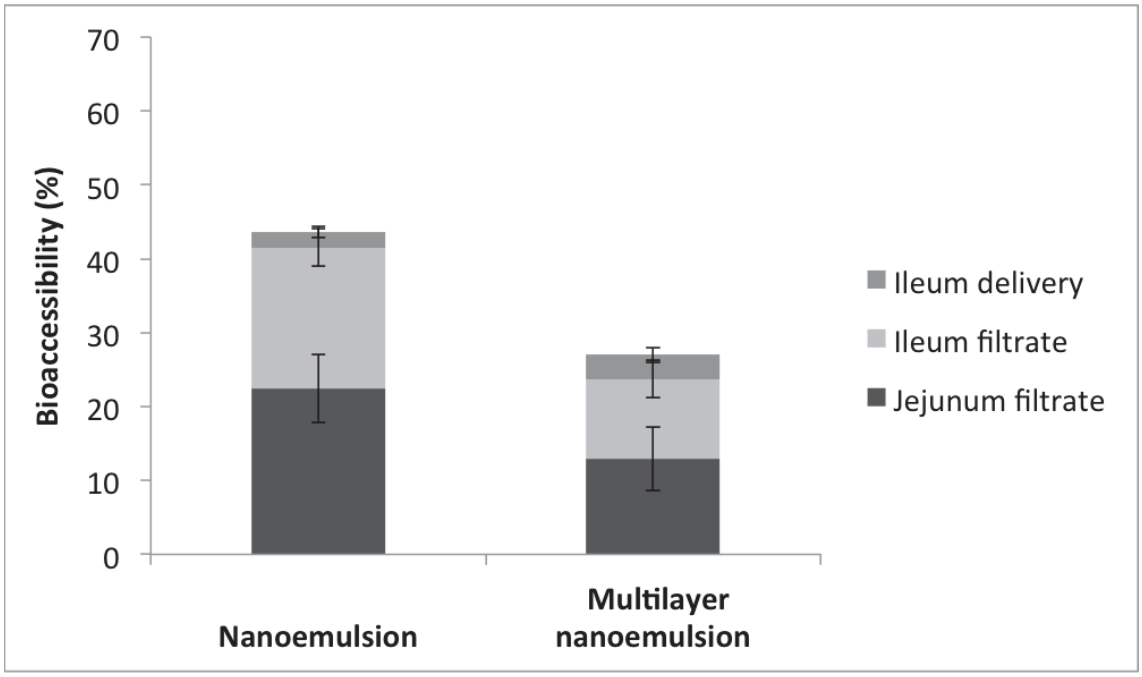

Figure 5.5 – Percentage of bioaccessibility as the nanosystems (nanoemulsion and multilayer nanoemulsion) undergo jejunal and ileal stages of dynamic *in vitro* digestion. The results are presented as the mean values of triplicate experiments.

The bioaccessibility of free curcumin solubilised in MCTs was also evaluated (data not shown), achieving only, 0.15 ± 0.01 % at the jejunal filtrate, while there was no evidence of curcumin at the ileal compartments. The reasons for the low bioaccessibility of the free curcumin in MCTs can be attributed to the poor solubility of curcumin in aqueous solutions, and to the lack of mixed micelles for

the solubilisation of curcumin and residues of curcumin that were found to be adhered to the dynamic digestion model walls after the digestion was completed, specially in the duodenum stage.

TEM micrographs showed that undigested nanosystems were still present after the *in vitro* digestion; due to this, the concentration of curcumin was measured at every stage of the digestion, from stomach to ileal delivery. Figure 5.6 shows the decrease of curcumin concentration with the digestion time, which is explained by the dilutions made due to the addition of gastric and intestinal secretions. Results showed that in the ileum filtrate the concentration of curcumin present in the multilayer nanoemulsion is significantly higher (p<0.05) than the concentration of curcumin present in the nanoemulsion (Figure 5.6). Under ileal conditions, curcumin is prone to chemical degradation; this result suggests that the multilayer nanoemulsion has the ability to protect (at least partially) the curcumin and encapsulated lipids from the action of lipase and bile salts and/or chemical degradation (Ting et al., 2014; Zou et al., 2015).

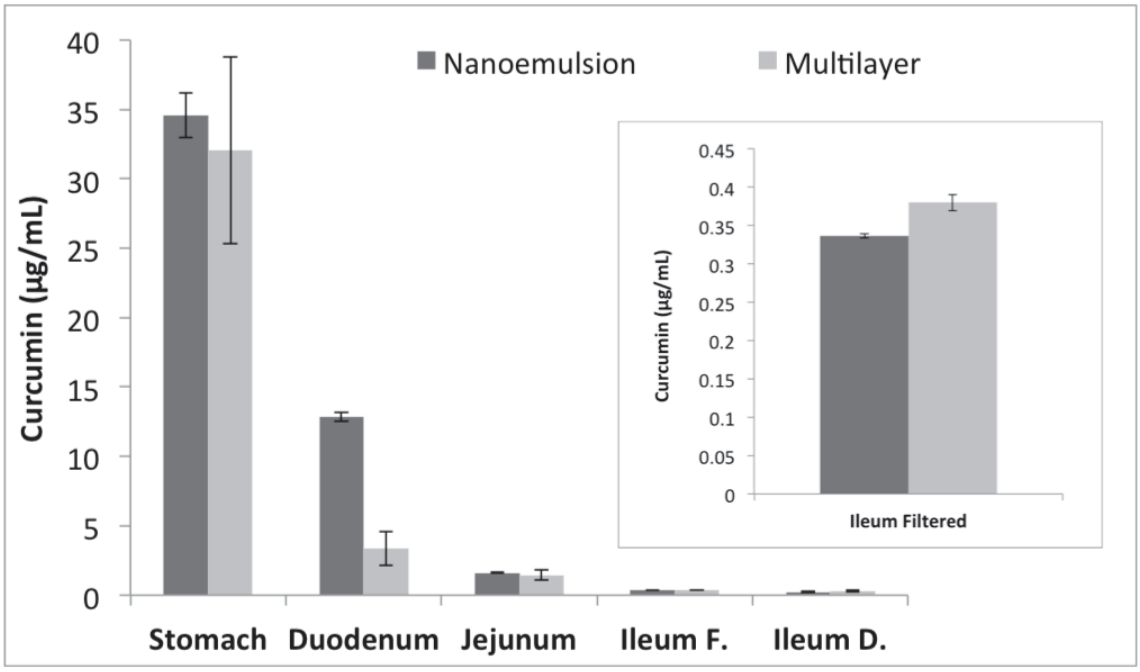

Figure 5.6 – Curcumin concentration during the different stages of dynamic *in vitro* digestion of the different nanosystems (nanoemulsion and multilayer nanoemulsion). The results are presented as the mean values of triplicate experiments. Ileum f. – Ileum filtrate; Ileum d. – Ileum delivery

5.3.3.4 Influence of polyelectrolytes in the antioxidant activity of curcumin

Figure 5.7 shows curcumin antioxidant activity, determined as the radical scavenging activity of curcumin according to the DPPH assay. Results showed that curcumin radical scavenging activity decreased during *in vitro* digestion, from 27.01 ± 1.39 % to 1.51 ± 0.12 % for the nanoemulsion and from 23.30 ± 1.27 % to 6.88 ± 0.87 % in the case of the multilayer nanoemulsions. The decrease of the antioxidant activity of curcumin could be explained by the degradation of curcumin during digestion. Curcumin is prone to chemical degradation at neutral pH and above, resulting in the formation of different reaction products, as trans-6-(4′-hydroxy-3′-methoxyphenyl)-2,4-dioxo-5-hexanal, ferulic acid, feruloylmethane, and vanillin (Zou et al., 2015). Also other factors, such as ionic strength, enzymatic degradation, mechanistic motilities or free radicals (e.g. hydroxyl radicals), can theoretically contribute to the degradation of curcumin and bioactive compounds (Ting et al., 2014). Figure 5.7 shows that from jejunal filtrate to ileal delivery the degradation of curcumin is significantly higher (p<0.05) for the nanoemulsions when compared with multilayer nanoemulsions. This result suggests that the polyelectrolyte layers are more effective in the protection of curcumin; explained by the fact that polyelectrolyte layers are sterically hindering curcumin from enzymatic or free radicals degradation. Nonetheless it may also be explained by the higher size and lower surface area of the multilayer nanoemulsion; i.e. if there are a lower surface area in contact with the surrounding aqueous phase, less curcumin would be in direct contact with any catalysts that could trigger curcumin degradation (Zou et al., 2015).

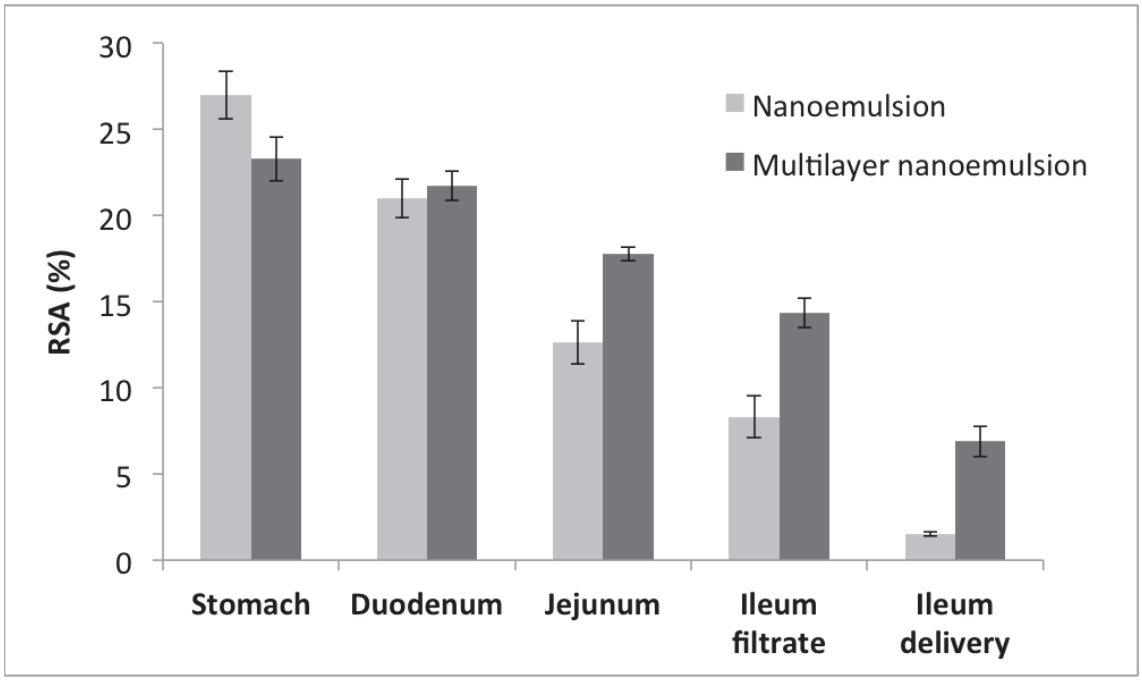

Figure 5.7 – Antioxidant capacity of curcumin nanosystems expressed in percentage of the radical scavenging activity (RSA) as the nanosystems undergo the different stages of dynamic *in vitro* digestion. The results are presented as the mean values of triplicate experiments.

5.3.4 Cytotoxicity assay

The evaluation of the cytotoxicity of the nanosystems is of utmost importance for safety reasons, if one of the objectives is the introduction of these nanosystems into food products.

The cytotoxicity of both nanosystems and of some of the materials used for their production were evaluated on the human colon adenocarcinoma Caco-2 cell line by using the CellTiter 96® AQueous One Solution Cell Proliferation Assay (MTS). The concentrations resulting in a 50 % decrease of cell viability, IC_{50}, were determined for the nanoemulsion, nanoemulsion multilayer and curcumin. Although curcumin did not present any intrinsic cytotoxicity (> 4.75 μg curcumin mL^{-1}), the results showed that nanoemulsion and multilayer nanoemulsion were toxic for Caco-2 cells after 4 h of incubation, with IC_{50} values of 1.125 ± 0.028 and 1.128 ± 0.079 μg nanosystem mL^{-1}, respectively, equivalent to 0.855 ± 0.02 μg curcumin mL^{-1} and 0.858 ± 0.06 μg curcumin mL^{-1} for the nanoemulsion and multilayer nanoemulsion, respectively (Table 5.1). In order to understand the cytotoxicity of the nanosystems the IC_{50} values for chitosan and SDS were determined. Chitosan did not show any cytotoxicity in the range of concentrations tested, relatively to the control (100 % of cell

viability) after 4 h of incubation (> 31.25 of μg chitosan mL^{-1}, Table 5.1). The IC_{50} value determined for SDS was 34.30 ± 2.18 μg SDS mL^{-1}, which was 3.3-fold lower than the IC_{50} values found for nanoemulsion and multilayer nanoemulsion (112.48 ± 2.81 μg SDS mL^{-1} and 112.81 ± 7.89 μg SDS mL^{-1}, respectively, Table 5.1). These results suggest that the decrease in the cell viability is caused by the presence of the SDS in the nanoemulsions and multilayer nanoemulsions. In fact, SDS is not recognized by EFSA for use in food products (EFSA, 2010), although FDA approves the use of SDS as surfactant for fruit juice drinks under 25 ppm (FDA, 2014a, b).

Table 5.1 – IC_{50} values of nanoemulsions, multilayer nanoemulsions, sodium dodecyl sulfate (SDS), curcumin and chitosan

Sample	μg mL^{-1}	μg SDS mL^{-1}
Nanoemulsion	1.125 ± 0.028	112.48 ± 2.81
Multilayer nanoemulsion	1.128 ± 0.079	112.81 ± 7.89
SDS	34.30 ± 2.18	34.30 ± 2.18
Curcumin	> 4.75	-
Chitosan	> 31.25	-

Despite of the cytotoxicity of both nanosystems, this work suggests that the use of droplets in the nano-scale by itself did not potentiate the cytotoxic effect of SDS; on the contrary, both nanosystems reduced the cytotoxicity of SDS by 3.3-fold, as can be seen in Table 5.1. This finding may contribute for arguing the existent opinion that nanostructures could be toxic only due to their small size.

5.4 Conclusions

The purpose of this study was to investigate the effect of nanosystems' interfacial composition on their stability during *in vitro* digestion, on lipids digestibility, curcumin bioaccessibility and antioxidant activity, using a dynamic gastrointestinal system. In addition, also the cytotoxicity of the nanosystems was evaluated.

Results showed that nanoemulsions can increase the bioaccessibility of curcumin, while polyelectrolyte layers were effective in the control of lipid digestibility, significantly delaying the lipid digestion rate and decreasing the extent of lipid digestion. Results also suggest that the use of polyelectrolytes was efficient in protecting curcumin from enzymes and bile salts, improving the antioxidant capacity of curcumin during digestion. Cytotoxicity assays revealed that the use of nanosystems *per se* did not influence the cytotoxicity; on the contrary, nanosystems containing SDS were 3.3-fold less toxic than SDS itself. This study suggests that the developed nanosystems can be used as platforms for the design of functional foods with different functionalities.

5.5 References

Ahmed K, Li Y, McClements DJ & Xiao H (2012) Nanoemulsion- and emulsion-based delivery systems for curcumin: Encapsulation and release properties. Food Chemistry 132(2), 799-807.

Burke SE & Barrett CJ (2003a) Acid−Base Equilibria of Weak Polyelectrolytes in Multilayer Thin Films. Langmuir 19(8), 3297-3303.

Burke SE & Barrett CJ (2003b) pH-Responsive Properties of Multilayered Poly(l-lysine)/Hyaluronic Acid Surfaces. Biomacromolecules 4(6), 1773-1783.

Cerqueira M, Pinheiro A, Silva H, Ramos P, Azevedo M, Flores-López M, Rivera M, Bourbon A, Ramos Ó & Vicente A (2014) Design of Bio-nanosystems for Oral Delivery of Functional Compounds. Food Engineering Reviews 6(1-2), 1-19.

Cerqueira MA, Bourbon AI, Pinheiro AC, Silva HD, Quintas MAC & Antonio AV, (2013). Edible Nano-Laminate Coatings for Food Applications, *Ecosustainable Polymer Nanomaterials for Food Packaging*. CRC Press, pp. 221-252.

EFSA (2010). Call for scientific data on food additives permitted in the EU and belonging to the functional classes of emulsifiers, stabilisers and gelling agents, Available at: http://www.efsa.europa.eu/en/dataclosed/call/ans091123.pdf. Accessed 17/03/2015.

FDA, (2014a). CFR - Code of Federal Regulations Title 21 - Food and Drugs.

FDA, (2014b). CFR - Code of Federal Regulations Title 21 - indirect food additives: adjuvants, production aids and sanitizers.

Guttoff M, Saberi AH & McClements DJ (2015) Formation of vitamin D nanoemulsion-based delivery systems by spontaneous emulsification: factors affecting particle size and stability. Food Chem 171(0), 117-122.

Harnsilawat T, Pongsawatmanit R & McClements DJ (2006) Characterization of β-lactoglobulin–sodium alginate interactions in aqueous solutions: A calorimetry, light scattering, electrophoretic mobility and solubility study. Food Hydrocolloids 20(5), 577-585.

Hu M, Li Y, Decker E, Xiao H & McClements D (2011) Impact of Layer Structure on Physical Stability and Lipase Digestibility of Lipid Droplets Coated by Biopolymer Nanolaminated Coatings. Food Biophysics 6(1), 37-48.

Hu M, Li Y, Decker EA & McClements DJ (2010) Role of calcium and calcium-binding agents on the lipase digestibility of emulsified lipids using an in vitro digestion model. Food Hydrocolloids 24(8), 719-725.

Hur SJ, Decker EA & McClements DJ (2009) Influence of initial emulsifier type on microstructural changes occurring in emulsified lipids during in vitro digestion. Food Chemistry 114(1), 253-262.

Jelezova I, Drakalska E, Momekova D, Shalimova N, Momekov G, Konstantinov S, Rangelov S & Pispas S (2015) Curcumin loaded pH-sensitive hybrid lipid/block copolymer nanosized drug delivery systems. European Journal of Pharmaceutical Sciences 78, 67-78.

Klinkesorn U & Julian McClements D (2010) Impact of Lipase, Bile Salts, and Polysaccharides on Properties and Digestibility of Tuna Oil Multilayer Emulsions Stabilized by Lecithin–Chitosan. Food Biophysics 5(2), 73-81.

Klinkesorn U & McClements DJ (2009) Influence of chitosan on stability and lipase digestibility of lecithin-stabilized tuna oil-in-water emulsions. Food Chemistry 114(4), 1308-1315.

Li Y, Hu M, Du Y, Xiao H & McClements DJ (2011) Control of lipase digestibility of emulsified lipids by encapsulation within calcium alginate beads. Food Hydrocolloids 25(1), 122-130.

Li Y, Hu M, Xiao H, Du Y, Decker EA & McClements DJ (2010) Controlling the functional performance of emulsion-based delivery systems using multi-component biopolymer coatings. European Journal of Pharmaceutics and Biopharmaceutics 76(1), 38-47.

Maljaars J, Peters HPF, Haddeman E & Masclee A (in press) M2078 Distribution of Small Intestinal Fat Delivery Influences Satiety and Food Intake. Gastroenterology 136(5), A-480.

Malvern I, (2011). Dynamic light scattering common terms defined, in: Instruments M (Ed.), Worcestershire, UK.

Mayer S, Weiss J & McClements DJ (2013) Behavior of vitamin E acetate delivery systems under simulated gastrointestinal conditions: Lipid digestion and bioaccessibility of low-energy nanoemulsions. Journal of Colloid and Interface Science 404, 215-222.

McClements DJ (2010) Design of Nano-Laminated Coatings to Control Bioavailability of Lipophilic Food Components. Journal of Food Science 75(1), R30-R42.

McClements DJ (2015) Enhancing nutraceutical bioavailability through food matrix design. Current Opinion in Food Science 4(0), 1-6.

McClements DJ & Li Y (2010) Structured emulsion-based delivery systems: Controlling the digestion and release of lipophilic food components. Advances in Colloid and Interface Science 159(2), 213-228.

McClements DJ & Xiao H (2012) Potential biological fate of ingested nanoemulsions: influence of particle characteristics. Food & Function 3(3), 202-220.

Minekus M, Jelier M, Xiao J-z, Kondo S, Iwatsuki K, Kokubo S, Bos M, Dunnewind B & Havenaar R (2005) Effect of Partially Hydrolyzed Guar Gum (PHGG) on the Bioaccessibility of Fat and Cholesterol. Bioscience, Biotechnology, and Biochemistry 69(5), 932-938.

Mu H & Høy C-E (2004) The digestion of dietary triacylglycerols. Progress in Lipid Research 43(2), 105-133.

Ozturk B, Argin S, Ozilgen M & McClements DJ (2014) Formation and stabilization of nanoemulsion-based vitamin E delivery systems using natural surfactants: Quillaja saponin and lecithin. Journal of Food Engineering 142(0), 57-63.

Pinheiro AC, Bourbon AI, Cerqueira MA, Maricato É, Nunes C, Coimbra MA & Vicente AA (2015) Chitosan/fucoidan multilayer nanocapsules as a vehicle for controlled release of bioactive compounds. Carbohydrate Polymers 115, 1-9.

Pinheiro AC, Coimbra MA & Vicente AA (2016) In vitro behaviour of curcumin nanoemulsions stabilized by biopolymer emulsifiers – Effect of interfacial composition. Food Hydrocolloids 52, 460-467.

Pinsirodom P, & P, K. L., (2005). Lipase assays, in: Wrolstad RE (Ed.), *Handbook of food analytical chemistry*. Wiley, Hoboken, NJ, pp. 371 - 383.

Porter CJH, Trevaskis NL & Charman WN (2007) Lipids and lipid-based formulations: optimizing the oral delivery of lipophilic drugs. Nat Rev Drug Discov 6(3), 231-248.

Rao J & McClements DJ (2013) Optimization of lipid nanoparticle formation for beverage applications: Influence of oil type, cosolvents, and cosurfactants on nanoemulsion properties. Journal of Food Engineering 118(2), 198-204.

Reis P, Raab T, Chuat J, Leser M, Miller R, Watzke H & Holmberg K (2008) Influence of Surfactants on Lipase Fat Digestion in a Model Gastro-intestinal System. Food Biophysics 3(4), 370-381.

Rufino MdSM, Alves RE, Brito ESd, Morais SMd, Sampaio CdG, Pérez - Jiménez J & Saura-Calixto FD (2007). Metodologia científica: determinação da atividade antioxidante total em frutas pela captura do radical livre DPPH., Available at: http://www.infoteca.cnptia.embrapa.br/handle/doc/426953. Accessed 22/08/2015.

Salvia-Trujillo L, Qian C, Martín-Belloso O & McClements DJ (2013) Influence of particle size on lipid digestion and β-carotene bioaccessibility in emulsions and nanoemulsions. Food Chemistry 141(2), 1472-1480.

Salvia-Trujillo L, Sun Q, Um BH, Park Y & McClements DJ (2015) In vitro and in vivo study of fucoxanthin bioavailability from nanoemulsion-based delivery systems: Impact of lipid carrier type. Journal of Functional Foods 17, 293-304.

Sambuy Y, De Angelis I, Ranaldi G, Scarino ML, Stammati A & Zucco F (2005) The Caco-2 cell line as a model of the intestinal barrier: influence of cell and culture-related factors on Caco-2 cell functional characteristics. Cell Biology and Toxicology 21(1), 1-26.

Silva H, Cerqueira M & Vicente A (2012) Nanoemulsions for Food Applications: Development and Characterization. Food and Bioprocess Technology 5(3), 854-867.

Silva HD, Cerqueira MA, Souza BWS, Ribeiro C, Avides MC, Quintas MAC, Coimbra JSR, Carneiro-da-Cunha MG & Vicente AA (2011) Nanoemulsions of β-carotene using a high-energy emulsification-evaporation technique. Journal of Food Engineering 102(2), 130-135.

Silva HD, Cerqueira MA & Vicente AA, (2015a). Chapter 56 - Nanoemulsion-Based Systems for Food Applications, in: Kharisov BI (Ed.), *CRC Concise Encyclopedia of Nanotechnology*. CRC Press by Taylor and Francis Group, USA.

Silva HD, Cerqueira MA & Vicente AA (2015b) Influence of surfactant and processing conditions in the stability of oil-in-water nanoemulsions. Journal of Food Engineering.

Silva HD, Pinheiro AC, Donsì F, Cerqueira MA, Ferrari G & Vicente AA, (2015c). Development and characterization of lipid-based nanosystems: Effect of interfacial composition on nanoemulsions behaviour.

Souza BWS, Cerqueira MA, Bourbon AI, Pinheiro AC, Martins JT, Teixeira JA, Coimbra MA & Vicente AA (2012) Chemical characterization and antioxidant activity of sulfated polysaccharide from the red seaweed Gracilaria birdiae. Food Hydrocolloids 27(2), 287-292.

Sun Y, Xia Z, Zheng J, Qiu P, Zhang L, McClements DJ & Xiao H (2015) Nanoemulsion-based delivery systems for nutraceuticals: Influence of carrier oil type on bioavailability of pterostilbene. Journal of Functional Foods 13, 61-70.

Ting Y, Jiang Y, Ho C-T & Huang Q (2014) Common delivery systems for enhancing in vivo bioavailability and biological efficacy of nutraceuticals. Journal of Functional Foods 7, 112-128.

Tokle T, Lesmes U, Decker EA & McClements DJ (2012) Impact of dietary fiber coatings on behavior of protein-stabilized lipid droplets under simulated gastrointestinal conditions. Food & Function 3(1), 58-66.

Tokle T, Lesmes U & McClements DJ (2010) Impact of Electrostatic Deposition of Anionic Polysaccharides on the Stability of Oil Droplets Coated by Lactoferrin. Journal of Agricultural and Food Chemistry 58(17), 9825-9832.

Troncoso E, Aguilera JM & McClements DJ (2012) Influence of particle size on the in vitro digestibility of protein-coated lipid nanoparticles. Journal of Colloid and Interface Science 382(1), 110-116.

Vachoud L, Zydowicz N & Domard A (2000) Physicochemical behaviour of chitin gels. Carbohydrate Research 326(4), 295-304.

Yang D, Wang X-Y, Ji C-M, Lee K-T, Shin J-A, Lee E-S & Hong S-T (2014) Influence of Ginkgo biloba extracts and of their flavonoid glycosides fraction on the in vitro digestibility of emulsion systems. Food Hydrocolloids 42, Part 1, 196-203.

Zhang C, Xu W, Jin W, Shah BR, Li Y & Li B (in press) Influence of anionic alginate and cationic chitosan on physicochemical stability and carotenoids

bioaccessibility of soy protein isolate-stabilized emulsions. Food Research International.

Zhao L, Du J, Duan Y, Zang Yn, Zhang H, Yang C, Cao F & Zhai G (2012) Curcumin loaded mixed micelles composed of Pluronic P123 and F68: Preparation, optimization and in vitro characterization. Colloids and Surfaces B: Biointerfaces 97, 101-108.

Zou L, Zheng B, Liu W, Liu C, Xiao H & McClements DJ (2015) Enhancing nutraceutical bioavailability using excipient emulsions: Influence of lipid droplet size on solubility and bioaccessibility of powdered curcumin. Journal of Functional Foods 15, 72-83.

CHAPTER 6

EVALUATING THE EFFECT OF CHITOSAN LAYER ON BIOACCESSIBILITY AND CELLULAR UPTAKE OF CURCUMIN NANOEMULSIONS

Since nanoemulsions produced with SDS revealed cytotoxicity torwards Caco-2 cells, in this chapter nanoemulsions were produced using whey protein isolate as the emulsifier. Also, the effect of the deposition of chitosan layer onto curcumin nanoemulsion was evaluated in terms of lipids digestibility and bioaccessibility of curcumin using a dynamic gastrointestinal model (simulating the stomach, duodenum, jejunum and ileum). Cytotoxicity, cellular antioxidant activity and permeability analyses of the undigested nanosystems were carried on Caco-2 cells.

This Chapter was adapted from:

Silva, H. D., Beldíková, E., Poejo, J., Abrunhosa, L., Serra, A. T., Duarte C. M., Brányikb, T., Cerqueira, M. A., Pinheiro, A. C. & Vicente, A. A. Evaluating the effect of chitosan layer on bioaccessibility and cellular uptake of curcumin nanoemulsions. *Food Hydrocolloids* (Submitted).

6.1 Introduction

Curcumin is a natural poliphenolic compound extracted from the rhizome of *Curcuma longa*, being commercially available as turmeric extracts, curcuminoids containing 70-80 % of curcumin, 15-25 % of demethoxycurcumin and 2.5-6.5 % of bisdemethoxycurcumin (Jayaprakasha et al., 2006; Siviero et al., 2015). Several studies suggest that curcumin exhibits a wide range of beneficial activities, such as antioxidant, anti-inflamatory, antimicrobial, anticancer, antiviral, anti-mutagen and wound healing (Jayaprakasha et al., 2006; Kaur et al., 2015; Liu et al., 2016; Siviero et al., 2015). However the use of curcumin is limited by their poor solubility in aqueous media (11 ng/mL), sensitivety to oxygen, pH, solvents and light (Plaza-Oliver et al., 2015; Siviero et al., 2015; Zhao et al., 2012). Hence, exploitation of curcumin as part of functional foods deeply relies on strategies that overcomes these limitations, triggering their incorporation into foods and beverages (Cerqueira et al., 2014; Pinheiro et al., 2016; Plaza-Oliver et al., 2015). Lipid-based nanosystems can be designed to overcome the limitations of the use of curcumin in the food industry. Lipid-based nanosystems such as nanoemulsions and multilayer nanoemulsions are delivery systems widely used to encapsulate lipophilic bioactive compounds, increasing their solubility in aqueous media, protecting them from environmental stresses, chemical, enzimatic and oxidative degradation, allowing their controlled release, improving their passage through gastrointestinal tract, enhancing lipid digestibility and promoting at the same time a greater bioaccessibility and bioavailability, while also enhancing the permeability of bioactive compounds across mucus layer and epithelium cells (Sun et al., 2015; Ting et al., 2014; Zou et al., 2015). The development of tailored lipid nanosystems relies on the final application, from nanosystems designed to delay lipids digestability, inducing satiation; to enhancing permeability across the intestinal membrane, improving bioavailability, potentiating the benefitial effects of curcumin, such as avoiding lipid peroxidatin and retarding the progress of chronic diseases (Maljaars et al., in press; Pinheiro et al., 2016; Ting et al., 2014). Generally, there are two pathways to transport bioactive compounds through the small intestine epithelium,

paracellular or transcellular pathway, enhancing the absorption of bioactive compounds in the gastrointestinal tract (Li et al., 2015a; Li et al., 2015b; Wang et al., 2015; Yu & Huang, 2012). In paracellular transport lipid-based nanosystems below 50 nm may be able to directly diffuse (passive diffusion) through the cell tight junctions (Li et al., 2015b; Wang et al., 2015). Transcellular transport represents the classic digestion-diffusion route, where the bioactive compounds entrapped within lipid-based nanosystems below 500 nm may be absorbed by the epithelial cells passing through the Caco-2 cell monolayer via passive or active transport mechanisms, such as macropinocytosis or endocytosis containing clathrin-mediated endocytosis, caveolae-mediated endocytosis, and clathrin- and caveolae-independent endocytosis (Li et al., 2015b; Yu & Huang, 2012). Also, lymphatic transport of the lipid-based nanosystems (sizes below 5 nm) can occur through M cells, which are located within Peyer's epithelium and hold high endocytosis capacity towards nanomaterials (Huang & Kuo, in press; Martins et al., 2015). Despite of the enourmous potential that lipid-based nanosystems present, theres a lack of knowledge about the behaviour of these systems after ingestion, from their behaviour during gastrointestinal tract, to their absorption through the instestine, evaluation of the bioavailability and potential toxicity (McClements, 2013; Pinheiro et al., 2016).

Therefore, the main purposes of this study were the understandment of the behavior of lipid based nanosystems under *in vitro* digestion and the evaluation of undigested nanosystems cytotoxicity, cellular antioxidant activity, apparent permeability coefficient and cellular uptake using Caco-2 cells line.

6.2 Materials and Methods

6.2.1 Materials

Neobee 1053 medium chain triglycerides (MCTs) is caprylic/capric triglyceride oil with a fatty acid distribution of 55 % of C8:0 and 44 % of C10:0. MCTs was kindly provided by Stepan (The Netherlands) and was used without further purification. Curcumin (Mw = 368.38 Da), DPPH, pepsin from porcine gastric mucosa (600 U mL^{-}1), lipase from porcine pancreas (40 U mL^{-}1), pancreatin

from porcine pancreas (8 × USP), bile extract porcine and the salts used for preparing the gastric and small intestinal electrolyte solutions, hydrochloric acid, sodium bicarbonate, Nile Red 9-diethylamino-5H-benzo[α]phenoxazine-5-one and dimethyl sulfoxide were purchased from Sigma-Aldrich (St Louis, MO, USA). Whey Protein Isolate (WPI) was purchased from Arla (Denmark), chitosan (deacetylation degree ≥ 95 %) from Golden-Shell Biochemical CO., LTD (Zhejiang, China) and sodium alginate from Manutex RSX, Kelco 104 International, Ltd. (Portugal) with Mw ≈ 15,900 Da and viscosity ≈ 200 cp (1 % aqueous solution with Brookfield Model LV – 60 rpm at 25 ºC). Lactic acid (90 %) was obtained from Acros Organics (Geel, Belgium). Sodium hydroxide and phenolphthalein were obtained from Panreac (Spain). Chloroform was obtained from Fisher Scientific (NJ, USA) and acetone from Fisher Chemical (UK). Distilled water (Milli-Q apparatus, Millipore Corp., Bedford, MA, USA) was used to prepare all solutions. For cell-based assays RPMI 1640 medium, Fetal Bovine Serum (FBS), Penicillin-Streptomycin (PS), trypsin/EDTA and Hanks' Balanced Salt Solution (HBSS) were obtained from Invitrogen (Paisley, UK). Phosphate buffered saline (PBS) powder, 2',7'-dichlorofluorescin diacetate (DCFH-DA), 2,2′-Azobis(2-methylpropionamidine) dihydrochloride (AAPH), quercetin and CelLytic™ MT Cell Lysis Reagent were obtained from Sigma-Aldrich (St. Louis, MO, USA). CellTiter 96® AQueous One Solution Cell Proliferation Assay (MTS) was obtained from Promega (Wisconsin, USA), Protease Inhibitor Cocktail Set III was purchased from Merck Millipore (Darmstadt, Germany), dimethyl sulfoxide (DMSO) was obtained from Carlo Erba Reagents Srl (Milan, Italy) and ethanol was purchased from Scharlab S.L. (Barcelona, Spain).

6.2.2 Experimental Procedures

6.2.2.1 Preparation of curcumin nanosystems

6.2.2.1.1 Curcumin nanoemulsion preparation

Curcumin oil-in-water nanoemulsions were prepared according to (Silva et al., 2015), with minor modifications. Briefly, 0.1 % (w/w) of curcumin was solubilized at 90 ºC in 10 % (w/w) of medium chain triglycerides (MCT's) and homogenized with 90 % (w/w) aqueous phase containing 1.5 % (w/w) of whey protein isolate

(WPI) dissolved in distilled water using an Ultra-Turrax homogenizer (T 25, Ika-Werke, Germany) during 2 min at 5000 rpm, followed by passage through a high-pressure homogenizer (EmulsiFlex-C3, Avestin, Canada) at 50 Psi, during 20 cycles of homogenization.

6.2.2.1.2 Curcumin multilayer nanoemulsion preparation

The multilayer nanoemulsions were formed through the deposition of chitosan solutions at pH 3 onto curcumin nanoemulsions using the LbL electrostatic deposition technique. The saturation method was applied, i.e. the layers were constructed by subsequent adsorption of polyelectrolytes from their solutions without the intermediate rinsing step (Adamczak et al., 2014). Briefly, anionic curcumin nanoemulsions were coated with a layer of positively charged chitosan solution, added drop wise with a syringe pump (NE-1000, New Era Pump Systems, Inc., USA) to fresh curcumin nanoemulsions, under stirring for 15 min. The concentration of chitosan solution used to form the surrounding layer was chosen empirically by analysing the results of zeta potential measurements (Adamczak et al., 2014; Madrigal-Carballo et al., 2010).

6.2.2.2 Nanosystems size measurements

The H_d and *PdI* of nanoemulsions and multilayer nanoemulsions were determined using DLS (Zetasizer Nano ZS-90, Malvern Instruments, Worcestershire, UK). The nanoemulsion samples were diluted 10× in distilled water at ambient temperature. The data was reported as the mean droplet diameter (hydrodynamic diameter, H_d). *PdI* is a dimensionless and indicates the heterogeneity (monodisperse or polydisperse) of particles size in a mixture (Malvern, 2011). Each sample was analysed in a disposable polystyrene cell (DTS0012, Malvern Instruments). The measurements were performed in duplicate, with three readings for each of them. The results are given as the average ± standard deviation of the six values obtained (Rao & McClements, 2013; Silva et al., 2011).

6.2.2.3 Nanosystems charge measurements

The droplet charge (*Zp*) of the nanoemulsions and multilayer nanoemulsions was determined using a particle micro-electrophoresis instrument (Zetasizer

Nano ZS-90, Malvern Instruments, Worcestershire, UK). Samples were diluted 100× in distilled water prior to measurements in order to avoid multiple scattering effects at ambient temperature and placing the diluted emulsions into disposable capillary cells (DTS 1060, Malvern Instruments) (Ozturk et al., 2014; Rao & McClements, 2013).

6.2.2.4 Stability of the nanosystems under storage

In order to evaluate the stability of nanoemulsion and multilayer nanoemulsion during storage, the H_d, *PdI* and *Zp* were evaluated during three months of storage at 4 ºC in the absence of light.

6.2.2.5 Nanosystems stability and curcumin release at gastrointestinal environmental conditions

The curcumin nanosystems stability under gastrointestinal environmental conditions was accessed by a dialysis method. 2 mL of aqueous curcumin nanosystems were added into a dialysis membrane (molecular weight cut-off 15 kDa; Cellu-Sep H1, Membrane filtration products, USA). The sealed dialysis membrane was then placed into 50 mL of buffer solution (phosphate buffer, PBS, for pH 7.4 and KCl–HCl buffer for pH 2) under magnetic stirring at 37 ºC. At appropriate time intervals, 0.5 mL of supernatant were taken and 0.5 mL of fresh acceptor medium was added to keep the volume of the release medium constant. The stability of the nanosystems and the released amount of curcumin from the nanosystems was evaluated by measuring the H_d after 54 h and the absorbance at 425 nm, maximum absorbance peak (Elisa Biotech Synergy HT, Biotek, USA). All stability/release tests were run at duplicate or triplicate. This assay was only performed to understand the stability of these nanosystems at the pH values of the gastrointestinal system.

6.2.2.6 In vitro *digestion*

6.2.2.6.1 Dynamic gastrointestinal model

A dynamic gastrointestinal system was used in the *in vitro* digestion experiments using the methodology developed by Pinheiro et al. (2016). This model simulates the main events that occur during digestion and consists of four compartments simulating the stomach, duodenum, jejunum and ileum.

Each compartment consists in two connected glass reactors with a flexible wall inside and water is pumped around the flexible walls to maintain the temperature at 37 ºC and to enable the simulation of the peristaltic movements (by the alternate compression and relaxation of the flexible walls). The changes in water pressure are achieved by peristaltic pumps which alter the flow direction according to the time controlled devices connected to them. The compartments are connected by silicone tubes and, at a predefined time, a constant volume of chyme is transferred. All compartments are equipped with pH electrodes and pH values are controlled by the secretion of HCl (1 mol L^{-1}) into the stomach and $NaHCO_3$ (1 mol L^{-1}) into the intestinal compartments. The gastric and intestinal secretions are added via syringe pumps at pre-set flow rates. The jejunum and ileum compartments are connected with hollow-fibre devices (SpectrumLabs Minikros®, M20S-100-01P, USA) to absorb digestion products and water from the chyme and to modify electrolyte and bile salts concentration of the chime (Pinheiro et al., 2016). It should be noted that, although at the mouth stage there may be changes in emulsions' size and interfacial characteristics, influencing the emulsions' fate in the gastrointestinal tract (McClements & Xiao, 2012; Pinheiro et al., 2016), this phase was not included once the sample is liquid (and therefore the mastication is not relevant and the residence time in the mouth is very low) and the samples do not contain starch (i.e. the primary enzyme present in saliva, amylase, would not act) (Pinheiro et al., 2016).

6.2.2.6.2 Experimental conditions

In vitro digestion was performed as described by other authors (Pinheiro et al., 2016) with minor modifications. A volume of 40 mL of curcumin nanosystems (both nanoemulsions and multilayer nanoemulsions) was introduced into the dynamic gastrointestinal system (gastric compartment) and the experiment was run for a total of 5 h, simulating average physiological conditions of GI tract by the continuous addition of gastric, duodenal, jejunal and ileal secretions. The gastric secretion consisted of pepsin and lipase in a gastric electrolyte solution (NaCl 4.8 g L^{-1}, KCl 2.2 g L^{-1}, $CaCl_2$ 0.22 g L^{-1} and $NaHCO_3$ 1.5 g L^{-1}), secreted at a flow rate of 0.33 mL min^{-1}. The pH was controlled to follow a predetermined curve (from 4.8 at t = 0 to 1.7 at t = 120 min) by secreting HCl (1 mol L^{-1}). The

duodenal secretion consisted of a mixture of 4% (w/v) porcine bile extract, 7% (w/v) pancreatin solution and small intestinal electrolyte solution (SIES) (NaCl 5 g L^{-1}, KCl 0.6 g L^{-1}, $CaCl_2$ 0.25 g L^{-1}) secreted at a flow rate of 0.66 mL min^{-1}. The jejunal secretion fluid consisted of SIES containing 10% (v/v) porcine bile extract solution at a flow rate of 2.13 mL min^{-1}. The ileal secretion fluid consisted of SIES at a flow rate of 2.0 mL min^{-1}. The pH in the different compartments of small intestine was controlled by the addition of 1 mol L^{-1} $NaHCO_3$ solution to set points of 6.5, 6.8 and 7.2 for simulated duodenum, jejunum and ileum, respectively. During *in vitro* digestion, samples were collected directly from the lumen of the different compartments (or jacket reactor), from the stomach, duodenal, jejunal and ileal filtrates and from the ileal delivery. The jejunal and ileal filtrates and ileal delivery were used to determine the bioaccessibility of curcumin. The samples were analysed in terms of H_d, Zp and free fatty acids. Both curcumin nanosystems were tested in the dynamic gastrointestinal model at least in triplicate.

6.2.2.7 Microscopy

The morphology of nanosystems was evaluated by transmission electron microscopy (TEM) (EM 902A, ZEISS, Germany) operating at 80 kV. TEM samples were prepared by depositing the nanoemulsion suspensions on a carbon-coated copper grid, and negatively stained with 1% (w/v) uranyl acetate for observation. Samples were air-dried before analyses. Also, the oil droplets in the emulsions were studied using an epifluorescence microscope (BX51 OLYMPUS, Tokyo, Japan) with an ×100 oil immersion objective lens. Samples were stained with Nile Red (9-diethylamino-5H-benzo[α]phenoxazine-5-one, 0.25 mg ml^{-1} in dimethyl sulfoxide, 1 : 10 (dye:sample), v/v), which enabled the oil droplets to become visible. Slides were prepared by taking 10 µL of the stained emulsion solution and placing in a glass microscope slide and covering with a glass cover slip.

6.2.2.8 Free fatty acids release

The digestion activity was measured by determining the amount of FFA released from curcumin nanoemulsions using a titration method (Pinsirodom, 2005). Briefly, 5 mL of jejunal filtrate, ileal filtrate and ileal delivery samples

were collected and 10 mL of acetone were added to quench the enzymes' activity and 3 drops of 1 % (w/v) phenolphthalein were added as an indicator. A direct titration with 0.1 mol L^{-1} NaOH using a burette was performed and the volume of NaOH added until the titration end point was determined and used to calculate the concentration of FFA produced by lipolysis. Therefore, the percentage of free fatty acids released was calculated from the number of moles of NaOH required to neutralize the FFA divided by the number of moles of FFA that could be produced from triglycerides if they were all digested (assuming 2 FFA produced per 1 triacylglycerol molecule) (Li et al., 2011; Pinheiro et al., 2016):

$$\%\ FFA = 100 \times \left(\frac{v_{NaOH} \times m_{NaOH} \times M_{lipid}}{w_{lipid} \times 2} \right) \quad \text{Eq. 6.1}$$

where v_{NaOH} is the volume of sodium hydroxide required to neutralize the FFA generated (in mL), m_{NaOH} is the molarity of the sodium hydroxide used (in mol L^{-1}), w_{lipids} is the total weight of MCT's oil initially present and M_{lipid} is the molecular weight of the MCT's oil (based on their average fatty acid composition the molecular weight of MCT's oil was considered to be 503 g mol^{-1}).

6.2.2.9 Curcumin bioaccessibility

It was assumed that the fraction of the original curcumin that ended up in the micelle phase was a measure of curcumin bioaccessibility (Ahmed et al., 2012) and that the mixed micelles that contained the bioaccessible curcumin fraction were able to pass the hollow-fibre membranes (i.e. corresponds to jejunal filtrate and ileal filtrate samples), while undigested emulsions were retained (Minekus et al., 2005). Curcumin bioaccessibility was determined based on the methodology described by other authors (Ahmed et al., 2012; Pinheiro et al., 2016). Briefly, 5 mL of the sample (jejunal or ileal filtrate) were vortexed with 5 mL of chloroform, and then centrifuged (Sigma 4K15, Germany) at 1750 rpm, at room temperature, for 10 min. The bottom chloroform layer was collected and the extraction procedure was repeated with the top layer. The second bottom chloroform layer was added to the previously set aside chloroform layer, mixed,

and analysed in a UV-VIS spectrophotometer (Elisa Biotech Synergy HT, Biotek, USA) at 425 nm (absorbance peak). The concentration of curcumin was determined from a previously prepared calibration curve of absorbance versus curcumin concentration in chloroform.

6.2.2.10 Cell culture

The Caco-2 cell line was selected for cytotoxicity experiments, cellular antioxidant activity evaluation and permeation studies. Caco-2 is a human intestinal epithelial cell line derived from a human colon adenocarcinoma, and is particularly useful since it forms a monolayer with many small intestinal functions (Matias et al., 2014). This cell line undergoes in culture a process of spontaneous differentiation that leads to the formation of a monolayer of cells, expressing several morphological and functional characteristics of the mature enterocyte (Sambuy et al., 2005). Caco-2 cell line were purchased from Deutsche Sammlung von Mikroorganismen und Zellkulturen (DSMZ, Braunschweig, Germany) and were routinely grown in RPMI 1640 culture medium supplemented with 10 % (v/v) of inactivated FBS and 1 % (v/v) of PS. Stock cells were maintained as monolayers in 75 cm^2 culture flasks. Cells were subcultured every week at a split ratio of 1 to 4 by treatment with trypsin/EDTA (0.25 %) and incubated at 37 ºC in a 5 % CO_2 humidified atmosphere (Matias et al., 2014). For all cell-based assays Caco-2 were used between passages 30 and 50.

6.2.2.11 Cytotoxicity assay

Caco-2 cells were seeded at a density of 2×10^4 cells/well in 96-well plate and the medium was changed every 48 h. The experiments were performed through method previously described by Serra and co-workers (2011), using completely differentiated cells (after reaching confluence, ~ 96 h) (Serra et al., 2011b; Serra et al., 2013). An initial stock solution of curcumin in ethanol was prepared (4 mg ml^{-1}). In the day of the assay, curcumin, nanoemulsion and nanoemulsion multilayer were diluted in RPMI medium supplemented with 0.5 % inactivated FBS (4.8 – 19.0 µg curcumin mL^{-1} and 31.25 – 250.00 µg chitosan mL^{-1}) and added to Caco-2 cells in triplicate. After 4 h of incubation at 37 ºC in a 5 % CO_2 humidified atmosphere, samples were removed and cells were washed twice

with PBS. Then, 100 µL of CellTiter 96® AQueous One Solution Cell Proliferation Assay reagent (MTS) diluted in RPMI 1640 medium supplemented with 0.5 % FBS was added to each well and left to react for 2 h, at 37 ºC in a 5 % CO_2 humidified atmosphere. MTS enters in cells and it is bio-reduced into a colored formazan product that is soluble in the culture medium. The quantity of formazan produced was measured spectrophotometrically at 490 nm in a microplate reader (EPOCH, Bio-Tek, USA) and is directly proportional to the number of living cells in culture. Results were expressed in terms of percentage of cellular viability relative to a group control (cells only with RPMI medium). Experiments were performed in triplicate in three independent assays.

6.2.2.12 Cellular antioxidant activity

Cellular Antioxidant Activity (CAA) was carried out by the method previously described by Wolfe and Liu (2007) with some modifications (Serra et al., 2011a). Briefly, Caco-2 cells were seeded at a density of 2×10^4 cells/well in a 96-well plate and the medium was changed every 48 h. After reaching confluence (~ 96 h), cells were washed twice with PBS and triplicate wells were treated for 1 h with 100 µL of different concentrations of curcumin (5 to 40 µg mL^{-1}) or nanoemulsion and multilayer nanoemulsion (0.95 to 7.60 µg mL^{-1}) plus 25 µmol L^{-1} of DCFH-DA diluted in PBS. Then, the medium was removed, cells were washed with PBS and 100 µL of 600 µmol L^{-1} of AAPH was added in each well. The 96-well microplate was placed into a fluorescence reader (FL800, Bio-Tek Instruments, Winooski, VT, USA) at 37 ºC. Emission at 530 ± 25 nm was measured after excitation at 485 ± 20 nm every 5 min for 1 h. Each plate included triplicate control and blank wells: control wells contained cells treated with DCFH-DA and oxidant (AAPH); blank wells contained cells treated with DCFH-DA without oxidant. Quercetin, previously dissolved in DMSO (20 mmol L^{-1}) was used as standard (1.25 – 10 µmol L^{-1}) for the calibration curve. CAA of samples was quantified as described by Wolfe and Liu (2007). Briefly, after blank and initial fluorescence subtraction, the area under the curve for fluorescence versus time was integrated to calculate the CAA value at each concentration of the sample:

$$CAA\ unit = 1 - \left(\int \frac{SA}{CA}\right) \quad \text{Eq. 6.2}$$

Where $\int SA$ is the integrated area under the sample fluorescence versus time curve and $\int CA$ is the integrated area of the control curve. The median effective concentration (EC_{50}) was determined for the sample from the median effect plot of log (f_a/f_u) versus log (dose), where f_a is the fraction affected (CAA unit) and f_u is the fraction unaffected (1-CAA unit) by the treatment. The EC_{50} values were stated as mean ± SD for triplicate sets of data obtained from the same experiment. Also, EC_{50} were converted to CAA values, expressed as micromoles of quercetin per mg of curcumin, using the mean EC_{50} value of quercetin from three independent experiments, 3.52 ± 0.42 µmol L^{-1}.

6.2.2.13 Permeability studies

For transport studies, Caco-2 cells were seeded in 12 mm i.d. Transwell® inserts (polycarbonate membrane, 0.4 µm pore size, Corning Costar Corp.) in 12-well plates at a density of $1x10^5$ cells/well. The basolateral (serosal) and apical (mucosal) compartments contained 1.5 and 0.5 mL of culture medium, respectively. Cells were allowed to grow and differentiate to confluent monolayers for 21 days by changing the medium (RPMI 1640 supplemented with 10 % of FBS and 1 % of PS) three times a week (Serra, 2010). By culturing them for 21 days, Caco-2 cells are spontaneously differentiated and tight junctions are formed between the cells, microvillus structures are formed on the apical cell surface and a variety of brush-border digestive enzymes, transporters and receptors are expressed (Langerholc et al., 2011; Shimizu, 2010). Transepithelial electrical resistance (TEER) of cells grown in Transwell was measured using an epithelial Volt-Ohm-meter (WPI, Berlin, Germany). The measurement of electrical resistance across the monolayer is a measure of passive ion transport across the cell and cell junctions and can be used as a criterion for the tightness of the cell monolayer in order to evaluate and determine the monolayer integrity. The TEER value was measured from the following equation:

$$TEER = \left(R_{monolayer} - R_{blank} \right) \times A \qquad \text{Eq. 6.3}$$

Where $R_{monolayer}$ is the resistance of the cell monolayer along with the filter membrane, R_{blank} is the resistance of the filter membrane and A is the surface area of the membrane (1.12 cm^2 in 12-well plates). Only monolayers with TEER value higher than 500 Ωcm^2 were used for experiments (Matias et al., 2014).

In the day of the experiment, the medium was removed and cells were washed twice with HBSS (pH 7.4, 37 ºC) to remove traces of RPMI medium. After washing, cells were incubated with transport buffer (HBSS) for 60 min at 37 ºC in a 5 % CO_2 incubator. For permeability transport studies, 500 µL of nanosystem (nanoemulsion and multilayer nanoemulsion) diluted in HBSS (19 µg curcumin mL^{-1}) was added to the apical compartment and 1.5 mL of transport buffer to the basolateral side. The transepithelial transport was followed as a function of time: after 0, 15, 30, 45, 60 and 120 min of incubation, TEER was measured and the basolateral and apical samples were collected and frozen until analysis. The apparent permeability coefficient (P_{app}) of nanoemulsions were calculated using the following equation:

$$P_{app} = \frac{\frac{dQ}{dt}}{Co \times A} \qquad \text{Eq. 6.4}$$

where *dQ/dt* is the cumulative transport rate (µg min^{-1}) defined as the slope obtained by linear regression of cumulative transported amount as a function of time (min), *Co* is the initial nanosystem concentration in the donor compartment and A is the membrane surface area (1.12 cm^2 in 12-well plates).

In addition, the cellular uptake of curcumin was also quantified. For this purpose, after 15, 30, 45, 60 and 120 min of incubation with samples, the Caco-2 monolayer was washed with 100 µL of HBSS to remove traces of nanoemulsions from the apical compartment and then cells were incubated for 5 min with 100 µL of CelLytic™ MT Cell Lysis Reagent containing 1 % (v/v) of Protease Inhibitor Cocktail (Matias et al., 2014). After scrapping, cells were collected and frozen until quantitative analysis by the high performance liquid chromatography (HPLC) method described below.

6.2.2.14 HPLC analysis of curcumin

The HPLC system comprised a Varian Prostar 210 pump, a Varian Prostar 410 autosampler and a Jasco FP-920 fluorescence detector (λ_{exc}=420 nm and

λ_{em}=540 nm). The instrument and the chromatographic data were managed by a Varian 850-MIB data system interface and a Galaxie chromatography data system, respectively. The chromatographic separation was performed on a C18 reversed-phase YMC-Pack ODS-AQ analytical column (250 x 4.6 mm I.D., 5 µm) that was fitted with a pre-column with the same stationary phase. The compounds were eluted using a flow rate of 1.0 mL min^{-1} during a 15 min isocratic run at a temperature of 30 °C. The injection volume was 20 µL. The mobile phase was a mixture of acetic acid (2 % v/v), pH 2.5, and acetonitrile (at a ratio of 47:53 v/v) that was filtered and degassed with a 0.2 µm membrane filter (GHP, Gelman). A calibration curve was prepared with standard solutions containing 0.1 to 10 µg mL^{-1} of curcumin in acetonitrile (Sigma-Aldrich). Curcumin, demethoxycurcumin, and bisdemethoxycurcumin were quantified by comparing the peak areas with the calibration curve. Retention times were 10.5, 11.5, and 12.5 min, respectively.

6.2.3 Statistical procedures

6.2.3.1 Data Analyses

Data analyses were performed using Microsoft Windows Excel 2011, using the Tukey's Multiple Comparison Test with a confidence interval of 95 % in GraphPad Prism 5 (GraphPad Software, Inc.) and using ANOVA in STATISTICA 7.0 (Statsoft, Tulsa, OK, USA).

Regarding the cell assays all data are expressed as means ± standard error and individual experiments were performed at least in triplicate. The statistical analysis was done using SigmaStat 3.0® software. All values were tested for normal distribution and equal variance. When homogeneous variances were confirmed, data were analysed by One Way Analysis of Variance (ANOVA) coupled with the Tukey's post-hoc analysis to identify means with significant differences (p value of p<0.001 was considered significant).

6.3 Results and Discussion

6.3.1 Curcumin nanosystems development and characterization

Different concentrations of WPI were tested aiming at preparing of curcumin nanoemulsions using 10 % (w/w) of MCTs as the oily phase (results not shown). The minimum concentration of WPI required to form stable nanoemulsions was found to be 1.5 % (w/w) presenting values of H_d of 186 ± 3.9 nm and a *PdI* of 0.124 ± 0.014, regarding the electrical charge (*Zp*) a value of -51.9 ± 2.4 mV was obtained.

For the development of multilayer nanoemulsions, the LbL electrostatic deposition technique was applied and the concentration of chitosan was controlled to avoid particle aggregation, using the saturation method, in which concentrations of chitosan were used without the need of centrifugation. The saturation concentration can than be empirically determined by monitoring the changes in the *Zp* measurements. A screening between 0 % and 0.1 % (w/w) was performed in order to evaluate the influence of chitosan in the nanoemulsions properties, i.e. H_d, *PdI* and *Zp*. The H_d, *PdI* and *Zp* of the multilayer nanoemulsion (first layer) were measured immediately after production.

Figure 6.1a shows that the addition of chitosan results in a change of *Zp* values, where the increase of chitosan concentrations (0 % to 0.1 %) changes the *Zp* values from highly negative to highly positive values, reaching a positive constant value around 42 mV, when the concentration ranged between 0.05 % to 0.1 % (w/w). This saw-like profile in the *Zp* values indicates that chitosan was adsorbed to the surface of the nanoemulsion, forming a multilayer nanoemulsion (Szczepanowicz et al., in press). At chitosan concentrations raging from 0.01 to 0.02 % (w/w) large “clumps” and oily droplets were observed at the upper surface of the samples This behaviour can be explained by the insufficient amount of chitosan present to coat all the nanoemulsion droplets, which is reflected by the *Zp* of the samples, achieving an increase from -51.9 mV for the nanoemulsion, to -15.1 mV and 0.8 mV for 0.01 % and 0.02 % w/w, respectively. In Figure 6.1b it is possible to observe the effect of these large clumps in the H_d of the samples, increasing the sizes and presenting a high *PdI*. The presence of clumps indicates that bridging

flocculation occurred. Charged polyelectrolytes can trigger bridging flocculation, as there is an insufficient amount of chitosan to completely coat the nanoemulsions, chitosan could link to the surface of more than one nanoemulsion droplet coupling nanoemulsions together (Cui et al., 2014; Guzey & McClements, 2006; Mora-Huertas et al., 2010). Similar behaviours were presented by Aoki and co-workers (2005) and Mun and co-workers (2005). Both authors verified that concentrations of chitosan below the saturation point resulted in droplets with negative surfaces, allowing chitosan to adsorb to the surface of two or more droplets simultaneously, forming large droplets aggregates and clumps (Aoki et al., 2005; Mun et al., 2005).

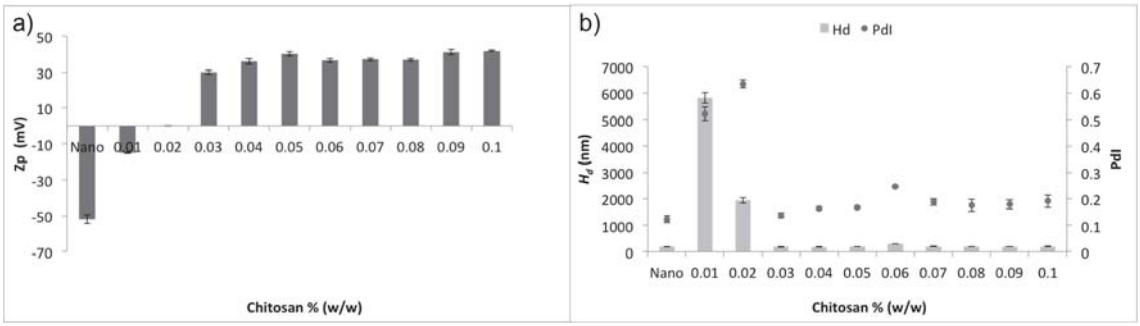

Figure 6.1 – Development of the 1st layer. a) Change in the zeta potential (*Zp*) as function of chitosan concentrations; b) Change in the hydrodynamic diameter (H_d) and polydispersity index (PdI) as function of chitosan concentrations. Bars indicate standard deviation (n = 3).

From 0.02 % to 0.1 % (w/w) a change from neutral to highly positive *Zp* was observed, suggesting that chitosan adsorbed to the surface of the nanoemulsions (Szczepanowicz et al., in press). Increasing the chitosan concentration above 0.5 % w/w did not increased the *Zp* value, leading to a constant value around 42 mV, however resulted in an increase of the H_d values from 189.1 ± 3.4 to 198.7 ± 5.4 nm, for 0.05 % and 0.1 % (w/w) of chitosan, respectively. It also promoted an increase of *PdI* values from 0.167 ± 0.004 to 0.191 ± 0.024, for the same range of concentrations. Results suggest that the nanoemulsions become saturated with chitosan, where the strong electrostatic repulsions present prevented droplet aggregation by bridging and depletion flocculation (Li et al., 2010; Pinheiro et al., 2016). Hence, 0.05 % (w/w) of chitosan was selected for the build up of the multilayer nanoemulsion, without significant excess of polyelectrolytes in solution. The developed multilayer

nanoemulsion presents a final H_d of 189.1 ± 3.4 nm, with a *PdI* of 0.167 ± 0.004 and a *Zp* value of 40.1 ± 1.2 mV. Transmission Electron Microscopy (TEM) confirms the mean droplet diameters achieved and confirmed the development of the nanosystems, Figure 6.2 presents a TEM microphotograph of the nanoemulsion and multilayer nanoemulsion (initial).

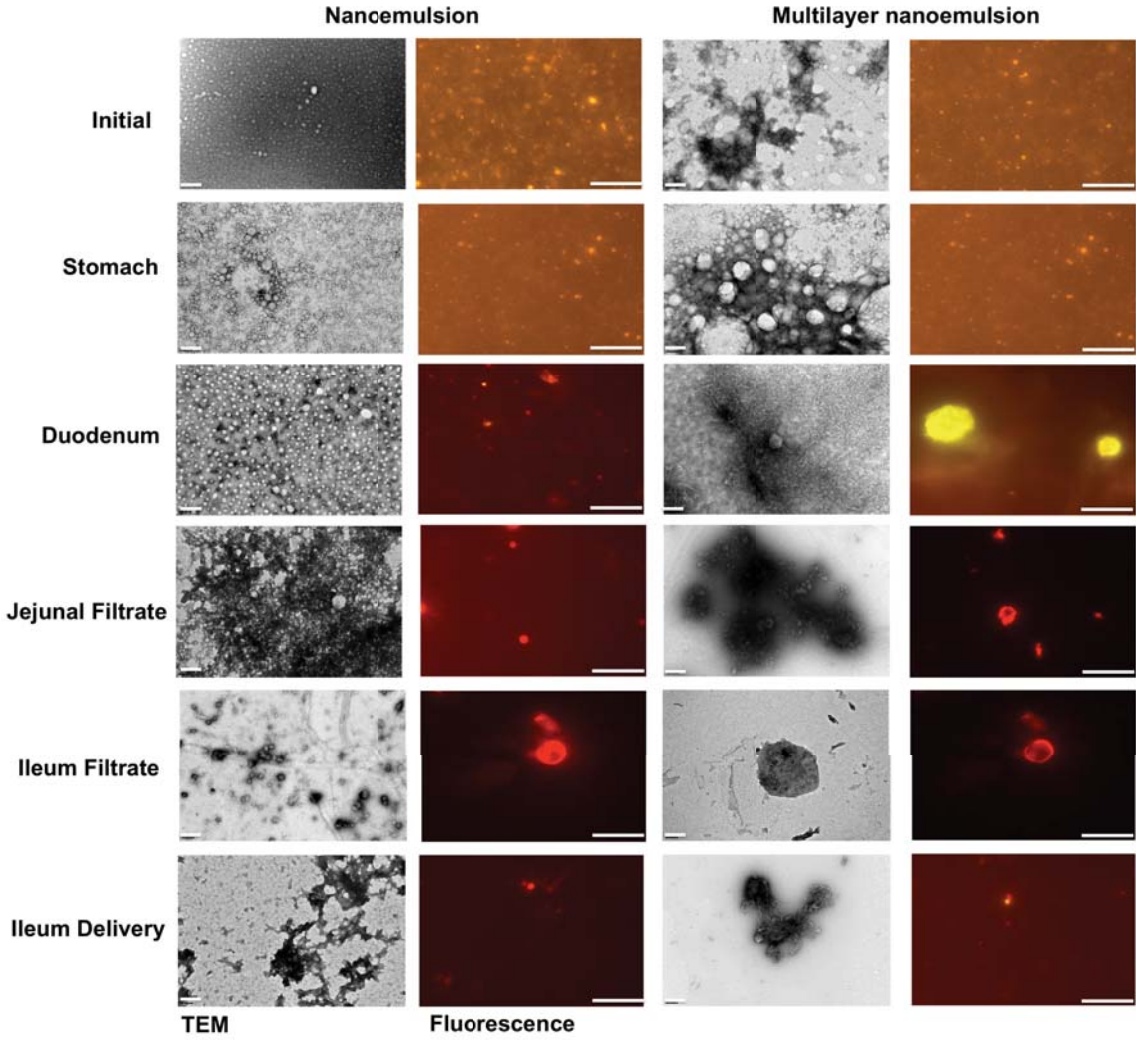

Figure 6.2 – TEM microphotographs of negatively stained nanosystems with uranyl 1% w/w and epifluorescence microphotographs stained with Nile Red as they undergo through the dynamic *in vitro* digestion. The scale bar for all TEM images and epifluorescent images are 400 nm and 20 μm, respectively.

6.3.2 Nanosystems stability under storage conditions

The developed nanosystems showed no macroscopic sign of instability phenomena (i.e. creaming or phase separation) after 35 days of storage. Figure 6.3 shows that curcumin nanoemulsions and multilayer nanoemulsions

maintained their H_d during storage. These results show that storage conditions do not statistically influence (p>0.05) (data not shown) the H_d values when compared to the values obtained after nanosystems production (please see Figure 6.3).

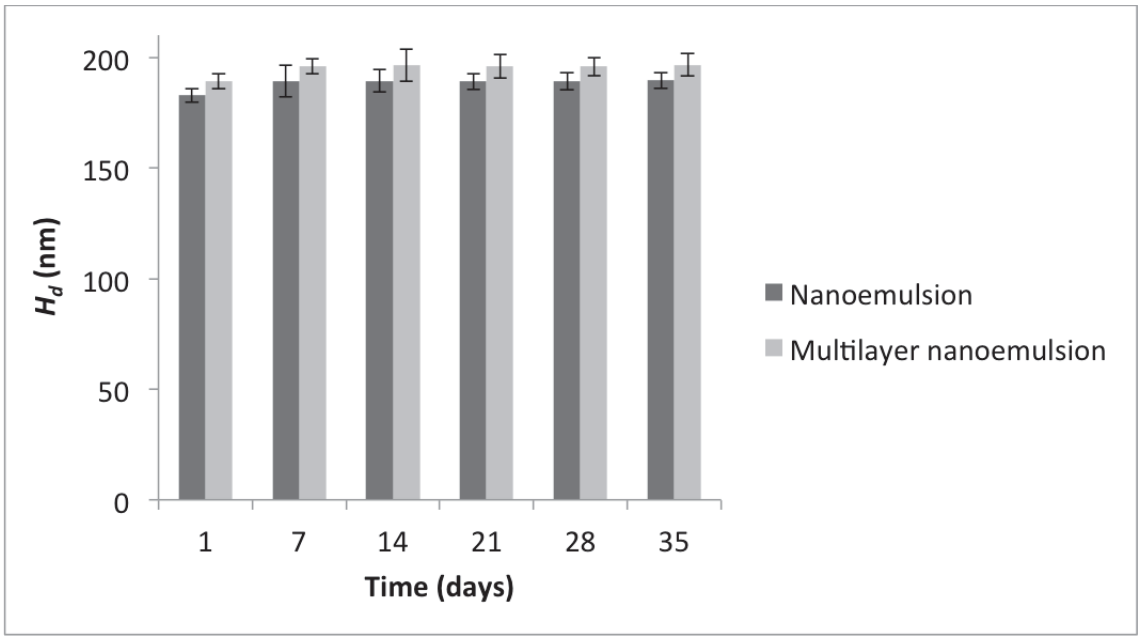

Figure 6.3 – Hydrodynamic diameter (H_d) during 35 days of storage for nanoemulsion and multilayer nanoemulsion. Bars indicate standard deviation (n = 3).

6.3.3 Evaluation of nanosystems responsiveness under gastrointestinal environmental conditions

The stability/responsiveness of both nanosystems was accessed at gastrointestinal conditions (i.e. at pH 2 and 7.4 at 37 ºC) during 54 h, by performing release assays and by measuring the absorbance of curcumin in the acceptor mediums. Also, after 54 h of release assays, the H_d and *PdI* of the nanosystems were evaluated in order to determine the changes in H_d and *PdI* values. At pH 7.4 none of the nanosystems released curcumin during the evaluation period, maintaining curcumin entrapped within the nanosystems. Considering the H_d stability, it was observed that after 54 h of assay, at pH 7.4, the nanosystems maintained values of H_d closer (p>0.05) to the initial value, with 187.3 ± 2.7 nm for the nanoemulsion and 189.1 ± 2.8 nm for the multilayer nanoemulsion. At these conditions, above the pK_a of chitosan, the amino groups are entirely deprotonated (Vachoud et al., 2000), although, it is feasible

that chitosan held some positive charge. Previous works showed that pK_a of charged groups can change when entangled between polyelectrolytes of oppositely charges, improving the stability of the multilayer nanoemulsion to pH changes (Burke & Barrett, 2003a, b; Li et al., 2010).

At pH 2, the nanoemulsions loss WPI to the acceptor medium (data not shown), being unstable at this pH after 54 h of assay thus rendering it impossible to measure H_d. However, for the multilayer nanoemulsions, the H_d remained stable after 54 h of assay, obtaining an H_d of 190.4 ± 3.1 nm, while no sign of curcumin was present in the acceptor medium (0 μg mL^{-1}, below the detection limit of 0.01 μg mL^{-1}). Curcumin is reported as having low solubility in aqueous systems, 11 ng mL^{-1}, which could explain the absence of curcumin release (Jelezova et al., 2015; Zhao et al., 2012).

6.3.4 Dynamic *in vitro* digestion

As showed in chapter 4, LbL technique can be used to modify the interfacial composition of nanoemulsions increasing the stability under gastrointestinal tract conditions, delaying lipid digestion (Hu et al., 2011; Klinkesorn & Julian McClements, 2010; Yang et al., 2014). These experiments evaluated the influence of a chitosan layer in the behaviour of the nanosystems under *in vitro* digestions, mimicking the human gastrointestinal tract.

6.3.4.1 Influence of chitosan on nanosystems characteristics during in vitro *digestion*

The effect of the deposition of a chitosan layer on the nanoemulsion H_d, morphology and *Zp* was evaluated at each stage of the *in vitro* digestion. Initially the nanosystems had a H_d of 186 and 189 nm for the nanoemulsion and multilayer nanoemulsion, respectively. After being subjected to stomach conditions, the nanoemulsion H_d values increased to 258.3 ± 26.7 nm (please see Figure 6.4) evidencing some coalescence phenomena, confirmed by the epifluorescence microscopy, Figure 6.2. For the multilayer nanoemulsion the H_d value obtained under the gastric conditions was 205.4 ± 16.8, which does not present a statistically significant difference (p>0.05) when compared with the initial value. From the epifluorescence microscopy, Figure 6.2, some larger droplets can be observed, nonetheless TEM micrographs confirm droplets in

the nano-size range. This behaviour can be related with the interfacial characteristics of systems and their surface charge. Under gastric conditions, both nanosystems are positively charged: the nanoemulsion presented a positive *Zp* of 29.7 ± 5.3 mV and the multilayer nanoemulsion presented a *Zp* of 36.6 ± 3.0 mV (Figure 6.5), exhibiting strong electrostatic repulsion between droplets and thus avoiding droplet aggregation, flocculation and coalescence (Klinkesorn & Julian McClements, 2010; Pinheiro et al., 2016; Zhang et al., in press). The change in the *Zp* values, from negative to positive, for nanoemulsions at gastric conditions can be attributed to changes in solutions conditions, pH and ionic strength. In fact, at pH below the isoelectric point (pI ~5.2) of WPI, the WPI-stabilized nanoemulsions would be positively charged, which is in agreement with other published works (Rodrigues et al., 2015).

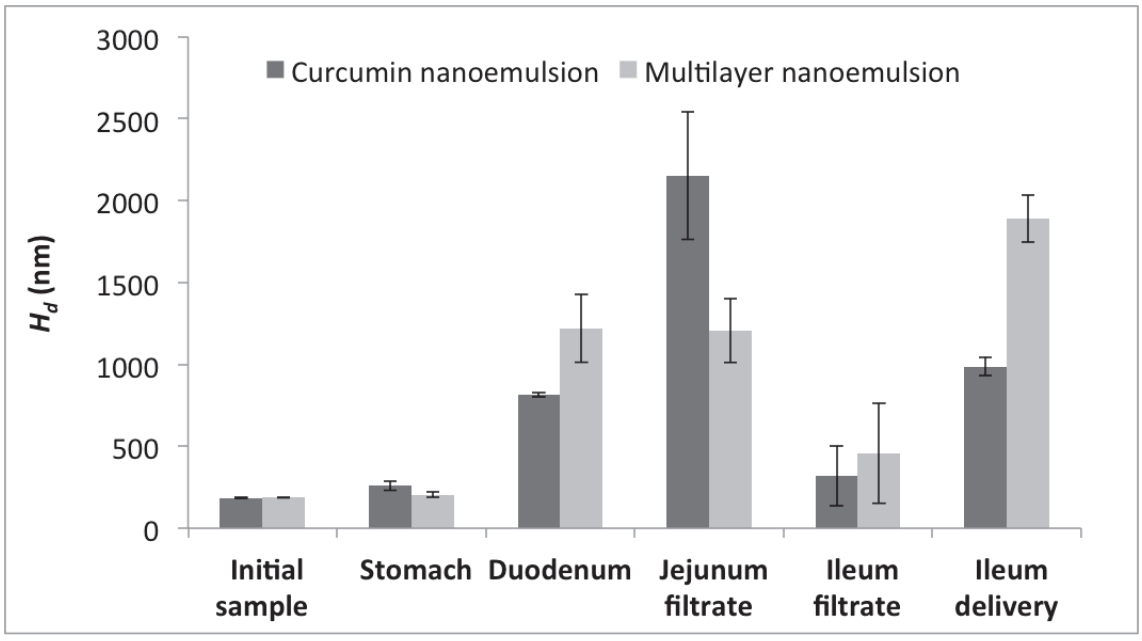

Figure 6.4 – Hydrodynamic diameter (H_d) for the nanosystems as they undergo through the dynamic *in vitro* digestion. Bars indicate standard deviation (n = 3).

Under intestinal conditions, both nanosystems exhibited an increase of the H_d due to particle aggregation either by flocculation or coalescence of droplets (Figure 6.2 and 6.4). At the duodenal stage, the H_d values increased to 815.2 ± 13.5 nm for the nanoemulsion, presenting a *Zp* value of -22.7 ± 7.2 mV; in the case of the multilayer nanoemulsion, the H_d increased to 1218.6 ± 205.7 nm and the *Zp* to -19.1 ± 2.7 mV. Microscopy analyses showed that at this stage,

both nanosystems exhibited droplets at the nano and micro-scale, confirming the H_d values presented in Figure 6.4. At jejunum and ileum stages both nanosystems presented a high H_d. For instance, in the jejunum the nanoemulsion had an H_d of 1831.0 ± 126.9 nm, whereas the multilayer nanoemulsion presented an H_d value of 1205.7 ± 193.9 nm. However, both nanosystems presented a smaller mean droplet diameter in the ileum filtrate than the one found in the jejunum filtrate and ileal delivery, justified by the filtration step performed in the hollow-fibre cartridge. For all the intestinal stages of digestion, sizes at the micro-scale were encountered (Figure 6.2), still, TEM analyses showed non-digested nanosystems at the nano-scale present in the jejunum and ileum stages of the digestion. The large H_d observed at the small intestine stage can be due to the fact that bile salts are able to displace WPI and chitosan from the droplets surface and lipase conducted the hydrolysis of the triacylglycerol molecules present into free fatty acids (FFA), monoacyglycerides and/or diacylglycerides (Pinheiro et al., 2016). This hydrolysis can also generate structures such as micelles, vesicles or other colloidal structures (Mu & Høy, 2004).

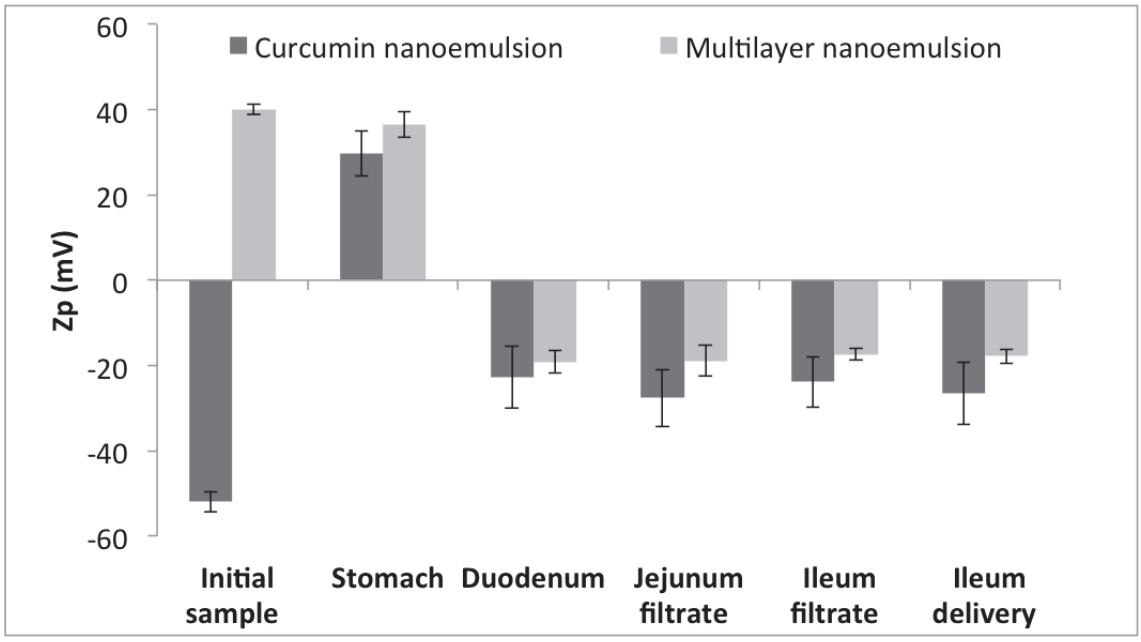

Figure 6.5 – Zeta potential values (*Zp*) for the nanosystems as they undergo through the dynamic *in vitro* digestion. Bars indicate standard deviation (*n* = 3).

Regarding the effect of intestinal conditions on the droplet charge, results show that the *Zp* values decreased, changing from positive to negative charges for both nanosystems, reaching to values ranged between -28 mV and -23 mV for the nanoemulsion and around -18 mV for the multilayer nanoemulsion (Figure 6.5). These results suggest that the presence of bile salts or free fatty acids might have displaced the WPI and chitosan from droplet surface or that bile salts or free fatty acids adsorbed onto the surface of the nanosystems (Klinkesorn & Julian McClements, 2010; Pinheiro et al., 2016; Salvia-Trujillo et al., 2015; Zou et al., 2015). There were no significant differences (p>0.05) between the values of *Zp* of both nanosystems at intestinal conditions.

6.3.4.2 Influence of chitosan layer on lipids digestion

The effect of chitosan layer in the lipids digestion was examined by the hydrolysis of the triacylglycerol molecules into free fatty acids (FFA) at each stage of the small intestine digestion (Figure 6.6). The deposition of a chitosan layer onto the nanoemulsion did not had a significant effect on the extent of lipid digestion, achieving a similar overall extent of released FFA (Figure 6.6), of 96.14 ± 1.36 % and 95.52 ± 4.93 % for curcumin nanoemulsion and multilayer nanoemulsion, respectively. These results suggest that the chitosan layer did not prevent lipid digestion, rather delaying it during the jejunum filtrate stage. In fact, some studies suggest that pancreatic lipase has the ability to hydrolyse chitosan, explaining the lack of efficiency of the developed layer (Pantaleone et al., 1992; Shin et al., 2001). Nonetheless, this study shows some differences in the rate at which the nanosystems were digested. In Figure 6.6 it is possible to see that in the jejunum the multilayer nanoemulsion presents a significantly lower (p<0.05) amount of FFA released when compared with the nanoemulsion, suggesting that the multilayer nanoemulsions were digested at a slower rate. At this stage, chitosan reduced the lipid digestion from 77.67 ± 1.19 % to 65.29 ± 2.92 %, being these results in agreement with previous studies (Klinkesorn & McClements, 2009; Pinheiro et al., 2016; Tokle et al., 2012). The decrease of the FFA release at jejunum when using chitosan layer may be explained by the ability of bile salts to form electrostatic complex with chitosan, reducing the digestibility of the lipids by sterically hindering the lipase, as seen in chapter 5 (Klinkesorn & Julian McClements, 2010; Klinkesorn & McClements, 2009). Also,

large aggregates of chitosan could restrict the access of lipase to the lipids (McClements & Li, 2010; Zhang et al., in press).

These results suggest that the presence of a chitosan layer on the nanoemulsions may be useful to control the rate of lipid digestion and FFA adsorption within the gastrointestinal tract, although being inefficient in preventing lipid digestion.

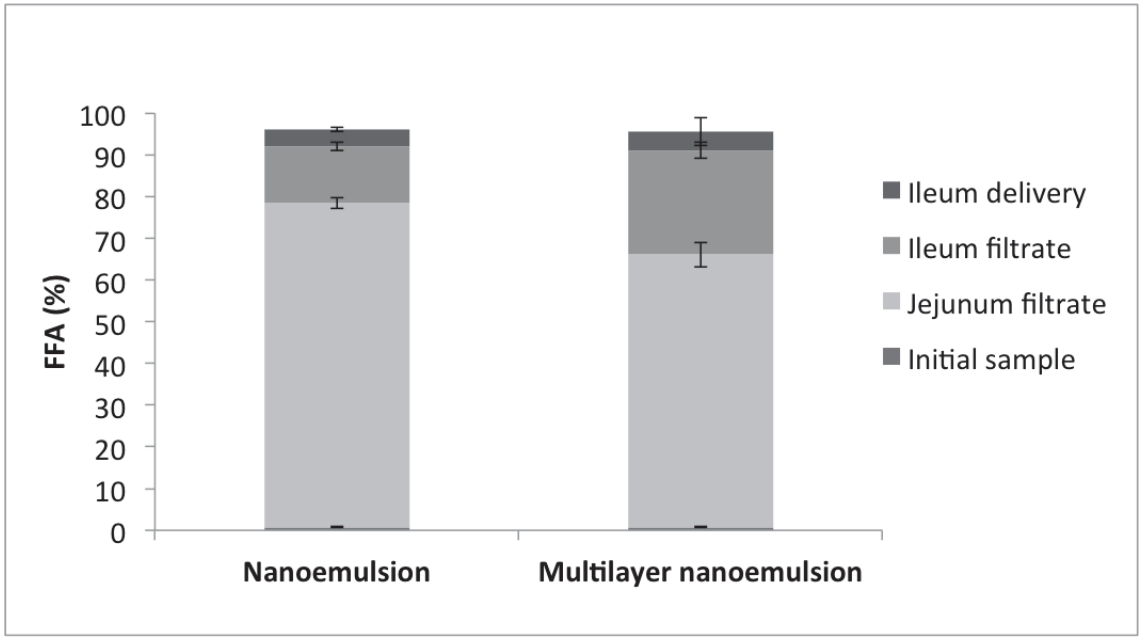

Figure 6.6 – Percentage of free fatty acids (FFA) released from the nanosystems as they undergo through the dynamic *in vitro* digestion. Bars indicate standard deviation (n = 3).

6.3.4.3 Influence of chitosan on curcumin bioaccessibility

Curcumin bioaccessibility from the nanosystems was measured as the curcumin concentration present in mixed micelles after digestion at jejunum filtrate, ileal filtrate and ileal delivery. Figure 6.7 shows that curcumin bioaccessibility increases during the digestion time, which can be explained by the ability of free fatty acids (FFA), monoacyglycerides and diacylglycerides to form mixed micelles capable of solubilize curcumin (Pinheiro et al., 2016). Also, Figure 6.7 shows that the use of a chitosan layer did not significantly increase (p<0.05) the curcumin bioaccessibility for multilayer nanoemulsion with 41.6 ± 6.23 % when compared to the nanoemulsion bioaccessibility with 31.55 ± 4.94 % (Figure 6.7). For both nanosystems, the bioaccessibility of curcumin was higher in the jejunal filtrate, when compared to the ileal filtrate fraction. When

comparing the results of the curcumin bioaccessibility at ileal filtrate between nanoemulsion and multilayer nanoemulsion, it can be observed that multilayer nanoemulsion present higher (p<0.05) bioaccessibility of curcumin regarding to nanoemulsions (15.5 ± 1.92 % and 9.3 ± 2.63 %, respectively). These results are in agreement with the FFA released from lipid digestion, Figure 6.6, i.e. the higher curcumin bioaccessibility observed in the ileal filtrate for the multilayer nanoemulsions, corresponds to the higher amount of FFA observed in the ileal filtrate. Since the access of lipases to lipids is crucial for a good bioaccessibility, the observed higher amount of FFA that could be part of mixed micelles could increase the solubility towards curcumin, increasing therefore its bioaccessibility (Pinheiro et al., 2016; Porter et al., 2007).

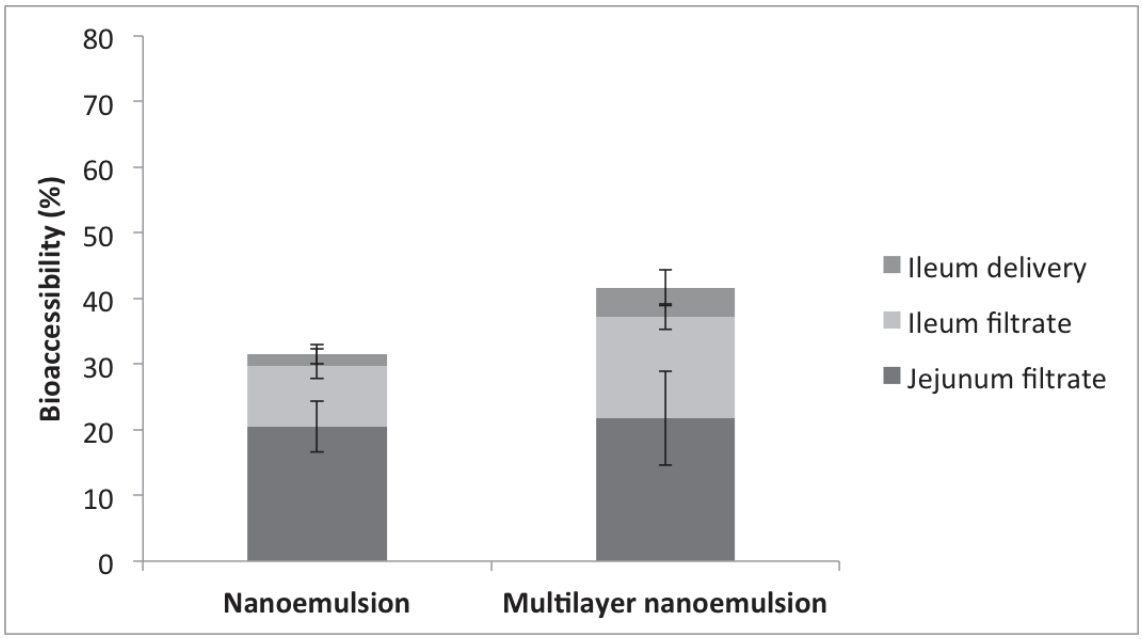

Figure 6.7 – Percentage of bioaccessibility as the nanosystems undergo through jejunal and ileal stages of the dynamic *in vitro* digestion. Bars indicate standard deviation (n = 3).

6.3.5 Cytotoxicity assay

The cytotoxicity of curcumin, nanosystems and chitosan were assessed using MTS test through the evaluation of Caco-2 cells viability. As shown in Figure 6.8, free curcumin and nanosystems were not toxic relatively to the control group (cells with RPMI medium), indicating that all samples had no effect in Caco-2 cell viability after 4 h of incubation in the tested concentrations (between 4.8 and 19 μg curcumin mL^{-1}). Furthermore, chitosan did not present

toxicity towards the control group (data not shown). These results ensure the safety of curcumin and nanosystems to be further tested for cellular antioxidant activity and for permeability studies.

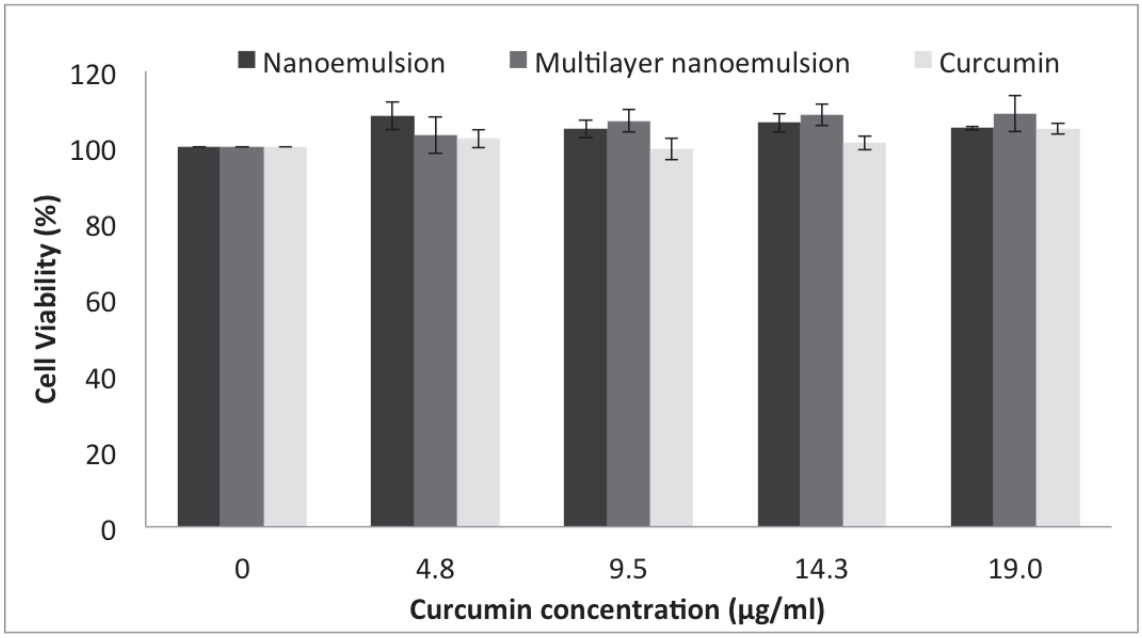

Figure 6.8 – Cell viability in percentage in function of curcumin concentration in terms of µg/mL. Bars indicate standard deviation (*n* = 3).

6.3.6 Cellular antioxidant activity

Curcumin is a well-known antioxidant compound (Pinheiro et al., 2016; Siviero et al., 2015; Zou et al., 2015). Several *in vitro* chemical antioxidant assays have been performed to evaluate the antioxidant activity of curcumin in the presence of different free radicals (Ak & Gülçin, 2008; Jayaprakasha et al., 2006). Nonetheless, the wide usage of these antioxidant chemical assays do not account for some physiological conditions that happens *in vivo*, such as, cell uptake, metabolism and distribution of the bioactive compounds (Wolfe & Liu, 2007). For this reason, in this work the cellular antioxidant activity (CAA) of free curcumin and curcumin entrapped within nanosystems (undigested) were quantified in the human cell model Caco-2. In this assay, dichlorofluorescein is trapped in the cells and is oxidized to fluorescent dichloroffluorescein. This method measures the ability of antioxidants to prevent the formation of fluorescent dichloroffluorescein by AAPH-generated peroxyl radicals (Serra, 2010; Wang & Joseph, 1999). Thus, the decrease in the cellular fluorescence

when compared to the control cells indicates the antioxidant activity of curcumin. Table 6.1 presents the EC_{50} (µg curcumin mL^{-1}) and *CAA* (µmol L^{-1} quercetin equivalents (QE) mg^{-1} curcumin) values for free curcumin and curcumin entrapped in the nanosystems. Table 6.1 shows that curcumin encapsulated in the nanosystems had higher *CAA* value than curcumin solubilized in ethanol (0.21 ± 0.01 µmol L^{-1} QE mg^{-1} curcumin). Nanosystems exhibited 8.5 and 9.9-fold higher values of *CAA* for nanoemulsion and multilayer nanoemulsion, 1.79 ± 0.08 µmol L^{-1} QE mg^{-1} curcumin and 2.08 ± 0.16 µmol L^{-1} QE mg^{-1} curcumin, respectively. Results show that *CAA* values of curcumin encapsulated in the nanosystems significantly (p<0.001) increased when compared to free curcumin, suggesting that nanoencapsulation of curcumin using WPI as emulsifier lead to an increase of the cellular antioxidant activity of curcumin in Caco-2 cells. The use of a chitosan layer did not have significant impact (p>0.001) in the *CAA* value, suggesting that chitosan did not enhance the cellular antioxidant capacity of curcumin. The enhanced *CAA* may be explained by the fact that free curcumin was solubilised in ethanol and cell media, which could limited the solubility of curcumin. On the other hand, curcumin encapsulated in the nanosystems has a larger surface area, therefore increasing the *CAA* values (Sessa et al., 2011; Yu et al., 2011). Another explanation may be the fact that curcumin suffers rapid hydrolysis at weak basic conditions (ethanol and media) that may induce their rapid degradation. Otherwise, both nanosystems could stabilize curcumin against hydrolysis (Yu et al., 2011). Yu and co-workers 2011, suggested that micelle encapsulation enhanced the *CAA* of curcuminoids in HepG2 cell line (liver hepatocellular carcinoma cells) by 2-fold when compared to free curcuminoids solubilised in DMSO (Yu et al., 2011), which is in accordance with our work.

Table 6.1 – EC_{50} (µg curcumin mL^{-1}) and *CAA* (µmol L^{-1} QE mg^{-1} curcumin) values for the inhibition of Peroxyl Radical-Induced DCFH Oxidation by curcumin and nanoemulsions (Mean ± SD, *n* =3)

Samples	EC_{50} (µg curcumin mL^{-1})	*CAA* (µmol L^{-1} QE mg^{-1} curcumin)
Curcumin	16.4 ± 0.6	0.21 ± 0.01
Nanoemulsion	1.97 ± 0.09	1.79 ± 0.08
Multilayer nanoemulsion	1.69 ± 0.13	2.08 ± 0.16

6.3.7 Permeability assays

The transport mechanisms of curcumin loaded in the lipid-based nanosystems (undigested) were evaluated using Caco-2 cell monolayers, aiming at simulationg the small intestine epithelium. The selected concentration of curcumin for the permeability studies was 19 µg mL^{-1} since at these concentrations the nanosystems did not show cytotoxicity. The apparent permeability coefficient (P_{app}) of most compounds ranges between 1.0×10^{-7} and 1.0×10^{-5} cm s^{-1}. Usually a poorly transported compound exhibits a P_{app} value of ~1.0×10^{-7} cm s^{-1}, whereas a well transported compound has a P_{app} value of ~1.0×10^{-5} cm s^{-1}. Otherwise, average permeable compounds will exhibit P_{app} values of ~1.0×10^{-6} cm s^{-1} (Gao et al., 2001; Sessa et al., 2014). The curcumin permeation rates for nanoemulsion and multilayer nanoemulsion are showed in Figure 6.9. The permeation rate for curcumin nanoemulsion was determined as $1.25 \pm 0.05 \times 10^{-6}$ cm s^{-1}, that falls in the range of the averagely permeable compounds. The rate of permeation of curcumin across the cells monolayer increased as function of time (data not shown) and the TEER values (not shown) did not change significantly (p>0.05), suggesting that curcumin permeated the cells monolayer through transcellular pathway (Li et al., 2015a; Sun et al., 2015; Yu & Huang, 2012). Nevertheless, these results do not show if nanoemulsions permeate directly across the Caco-2 cell monolayers (Yu & Huang, 2012). Also, the permeation rate for curcumin multilayer nanoemulsion

was determined as 1.93 ± 0.02 × 10^{-6} cm s^{-1} (Figure 6.9), 1.55-fold higher (p<0.05) than the value obtained for the nanoemulsion. Chitosan is known for its ability to facilitate the widening of tight junctions, enhancing the paracellular transport of bioactive compounds, such as curcumin, across the Caco-2 cells monolayer (Smith et al., 2004; Ting et al., 2014). In our study, the presence of chitosan significantly decreased (p<0.05) the TEERS value, suggesting that curcumin multilayer nanosystem were also able to directly diffuse through Caco-2 cell tight junctions. A reduction of ~90 % in TEER values can indicate that lipid-based nanosystems could disrupt the tight junctions, enhancing the transport of the bioactive compounds via paracellular pathway (Li et al., 2015b; Wang et al., 2015). Despite the reduction of the TEER values, Caco-2 cells monolayer did not shown visual signs of damage. Thus, these results suggest that both transcellular and paracellular pathways may exist at the same time when nanoemulsions with a chitosan layer are absorbed.

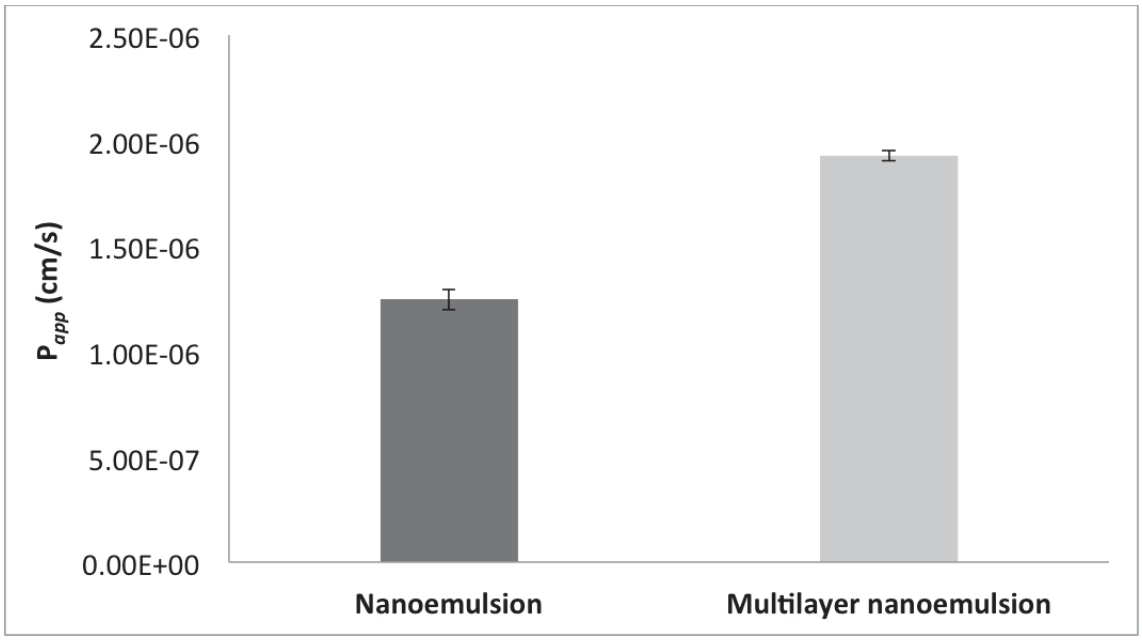

Figure 6.9 – The apparent permeability coefficient (P_{app}) for nanoemulsion and multilayer nanoemulsion in terms of curcumin after 2 h of incubation time. The results are presented as the mean values of duplicates experiments.

In addition, the cellular uptake of curcumin delivered by nanoemulsions and multilayer nanoemulsions was quantified (Figure 6.10). The use of a chitosan layer significantly increased the cellular uptake by endocytosis from 4.44 ±

0.11 % to 10.50 ± 0.15 %, which represents an increase of 2.36-fold on the cellular uptake. Since size and surface properties (such as charge and hydrophobicity) of the nanosystems governs the cellular uptake, this result may be explained by the positive charges that the multilayer nanoemulsion had, due chitosan amino groups, being the multilayer nanoemulsion internalized into the Caco-2 cells, whereas the negative charge of WPI due to electrostatic repulsions can decrease the uptake efficiency (Li et al., 2015b). Hydrophilic polyelectrolytes such as chitosan can enhance nanosystems transport through the Caco-2 cells via specific interaction between nanosystems and intestinal epithelium (des Rieux et al., 2006; McClements, in press). For instance Harush-Frenkel and co-workers (2007) reported that negative nanoparticles, due to repulsions between the nanoparticles and negative charged HeLa cells, had a lower cellular uptake, when compared with positive charged nanoparticles (Harush-Frenkel et al., 2007; Li et al., 2015b).

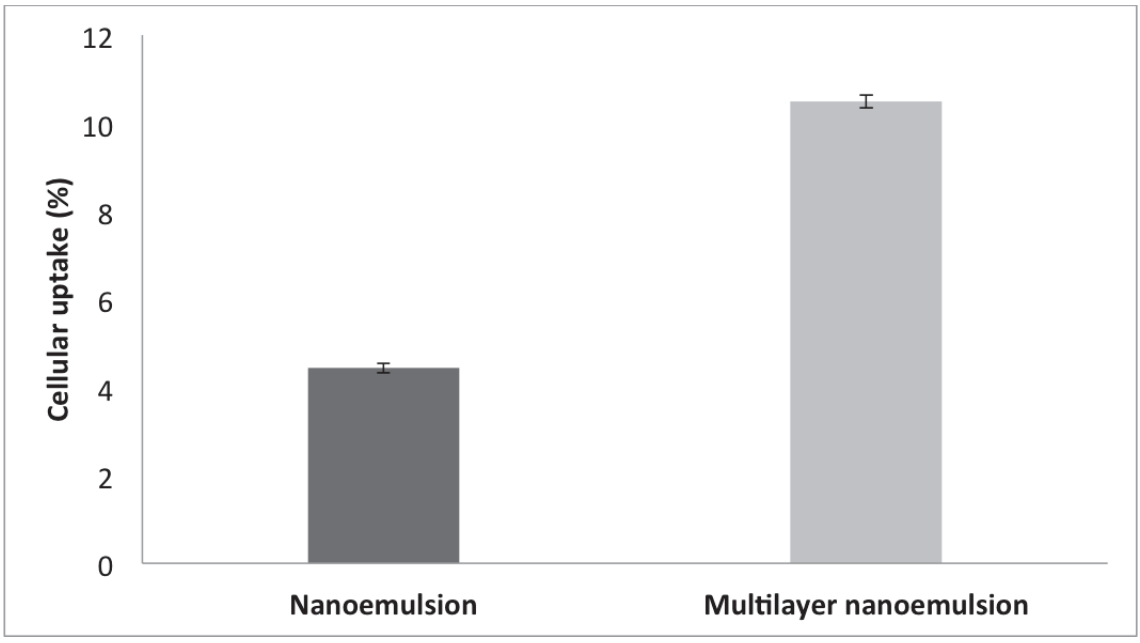

Figure 6.10 – Cellular uptake in percentage for nanoemulsion and multilayer nanoemulsion. The results are presented as the mean values of duplicates experiments.

The mass balance performed (data not shown) presented a low value of curcumin recovery (between 30 % to 40 %), which suggests that curcumin could have been metabolized by the Caco-2 cells, accumulated in the cell monolayer, bind to the plate, as well as lost during the washing step or during

sample preparation for HPLC (Cyprotex; Li et al., 2015b; McClements, in press). Curcumin nanosystems after being internalized in the Caco-2 cells may have been consumed in metabolic processes such as reduction, conjugation, dehydroxylation, cyclization, and methylation (Li et al., 2015b; McClements, in press). In fact, curcumin undergoes metabolic O-conjugation to curcumin glucuronide and curcumin sulfate and bioreduction to tetrahydrocurcumin, hexahydrocurcumin, octahydrocurcumin, and hexahydrocurcuminol (Prasad et al., 2014).

6.4 Conclusions

The purpose of this study was to develop lipid-based nanosystems, while evaluating the effect of a chitosan layer on nanosystems stability during *in vitro* digestion, on lipids digestibility and curcumin bioaccessibility. Also the cytotoxicity, cellular antioxidant activity and transport properties through a Caco-2 cell monolayer of undigested nanosystems were evaluated. Results showed that both nanosystems (nanoemulsion and multilayer nanoemulsion) can increase the bioaccessibility of curcumin. Also, results suggest that WPI nanoemulsions and chitosan-coated nanoemulsions can significantly increase the cellular antioxidant activity of curcumin, suggesting that both systems can be used for the delivery of water-insoluble curcumin. Permeability assays performed in Caco-2 cells showed that the use of chitosan can enhance the apparent permeability coefficient of curcumin by 1.55-fold. Although the permeation rate multilayer nanoemulsion was higher than that of nanoemulsion, both the transcellular and paracellular pathways may exist at the same time.

This study suggests that food grade lipid-based nanosystems can be designed as delivery systems offering the opportunity to create functional foods able to maximize curcumin antioxidant capacity.

6.5 References

Adamczak M, Kupiec A, Jarek E, Szczepanowicz K & Warszyński P (2014) Preparation of the squalene-based capsules by membrane emulsification method and polyelectrolyte multilayer adsorption. Colloids and Surfaces A: Physicochemical and Engineering Aspects 462, 147-152.

Ahmed K, Li Y, McClements DJ & Xiao H (2012) Nanoemulsion- and emulsion-based delivery systems for curcumin: Encapsulation and release properties. Food Chemistry 132(2), 799-807.

Ak T & Gülçin İ (2008) Antioxidant and radical scavenging properties of curcumin. Chemico-Biological Interactions 174(1), 27-37.

Aoki T, Decker EA & McClements DJ (2005) Influence of environmental stresses on stability of O/W emulsions containing droplets stabilized by multilayered membranes produced by a layer-by-layer electrostatic deposition technique. Food Hydrocolloids 19(2), 209-220.

Burke SE & Barrett CJ (2003a) Acid−Base Equilibria of Weak Polyelectrolytes in Multilayer Thin Films. Langmuir 19(8), 3297-3303.

Burke SE & Barrett CJ (2003b) pH-Responsive Properties of Multilayered Poly(l-lysine)/Hyaluronic Acid Surfaces. Biomacromolecules 4(6), 1773-1783.

Cerqueira M, Pinheiro A, Silva H, Ramos P, Azevedo M, Flores-López M, Rivera M, Bourbon A, Ramos Ó & Vicente A (2014) Design of Bio-nanosystems for Oral Delivery of Functional Compounds. Food Engineering Reviews 6(1-2), 1-19.

Cui J, van Koeverden MP, Müllner M, Kempe K & Caruso F (2014) Emerging methods for the fabrication of polymer capsules. Advances in Colloid and Interface Science 207, 14-31.

Cyprotex Caco-2 permeability assay, Available at: http://www.cyprotex.com/admepk/in-vitro-permeability/caco-2-permeability. Accessed 27/10/2015.

des Rieux A, Fievez V, Garinot M, Schneider Y-J & Préat V (2006) Nanoparticles as potential oral delivery systems of proteins and vaccines: A mechanistic approach. Journal of Controlled Release 116(1), 1-27.

Gao J, Hugger ED, Beck-Westermeyer MS & Borchardt RT, (2001). Estimating Intestinal Mucosal Permeation of Compounds Using Caco-2 Cell Monolayers, *Current Protocols in Pharmacology*. John Wiley & Sons, Inc.

Guzey D & McClements DJ (2006) Formation, stability and properties of multilayer emulsions for application in the food industry. Advances in Colloid and Interface Science 128-130, 227-248.

Harush-Frenkel O, Debotton N, Benita S & Altschuler Y (2007) Targeting of nanoparticles to the clathrin-mediated endocytic pathway. Biochemical and Biophysical Research Communications 353(1), 26-32.

Hu M, Li Y, Decker E, Xiao H & McClements D (2011) Impact of Layer Structure on Physical Stability and Lipase Digestibility of Lipid Droplets Coated by Biopolymer Nanolaminated Coatings. Food Biophysics 6(1), 37-48.

Huang Y-C & Kuo T-H (in press) O-carboxymethyl chitosan/fucoidan nanoparticles increase cellular curcumin uptake. Food Hydrocolloids.

Jayaprakasha GK, Jaganmohan Rao L & Sakariah KK (2006) Antioxidant activities of curcumin, demethoxycurcumin and bisdemethoxycurcumin. Food Chemistry 98(4), 720-724.

Jelezova I, Drakalska E, Momekova D, Shalimova N, Momekov G, Konstantinov S, Rangelov S & Pispas S (2015) Curcumin loaded pH-sensitive hybrid lipid/block copolymer nanosized drug delivery systems. European Journal of Pharmaceutical Sciences 78, 67-78.

Kaur K, Kumar R & Mehta SK (2015) Nanoemulsion: A new medium to study the interactions and stability of curcumin with bovine serum albumin. Journal of Molecular Liquids 209, 62-70.

Klinkesorn U & Julian McClements D (2010) Impact of Lipase, Bile Salts, and Polysaccharides on Properties and Digestibility of Tuna Oil Multilayer Emulsions Stabilized by Lecithin–Chitosan. Food Biophysics 5(2), 73-81.

Klinkesorn U & McClements DJ (2009) Influence of chitosan on stability and lipase digestibility of lecithin-stabilized tuna oil-in-water emulsions. Food Chemistry 114(4), 1308-1315.

Langerholc T, Maragkoudakis PA, Wollgast J, Gradisnik L & Cencic A (2011) Novel and established intestinal cell line models – An indispensable tool in food science and nutrition. Trends in Food Science & Technology 22, Supplement 1, S11-S20.

Li M, Cui J, Ngadi MO & Ma Y (2015a) Absorption mechanism of whey-protein-delivered curcumin using Caco-2 cell monolayers. Food Chemistry 180, 48-54.

Li Y, Hu M, Du Y, Xiao H & McClements DJ (2011) Control of lipase digestibility of emulsified lipids by encapsulation within calcium alginate beads. Food Hydrocolloids 25(1), 122-130.

Li Y, Hu M, Xiao H, Du Y, Decker EA & McClements DJ (2010) Controlling the functional performance of emulsion-based delivery systems using multi-component biopolymer coatings. European Journal of Pharmaceutics and Biopharmaceutics 76(1), 38-47.

Li Z, Jiang H, Xu C & Gu L (2015b) A review: Using nanoparticles to enhance absorption and bioavailability of phenolic phytochemicals. Food Hydrocolloids 43, 153-164.

Liu Y, Cai Y, Jiang X, Wu J & Le X (2016) Molecular interactions, characterization and antimicrobial activity of curcumin–chitosan blend films. Food Hydrocolloids 52, 564-572.

Madrigal-Carballo S, Lim S, Rodriguez G, Vila AO, Krueger CG, Gunasekaran S & Reed JD (2010) Biopolymer coating of soybean lecithin liposomes via layer-by-layer self-assembly as novel delivery system for ellagic acid. Journal of Functional Foods 2(2), 99-106.

Maljaars J, Peters HPF, Haddeman E & Masclee A (in press) M2078 Distribution of Small Intestinal Fat Delivery Influences Satiety and Food Intake. Gastroenterology 136(5), A-480.

Malvern I, (2011). Dynamic light scattering common terms defined, in: Instruments M (Ed.), Worcestershire, UK.

Martins J, Ramos Ó, Pinheiro A, Bourbon A, Silva H, Rivera M, Cerqueira M, Pastrana L, Malcata FX, González-Fernández Á & Vicente A (2015) Edible Bio-Based Nanostructures: Delivery, Absorption and Potential Toxicity. Food Engineering Reviews, 1-23.

Matias A, Nunes SL, Poejo J, Mecha E, Serra AT, Madeira PJA, Bronze MR & Duarte CMM (2014) Antioxidant and anti-inflammatory activity of a flavonoid-rich concentrate recovered from Opuntia ficus-indica juice. Food & Function 5(12), 3269-3280.

McClements DJ (2013) Edible lipid nanoparticles: Digestion, absorption, and potential toxicity. Progress in Lipid Research 52(4), 409-423.

McClements DJ (in press) Encapsulation, protection, and release of hydrophilic active components: Potential and limitations of colloidal delivery systems. Advances in Colloid and Interface Science(0).

McClements DJ & Li Y (2010) Structured emulsion-based delivery systems: Controlling the digestion and release of lipophilic food components. Advances in Colloid and Interface Science 159(2), 213-228.

McClements DJ & Xiao H (2012) Potential biological fate of ingested nanoemulsions: influence of particle characteristics. Food & Function 3(3), 202-220.

Minekus M, Jelier M, Xiao J-z, Kondo S, Iwatsuki K, Kokubo S, Bos M, Dunnewind B & Havenaar R (2005) Effect of Partially Hydrolyzed Guar Gum (PHGG) on the Bioaccessibility of Fat and Cholesterol. Bioscience, Biotechnology, and Biochemistry 69(5), 932-938.

Mora-Huertas CE, Fessi H & Elaissari A (2010) Polymer-based nanocapsules for drug delivery. International Journal of Pharmaceutics 385(1–2), 113-142.

Mu H & Høy C-E (2004) The digestion of dietary triacylglycerols. Progress in Lipid Research 43(2), 105-133.

Mun S, Decker EA & McClements DJ (2005) Influence of Droplet Characteristics on the Formation of Oil-in-Water Emulsions Stabilized by Surfactant−Chitosan Layers. Langmuir 21(14), 6228-6234.

Ozturk B, Argin S, Ozilgen M & McClements DJ (2014) Formation and stabilization of nanoemulsion-based vitamin E delivery systems using natural surfactants: Quillaja saponin and lecithin. Journal of Food Engineering 142(0), 57-63.

Pantaleone D, Yalpani M & Scollar M (1992) Unusual susceptibility of chitosan to enzymic hydrolysis. Carbohydrate Research 237, 325-332.

Pinheiro AC, Coimbra MA & Vicente AA (2016) In vitro behaviour of curcumin nanoemulsions stabilized by biopolymer emulsifiers – Effect of interfacial composition. Food Hydrocolloids 52, 460-467.

Pinsirodom P, & P, K. L., (2005). Lipase assays, in: Wrolstad RE (Ed.), *Handbook of food analytical chemistry*. Wiley, Hoboken, NJ, pp. 371 - 383.

Plaza-Oliver M, Baranda JFSd, Rodríguez Robledo V, Castro-Vázquez L, Gonzalez-Fuentes J, Marcos P, Lozano MV, Santander-Ortega MJ & Arroyo-Jimenez MM (2015) Design of the interface of edible nanoemulsions to

modulate the bioaccessibility of neuroprotective antioxidants. International Journal of Pharmaceutics 490(1–2), 209-218.

Porter CJH, Trevaskis NL & Charman WN (2007) Lipids and lipid-based formulations: optimizing the oral delivery of lipophilic drugs. Nat Rev Drug Discov 6(3), 231-248.

Prasad S, Tyagi AK & Aggarwal BB (2014) Recent Developments in Delivery, Bioavailability, Absorption and Metabolism of Curcumin: the Golden Pigment from Golden Spice. Cancer Res Treat 46(1), 2-18.

Rao J & McClements DJ (2013) Optimization of lipid nanoparticle formation for beverage applications: Influence of oil type, cosolvents, and cosurfactants on nanoemulsion properties. Journal of Food Engineering 118(2), 198-204.

Rodrigues RM, Martins AJ, Ramos OL, Malcata FX, Teixeira JA, Vicente AA & Pereira RN (2015) Influence of moderate electric fields on gelation of whey protein isolate. Food Hydrocolloids 43, 329-339.

Salvia-Trujillo L, Sun Q, Um BH, Park Y & McClements DJ (2015) In vitro and in vivo study of fucoxanthin bioavailability from nanoemulsion-based delivery systems: Impact of lipid carrier type. Journal of Functional Foods 17, 293-304.

Sambuy Y, De Angelis I, Ranaldi G, Scarino ML, Stammati A & Zucco F (2005) The Caco-2 cell line as a model of the intestinal barrier: influence of cell and culture-related factors on Caco-2 cell functional characteristics. Cell Biology and Toxicology 21(1), 1-26.

Serra AT, (2010). Valorization of traditional portuguese apples and cherries biochemical characterization and development of functional ingredients, *Instituto de Tecnologia Química e Biológica*. Universidade Nova de Lisboa.

Serra AT, Duarte RO, Bronze MR & Duarte CMM (2011a) Identification of bioactive response in traditional cherries from Portugal. Food Chemistry 125(2), 318-325.

Serra AT, Matias AA, Almeida APC, Bronze MR, Alves PM, de Sousa HC & Duarte CMM (2011b) Processing cherries (Prunus avium) using supercritical fluid technology. Part 2. Evaluation of SCF extracts as promising natural chemotherapeutical agents. The Journal of Supercritical Fluids 55(3), 1007-1013.

Serra AT, Poejo J, Matias AA, Bronze MR & Duarte CMM (2013) Evaluation of Opuntia spp. derived products as antiproliferative agents in human colon cancer cell line (HT29). Food Research International 54(1), 892-901.

Sessa M, Balestrieri ML, Ferrari G, Servillo L, Castaldo D, D'Onofrio N, Donsì F & Tsao R (2014) Bioavailability of encapsulated resveratrol into nanoemulsion-based delivery systems. Food Chemistry 147(0), 42-50.

Sessa M, Tsao R, Liu R, Ferrari G & Donsì F (2011) Evaluation of the Stability and Antioxidant Activity of Nanoencapsulated Resveratrol during in Vitro Digestion. Journal of Agricultural and Food Chemistry 59(23), 12352-12360.

Shimizu M (2010) Interaction between Food Substances and the Intestinal Epithelium. Bioscience, Biotechnology, and Biochemistry 74(2), 232-241.

Shin SS, Lee YC & Lee C (2001) THE DEGRADATION OF CHITOSAN WITH THE AID OF LIPASE FROM RHIZOPUS JAPONICUS FOR THE PRODUCTION OF SOLUBLE CHITOSAN. Journal of Food Biochemistry 25(4), 307-321.

Silva HD, Cerqueira MA, Souza BWS, Ribeiro C, Avides MC, Quintas MAC, Coimbra JSR, Carneiro-da-Cunha MG & Vicente AA (2011) Nanoemulsions of β-carotene using a high-energy emulsification-evaporation technique. Journal of Food Engineering 102(2), 130-135.

Silva HD, Cerqueira MA & Vicente AA (2015) Influence of surfactant and processing conditions in the stability of oil-in-water nanoemulsions. Journal of Food Engineering.

Siviero A, Gallo E, Maggini V, Gori L, Mugelli A, Firenzuoli F & Vannacci A (2015) Curcumin, a golden spice with a low bioavailability. Journal of Herbal Medicine 5(2), 57-70.

Smith J, Wood E & Dornish M (2004) Effect of Chitosan on Epithelial Cell Tight Junctions. Pharmaceutical Research 21(1), 43-49.

Sun Y, Xia Z, Zheng J, Qiu P, Zhang L, McClements DJ & Xiao H (2015) Nanoemulsion-based delivery systems for nutraceuticals: Influence of carrier oil type on bioavailability of pterostilbene. Journal of Functional Foods 13, 61-70.

Szczepanowicz K, Bazylińska U, Pietkiewicz J, Szyk-Warszyńska L, Wilk KA & Warszyński P (in press) Biocompatible long-sustained release oil-core polyelectrolyte nanocarriers: From controlling physical state and stability to biological impact. Advances in Colloid and Interface Science.

Ting Y, Jiang Y, Ho C-T & Huang Q (2014) Common delivery systems for enhancing in vivo bioavailability and biological efficacy of nutraceuticals. Journal of Functional Foods 7, 112-128.

Tokle T, Lesmes U, Decker EA & McClements DJ (2012) Impact of dietary fiber coatings on behavior of protein-stabilized lipid droplets under simulated gastrointestinal conditions. Food & Function 3(1), 58-66.

Vachoud L, Zydowicz N & Domard A (2000) Physicochemical behaviour of chitin gels. Carbohydrate Research 326(4), 295-304.

Wang H & Joseph JA (1999) Quantifying cellular oxidative stress by dichlorofluorescein assay using microplate reader1. Free Radical Biology and Medicine 27(5–6), 612-616.

Wang J, Ma W & Tu P (2015) The mechanism of self-assembled mixed micelles in improving curcumin oral absorption: In vitro and in vivo. Colloids and Surfaces B: Biointerfaces 133, 108-119.

Wolfe KL & Liu RH (2007) Cellular Antioxidant Activity (CAA) Assay for Assessing Antioxidants, Foods, and Dietary Supplements. Journal of Agricultural and Food Chemistry 55(22), 8896-8907.

Yang D, Wang X-Y, Ji C-M, Lee K-T, Shin J-A, Lee E-S & Hong S-T (2014) Influence of Ginkgo biloba extracts and of their flavonoid glycosides fraction on the in vitro digestibility of emulsion systems. Food Hydrocolloids 42, Part 1, 196-203.

Yu H & Huang Q (2012) Improving the Oral Bioavailability of Curcumin Using Novel Organogel-Based Nanoemulsions. Journal of Agricultural and Food Chemistry 60(21), 5373-5379.

Yu H, Li J, Shi K & Huang Q (2011) Structure of modified E-polylysine micelles and their application in improving cellular antioxidant activity of curcuminoids. Food & Function 2(7), 373-380.

Zhang C, Xu W, Jin W, Shah BR, Li Y & Li B (in press) Influence of anionic alginate and cationic chitosan on physicochemical stability and carotenoids bioaccessibility of soy protein isolate-stabilized emulsions. Food Research International.

Zhao L, Du J, Duan Y, Zang Yn, Zhang H, Yang C, Cao F & Zhai G (2012) Curcumin loaded mixed micelles composed of Pluronic P123 and F68:

Preparation, optimization and in vitro characterization. Colloids and Surfaces B: Biointerfaces 97, 101-108.

Zou L, Zheng B, Liu W, Liu C, Xiao H & McClements DJ (2015) Enhancing nutraceutical bioavailability using excipient emulsions: Influence of lipid droplet size on solubility and bioaccessibility of powdered curcumin. Journal of Functional Foods 15, 72-83.

CHAPTER 7

GENERAL CONCLUSIONS

This chapter provides the overall conclusions of this thesis, as well as recommendations and suggestions for future work.

7.1 Conclusions

The work presented in this thesis is the result of a systematic study that aimed at the development of lipid-based nanosystems for controlled release of lipophilic bioactive compounds in the gastrointestinal tract. In order to fulfil this main objective this thesis followed the development and characterization of nanoemulsions and multilayer nanoemulsions, with the further incorporation of curcumin as model bioactive compound, and the evaluation of their behaviour when subjected to digestion in a dynamic artificial gastrointestinal system. The cytotoxicity of the developed lipid-based nanosystems was also addressed, as well the cellular uptake and apparent permeability coefficient of curcumin through Caco-2 cells. The main contributions of this thesis are summarized below:

- The high-pressure homogenization technique successfully produced nanoemulsions using different surfactants or proteins, which were kinetically stable during storage (at least 28 days);
- Homogenization pressure, surfactant type and oil concentration were found to be critical to achieve the desired hydrodynamic diameter, polydispersity index and zeta potential of nanoemulsions;
- The use of small molecules' surfactants such as SDS lead to smaller droplet sizes due to the faster adsorption kinetics to the interface that reduced size and recoalescence phenomena. The increase of surface charge may slow down the creaming rate, due to the increase of repulsive forces between droplets. Anionic nanoemulsions displayed the highest stability against creaming after 1 year of storage;
- LbL assembly technique, using chitosan and alginate, can be used to successfully change the surface characteristics of curcumin nanoemulsions;
- The deposition of chitosan and alginate results in the formation of a stable multilayer structure, mainly due to electrostatic interactions between the polyelectrolytes, whereas interactions such as hydrogen bonds might also be involved;

- Lipid-based nanosystems were stable to changes in temperature and present pH-responsiveness;
- Curcumin release from lipid-based nanosystems suggested an anomalous behaviour, being relaxation of the polymers/surfactant the main transport phenomenon observed;
- Anionic nanoemulsions can increase curcumin bioaccessibility, while polyelectrolyte layers were effective in the delaying the lipid digestibility;
- The build-up of a multilayer nanoemulsion with three layers was efficient in protecting curcumin from enzymes and bile salts, improving the antioxidant capacity of curcumin during digestion;
- The use of WPI nanoemulsions and chitosan-coated nanoemulsions can significantly increase the cellular antioxidant activity of curcumin;
- The use of chitosan as a coating can enhance curcumin apparent permeability coefficient when compared to nanoemulsions;
- The permeation rate of the lipid-based nanosystems through Caco-2 cells monolayer suggests that transcellular and paracellular pathways may exist at the same time.

Briefly, this thesis showed that it is possible to tailor nanoemulsions and multilayer nanoemulsions by combining high-pressure homogenization and the LbL technique. The developed work clarified the release mechanism involved in this type of systems, enlightening the impact of temperature, solvent and surface properties. Furthermore, this thesis contributed to the understanding of the behaviour of lipid-based nanosystems during digestion and the knowledge of their cytotoxicity and permeation mechanism using Caco-2 cells. The developed lipid-based nanosystems can be used as platforms for the design of functional foods with different functionalities.

7.2 Recommendations

Even though the main purposes of this thesis have been accomplished, work still needs to be done in order to better understand how lipid-based nanosystems will behave inside the human body and to elucidate consumers' awareness and knowledge towards nanotechnology. Thus, some recommendations for improvements of the present work and guidelines for future work in nanotechnology applied to food science can be advanced:

- The behaviour of the lipid-based nanosystems should be evaluated in real food systems;
- Assessment of nanosystems behaviour under more complex in vitro digestion models, being these able to contemplate the intestinal microflora influence;
- The apparent permeability coefficient using Caco-2 and HT29 cells monolayer, in order to mimic the epithelial mucus layer, should be determined;
- The transport phenomena using M cells should be studied in order to better understand the internalization of bioactive compounds;
- Bioactive compounds bioavailability after nanosystem digestion on the dynamic gastrointestinal system in combination with the use of human intestinal cells, such as Caco-2 and HT29, should be re-evaluated, resulting in a more reliable value of bioavailability of bioactive compounds;
- Further studies regarding the cellular uptake, in order to clarify and quantify curcumin metabolites after cell internalization should be made;
- *In vivo* studies in animals (rats) and further comparison with the results obtained with the dynamic *in vitro* gastrointestinal system should be performed;
- *In vivo* studies should be made in order to clarify the consumers' opinion towards nanotechnology.

SUPPLEMENTARY MATERIAL

Table S4.1 – FTIR characteristic peaks of MCTs, curcumin, SDS, chitosan and alginate with references

Wavelength (cm^{-1})	MCT's	Curcumin	SDS	Chitosan	Alginate	References
3700 – 3000					OH stretch	(Lawrie, et al., 2007)
3507		OH group				(Mohan, et al., 2012)
3354				Stretching vibration of the NH group		(Pawlak, et al., 2003)
3339		Vibration of the free hydroxyl-group of phenol (Ar-OH)				(Hee-Je Kim, et al., 2013)
3295				Stretching of the OH and NH groups		(Lawrie, et al., 2007)
2956			Asymmetric CH_3 stretching vibrational			(Viana, et al., 2012)
2954	Symmetric stretching vibration shoulder of the aliphatic CH_3 group					(N. Vlachos, et al., 2006)

2924 and 2855	Symmetric and asymmetric stretching vibration of the aliphatic CH_2 group			(N. Vlachos, et al., 2006; Yang, et al., 2005)
2924			Stretching of the CH group	(Mukhopadhyay, et al., 2015; Pawlak, et al., 2003)
2922 and 2853			CH stretch	(Lawrie, et al., 2007)
2917		Asymmetric CH_2 stretching vibrational		(Viana, et al., 2012)

2874			OH stretching	(Li, et al., 2008)
2873		Symmetric CH_3 stretching vibrational		(Viana, et al., 2012)
2849		Symmetric CH_2 stretching vibrational		(Viana, et al., 2012)
1741	Ester carbonyl functional group of the triglycerides			(N. Vlachos, et al., 2006; Yang, et al., 2005)
1648			Carbonyl (C=O) stretching of the secondary amide (amide I band)	(Lawrie, et al., 2007; Li, et al., 2008; Pawlak, et al., 2003)
1626	Stretching of the C=C and C=O of			(Mangolim, et al., 2014; Mohan, et al., 2012)

		the inter ring chain			
1601		Symmetric stretching vibrations of the aromatic ring C=C			(Mangolim, et al., 2014; Mohan, et al., 2012)
1592				Asymmetric CO_2^- stretch	(Lawrie, et al., 2007)
1591			NH_2 in amino group		(Pawlak, et al., 2003)
1505		Stretching of C=O; in plane bending of CCC and in plane bending of C=O			(Mangolim, et al., 2014; Mohan, et al., 2012)
1468			CH_2 scissoring mode and in plane bending of the CH_2 group		(Viana, et al., 2012)
1458	CH bending (scissoring)				(Yang, et al., 2005)
1455		Vibrational mode of C-O elongation of the alcohol group			(Hee-Je Kim, et al., 2013)
1427		In plane bending of CCC; in plane bending of CCH			(Mangolim, et al., 2014)

		and in plane bending of C-OH of the aromatic rings				
1418	Rocking vibrations of CH bonds of cis-disubstituted olefins			CH_2 bending		(Lawrie, et al., 2007; N. Vlachos, et al., 2006)
1408					Symmetric CO_2^- stretch	(Lawrie, et al., 2007; Shi, et al., 2006)
1378	Bending vibrations of CH2 groups		CH_3 umbrella mode	CH_3 symmetrical deformation in amide group		(Lawrie, et al., 2007; Viana, et al., 2012; N. Vlachos, et al., 2006)
1377		Vibrational mode of C-O elongation of the phenol group				(Hee-Je Kim, et al., 2013)
1323				CH_2 stretching vibration attributed to pyranose ring		(Pawlak, et al., 2003)
1315		In plane bending CCH of the inter-ring chain (C10 and C11)				(Mangolim, et al., 2014)
1298					Skeletal vibration	(Lawrie, et al., 2007)
1272		Enol C-O				(Mohan, et al., 2012)

1258			CO group		(Pawlak, et al., 2003)
1248 and 1217		SO_2 asymmetric vibrational			(Viana, et al., 2012)
1224 and 1153	Stretching vibration of the C O ester groups				(N. Vlachos, et al., 2006)
1151		In plane bending of the CCH of aromatic rings and in plane bending C-OH of the enolic group coupled to in plane bending of C=CH in the inter-ring chain			(Mangolim, et al., 2014)
1150			Asymmetric stretch C-O-C and C-N stretch		(Lawrie, et al., 2007; Pawlak, et al., 2003)
1082 and 1027				Asymmetric stretch C-O-C	(Lawrie, et al., 2007)
1081		SO2 symmetric vibrational			(Viana, et al., 2012)
1026			Skeletal vibration of C-O stretching		(Lawrie, et al., 2007)

1024		C-O-C	(Hee-Je Kim, et al., 2013; Mohan, et al., 2012)
962		Bending vibrations of C-H bond of alkene group ($RCH=CH_2$)	(Hee-Je Kim, et al., 2013)
855		Out of plane bending CH of aromatic and skeletal CCH	(Mangolim, et al., 2014)
815		Bending vibrations of C-H bond of alkene group (RCH=CH2)	(Hee-Je Kim, et al., 2013)
724	Overlapping of the CH_2 rocking vibration and the out-of-plane vibration of cis-disubstituted olefins		(N. Vlachos, et al., 2006)
714		Cis CH vibration of the aromatic ring	(Mohan, et al., 2012)

References

Hee-Je Kim, Dong- Jo Kim, Karthick, S. N., Hemalatha, K. V., C. Justin Raj, Sunseong Ok, & Choe, Y. (2013). Curcumin Dye Extracted from Curcuma longa L. Used as Sensitizers for Efficient Dye-Sensitized Solar Cells. *International Journal of Electrochemical Science*(8), 8320 - 8328.

Lawrie, G., Keen, I., Drew, B., Chandler-Temple, A., Rintoul, L., Fredericks, P., & Grøndahl, L. (2007). Interactions between Alginate and Chitosan Biopolymers Characterized Using FTIR and XPS. *Biomacromolecules, 8*(8), 2533-2541.

Li, P., Dai, Y.-N., Zhang, J.-P., Wang, A.-Q., & Wei, Q. (2008). Chitosan-Alginate Nanoparticles as a Novel Drug Delivery System for Nifedipine. *International Journal of Biomedical Science : IJBS, 4*(3), 221-228.

Mangolim, C. S., Moriwaki, C., Nogueira, A. C., Sato, F., Baesso, M. L., Neto, A. M., & Matioli, G. (2014). Curcumin–β-cyclodextrin inclusion complex: Stability, solubility, characterisation by FT-IR, FT-Raman, X-ray diffraction and photoacoustic spectroscopy, and food application. *Food Chemistry, 153*, 361-370.

Mohan, P. R. K., Sreelakshmi, G., Muraleedharan, C. V., & Joseph, R. (2012). Water soluble complexes of curcumin with cyclodextrins: Characterization by FT-Raman spectroscopy. *Vibrational Spectroscopy, 62*, 77-84.

Mukhopadhyay, P., Chakraborty, S., Bhattacharya, S., Mishra, R., & Kundu, P. P. (2015). pH-sensitive chitosan/alginate core-shell nanoparticles for efficient and safe oral insulin delivery. *International Journal of Biological Macromolecules, 72*, 640-648.

Pawlak, A., & Mucha, M. (2003). Thermogravimetric and FTIR studies of chitosan blends. *Thermochimica Acta, 396*(1–2), 153-166.

Shi, X., Du, Y., Sun, L., Zhang, B., & Dou, A. (2006). Polyelectrolyte complex beads composed of water-soluble chitosan/alginate: Characterization and their protein release behavior. *Journal of Applied Polymer Science, 100*(6), 4614-4622.

Viana, R. B., da Silva, A. B. F., & Pimentel, A. S. (2012). Infrared Spectroscopy of Anionic, Cationic, and Zwitterionic Surfactants. *Advances in Physical Chemistry, 2012*, 14.

Vlachos, N., Skopelitis, Y., Psaroudaki, M., Konstantinidou, V., Chatzilazarou, A., & Tegou, E. (2006). Applications of Fourier transform-infrared spectroscopy to edible oils. *Analytica Chimica Acta, 573–574*, 459-465.

Vlachos, N., Skopelitis, Y., Psaroudaki, M., Konstantinidou, V., Chatzilazarou, A., & Tegou, E. (2006). Applications of Fourier transform-infrared spectroscopy to edible oils. *Analytica Chimica Acta, 573–574*, 459–465.

Yang, H., Irudayaraj, J., & Paradkar, M. M. (2005). Discriminant analysis of edible oils and fats by FTIR, FT-NIR and FT-Raman spectroscopy. *Food Chemistry, 93*(1), 25-32.